2019

Role of Neutrophils in Osteoarthritis and Rheumatoid Arthritis and Their Metabolomics

Dong Zhan
Faculty of Medicine

Role of Neutrophils in Osteoarthritis and Rheumatoid Arthritis and Their Metabolomics

Mr. Dong Zhan

A Dissertation Submitted in Partial Fulfillment of the Requirements for the Degree of Doctor of Philosophy in Biomedical Sciences and Biotechnology
Common Course
FACULTY OF MEDICINE
Chulalongkorn University
Academic Year 2019

บทบาทของนิวโทรฟิลและการศึกษาเมแทบอโลมิกส์ในโรคข้อเสื่อมและโรคข้ออักเสบรูมาทอยด์

นายตง เฉิน

วิทยานิพนธ์นี้เป็นส่วนหนึ่งของการศึกษาตามหลักสูตรปริญญาวิทยาศาสตรดุษฎีบัณฑิต
สาขาวิชาชีวเวชศาสตร์และชีวเทคโนโลยี ไม่สังกัดภาควิชา/เทียบเท่า
คณะแพทยศาสตร์ จุฬาลงกรณ์มหาวิทยาลัย
ปีการศึกษา 2562

Thesis Title	Role of Neutrophils in Osteoarthritis and Rheumatoid Arthritis and Their Metabolomics
By	Mr. Dong Zhan
Field of Study	Biomedical Sciences and Biotechnology
Thesis Advisor	Professor Doctor Sittisak Honsawek
Thesis Co Advisor	Professor Robert John Moots Helen Louise Wright Professor Steven W. Edwards

Accepted by the FACULTY OF MEDICINE, Chulalongkorn University in Partial Fulfillment of the Requirement for the Doctor of Philosophy

..... Dean of the FACULTY OF MEDICINE
(Professor SUTTIPONG WACHARASINDHU)

DISSERTATION COMMITTEE

..... Chairman
(Professor KANYA SUPHAPEETIPORN)

..... Thesis Advisor
(Professor Doctor Sittisak Honsawek)

..... Thesis Co-Advisor
(Professor Robert John Moots)

..... Thesis Co-Advisor
(Helen Louise Wright)

..... Thesis Co-Advisor
(Professor Steven W. Edwards)

..... Examiner
(Professor AREE TANAVALEE)

..... Examiner
(Assistant Professor TRAIRAK PISITKUN)

..... Examiner
(JAMES ANTHONY GALLAGHER)

..... External Examiner
(Korbtham Sathirakul)

ตง เฉิน : บทบาทของนิวโทรฟิลและการศึกษาเมแทบอโลมิกส์ในโรคข้อเสื่อมและโรคข้ออักเสบรูมาทอยด์. (Role of Neutrophils in Osteoarthritis and Rheumatoid Arthritis and Their Metabolomics) อ.ที่ปรึกษาหลัก : ศ.สิทธิศักดิ์ หรรษาเวก, อ.ที่ปรึกษาร่วม : ศ.โรเบิร์ต จอห์น มูทส์,ฮเลน ลูอีส ไรท์,ศ.สตีเว็น ดับบลิว เอ็ดเวิร์ด

Fibroblast-like synoviocytes (FLS) มีบทบาทสำคัญต่อการเกิดการอักเสบของเยื่อบุข้อในผู้ป่วยโรคข้อเข่าเสื่อมและโรคข้ออักเสบรูมาทอยด์ การศึกษาก่อนหน้าพบว่า Neutrophil-derived microvesicles (NDMV) สามารถป้องกันกระดูกอ่อนและออกฤทธิ์ป้องกันการอักเสบในเซลล์เป้าหมายได้ การศึกษาครั้งนี้มีวัตถุประสงค์เพื่อดูการแสดงออกของ inflammatory cytokine ที่สร้างขึ้นโดย FLS ที่ได้จากการกระตุ้นโดย TNFα ซึ่งมีการปรับสภาพด้วย NDMV โดย FLS ที่แยกได้จาก synovium ของผู้ป่วยโรคข้อเข่าเสื่อมจะนำมาวิเคราะห์ด้วย flow cytometry การศึกษาครั้งนี้ได้ทำการสกัด neutrophil จากเลือดอาสาสมัครสุขภาพดีด้วยการปั่นด้วย cytospin และ flow cytometry หลังจากนั้น NDMV ซึ่งได้จาก neutrophil ที่กระตุ้นโดย TNFα จะถูกนำมาวิเคราะห์ด้วยกล้อง electron , nanoparticle tracking analysis และ flow cytometry ต่อมา MicroRNA ของ NDMV จะถูก sequence โดย Illumina NextSeq500 ภายหลังการปรับสภาพด้วย NDMV จะทำการวัด FLS viability ด้วยวิธี MTT assay การศึกษา internalisation ของ NDMV ที่ถูกติดฉลากด้วยสารเรืองแสงทำโดย flow cytometry และกล้อง confocal โดยระดับ inflammatory cytokine ของ FLS ที่ได้จากส่วนใสของการเพาะเลี้ยงจะวัดปริมาณโดยเทคนิค Bio-Plex suspension array system ผลการศึกษาพบว่า FLS จาก passage 4 ที่ได้จาก OA synovium มี purity สูงที่สุด (≥95%) สามารถ สกัด neutrophil ได้ (>98%) ภายหลังการกระตุ้นด้วย TNFα 50 ng/ml เป็นเวลา 20 นาที ซึ่งทำก่อนขั้นตอนการเตรียม NDMV โดย NDMV ที่สกัดได้นั้น (200 - 500nm) พบการแสดงออกของ Annexin V และ CD63 มากกว่า neutrophil ที่ไม่ได้รับการกระตุ้น นอกจากนี้ยังพบว่าการบ่ม FLS ด้วย NDMV โดยมีอัตราส่วน 1:100 จะมีผลต่อการนำเข้าของเซลล์ที่แปรผันตามเวลา โดยไม่พบความแตกต่างของ cell viability ใน 35% ของ FLS ที่บ่มด้วย NDMV เป็นเวลา 6-24 ชั่วโมง พบว่า 74 และ 26 ยีนเป้าหมายของ MAPK NDMV-carried microRNAs เกิดปฏิกิริยากับการถ่ายทอดสัญญาณของเซลล์โดยส่งผ่านโปรตีน PI3K-Akt และ MAPK อย่างมีนัยสำคัญทางสถิติ ($p<0.0001$) ซึ่ง TNFα (10ng/ml) สามารถกระตุ้นการแสดงออกของ cytokines และ chemokines จาก synoviocyte และพบว่า NDMV down-regulated ทำให้เกิดการแสดงออกของ of IL-5, IL-6, IL-8. MCP-1, IFNγ and MIP-1β ($p<0.01$) อย่างมีนัยสำคัญทางสถิติ การศึกษาครั้งนี้แสดงให้เห็นว่า NDMV จะถูก internalise โดย FLS และยับยั้งการหลั่ง inflammatory cytokine ที่ถูกกระตุ้นด้วย TNFα ผ่านทาง NDMV-carried microRNAs ที่ควบคุมเชิงลบในขั้นตอน post-transcriptional ของการถ่ายทอดสัญญาณของเซลล์โดยส่งผ่านโปรตีน PI3K-Akt และ MAPK.

สาขาวิชา	ชีวเวชศาสตร์และชีวเทคโนโลยี	ลายมือชื่อนิสิต .....
ปีการศึกษา	2562	ลายมือชื่อ อ.ที่ปรึกษาหลัก .....
		ลายมือชื่อ อ.ที่ปรึกษาร่วม .....
		ลายมือชื่อ อ.ที่ปรึกษาร่วม .....

5874851030 : MAJOR BIOMEDICAL SCIENCES AND BIOTECHNOLOGY
KEYWORD: osteoarthritis, rheumatiod arthritis, neutrophils, neutrophils-derived microvesicles, synovitis, fibroblast-like synoviocytes, cytokines, microRNA

Dong Zhan : Role of Neutrophils in Osteoarthritis and Rheumatoid Arthritis and Their Metabolomics. Advisor: Prof. Doc. Sittisak Honsawek Co-advisor: Prof. Robert John Moots, Helen Louise Wright,Prof. Steven W. Edwards

Objectives: Fibroblast-like synoviocytes (FLS) plays a function in the development of synovitis in osteoarthritis (OA) and rheumatoid arthritis (RA). Neutrophil-derived microvesicles (NDMV) can protect cartilage and possess anti-inflammatory effects on recipient cells. We investigated the expression of inflammatory cytokines produced by TNFα-stimulated FLS which were pre-treated with NDMV. Methods: FLS isolated from the synovium of patients with OA were characterized by flow cytometry. Neutrophils were isolated from healthy volunteer blood and were characterized by cytospin and flow cytometry. NDMV, generated from TNFα-stimulated neutrophils, were characterized by electron microscopy, nanoparticle tracking analysis and flow cytometry. MicroRNA of NDMV were sequenced by Illumina NextSeq500. MTT assay was used to measure FLS viability after NDMV treatment, while internalisation of fluorescently labelled NDMV was measured by flow cytometry and confocal microscopy. Cytokines levels in FLS cultured supernatants were quantified by the Bio-Plex suspension array system. Results: High purity (≥95%) of FLS at passage 4 were prepared from OA synovium. Isolated neutrophils (>98%) were treated for 20min treatment with 50ng/ml TNFα prior to preparation of NDMV. Isolated NDMV (200 to 500nm) expressed more Annexin V and CD63 than untreated neutrophils. Incubation of FLS with NDMV at a ratio of 1:100 resulted in a time-dependent uptake, with 35% of FLS containing NDMV over a 6-24h time-period, with no significant change in cell viability. 74 and 26 target genes of NDMV-carried microRNAs were predicted to interact with the PI3K-AKT and MAPK signaling pathways (p<0.0001). TNFα (10ng/ml) stimulated the expression of a number of cytokines and chemokines from synoviocytes and NDMV down-regulated this TNFα-induced expression of IL-5, IL-6, IL-8. MCP-1, IFNγ and MIP-1β (p<0.01). Conclusions: NDMV are internalised by FLS and inhibit TNFα-stimulated inflammatory cytokine secretion via NDMV-carried microRNAs negatively regulating post-transcriptional control of PI3K-Akt and MAPK signaling pathways.

Field of Study:	Biomedical Sciences and Biotechnology	Student's Signature .....
Academic Year:	2019	Advisor's Signature .....
		Co-advisor's Signature .....
		Co-advisor's Signature .....

ACKNOWLEDGEMENTS

Without generous assistance and precious support from kindhearted people around me, it would not have been possible to complete this tough work to only some of whom it is possible to give mention here.

During the period of pursuing my PhD degree, Professor Sittisak Honsawek, Professor Robert Moots, Professor Steven Edwards and Dr Helen Wright always gave me excellent guidance, wise suggestions and experiment-related technique improvement, as well as they inspired debates and discussions and encourage me to overcome difficulties. Please allow me to express my sincere appreciation to them.

I would like to thank warmhearted and friendly teachers, staffs and labmates from Chulalongkorn University, University of Liverpool and their affiliated hospitals (King Chulalongkorn Memorial Hospital and Aintree University Hospital).

Many thanks to my father, mother, father-in-law, mother-in-law, wife, brother, daughter and son to give me selfless and generous support and help. Thanks to the understanding from my colleagues of Kunming Medical University.

Thanks to scholarships from Graduate School, Chulalongkorn University (The 100th Anniversary Chulalongkorn University for Doctoral Scholarship and Overseas Research Experience Scholarship for Graduate Students) and China Scholarship Council.

Thanks to myself also.

Dong Zhan

TABLE OF CONTENTS

Page

LIST OF TABLES

Page

LIST OF FIGURES

Page

PREFACE

There is only one form of heroism in the world:
to see the world as it is, and to love it.
—Romain Rolland—

OA and RA are the two most prevalent forms of arthritis. Synovitis is detectable in affected joints of both conditions. Until recently, medical doctors and clinical scientists have had to face a shortage and limitation of effective treatments and even newer therapies are not always effective. It is therefore necessary to explore the role of novel therapies to improve joint function and relieve symptoms. Extracellular vesicles (EV) are a useful form of communication between cells, while neutrophil-derived microvesicles (NDMV), generated from stimulated neutrophils are reported to inhibit inflammation in some recipient cells. NDMV can also regulate chondrocytes to protect cartilage. My supervisor from Chulalongkorn University is an expert in OA, and supervisors from University of Liverpool are specialists in RA and neutrophils. It is appropriate to combine two research fields of FLS, neutrophils and NDMV. This research may eventually lead to NDMV applications in clinical practice for the treatment of inflammatory diseases.

Chapter 1 contains a brief description of research questions in osteoarthritis (OA) and rheumatoid arthritis (RA) and neutrophil-derived microvesicles (NDMV). The objectives, experimental design and hypothesis of the research in this thesis are stated in this opening chapter. Chapter 2 provides an overview of the current research developments and outstanding issues in OA, RA and NDMV. Synovitis is a common feature of both OA and RA whereas NDMV have the capability to inhibit the inflammatory response of recipient cells. In Chapter 3, experimental materials and methods are described to culture FLS, isolate NDMV, evaluate the characteristics of cells and NDMV, measure levels of cytokines and analyse microRNAs in neutrophils and NDMV. Bioinformatic methods were used to predict target genes of these microRNAs. In Chapter 4, after data were statistically analysed, experimental results are presented and the results section is composed of 4 parts: FLS culture and characterisation; neutrophil isolation and functional properties; NDMV isolation and

properties; the effects of NDMV on FLS. Chapter 5 contains discussion of the major findings in this research and the limitations. In Chapter 6 we speculate that NDMV could modulate FLS to prevent an inflammatory response through microRNA. We propose that NDMV have potential merit as a novel therapeutic approach for OA and RA patients.

Chapter 1. INTRODUCTION

1.1 Problem description

Osteoarthritis (OA) is often wrongly considered to be a disease of "tear and wear" and a primary defect of cartilage in synovial joints, and low-grade and chronic inflammation is often present in the synovium of affected joints. Rheumatoid arthritis (RA) is an autoimmune disorder that affects multiple organs. Its main manifestation is high-grade inflammation in tissues, especially the synovium that can result in cartilage and bone erosion. Hence, although OA and RA are two entirely different types of arthritis, both are associated with cartilage damage and synovial inflammation (synovitis) to various degrees. Synovitis in RA is extensive, involving the whole synovium in affected joints, but in OA synovitis appears in discrete locations of synovium named after "inflamed area" with hyperplasia and hypervascularity (Deligne et al., 2015).

Macrophages and T cells are two predominant immune cells that migrate from the blood stream to the synovium in OA and RA. Neutrophils are, however, the major infiltrating cell (about 50.6%) in the synovial fluid (SF) of RA joints, in comparison to OA, where neutrophils are typically less abundant (11.3%) (Rolle et al., 2019). An earlier study reported that the absolute number of neutrophils in OA SF (5ml) was 70.50%, which is lower than that in RA SF 79.17% (Abd-El-Hafez et al., 2014). Beside cartilage loss and low-grade synovitis, OA is also characterized by osteophytes, sclerosis and subchondral bone cysts. Another frequently observed histological feature in RA is a synovial pannus, induced by long-term synovitis and Figure 1 illustrates the differences in synovial joints between OA and RA compared to normal, healthy control joints. The occurrence of OA increases with age and is two-fold greater in those over 60 years, with a predominance in females. While the prevalence of RA is also higher in females, the age of onset is typically lower than in OA (Woolf and Pfleger, 2003). Both OA and RA result in pain, dysfunction and potentially

failure of joints, diminishing the quality of life. They also bring heavy social and economic burden both for governments and families. It is necessary to develop novel, effective and safe therapies for the improvement of human health, otherwise these diseases will continue to negatively influence millions of families across the world.

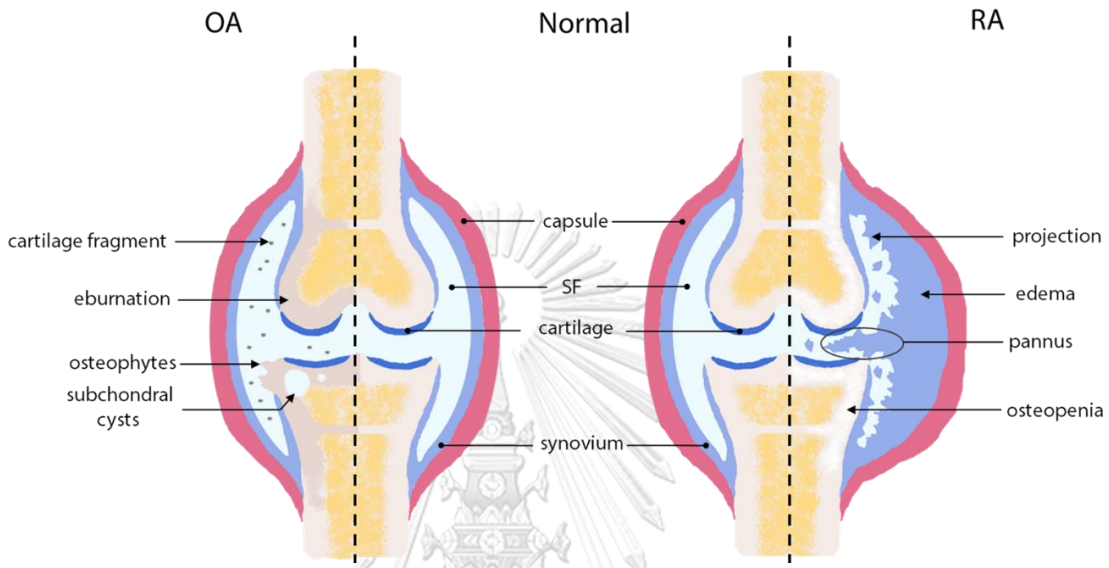

Figure 1. Schematic diagram comparing synovium, subchondral bone and synovial fluid between normal, OA and RA knee joints. Hyaline cartilage covers the ends of opposing articulated bones. Articular capsule is composed of fibrous membrane/capsule (outer layer) and synovial membrane/synovium (inner layer). Synovial fluid (SF) filled in potential joint cavity. OA knee is characterized with cartilage degradation and loss and cartilage fragments could be found in SF. Osteophytes also appears around the cartilage. Subchondral bone presents eburnation and cysts. In RA knee, pathological manifestations are mainly on synovium: overgrowth (projection and pannus) and edema results from high-grade synovitis. Osteopenia could appear in subchondral bone of RA. T cells and macrophages are two major cellular types found in the synovium and SF of arthritis. Neutrophils are recruited to either in the synovial cavity or membrane to spread inflammation and enhance joint destruction.

NDMV are one type of extracellular vesicles (EV) that are generated by neutrophils exposed to various stimulants, such as N-formyl-methionyl-leucyl-

phenylalanine (fMLP), interleukin (IL)-6 and Tumor Necrosis Factor alpha (TNFα). Although neutrophils are the predominant type of leukocytes (60-70%) in the circulation of healthy individuals, platelet-derived, rather the neutrophil-derived MV form the majority of total EV in circulating blood (Daniel et al., 2006). In RA the level of platelet-derived MV's positively correlates with disease activity, as determined by the disease activity score-28 (DAS28) (Knijff-Dutmer et al., 2002). NDMV have the potential to increase inflammation in endothelial cells in various vascular tissues such as brain microvessels, coronary arteries and umbilical veins (Ajikumar et al., 2019). Other pro-inflammatory mediators, such as IL-1β, IL-6, IL8, reactive oxygen species (ROS) etc., are expressed by endothelial cells exposed to NDMV (Mesri and Altieri, 1999, Mesri and Altieri, 1998). However, whether NDMV's perform an anti- or pro- inflammatory role depends on the recipient cell. For example, NDMV's exert a pro-inflammatory effect on endothelial cells, but an anti-inflammatory effect on myeloid cells (L Johnson et al., 2014).

In inflammation, whether induced by external factors (such as infection) or internal stimuli (such as in RA) stimuli, NDMV may be rapidly generated by infiltrating neutrophils at inflammatory sites. NDMV's down-regulate pro-inflammatory cytokines (IL-8, IL-10 and TNFα) expression from monocyte-derived macrophages and, conversely, elevation of the anti-inflammatory cytokine, Transforming Growth Factor beta (TGFβ) (Headland and Norling, 2015). The anti-inflammatory function of NDMV not only relies on surface proteins on NDMV membranes, but also on the content of NDMV. NDMV can be loaded with high levels of Annexin A1 and A5, myeloperoxidase, phosphatidylserine, etc. (Dalli et al., 2013). Microvesicles (MV) from the plasma of healthy volunteers contained substantial microRNAs and there were an identical 71 different microRNAs that were also found in monocytes (Hunter et al., 2008). It was reported that the proportion of CD66b+ (a neutrophil CD marker) on the MV was less than 5%. However, the CD66b+ MV percentage was highest among other cells derived MV (CD14+ or CD3+) from SF of RA. It may therefore be speculated that NDMV's possess microRNAs that could exert an influence on synovitis. In fact, exosomes (Exo) selectively assemble specific microRNAs, such as microRNA-320, 451 and 150, and MV selectively are loaded with pre-matured microRNAs (Chen et al., 2009, Guduric-Fuchs et al., 2012).

Recently, a study from Gomez *et al*. suggested that NDMV could up-regulate inflammatory cytokine expression in endothelial cells of the coronary artery via their cargo of miR-155 (Gomez et al., 2020).

Fibroblast-like synoviocytes (FLS) are the main cells types that forms the intimal layer of the synovium. They not only produce the lubricating synovial fluid essential for normal joint function, but also inflammatory- or metabolic-mediators to modulate the local joint environment. FLS treated by IL-1, IL-6 or TNFα etc. were commonly used to develop the cellular model of synovitis in *in vitro* studies. T cell-derived and monocyte-derived microvesicles (TDMV and MDMC) could induce FLS to up-regulate cyclooxygenase-2 (COX-2) gene expression and prostaglandin E2 (PGE2) levels, thereby promoting an inflammatory response, together with increased pro-angiogenetic chemokines expression, and elevated matrix metalloproteinases (MMP)-1, 3, 9 and 13 (Reich et al., 2011, Jungel et al., 2007, Distler et al., 2005b). Headland *et al.* proposed that NDMV could mediate a beneficial effect on chondrocytes (Headland et al., 2015), while Rhys *et al.* showed that the secretion of inflammatory cytokines was suppressed in FLS that had been co-cultured with macrophages treated by NDMV (Rhys et al., 2018). Eken *et al*. reported that NDMV could inhibit macrophage function through various signaling pathways, for example, via phosphatidylinositol 3-kinase-protein kinase B (PI3K-AKT), the MER proto-oncogene tyrosine kinase (MerTK) pathway and the Toll-like receptor (TLR)-2 pathway (Eken et al., 2013, Eken et al., 2010).

1.2 Aims

In the view of previous findings, the aim of this thesis was to investigate the direct impact of NDMV on the function of FLS and to determine how this interaction could affect inflammation. Highly-purified FLS, obtained by primary synoviocyte culture, were used to generate a cellular model of synovitis induced *in vitro* by TNFα exposure. Secondly, highly-pure populations of neutrophils were stimulated to generate NDMV and their properties and characteristics, including their microRNAs were investigated. The level of inflammatory cytokine s from FLS with or without treatment with NDMV were measured. The probable mechanism of these effects of NDMV-mediate changes in FLS function were analyzed via NDMV-containing

microRNAs and their predicted effects of the regulation of target genes by bioinformatic approaches.

1.3 Flowchart of experimental design

The experimental plan is divided into four parts: neutrophil isolation and their functional assays; FLS culture and characteristics; NDMV isolation, purification and properties assay, determination of the effect of NDMV to FLS. High purity of neutrophils and FLS are essential for the optimal analysis of data from the subsequent experiments.

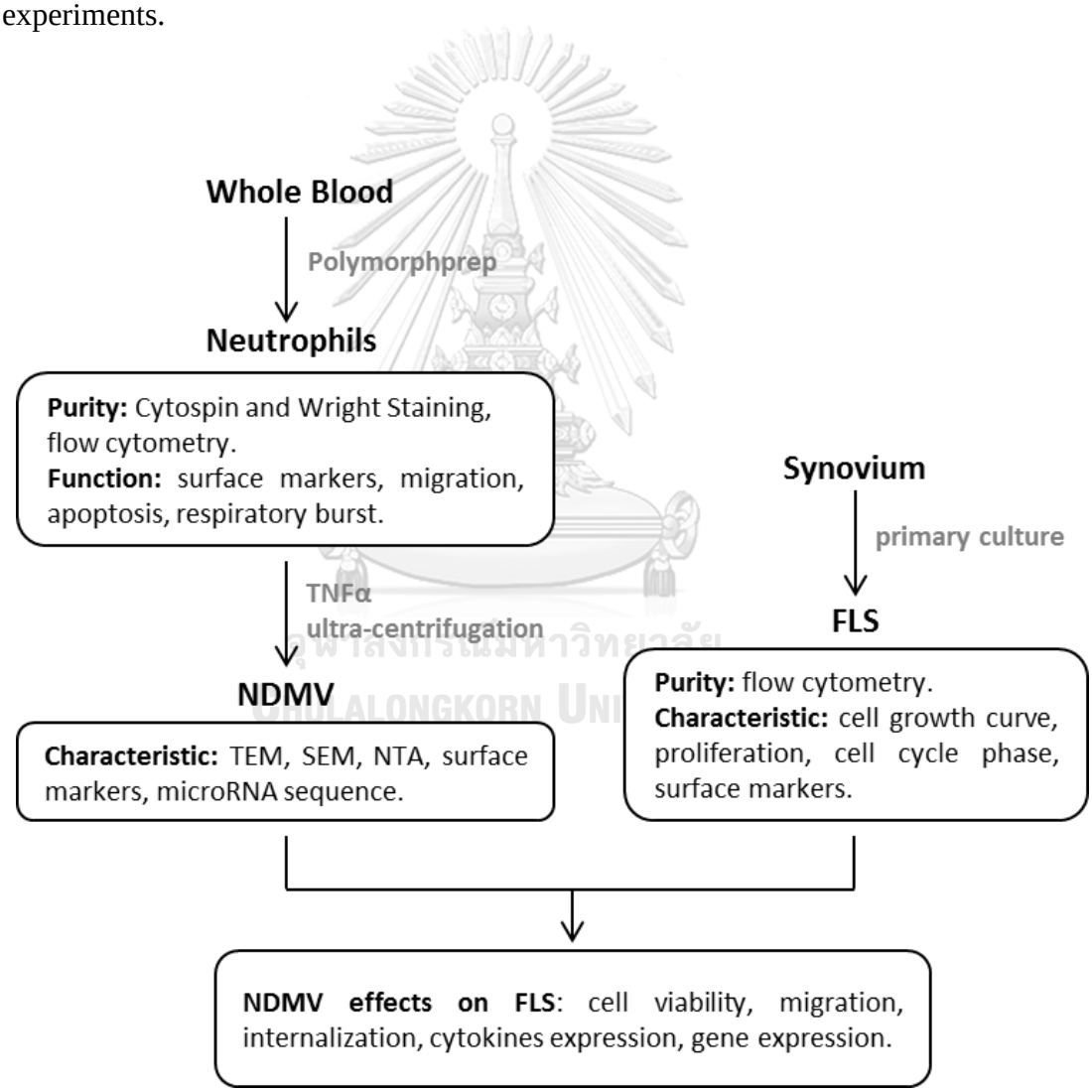

Figure 2. Flowchart of experiment design. This research work consists neutrophils, FLS and NDMV isolation and detection, and NDMV effects on FLS.

1.4 Hypothesis

- FLS cultured *in vitro* maintain their capabilities of proliferation and inflammatory response.
- Neutrophils remain functional and non-apoptotic after treatment by high-dose and short -term exposure to TNFα prior to generation of NDMV.
- NDMV are loaded abundant microRNAs that are different to those expressed in intact neutrophils.
- FLS internalize NDMV to suppress inflammatory cytokine secretion via packaged microRNAs regulating post-transcription regulation of the PI3K-AKT and MAPK signaling pathways.

Chapter 2. BACKGROUND AND LITERATURE REVIEW

Arthritic conditions are characterized by joint pain and loss of function and can be categorized into more than 100 different types. Redness, swelling, heat, pain and dysfunction are five major clinical components of arthritis. Osteoarthritis (OA) and Rheumatoid Arthritis (RA) are the two most prevalent types of arthritis and affect both males and females. Although OA and RA have some similarities in symptoms and signs, their etiologies, diagnosis and therapies are very different. The aetiology of OA has not been fully elucidated. It has traditionally been thought to be caused by mechanical wear and tear on overloaded or overused joints, resulting in cartilage damage. In contrast, RA is an autoimmune disorder, where the immune system mediates damage to joints and other organs in the absence of infection. Despite extensive ongoing research worldwide, the full etiologies of these disease, and hence the most effective treatments for these important conditions remain only partly known.

2.1 Osteoarthritis (OA)

OA was first described over 230 years ago. In 1782, William Heberden (1710–1801), a physician of the United Kingdom (UK), recorded symptoms and described the OA "Digitorum Nodi" which were later renamed Heberden's nodes (Dequeker and Luyten, 2008). In 1859, the term RA was proposed by Alfred Baring Garrod who considered OA and RA to be two different diseases. In 1987, the American College of Rheumatology (ACR) defined OA as "a heterogeneous group of conditions that lead to joint symptoms and signs, which are associated with defective integrity of articular cartilage, in addition to related changes in the underlying bone at the joint margins" (Arnett et al., 1988).

OA is recognized as a joint disease caused by articular cartilage loss in focal areas in synovial joints. It is associated with articular bone and capsule pathological changes: osteophytes, subchondral bone sclerosis, capsule thickening, etc. Both

weight-bearing joints (coxafemoral, tibiofemoral, talocrural, and intervertebral joints) and non-weight-bearing joints (interphalangeal joints of fingers or toes, etc.) can be affected. Histologically, cartilage is a type of connective tissue without vessels and nerve supply, therefore, the shortage of oxygen and nutrients attenuates the viability of chondrocytes and their potential for tissue repair. The clinical manifestations of OA include pain or tenderness, crepitus and limitation of movement in affected joints.

2.1.1 Risk factors of OA

Although the pathogenesis of OA is still unclear, its risk factors are known to be multifactorial. It is distinguished from other types of arthritis by massive loss, and failure of cartilage restoration. Multiple factors can contribute to accelerated cartilage damage and impaired cartilage repair. Systematic factors include ageing, gender, genetics, nutrients, bone density, smoking, etc. and local factors include occupation, biomechanical stress, trauma, muscle strength, inflammation, infection, manual labor, etc. (Garstang and Stitik, 2006). Ageing is a major factor in OA (Valdes and Stocks, 2018, Sacitharan, 2019). The disease progresses gradually and methods to reverse this joint destruction have yet to be discovered. Current treatment therefore focuses on symptomatic care with physiotherapy or painkillers leading to joint replacement surgery where required.

2.1.2 Categories of OA

OA is categorized into two types: primary and secondary, according to the classification of OA causes (Doherty et al., 1983). Primary OA is also called idiopathic OA, as no definite cause has yet been identified. It could be caused by natural ageing of the musculoskeletal system and appears to have families- and genetic-predispositions. Primary OA can be subdivided into common nodal OA occurring in most synovial joints and the less frequent erosive OA in distal interphalangeal joints. Multiple factors appear to underlie secondary OA, including joint trauma and/or infection, congenital deformity, metabolic disorders, systemic diseases, vocations, etc. In comparison to primary OA, secondary OA is linked more closely with known underlying causes.

2.1.3 Epidemiology of OA

Osteoarthritis is the third most frequent diagnosis made by general practitioners among older adults. It not only causes pain, but it also reduces the quality of life. As

OA progresses, patients may have to adapt to the disability resulting from reduced joint function. According to the World Health Organization (WHO), approximately 9.6% of male adults over 60 years old report OA-related symptoms, with a 2-fold higher prevalence in females (Woolf and Pfleger, 2003). The prevalence of OA is high across the world. In the United States (US), the National Institutes of Health (NIH) reported that there were about 40,000,000 individuals with OA in in 2008, and this was predicted to rise by 20,000,000 some twenty years later (Lawrence et al., 2008). OA symptoms in the knee are reported by 15% of Americans over the age of 60 years (Jordan et al., 2007). Versus Arthritis, the largest charity for arthritis research and care in the UK, reported that one fifth adults over the age of 45 suffered from knee OA in England. They estimate the prevalence rate of knee OA is therefore 15% to 21% of the population in England (Versus Arthritis, 2013).

In general, the prevalence of knee OA was reported as 7.9% in Asia, with some variation between countries. The incidence of knee OA was 7.5% in mainland of China, while in Thailand, researchers investigated rural regions by questionnaire and reported that the prevalence of OA was 11.3% (Chaiamnuay et al., 1998). Furthermore, there is a contrast between rural and urban regions: 13.7% of symptomatic knee OA in rural areas, compared to 6.0% in urban areas (Fransen et al., 2011). The difference in prevalence of OA with gender and age are well known. For example, the incidence of OA in females from 65 to 74 years constitutes the highest incidence with 1.4% diagnosed per each year while for men, over 75 years, it the incidence of OA is about 0.9% per year (Woolf and Pfleger, 2003). This positive correlation between age and incidence of OA is similar worldwide (Woolf and Pfleger, 2003, Sacitharan, 2019). In Queensland, Australia, researchers found that the incidence of primary OA was 88% in female OA patients. In contrast, the incidence of secondary OA was greater in male patients at roughly 82% (Cooper et al., 2013).

2.1.4 Diagnosis of OA

According to the diagnostic criteria from the American College of Rheumatology in 1986, knee OA is diagnosed by clinical manifestations, radiographic features and laboratory tests (Altman et al., 1986). Therefore, a diagnosis of knee OA is made from a combination of clinical, radiographic and laboratory examinations. Table 1-3 shows the diagnostic process for this diagnosis.

Table 1. Clinical diagnosis criteria of knee OA based on ACR.

If 1 plus at least 3 items from 2-7 are present:
1. Knee pain for most days of previous month
2. Crepitus on active joint motion
3. Morning stiffness lasting 30 min or less
4. Age 50 years or older
5. Bony enlargement of the knee on examination
6. Bony tenderness
7. No palpable warmth

Table 2. Clinical and radiographic diagnosis criteria of knee OA based on ACR.

If 1 and 2 plus at least 1 item from 3-6 are present:
1. Knee pain for most days of previous month
2. Osteophytes at joint margins on radiographs
3. Age 50 years or older
4. Crepitus on active joint motion
5. Morning stiffness lasting 30 min or less
6. No palpable warmth

The severity of knee OA is evaluated by the Kellgren-Lawrence (KL) Grading System according to X-ray images conducted by radiologists. Grade 1 to 4 is used to quantify each knee of each OA patient (Table 4). However, the ACR criteria are not reliable to confirm non-serious OA at an early stage but it has advantages for the identification of advanced OA stages with later findings (Peat et al., 2006).

Table 3. Clinical and laboratory diagnosis criteria of knee OA based on ACR.

If 1 plus at least 5 items from 2- are present:
1. Knee pain for most days of previous month
2. Crepitus on active joint motion
3. Morning stiffness lasting 30 min or less
4. Age 50 years or older
5. Bony enlargement of the knee on examination
6. Bony tenderness
7. No palpable warmth
8. Erythrocyte sedimentation rate (Westergren) < 40mm/h
9. Rheumatoid factor < 1:40
10. Synovial fluid signs of OA: clear, viscous or white blood cell count < 2 cells/ml

Table 4. The Kellgren-Lawrence Grading System on X-ray examination.

Grade 1: Unlikely narrowing of the joint space, possible osteophytes.
Grade 2: Small osteophytes, possible narrowing of the joint.
Grade 3: Multiple, moderately sized osteophytes, definite joint space narrowing, some sclerotic areas, possible deformation of bone ends.
Grade 4: Multiple large osteophytes, severe joint space narrowing, marked sclerosis and definite bony end deformity.
Note: Joint space narrowing-bone is visible on X-ray but the articular cartilage that covers it is not; a normal joint therefore appears to have a space between the bones; any decrease in space implies a reduction in cartilage cover. Osteophytes is small bony projections that form around joint margins, that are responsible for limiting the range of motion and can cause of pain. Sclerosis, defined as pathological "hardening" and is a sign of osteoarthritis, seen as increased white areas in the bone at the joint margins.

2.1.5 Treatment of OA

OA is a condition still lacking effective treatments that can target the underlying problem. Pain and stiffness are prominent symptoms OA and relieving these symptoms to maximise quality of life, underpins all therapeutic strategies. Pharmacological treatments focus on analgesia and acetaminophen (paracetamol) is recommended to control moderate pain (Zhang et al., 2007) while non-steroidal anti-inflammatory drugs (NSAID) are also often used, but can produce side effect such as gastric ulcer, hepatotoxicity, bleeding (Osani et al., 2019). For surgical treatment, intra-articular corticosteroid or hyaluronic acid injection may reduce knee pain and lubricate joint movement. Synovial excision may decrease synovial inflammation and joint pain, when coupled with intra-articular lavage. Tibial wedge osteotomy is a potential option for some patients who have a relatively small varus angulation (less than 10 degrees) and stable ligamentous support. Joint replacement/arthroplasty is an effective treatment for OA patients with severe manifestations or disability, particularly in the knee. Physical therapy can help to improve muscle strength, stabilize the joint and hence decrease pain. Other conservative therapies include acupuncture, electrotherapy and ultra-sonic therapy. Intraarticular mesenchymal stem cell (MSC) injection has the potential has the potential to help repair cartilage and reduce pain (Mancuso et al., 2019). but as yet there is insufficient data to support its use. Knee joint distraction is new therapy that has the potential to decrease cartilage physical stress. One study reports joint function was improved and pain was relieved effectively by this technique (Takahashi et al., 2019).

2.1.6 Synovitis of OA

Cartilage loss is a well-known feature of OA. However, inflammation is also becoming recognized to be an important factor. Synovial inflammation/synovitis in OA has been shown by histological, radiographic and arthroscopic examinations (Guermazi, 2019, Rein et al., 2019). Such synovitis is related to the clinical manifestation, joint structure changes and likely contributes to the pathophysiological process. A previous study has reported that whilst synovitis is often present in patients with early OA, it was not apparent in advanced disease (Haywood et al., 2003). Different grades of synovitis, from mild to moderate, were observed in OA histological samples on microscopy. Magnetic resonance imaging (MRI) and

ultrasound Doppler have confirmed synovitis in early stage of OA, consistent with inflammatory findings on histology (Pearle et al., 2007, Guermazi, 2019, Sarmanova et al., 2016) and radiographic severity of X-ray. In a cross-sectional study, investigators found that the Odds Ratio (OR) of synovitis score on contrast-enhanced MRI increased with Kellgren & Lawrence (KL) grades in knee OA patients (Guermazi et al., 2014). In the rabbit OA model, researchers found that the severity of OA caused by meniscectomy could be worsen with synovitis induced by calcium pyrophosphate dihydrate (Fam et al., 1995).

2.2 Rheumatoid Arthritis (RA)

RA is common type of arthritis, caused by an autoimmune mediated chronic inflammation of joints. It is also a systematic disorder that can cause problems in extra articular areas including the lungs and cardiovascular system. RA typically affects the small synovial joints in the hands or toes, such as the metacarpophalangeal (MCP) and proximal interphalangeal (PIP) joints, but other synovial joints such as in the in the upper and lower limbs are also often affected.

The pathogenesis of RA appears to involve multiple factors that include abnormal immunity, genetic background and smoking. Before syndromes and signs commence, the immune system of RA patients may show some differences from those of healthy control individuals. Anti-citrullinated protein antibodies (ACPA) and rheumatoid factor (RF) can be detected more than 10 years prior to the onset of symptoms (Wegner et al., 2010). The epitope of ACPA recognizes exo- or (modified) endogenous antigens to form circulating soluble antigen-antibody immune complexes, which may combine with RF to promote their activity (Arend and Firestein, 2012). These antigen-antibody complexes can stimulate innate immunity in the synovium and cause inflammation. Synovitis increases vascular permeability to recruit more inflammatory cells and produce more inflammatory cytokines in the synovial fluid (SF). The greatest genetic susceptibility to RA is located within the class II major histocompatibility complex (MHC) (Okada et al., 2014).

2.2.1 Risk factors of RA

What causes RA is also still unclear, but multiple factors are likely to be involved. A case-control study reported that up to 40% of descendants could inherit RA related

genes from their parents (Frisell et al., 2013). Researchers also found that the risk of inheriting RA from a parent who is RF/ACPA positive rises to 50%". Patients with RF/ACPA+ RA tend to present at an earlier age than those without. Multiple gene loci are confirmed to be risk factors: these include human leukocyte antigen (HLA)-DRB1, STAT4, TRAF1, FOXO3, etc. (Gregersen et al., 1987, Kurreeman et al., 2007, Mohamed et al., 2012, Lee et al., 2013). Age and gender are other risk factors. The incidence of RA is increased two fold in females compared to males (Myasoedova et al., 2010). Environmental risk factors, such as smoking induced citrullination of protein, also play role in RA occurrence (Tobón et al., 2010).

2.2.2 Categories of RA

According to the classification criteria established by the American College of Rheumatology and European League Against Rheumatism (EULAR), RA can be categorized into 3 types/phase depending upon disease progress (Aletaha et al., 2010a). These are: Phase 1/Early RA: clinical manifestation and laboratory examination that supports RA diagnosis and the presence of early synovitis; Phase 2/Developing RA: considering clinical and laboratory results to deduce RA and the possibility of developing possibility-constant inflammatory or erosive arthritis; Phase 3/Definite RA: integrating information of Phase 1 and 2 to improve grading system and confirm RA.

2.2.3 Epidemiology of RA

In a Global Burden of Disease 2010 study, the incidence of RA was estimated to be around 0.24% worldwide (Cross et al., 2014), while in an earlier study, the incidence of RA was considered to be higher, between 0.4-1.3% (Felson, 1990). The reasons for this apparent decline in RA prevalence over time are unclear. In developed countries, the RA prevalence rate ranges from 0.5% to 1% in adults (Gabriel and Michaud, 2009). In Woolf and Pfleger's study, it appears to be the prevalence of RA in developing countries that was higher than that of developed countries in the populations <60 years old. However, individuals > 60-years of age from developed countries had higher RA prevalence than developing countries (Woolf and Pfleger, 2003). In the UK, the prevalence of RA is 1.16% in UK females and 0.44% in UK males, while in Asian countries, RA prevalence is 0.2-0.93% in mainland China, and 0.12% in Thailand (Chaiamnuay et al., 1998, Zeng et al., 2008).

2.2.4 Diagnosis of RA

RA diagnosis is currently based on the 2010 ACR/EULAR classification criteria. The scoring system includes clinical features, serology, duration of symptoms and laboratory examination. A total score equal or greater than 6 suggests RA (Table 5).

Table 5. The ACR and EULAR classification criteria for RA.

Joint distribution (0–5 points) Points	**points**
Joint involvement: Any swollen or tender joint (excluding DIP of hand and feet, 1st MTP, 1st CMC) or additional evidence from MRI/ultrasound may be used to identify additional joints (include: temporomandibular, sternoclavicular, acromioclavicular, and others as reasonably expected in RA).	
1 large joint (shoulder, elbow, hip, knee, ankles)	0
2–10 large joints	1
1–3 small joints (MCP, PIP, MTP 2–5, thumb IP, wrist); large joints not counted Does not include: DIP, 1st CMC, 1st MTP	2
4–10 small joints (large joints not counted)	3
<10 joints (at least one small joint)	5
Serology (0–3 points)	**points**
Serology: Negative: ≤ULN (for the respective lab), Low positive: >ULN but ≤3×ULN, High positive: >3×ULN Where RF is only available qualitatively, a positive result should be scored as 'low-positive' for RF	
Negative RF and negative ACPA	0
Low positive RF or low positive ACPA	2
High positive RF or high positive ACPA	3

These criteria permit an earlier diagnosis of RA compared to previous ones. The following steps are suggested as an approach to the evaluation of patients with early RA (Table 6).

Continued Table 5.

Symptom duration (0–1 points)	**points**
Symptom duration refers to the patient's self-report on the maximum duration of signs and symptoms of any joint that is clinically involved at the time of assessment.	
<6 weeks	0
≥6 weeks	1
Acute phase reactants (0–1 points)	
Normal CRP and ESR	0
Abnormal CRP or abnormal ESR	1
Normal/abnormal ESR/CRP is determined by local laboratory standards	
Score ≥6 is classification of RA	**Total:**
A score of 6/10 needs to be achieved from four domains including: Joint activity (0–5 points), serology (0–3 points), symptom duration (0–1 point), and acute phase response (0–1 point). ACPA, anti-citrullinated protein/peptide antibodies; CRP, C-reactive protein; DIP, distal interphalangeal; ESR, erythrocyte sedimentation rate; MCP, metacarpophalangeal; MTP, metatarsophalangeal; RF, rheumatoid factor; ULN, upper limit of normal.	

Table 6. Approaches to early RA diagnosis.

• Recognize the presence of inflammatory arthritis.
• Exclude diseases other than RA or UA (undifferentiated arthritis) that present as an early inflammatory arthritis (e.g. SLE, psoriatic arthritis, or other spondyloarthropathy).
• Estimate the risk of developing persistent or erosive irreversible arthritis in patients with RA or UA by using a combination of clinical features, laboratory tests and imaging techniques.

2.2.5 Treatments of RA

Nowadays, the optimal strategy to manage RA, accepted by most Rheumatologists, includes early detection, early diagnosis and early treatment. The goal of RA

treatment is to suppress the underlying inflammation and hence reduce symptoms and prevent irreversible joint damage. Therefore, RA management encourages more dynamic use of medication (Guidelines, 2002). Treatment normally starts with a synthetic DMARD, typically methotrexate as soon as possible after diagnosis (Aletaha et al., 2010b). Other DMARDs such as Leflunomide and hydroxychloroquine can also be used (Ruderman, 2012). Failure of or intolerance to these conventional synthetic DMARDs can allow the subsequent use of a biologic or targeted synthetic DMARD (Salt and Crofford, 2012).

2.2.6 Synovitis of RA

Synovitis is a key feature in RA which if untreated, this can lead to destruction of adjacent tissues including cartilage and bone. The arthroscopic appearance of inflamed RA synovium shows hypergenesis of synoviocytes and capillary vessels that form a pannus (Orr et al., 2017). Histologically, inflammatory cells including macrophages, neutrophils, and lymphocytes infiltrate intimal and sub-intimal layers (Tak et al., 1997). The resulting pannus damages adjacent cartilage and bone, with ultimate destruction of the joint (Mullan et al., 2007) and destructive changes observed by imaging (Tak et al., 1997, Orr et al., 2017, Van der Heijde, 1996).

2.3 Heterogeneity of OA and RA synovitis

2.3.1 Synovium

Synovial joints are composed of a joint cavity, cartilage of adjoined bone and articular capsule. The synovial membrane/synovium comprises the inner layer of the capsule and contains an intimal layer and subintimal layer. The intimal layer is 20-40μm thick and borders the joint cavity. The subintimal layer, approximately 5mm thick is classified into three types: areolar, adipose and fibrous (Figure 3A) (Prieto-Potin et al., 2015). The intimal layer of synovium is composed of two diverse cells: Type A and B (Figure 3B) (IWANAGA et al., 2000).

Type A/Macrophage-like synoviocytes (MLS) originate from monocytes or macrophages from the circulating bloodstream (Smith, 2011). They are CD168+ and CD68+ cells, with increased activity of non-specific esterase and they possess high expression of immunoglobin receptor FcγRIIIa (Orr et al., 2017). Although MLS proliferation is low in the intimal synovium, these cells still have the ability of

phagocytosis (Bartok and Firestein, 2010). Type B/Fibroblast-like synoviocytes (FLS) originate from local tissue to produce synovial fluid and its components. The synovium is responsible for supplying metabolites and oxygen to chondrocytes for producing cartilage through secretion of SF, together with removing metabolic waste, carbon dioxide and degraded matrix. Hyaluronic acid and lubricin, secreted by FLS, can diminish the friction among focal areas of articular cartilages. Abnormal synovium, usually caused by inflammation, cannot maintain the homeostasis of joint environment leading to loss of the joint function.

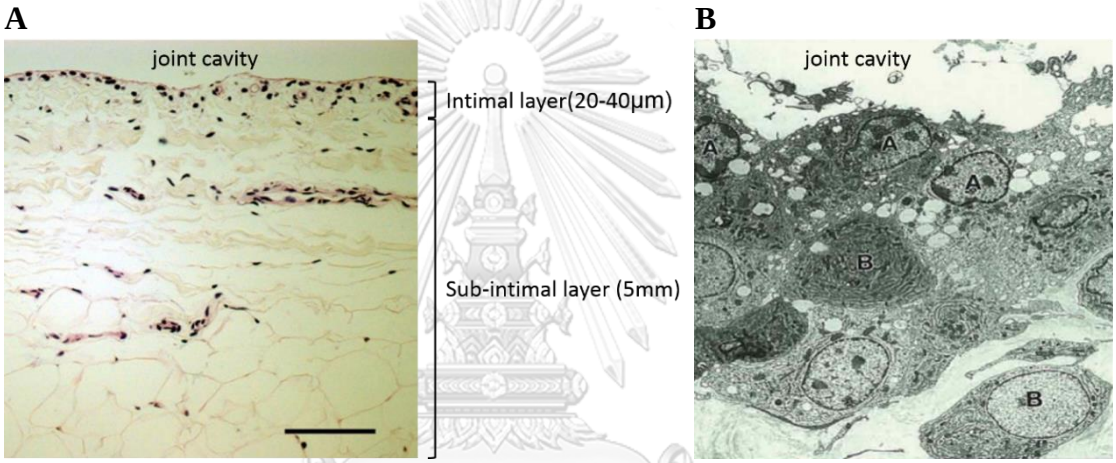

Figure 3. Images of synovium layers and cellular types in the intimal layer of synovium, reproduced from the ectoderm. (A) Synovium two layers and their thickness (Prieto-Potin et al., 2015). Scale bar: 100μm. (B) Electron-microscopic image of cellular types in the intimal layer of synovium (IWANAGA et al., 2000). ×2,800 magnification. A, type A synoviocytes; B, type B synoviocytes.

2.3.2 Low- and high-grade synovitis of OA and RA

OA is an articular disease with low-grade synovitis with extensive publications have documenting synovial inflammation in OA (De Lange-Brokaar et al., 2012, Lana and Rodrigues, 2019). In Hematoxylin and Eosin (HE) stained slides of OA synovium, the intimal layer contains hyperplasia of synoviocytes. Meanwhile, capillary proliferation is observed in the sub-intimal layer. Simultaneously, inflammatory cells infiltrate into the synovium of both OA and RA, and release cytokines to regulate local

inflammation. Synovitis of OA is much less extensive than that found in RA, but greater than in normal healthy joints.

2.3.3 Synovitis score of OA and RA

Synovitis evaluation systems are widely used to score the severity of synovitis in arthritis. The most popular is Krenn's Scoring System that includes the thickness of the intimal layer, cells number in synovial stroma and inflammatory cells number (Krenn et al., 2006). Table 7 illustrates the synovitis comparison among control (C), OA and RA. It is noticeable that the synovitis score of OA (mean range 2-3) is higher than that of healthy controls (mean<1.5), but much less than in RA (mean>5). In the Prieto-Potin *et al.* study, the OA group was divided into two sub-groups: non-inflamed (score range 0-1) and inflamed (score range 2-3) OA (Prieto-Potin et al., 2015). Synovitis was not present in all OA patients, but was present at high grade in each RA specimen.

2.3.4 Synovitis with infiltrated cells of OA and RA

The number of infiltrating inflammatory cells in normal control was less than in OA, which in turn was less than in RA. Most researchers report that the major cell type infiltrated into the synovium of both OA and RA were macrophages and T cells. Compared with infiltrated macrophages that infiltrated into the RA synovium, macrophages infiltrated into OA synovium possess higher ability to perform phagocytosis (Wood et al., 2019). Although T cells accumulated in the synovium of OA and RA, the CD4+/CD8+ T cell ratio was 2-2.5 in OA and 10-100 in RA (Steiner et al., 1999).

Table 7. Summary of synovitis score and infiltrated cells in the sub-intimal layer in comparison of normal control (C), OA and RA.

Sample (size)	Specimen	Evaluation	Findings	Ref.
C(5), OA(8), RA(16).	Arthroscopy, arthroplasty.	HE, IHC	T cells in synovium: C: 4, OA: 6; RA: 16; B cells in synovium: C: 1, OA: 1, RA: 0; Macrophages in synovium: C: 5, OA: 7, RA: 13.	(Smith et al., 1992)
C(5), OA(5), RA(5)	Arthroplasty	HE, IHC	Moderate/abundant mononuclear cells, few giant cells in synovium of OA and RA; No difference between OA and RA in infiltrated cells types.	(Furuzawa-Carballeda and Alcocer-Varela, 1999)
C(9), OA(12), RA(10)	Arthroscopy, biopsy.	HE, IHC	Infiltrated cells: T cells: C<OA<RA; B cells: C<OA<RA; Plasma cell: C<OA<RA; phagocyte: C<OA>RA; detritus-rich in OA and its synovium infiltrated with neutrophils and multinucleated giant cells.	(Oehler et al., 2002)
C(49), OA(212), RA (246)	Synovectomy	Krenn's Synovitis score	Synovitis score: C: 0.77, OA: 2.45; RA: 5.13	(Krenn et al., 2006)
C(9), OA(12), RA(10)	Arthroscopy, arthroplasty	Krenn's Synovitis score, HE	Synovitis score: C: 1.38, OA: 2.6; RA: 6.0; More T cells, B cells and microphages infiltrate in synovium of RA.	(Diaz‐Torne et al., 2007)

Continued Table 7.

Sample (size)	Specimen	Evaluation	Findings	Ref.
C(10), OA(25), RA(28)	Arthroscopy, arthroplasty	Krenn's Synovitis score, HE, IHC	Synovitis score: C: 1.38, OA: 2.23, RA: 5.74; Infiltrated cells: T cells: C: 27.7, OA: 67.2, RA: 552.9; B cells: C: 2.3, OA: 16.5, RA: 251.4; Plasma cells: C: 0.3, OA: 23.3, RA: 625.5; Macrophages: C: 8.2, OA: 19.3, RA: 26.9.	(Pessler et al., 2008b)
C(33), OA(221), RA(341)	Synovectomy	Krenn's Synovitis score, HE	Synovitis score: C: 0.50, OA: 2.0; RA: >4.	(Slansky et al., 2010)
OrthA(15), OA(14), RA(69)	Needle biopsy	Krenn's Synovitis score, HE, IHC	Synovitis score: OrthA: 2, OA: 3, RA: 4; Infiltrated cells: T cells: OrthA: 13.2, OA: 113.2, RA: 578.9; B cells: OrthA: 15.8, OA: 18.4, RA: 384.2; Plasma cells: OrthA: 21.1, OA: 21.1, RA: 600.0; Macrophages: OrthA: 48.0, OA: 30.0, RA: 530.3.	(Mo et al., 2011)
C[#](21), OA(42), RA(21)	Arthroplasty	Krenn's Synovitis score, HE, IHC	Synovitis score: C/OANI < OAI <RA; Infiltrated cells: MGC+ synovium%: C/OANI < OAI <RA; MGC diameter: OA<RA; Priority MGC types: OA: Langhans-like; RA: Langhans-like and Foreign body-like.	(Prieto-Potin et al., 2015)

Continued Table 7.

Types (size)	Specimen	Evaluation	Findings	Ref.
Note: C is control; OrthA is orthropathy arthritis; OANI is OA with non-inflammation; OAI is OA with inflammation; MGC is multinucleated giant cells; # means controls from post-mortem (PM).				

Similarly, the ratio of Th1/Th2 was higher in RA (6.1) than in OA (1.5) (Yudoh et al., 2000). B cells and plasma cells were the minority cell types in OA and RA synovium, and their numbers were greater in RA (Pessler et al., 2008a). Neutrophils were rarely found in OA, but were one of the most abundant cells in synovial fluid (SF) of RA (Tak et al., 1997, Pessler et al., 2008b, Saito et al., 2002). When plentiful detritus existed in OA, neutrophils and multinucleated giant cells (MGC) would accumulated in the synovium (Oehler et al., 2002). Natural killer (NK) cells and dendritic cells (DC) also were found in OA and RA synovium, but the numbers were lower than neutrophils and MGC (Pettit et al., 2001). More and more highly active NK cells were detected in synovial fluid of RA (Yamin et al., 2019), while mast cells and adipocytes of synovitis were fewer in OA than RA (Gotis-Graham and McNeil, 1997, Shanaj and Donlin, 2019).

Synovitis also is also detectable in other forms of inflammatory arthritis including psoriatic arthritis, juvenile idiopathic arthritis and Lyme arthritis (Moll et al., 2009, Collado et al., 2013, Jutras et al., 2019).

2.4 Extracellular vesicles

There has been an increasing interest over past decades in extracellular vesicles (EV) originating from various cells. EV are released from cells and are comprised of cellular membranes (including membrane proteins) together with plasma protein, nucleic acid, and carbohydrates. EV are considered as the transportable packages, transferring information from donor cells to target cells. The physiological and pathological features of recipient and donor cells can be influenced during EV release and subsequent internalization. EV are vesicles with a phospholipid bilayer released

by conserved methods from prokaryotes, eukaryotes and plant cells. Over the years, interest in EV in the literature has grown exponentially (this data website link is https://academic.microsoft.com/topic/2992929900), especially after 2012 (Figure 4).

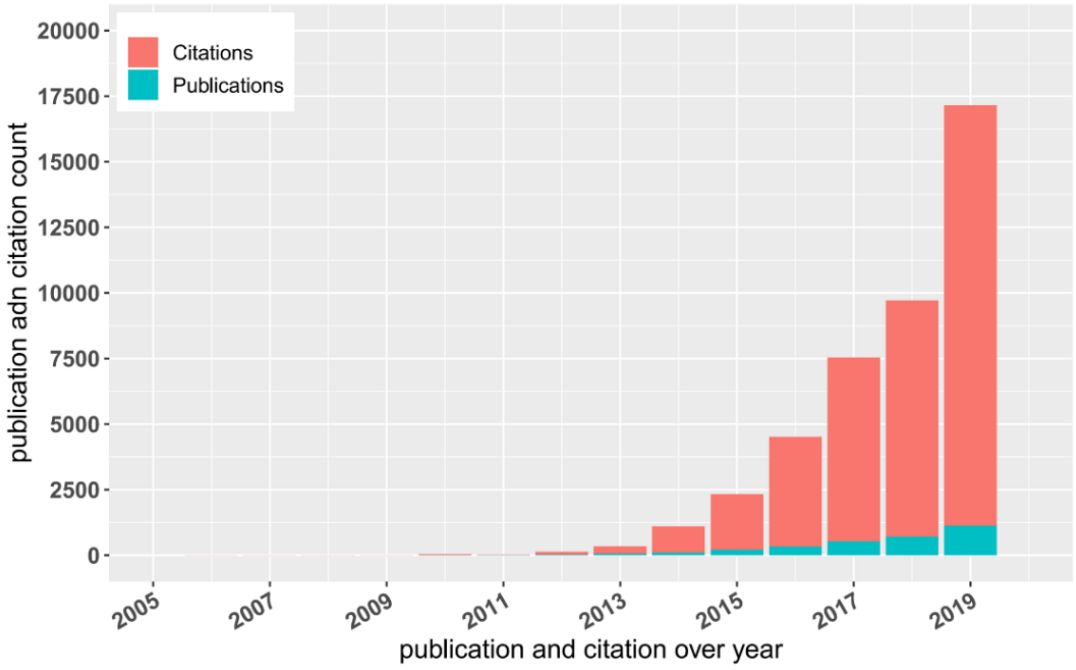

Figure 4. Publication and citation of EV related research and review papers from 2005 to 2019.

2.4.1 EV classification

The EV family has been expanded from classically-defined EV (exosomes (Exo), microvesicles (MV), apoptotic bodies (AB)) to large oncosomes (released by cancer cells). The assembly mechanisms of these different family members are essentially different. Exosomes are produced by inward budding of cellular membrane to initially form endosomes, which then generate multivesicular bodies (MVB) to fuse with phospholipid membranes (Cocucci and Meldolesi, 2015). MVB are released by exocytosis into the intercellular space. Exosomes range in size from 50-100 nm. After appropriate stimulation, they are released by outward budding. Their diameter is 100/200-1000 nm. AB are produced by apoptotic cells and their size is 800-5,000nm. The diameter of oncosomes is larger than other EV at approximately 20μm

(Crescitelli et al., 2013, Meehan et al., 2016). The different characters of Exo and MV are illustrated in Table 8.

Table 8. Different and analogous properties of microvesicles and exosomes.

Property	**Microvesicles**	**Exosomes**
Assembly manner	Outward budding	MVB
Size (nm)	100-1,000	50-100
Protein (membrane and plasma)	High	Low
RNAs	+	Low
DNA	N/A	N/A
MVB exocytosis	N/A	High
Releasing time	Seconds	Delayed
Fusion with target cells	+	+
membrane fusion with target cells	+	+
Endocytosis by target cells	+	+
Navigation of EV mixtures	+	+
Diagnosis and therapy	+	+

2.4.2 MV in OA and RA

EV can be detected by electron microscopy (EM) and nanoparticle tracking analysis (NTA) SF of both OA and RA. Isolated EV are composed of Exo and MV and the mean of total EV protein in OA was 0.14mg/ml which was less than RA (0.88mg/ml) (Gyorgy et al., 2012). SF EV from OA and RA contained abundant proteins originating from cellular plasma, such as albumin, actin, and myosin, and also clusterin in SF of OA and RA patients (Gyorgy et al., 2012) . However, protein types and compositions were not merely different in OA and RA (Gyorgy et al., 2012). It was found that CD3 and CD8 were expressed at significantly higher levels in RA EV than in OA EV. While Annexin V, CD4, CD14, CD19, CD41a and RANK, RANKL were found at higher levels in RA EV than in OA EV, these differences were not significant (Gyorgy et al., 2012). It was also found that MV were generated by granulocytes and monocytes in RA SF, platelet-derived MV predominated in RA

plasma. Other investigators have reported that platelet-derived MV are increased in RA blood and correlated positively with RA disease activity score 28 (DAS-28) (Knijff-Dutmer et al., 2002). In contrast, Headland *et al*. reported that MV from RA SF expressed higher levels of Annexin A1, CD66b, CD14 and CD3 than plasma MV. In fact, annexin A1+ MV also expressed the neutrophil marker CD66b indicating that the MV were generated from neutrophils in RA patients (Headland et al., 2015).

2.4.3 MV impact on FLS

In an *in vitro* study, MV generated from T cells and monocytes could increase expression of MMP-1, 3, 9 and 13 by FLS, regulated in a time-dependent manner (Distler et al., 2005a) These MV also up-regulated cytokines (IL-6, 8) and monocyte chemoattractant protein (MCP) 1 and 2 of FLS derived from OA and RA synovial membranes. When FLS were pre-treated with receptor antibodies to IL-1β and TNFα receptor antibodies, MV still could promote MMP1 and IL-6 expression (Distler et al., 2005a). Furthermore, T cells and monocytes derived MV elevated cellular mediators (CXCL-1, CXCL-2, CXCL-3, etc.) which could pro-angiogenic function in FLS to improve hypervascularity of the synovium. In addition, MV either up-regulated these mediators and improve immigration of the endothelial cells as well (Reich et al., 2011).

2.5 Neutrophil-derived microvesicles (NDMV)

2.5.1 Abundant NDMV in inflammatory sites

Although the lifespan of neutrophils is relatively short (Elbim et al., 2009), they are still the most abundant leukocyte type in circulation and are involved in innate immunity (Summers et al., 2010). NDMV are present in low concentrations in healthy blood/serum, but increase in inflammation (L Johnson et al., 2014). The majority of MV in the venous blood in healthy controls are platelet-derived, but NDMV will predominate at the foci of inflammation and infection. For instance, NDMV levels were increased 14 fold higher in blister induced by Cantharidin compared to levels in serum, but the number of neutrophils was 10 times less in blisters than in blood (Daniel et al., 2006, Dalli et al., 2013).

2.5.2 Proteins of NDMV

The NDMV diameter range is 100 to 1,000nm, as identified by EM, Nanoparticle Tracking Analysis (NTA) and flow cytometry. The common proteins expressed on NDMV include: phosphatidylserine and annexin A1 (Dalli et al., 2008). NDMVs also express identical membrane proteins as neutrophils: CD11b, CD62L, CD66b, CD18, CD55 and Fc receptors and also several neutrophil granule-proteins (Gasser et al., 2003, Dalli et al., 2013, Headland et al., 2015).

2.5.3 Stimulants for NDMV generation

NDMV can be generated *in vitro* by treatment with various agonists, cytokines, pathogens and proteins, such as *Mycobacterium tuberculosis*, *Staphylococcus aureus*, fMLP, LPS, IL-8, TNFα, anti-neutrophil cytoplasmic antibody (ANCA), nitric oxide, as well as ultraviolet light (Hong, 2018). Table 9 lists that various reagents that have been used to stimulate neutrophils to generate microvesicles after varying exposure times, concentrations and temperatures. Differential centrifugal force is frequently used to isolate microvesicles.

Table 9. Summary of used reagents, concentration and times to stimulate neutrophils to generate MV, and centrifuge force used for MV isolation.

No	Neutrophil (cells/ml)	Treatment			Isolation	Ref.
		Reagent	Conc.	Time		
1	20×10^6	TNFα	50ng/ml	20min	1) 13,000g, 4 ºC, 2min; AB. 2) 20,000g, 4 ºC, 30min; MVs. 3) 100,000g, 4 ºC, 60min; Exo.	(Rhys et al., 2018)
2	10^6	fMLP	0.5-1μM	20-30min	1) 13,000g, 4 ºC, 10min; CD. 2) 100,000g, 4 ºC, 60min; MVs.	(Finkielszstein et al., 2018)
		PMA	200nM	20-30min		
		IFNγ	100ng/ml	20-30min		

Continued Table 9.

No	Neutrophil (cells/ml)	Treatment			Isolation	Ref.
		Reagent	Conc.	Time		
3	20×10^6	fMLP	1μM	20 min	1) 3,000g, 4 °C, 10min; CD. 2) 100,000g, 4 °C, 60min; MV.	(Slater et al., 2017)
		PMA	200nM	20 min		
		latrunculin B + fMLP	1μM + 1μM	5min +15min		
4	10×10^6	PMA	10 nM	30min	1) centrifugal filter devices (10 kDa MWcutoff). 2) 160,000g, 4 °C, 40min; MV.	(Turbica et al., 2015)
5	9×10^6	opsonized S aureus	10^8/mL	20min	1) filtered through a 5-μmpore sterile filter (Sterile Millex Filter Unit, Millipore). 2) filtered fraction was sedimented again (15,700g, 4 °C, 10min; MV).	(Timar et al., 2013)
		PMA	100nM	20min		
		fMLP	1μM	20min		
		TNF	20 ng/mL	30min		
		LPS	100 ng/mL	120 min		
		CXCL-12	100 ng/mL	5 min		
		S aureus	10^8/mL	20min		
6	20×10^6	TNFα	50 ng/ml	20min	1) 13,000g, 4 °C, 2min; remove platelets. 2) 100,000g, 4 °C, 60min; MV.	(Headland et al., 2015)
		IL-8	50 ng/ml	2h		
		PMA	100 nM	4h		
7	5×10^6	LPS	100 μg/ml	2h	0.2 μm filtration and resuspended in the cell free plasma.	(Chen et al., 2015)
		PMA	1 μM	2h		

Continued table 9.

No	Neutrophil (cells/ml)	Treatment			Isolation	Ref.
		Reagent	Conc.	Time		
8	20×10^6	fMLP	1µM	30min	15,700g, 4ºC, 10min; MV.	(Pliyev et al., 2014)
		IL-8	20 ng/ml	30min		
		C5a	100 ng/ml	30min		
		zymosan	100 µg/ml			
		calcium ionophore	2 µM	20 min		
9	10×10^6	PMA	200 nM	30 min	100,000g for 45 min at 4°C. MV.	(Pitanga et al., 2014)
		LPS	10 µg/ml	2h		
		UV	N/A	20min		
10	20×10^6	fMLP	1µM	20min	100,000g, 4 ºC, 60min; MV.	(Dalli et al., 2014, Dalli et al., 2013, Dalli et al., 2008)
11	20×10^6	fMLP	1µM	20min	160,000g, 4 ºC, 45min; MV.	(Eken et al., 2013)
12	5×10^6	TNFα	2 ng/ml	15min	5000g, 4 ºC, 45min to remove cells and large debris then freeze.	(Hong et al., 2012b)
13	10×10^6	M. tuberculosis or M. bovis	10^7 bacilli/ml)	2h	100,000g, 4 ºC, 60min; MV.	(Duarte et al., 2012)
14	10^6	PMA	10nM	5min	N/A	(Gonzalez-Cano et al., 2010)

Continued Table 9.

No	Neutrophil (cells/ml)	Treatment			Isolation	Ref.
		Reagent	Conc.	Time		
15	10×10^6	fMLP	1μM	20min	concentrated with Centriprep centrifugal filter devices (MW10,000 cut-off; Millipore).	(Eken et al., 2010)
16	5×10^6	L-NAME	30μ mol/L	1h	100,000g, 4 ºC, 120min; MV.	(Nolan et al., 2008)
		D-NAME	30μ mol/L	1h		
		fMLP	10μmol/L	1h		
17	10×10^6	fMLP	1μM	20min	concentrated with Centriprep centrifugal filter devices (MW10,000 cut-off; Millipore).	(Gasser and Schifferli, 2004)
		C5a	100 ng/mL	20min		
18	10×10^6	fMLP	1μM	20min	concentrated with Centriprep centrifugal filter devices (MW10,000 cut-off; Millipore)	(Gasser et al., 2003)
		ionomycin	5μM	20min		
		PMA	10 nM	20min		
19	20×10^6	fMLP	0.1 μM/1μ M	15min	1) 200,000g, 4 ºC, 60min; MV.	(Hess et al., 1999)
		PMA	1 nM/10 nM	15min		
		ionomycin	0.5 μM/5μ M	15min		

Continued Table 9.

No	Neutrophils (cells/ml)	Treatment			Isolation	Ref.
		Reagent	Conc.	Time		
20	N/A	UV-B-irradiation	90mJ/cm^2	20min	1) 1.2 μm pore filter 2) 100,000g, 4 °C, 45min; MV.	(Shen et al., 2017)
21	9×10^6	fMLP	10 μmol/L	60min	1) 500g, 5min; 2) 1,500g, 5min; 3) 20,000g, 30min; MV.	(Ajikumar et al., 2019)

apoptotic bodies (AB); microvesicles (MV); exosomes (Exo); cell debris (CD); ultraviolet light (UV).

2.5.4 Effect of NDMV on target cells

NDMV can regulate cytokine and chemokine expression of target cells, but the precise response depends on the properties and functions of the recipient cells (L Johnson et al., 2014). NDMV stimulated the Mitogen-activated Protein Kinase/c-Jun N-terminal kinases 1 (MAPK/JNK1) signaling pathway of endothelial cells to produce IL-6, IL-8, MCP-1, adhesion molecule (Mesri and Altieri, 1999, Hong et al., 2012a). It has alos been reported that NDMV interacted with CD18 of endothelial cells to upregulate ICAM-1 and reactive oxygen species (ROS) (Hong et al., 2012a). Moreover, NDMV upregulate tissue factors to promote a procoagulant effect (Mesri and Altieri, 1999).

Previous studies have reported that NDMV can play an anti-inflammatory role. For endothelial cells, NDMV were able to decrease NF-κB, CCL8 and STAT1 levels in endothelial cells to inhibit pro-inflammatory responses (Dalli et al., 2013). NDMV could down-regulate inflammatory effects of macrophages via inhibiting phagocytosis and NF-κB activation, as well as promoting expression of lipid resolving factors (Eken et al., 2010). Other cytokines produced by macrophages also were down-regulated by NDMV, such as IL-8 and TNFα, but NDMV increased the expression of TGF-β1 that has an anti-inflammatory effect on macrophages (Gasser and Schifferli,

2004). Eken *et al*. demonstrated that NDMV could inhibit the macrophage inflammatory response via the PI3K/Akt pathway and MerTK (Mer-receptor tyrosine kinase) pathways (Cumpelik et al., 2016, Eken et al., 2010). Additionally, NDMV can also modulate phagocytotic function of monocyte-derived dendritic cells (DC) and up-regulate their TGF-β1 expression (Eken et al., 2008). IFN-γ and TNFα expressed by NK cells was blocked by co-culture with NDMV, despite TGF-β1 levels increasing in culture medium (Pliyev et al., 2014). Furthermore, neutrophil adherence and erythrocyte aggregation can be affected by NDMV through their expressed Annexin A1 and complement receptor 1 (Gasser and Schifferli, 2005, Dalli et al., 2008). NDMV interact with MerTK and Formyl Peptide Receptor (FPR)-2 of macrophage through their delivered phosphatidylserine and Annexin A1.

2.5.5 Relevant studies about NDMV effects on OA and RA

Exogenous NDMV are capable of decreasing IL-8 and prostaglandin E2 expression in chondrocytes (Headland et al., 2015). The consequences of this may be that inflammation is decreased and cartilage would be protected and restored, as well as gradually increasing the extracellular matrix of cartilage (Headland et al., 2015). The same research group identified that TNFα induced NDMV could modulate macrophages to affect FLS of RA. The TGF-β increasing of LPS induced macrophages, was enhanced by NDMV, while in contrast, up-regulation of cytokines (IL-1β, IL-10, IL-12), MHC II and CD86 of LPS induced macrophages was inhibited by NDMV. After FLS were co-cultured with NDMV-activated macrophages, the levels of IL-6, TNFα, MCP-1 and CD55 were all decreased (Rhys et al., 2018).

2.6 Summary

Low grade inflammation characterizes many forms of OA but the mechanisms responsible are not fully defined. NDMV have shown anti-inflammatory potential in some situations, but their role in down-regulating inflammatory responses of FLS from OA patients has not been reported. This thesis, therefore, aims to establish the effects of NDMV on FLS function and viability, and in particular to determine if they can down-regulate chemokine and cytokine expression from TNFα stimulated FLS isolated from OA patients.

Chapter 3. MATERIALS AND METHODS

Ethics

The thesis referred to research about human bio-specimens and personal information, therefore, this research proposal was submitted to the Institutional Review Board (IRB) of Faculty of Medicine, Chulalongkorn University. Ethics committee approved the proposal which was annotated as 565/59 to allow us to collect tissue and blood from patients and healthy volunteers. All processes were conducted in compliance with the guidelines of Declaration of Helsinki (7th version). All subjects gave written informed consent before participation.

Part A: FLS Culture and Testing

3.1 OA patients

The diagnosis of OA was based on the ACR criteria by surgeons from Department of Orthopaedics, Chulalongkorn Memorial Hospital. Patients with knee trauma, operation or history of other chronic inflammatory or immunological diseases were not included in this study. Fifteen knee OA patients were recruited to donate their synovium at the time of total knee replacement (TKR).

Synovium samples were saved in sterile collection bottles surrounded by ice and carried into cell culture room within 1h. Their age ranged from 58 to 81 with an average age of 70.33±1.81 (mean ± S.E.) years. There were 12 female patients with knee OA (~80%), and 3 knee OA patients were male (~20%). The average of Body Mass Index (BMI) was 25.56±0.92kg/m^2 over than the overweight criteria of 25 kg/m^2. BMI minimum of knee OA patient is 20.08 kg/m^2 of a female OA patient and maximum is 32.65 kg/m^2 of a female patient also. Two patients KL scores were highest to 4, but the severity of 10 patients were scored to 2. All patients bore different levels of pain from 3 to 9. Their pain average was 5.33±0.53 kg/m^2. Beside KL grading system was used to evaluate severity of knee OA by radiographic and symptomatic examination, Knee injury and Osteoarthritis Outcome Score (KOOS), Indices of Severity and disease activity for Osteoarthritis (ISOA) and Western Ontario and McMaster Universities Arthritis Index (WOMAC) were also utilized to evaluate pain, symptoms and joint function. The average of these three knee OA evaluation systems were 24.16±2.85, 13.27±0.64 and 156.80±12.54, respectively (Table 10).

Table 10. Basic characteristics of primary knee OA groups.

No.	Age (year)	Gender (F/M)	BMI (kg/m^2)	KL	VAS (0-10)	KOOS	ISOA	WOMAC
1	72	F	20.08	4	5	25.00	17	105.00
2	69	F	26.64	3	3	25.00	15	115.59
3	65	M	29.05	3	6	43.75	10	253.82
4	58	F	25.10	2	5	31.25	11	208.53
5	64	F	27.06	2	3	12.50	15	168.68
6	61	F	24.09	2	3	18.75	14	148.97
7	73	F	23.11	2	4	18.75	14	155.44
8	77	F	22.06	3	9	12.50	13	202.06
9	77	M	21.33	4	3	12.50	17	52.21
10	65	F	25.24	2	8	12.50	14	121.62
11	73	F	27.34	2	7	12.50	13	160.88
12	81	M	22.77	2	7	37.50	11	155.29
13	67	F	25.68	2	4	37.50	14	201.62
14	81	F	32.65	2	8	37.50	13	155.00
15	72	F	31.20	2	5	25.00	8	147.21

Note: KL represent the score by Kellgren and Lawrence grading system; KOOS is knee injury and osteoarthritis outcome score; ISOA is indices of severity and disease activity for osteoarthritis; WOMAC presents Western Ontario and McMaster Universities arthritis index; VAS presents visual analogue scale.

3.2 Explant tissue culture

Synovium samples were moved from the tissue bottle to a sterile dish and washed with normal saline at least 3 times to remove residual blood and to identify fat tissue (yellow) and synovium (white) in aseptic conditions (Figure 5A). All fat tissue was removed and only white tissue left by the scalpel or scissors. White synovium was dissected into 2-3mm sections. Each section was picked with syringe needle and placed into bottom of a flask. 5-10 drops of synoviocyte culture medium (DMEMα and 10% FBS, 100U/ml penicillin G, 100mg/ml streptomycin and 2.5mg/ml amphotericin B) were added gently on each section to avoid tissue debris floating in medium (Figure 5B & D).

The flask was places in a 37 °C incubator (Forma Steri-Cycle i160 CO2 Incubator, Thermo Scientific, Massachusetts, US) with 5% CO_2 and culture medium was changed carefully every 3 days by using 1ml syringe. After 14 days of tissue culture, massive single cells were observed growing away from the tissue sections and attached to the flask (Figure 5C). 5ml PBS was filled into the flask twice to wash away all tissue debris. Next, 0.25% trypsin (2.5ml) was added to the flask and incubated for 5min. Culture medium (2.5ml) was added to cease the trypsinization. Cell suspension was centrifuged at room temperature by 250g for 10min. The cell pellet was resuspended into 5ml culture medium, and then transferred into the flask to culture in 37°C incubator with 5% CO_2 atmosphere. Culture medium was changed every 3 days and cells were split until passage 4 for further usage.

The synoviocytes culture medium was composed of DMEMα and 10% FBS, 100U/ml penicillin G, 100mg/ml streptomycin and 2.5mg/ml amphotericin B.

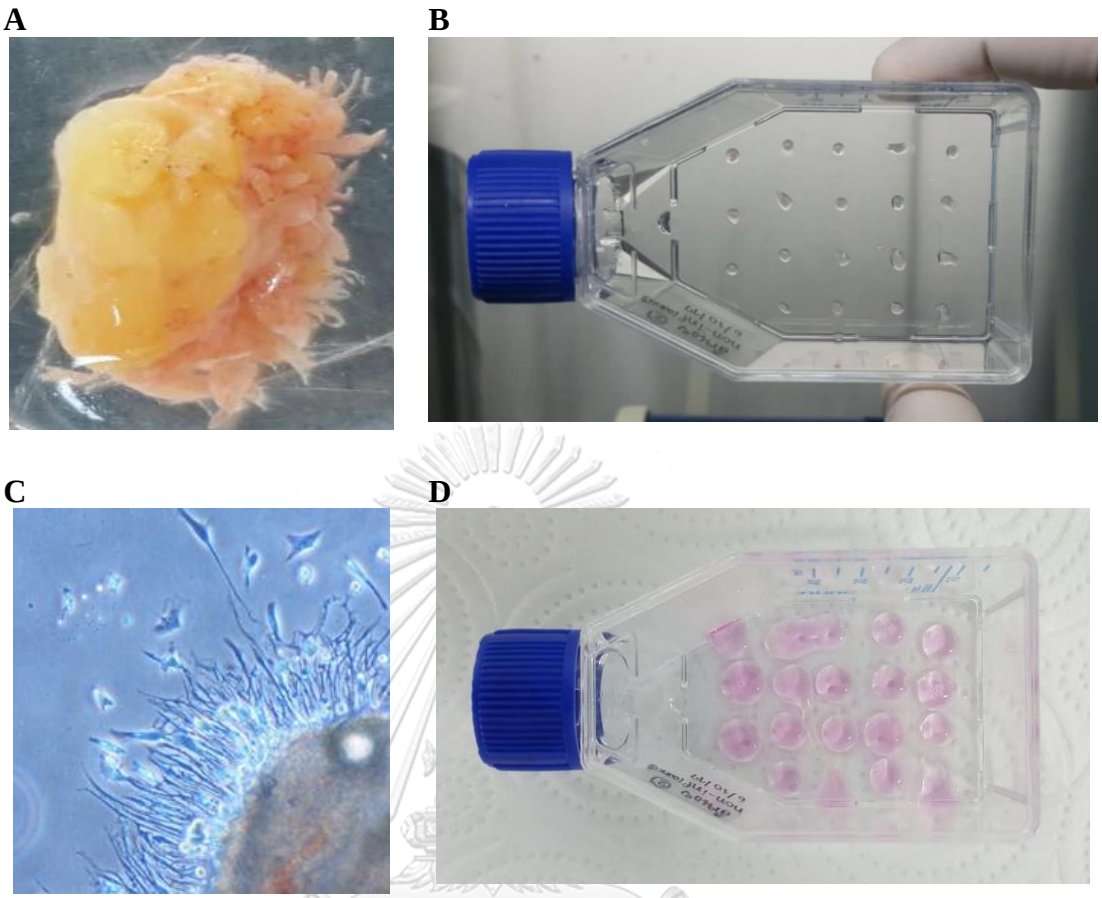

Figure 5. Process of primary synoviocytes culture by explant culture method. (A) The synovium (white or pink) was identified from the adipose tissue (yellow) after washing with normal saline. (B & D) The synovium debris were seeded on the bottom of the flask and added in a few drops of culture media. (C) Single cells started to secede from tissue blocks and grow around tissue.

3.3 Dispersed cell culture

Under aseptic conditions, synovium tissue in sterile bottle was transferred to a plastic dish and washed 3 times by PBS to remove residual blood from the tissue. Fat tissue was discarded as much as possible and white synovium was minced by scalpel or scissors. The synovium mince was transferred into a centrifuge tube filled with 1ml 0.25% trypsin and incubated for 15min at 37°C and 5% CO_2 atmosphere (Figure 6A). The ratio of mince volume to trypsin volume was 1:10. Subsequently, this mixture was centrifuged at 100g for 5min to remove supernatant and trypsin (Figure 6B). Pelleted mince was digested in 1ml HBSS with collagenase (1mg/ml) for 2h at 37 °C with 5% CO_2 (Figure 6C). The centrifuge tube was shaken every 15min for 30s. Then the mixture was centrifuged at 250g for 5min to discard supernatant and collagenase (Figure 6D). Pelleted mince was suspended in 5ml culture medium and filtered through 100µm nylon mech to removed tissue blocks. Collected single cells were cultured in a flask and non-adherent cells were removed by culture medium changes on day 1, 3 and 7. Attached cells were cultured and passaged conventionally until fourth passage for further usage.

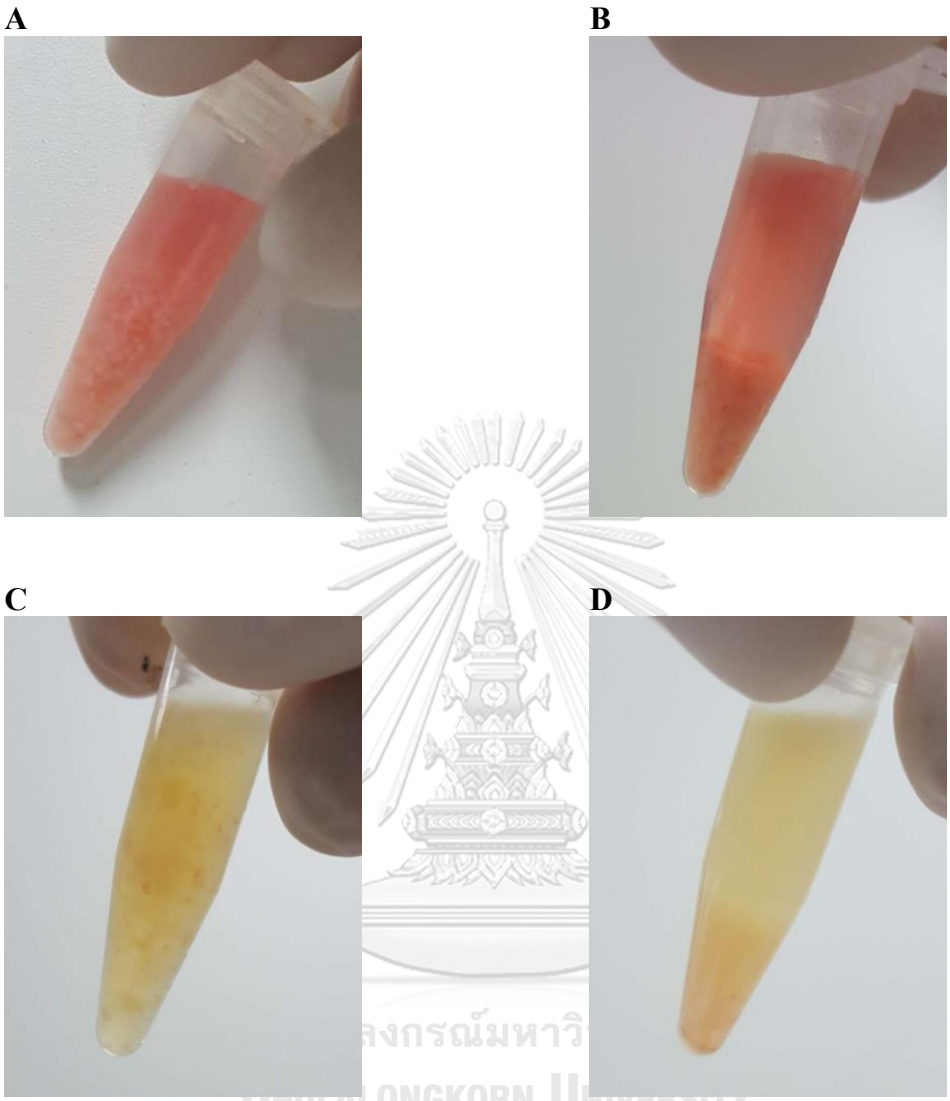

Figure 6. Process of primary synoviocytes culture by dispersed cell culture method. (A) The minced synovium was digested with 0.25% trypsin. (B) Trypsin digested minces were centrifuged into tissue pellets. (C) The second enzyme, 1mg/ml collagenase, was added to digest tissue pellets. (D) Collagenase digested pellets were centrifuged to pellet dispersed cells for routine culture.

3.4 Cells confluence measurement

Cells are commonly sub-cultured when their confluence achieves 80-90%. Cell confluence was measured via captured pictures by invert light microscopy and analysed by ImageJ. The time for cells to proliferate to 85% confluence was recorded and analysed. Cells from explant and dispersed cell cultured were seeded in tissue culture flask T25 (ThermoFisher, NY, US) and cells images were captured by light microscope (Eclipse TS100 Nikon, Japan) with 4-fold objective (Figure 7A). ImageJ and PHANTAST FIJI plugin were used to measure cell confluence. The raw image was opened in File option and converted into 32-bit grey image in the function menu: Image-Type-32bit. The plugins of PHANTAST was opened in Plugins-Segmentation-PHANTAST. In Segmentation Parameters window, sigma and epsilon of local contrast thresholding was set as 4 and 0.02. In output options, compute confluency of measurements was selected, as well as new mask image (Figure 7B) and selection overlay on original image (Figure 7C) of Image Output were ticked in checkbox. The new mask image was used to analyse by click on “OK”. The Result Table would show confluency in percentage.

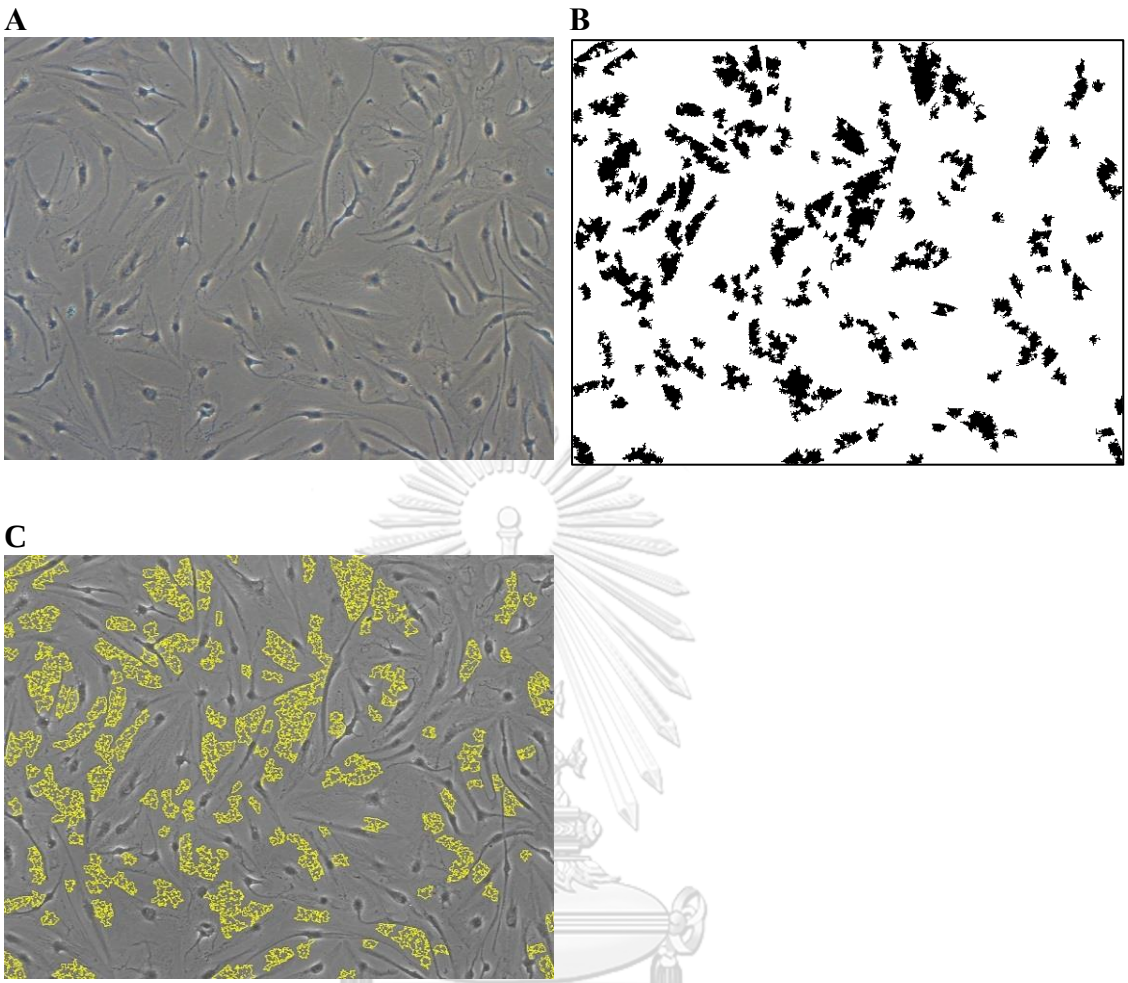

Figure 7. Cell confluency measured with ImageJ and PHANTAST plugin. (A) show original image captured by phase contract light microscope. (B) The new mask image was obtained by PHANTAST plugin, the white area represents cellular confluency and the black colour is area without cells. (C) The merged image of original image (A) and the image of acellular adhesion area (B), the yellow colour shows area without cells.

3.5 Mycoplasma contamination detection by PCR

Cultured cells were directly harvested with plastic scrapers in culture media (without removing culture media or washing cells). Cells and media were moved into centrifuge tube and boiled for 10min in the water bath. The cell suspension was centrifuged at 1,500g for 5min at 4°C. 4µl supernatant was added into a PCR reaction system which was prepared according to the manufactures protocol (mycoplasma PCR detection kit, HuaBio, Hangzhou, China).

The components of reaction mixture (25µl) consisted of 20µl PCR solution, Taq enzyme solution 1µl and sample supernatant or positive or negative control solution. The mixtures were prepared in PCR tubes (Thermo Scientific, Massachusetts, US) which were placed in a PCR Mastercycler (Eppendorf, CA, US). The conditions for PCR amplification was conducted according to the manufactures protocol as follows: initial denaturation at 94 °C for 5min, 30 amplification cycle at 94 °C for 30s, 56°C for 30s, 72°C for 45s, and final extension at 72°C for 5min. PCR products were load into wells of 1% agarose gel for electrophoresis for 30min at 120V. Gels were stained with 5% ethidium bromide in water for 15min and visualized on ultraviolet transilluminator: Gel Doc XR+ Imager (Biorad, California, US).

3.6 Cell growth curve

0.25% trypsin was used to harvest passage 1 and 4 cells of primary culture. Cell concentration was diluted into 10^5cell/ml with synoviocyte culture medium. 100µl cell suspension (1,000 cells) was seeded into each well of a 24-well plate and replenished with culture medium to 1000µl. When cells were cultured in the incubator for each 24h, cells of one well would be harvested by adding 500µl 0.25% trypsin. Digestion was stopped by supplementing with 500µl culture medium. 5µl cells suspension and 5µl trypan blue (volume ratio 1:1) were mixed and pipetted gently for counting cell number on the hemocytometer chamber. Three wells were used to calculate cell numbers for each day. Cell culture continued for 8 days and the culture medium was replaced every 3 days.

To characterize the growth of diploid primary cells, population doubling time was calculated in P1 and P4 from explant culture and dispersed cell culture. The following equation was used to calculate doubling time (DT):

$$DT = \frac{T \cdot ln2}{lnN_t - lnN_0}$$

DT is doubling time of primary cells.

T is cell cultured time, 8 days or 192 hours.

N_t is the cell number after 192 hours culture.

N_0 is the cell number at the beginning of the seeding: 1,000 cells per well.

3.7 Cell cycle phase

Cells from passage 1 and 4 of primary culture were harvested with 0.25% trypsin. After centrifuging cells suspension at 250g for 5min, 10^6 cells were resuspended in ice-cold PBS with 70% ethanol (3ml) and vortexed for 3s. Then cells were incubated at 4°C for 15min in fridge. Cells were pelleted by centrifugation at 250g for 5min and washed twice by cold PBS. Washed cells were resuspended in 500µl PI-solution that consisted of PBS, 50 µg/ml PI, 0.1 mg/ml RNase A and 0.05% Triton X-100. The mixture was incubated for 40min at room temperature (RT). After refilling 3ml PBS to stop staining, cells were centrifuged at 250g for 5min again. Cells pellet was resuspended in 1000µl PBS to be ready for flow cytometry analysis: BD LSR II (San Jose, CA, USA). PI fluorescent signal was detected with in the channel of PE/Texas Red.

3.8 Flow cytometry for fibroblast CDs expression

Primary synoviocytes from passage 1 and 4 were harvested by adding 0.25% trypsin (2.5ml) for 5min, and then supplimented with 2.5ml synoviocyte culture media to stop digestion. After cell suspension was centrifuged at 900g for 3min, cell concentration was adjusted to be 10^7cell/ml with culture medium. 100µl cells suspension was moved into 1000µl PBS with 10% FBS and centrifuged at 900g for 3 min. Cells pellet was resuspended in 100µl PBS supplemented with 10% FBS. Four single-labels antibodies (FITC-CD90, FITC-CD64, PE-CD55, APC-CD11b) with volume of 5µl were respectively added into cell suspensions. After brief vortexing, cell suspensions with anti-human CDs were incubated at RT in the dark for 30min. Subsequently cells suspension was replenished PBS with 10% FBS up to 1000µl and centrifuged at 900g for 3min. Cell pellets were resuspended in 500µl PBS with 10% FBS followed by 500µl PBS with 4% paraformaldehyde (PFA) to fix cells at RT for 15min in dark. Cell suspensions with fixing solution were centrifuged again to acquired cells pellet which were resuspended in 1000µl PBS with 10% FBS to be ready for flow cytometry test in FITC, PE or APC channels.

Part B: Neutrophils Isolation and Functional Assays

3.9 Healthy volunteers

Peripheral blood from ten healthy volunteers was collected into lithium-heparin tubes (Greiner Bio-One, Chonburi, Thailand). Random urine specimens were collected in 5ml urine containers by volunteers, then stored at 4^{o}C for laboratory testing. The urine and blood characteristics of all volunteers are summarized in more detail in Table 11-13. In urinalysis, all volunteer urines were clear and light yellow. The value of urine pH ranged from 5.5 to 7.5. The specific gravity of one urine was 10.21 higher than normal reference maximum. The protein, glucose, ketones, bilirubin, urobilinogen, nitrite, blood and leukocyte in all urine were normal. In blood chemical examination, 3 volunteers were found to have abnormal levels of cholesterol, triglyceride and alkaline phosphatase, but they did not complain any discomfort or signs and physicians did not find any clinical syndromes. All volunteers were normal in the hematological examination.

Table 11. The urinalysis of volunteers who donated their whole blood.

Item	Minimum	Maximum	Mean	95% CI		Ref.
				Lower	Upper	
pH	5.5	7.5	6.0	5.6	6.4	5.0-8.0
Specific Gravity	1.008	1.028	1.017	1.014	1.021	1.015-1.025

Note: The urea of all volunteers was yellow and clear. It was negative in protein, glucose, ketones, bilirubin, urobilinogen, nitrite, blood and leukocyte (esterase) of all volunteers. And the number of their RBC (/HPF) and WBC (/HPF) in urea were 0-3, epithelial cell (/HPF) was 0-2, bacteria (/HPF) were none, rare or few. The casts (/LPF), crystal (/HPF) and mucus were found in their urine.

Table 12 The blood chemicals tests of blood-donating volunteers.

Item	Minimum	Maximum	Mean	95% CI		Ref.
				Lower	Upper	
Uric Acid (mg/dL)	3.4	5.9	4.8	4.4	5.3	2.6-6.0
Cholesterol (mg/dL)	110.0	202.0	168.6	149.3	187.9	<200
HDL (mg/dL)	45.0	85.0	64.3	55.4	73.2	>40
LDL (mg/dL)	94.0	155.0	124.1	112.2	136.0	<160
Triglyceride (mg/dL)	35.0	234.0	100.8	65.9	135.7	45-150
AST (U/L)	18.0	26.0	21.1	19.8	22.4	5-35
ALT (U/L)	10.0	24.0	18.1	15.0	21.2	0-40
ALP (U/L)	41.0	100.0	76.0	65.2	86.8	30-120
FBG (mg/dL)	82.0	99.0	92.4	89.3	95.5	65-100
BUN (mg/dL)	7.0	18.0	12.7	10.7	14.7	8-20
Creatinine (mg/dL)	0.6	1.0	0.8	0.7	0.8	0.5-1.0
eGFR (mL/min)	86.5	111.1	100.6	96.6	104.6	>60
fasting plasma glucose (mg/dL)	71.0	98.0	83.9	78.8	89.0	70-99
alkaline phosphatase (U/L)	45.0	121.0	104.1	91.0	117.2	40-120
CK-MB (U/L)	13.0	23.0	19.3	17.4	21.2	0-24
sodium/Na(mmol/L)	136.0	145.0	139.4	137.6	141.2	136-145
potassium/K(mmol/L)	3.1	4.4	3.9	3.6	4.1	3.4-4.5

Table 13. The haematological tests of blood-donating volunteers.

Item	Minimum	Maximum	Mean	95% CI		Ref.
				Lower	Upper	
red cell (10^6/μl)	3.7	5.1	4.4	4.1	4.7	3.5-5.5
hemoglobin(g/dl)	11.5	15.6	13.7	12.8	14.6	12-16
platelet (10^3/ μl)	156.0	433.0	289.5	232.4	346.6	150-450
white blood (10^3/μl)	6.2	10.3	7.8	6.9	8.6	4.5-11.0
neutrophils %	44.2	69.5	59.7	54.8	64.6	40.0-70.9
neutrophils (10^3/μl)	2.9	7.1	4.7	3.9	5.4	1.8-7.8
lymphocytes %	23.2	41.2	34.1	31.0	37.3	22.2-43.6
lymphocytes (10^3/μl)	1.8	3.4	2.6	2.3	2.9	1.0-4.8
monocytes %	3.3	6.8	4.9	4.2	5.6	0-7.3
monocytes (10^3/μl)	0.2	0.6	0.4	0.3	0.4	0-0.8
eosinophils %	1.9	3.5	2.8	2.5	3.1	0-4.1
eosinophils (10^3/μl)	0.12	0.35	0.22	0.18	0.27	0-0.45
basophils %	0.1	1.3	0.9	0.6	1.2	0-1.8
basophils (10^3/μl)	0.0	0.1	0.1	0.0	0.1	0-0.2
prothrombin time (s)	9.9	13.9	12.0	11.3	12.7	10.0-14.5
APTT	20.30	32.70	25.84	23.54	28.14	20.0-32.7

3.10 Neutrophils isolation

Blood of 50ml was layered over an equal volume of Polymorphprep (Axis-Shield, Oslo, Norway) reagent and centrifuged at 500g for 30min at 25°C. Peripheral blood mononuclear cells (PBMC) layer was removed after centrifugation, polymorphonuclear (PMN) leukocytes were collected by pipette, washed with RPMI 1640 medium (Gibco, NY, US) and centrifuged to remove reagents and platelets. Contaminating erythrocytes were lysed in red blood cell lysis buffer (Roche, Mannheim, Germany) for 3min in the dark. After centrifugation at 400g for 3min, pelleted neutrophils were resuspended in RPMI 1640 with 5% vesicle-free serum to give a concentration of 2×10^7 cells/ml for further experiment and subsequent preparation of microvesicles (Figure 8). Each volunteer donated blood for each independent experiment.

Vesicle-free serum was prepared by ultra-centrifugation of human AB serum (EMD Millipore, MA, US) at 200,000g for 2h at 4°C. The supernatant was retained while the pelleted vesicles were discarded. Isolated neutrophil purity was examined by cytospin and flow cytometry.

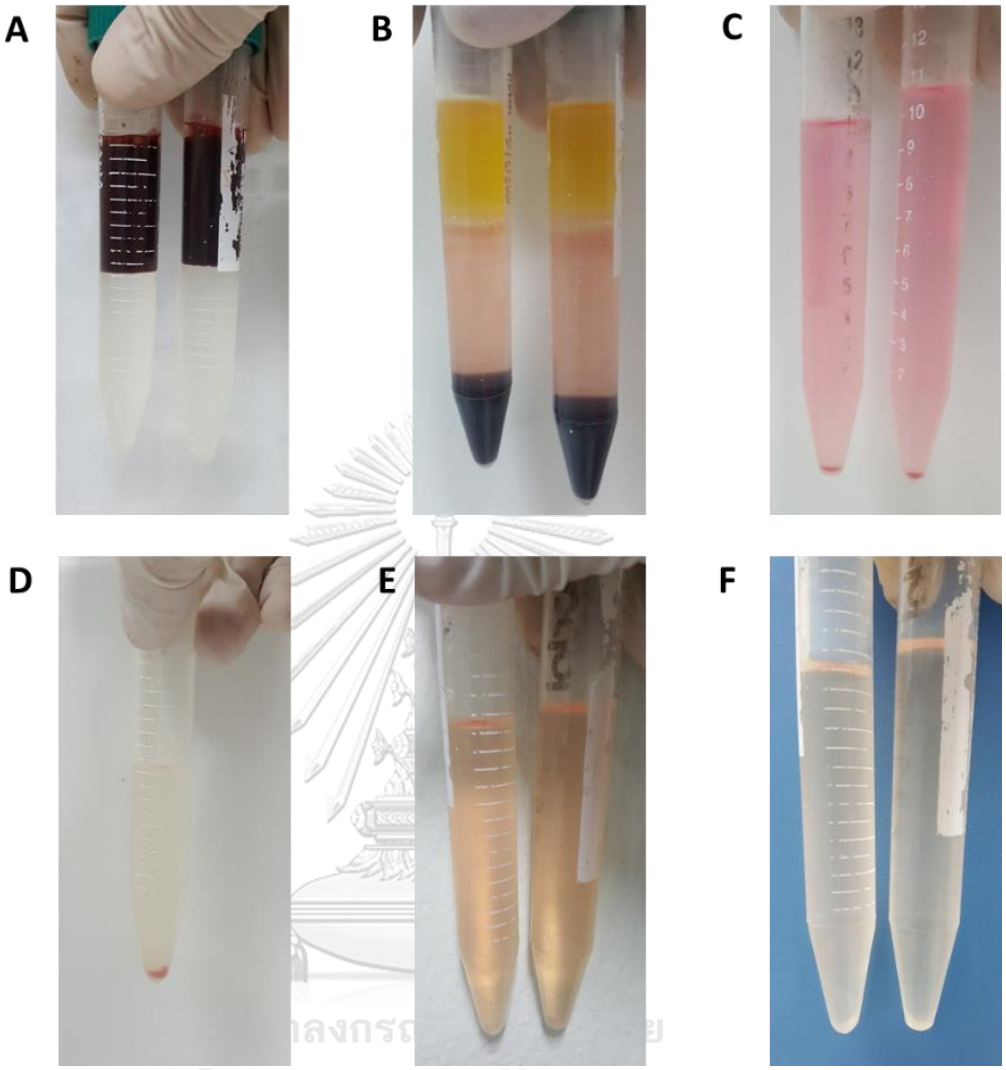

Figure 8. The progress of PMN isolation by polymorphprep. (A) Layer peripheral blood onto polymorpheprep solution. (B) The blood was separated into 6 layers: plasma, monocyte layer, solution layer, PMN layer, solution layer and erythrocytes layer after centrifugation. (C) The PMN layer was gathered and resuspended by RPMI 1640 medium, then centrifugated to obtain the cell pellets. (D) The supernatant was removed and red blood cell lysis buffer added. (E) Erythrocytes were lysed for 3min. (F) After centrifugation, the white pellet was resuspended with appropriate in RPMI 1640 with 5% vesicle-free serum.

3.11 Cytospin and wright staining for neutrophils purity

Freshly isolated neutrophils (100,000 cells) were resuspended in 200uL PBS with 10mM EDTA and removed to cytospin funnel (Tharmac, Germany). After centrifugation 50g for 5min at RT, the glass slide was allowed to air dry for 2min. Wright's solution (Merck, Wright's eosin methylene blue solution) was used to stain cells for 5min, before rinsing with deionized water twice. Dry glass slides were placed on light microscope (Nikon, Upright Microscope Eclip 50i) to count neutrophil amount and calculate purity.

3.12 Flow cytometry for neutrophils purity

Fresh isolated neutrophils (cell concentration 2×10^7 cells/ml) 2.5µl was suspended in 50µl PBS with 5% FBS. An equal volume of 4% paraformaldehyde in PBS was added for 15min at RT in the dark. After centrifugation with 900g for 3min, the supernatant was discarded and the cell pellet was resuspended in 200µl PBS with 5% FBS. Cells were analyzed by flow cytometry: BD LSR II (San Jose, CA, USA). The trigger of flow cytometry was set on the SSC. The used voltage of photomultiplier tube was set on 630V and trigger threshold was set on 0. The noise background was adjusted with deionized water by technicians.

3.13 Transwell assay

5g poly-2-hydoroxyethyl methacrylate (poly-HEMA) (Sigma-Aldrich, Missouri, US) was dissolved in 100ml of 95% Ethanol at 65°C overnight to obtain 50mg/ml ploy-HEMA solution. To coat the lower chamber, each well of a 24-well plate was filled with 200µl 50 mg/ml poly-HEMA and incubated overnight at RT. The Millicell hanging cell culture insert with 3.0µm pore size was settled in each well, then both upper and lower chambers were washed with PBS twice. 800µl RPMI 1640 medium with 10^{-8}mol/L N-Formyl-L-methionyl-L-leucyl-L-phenylalanine (fMLP) was added into each lower chamber. After the upper chamber was inserted in lower chamber for 5min, 200µl RPMI 1640 medium with 5×10^6cells neutrophils was added into upper chamber. The plate was incubated in for 90min with 5% CO_2 atmosphere at 37°C. In the lower chamber, 800µl RPMI medium was gently aspirated several times and

removed to new tube which is replenished 200µl RPMI medium to achieve 1000µl in total volume. The sum of migrated neutrophils was counted by hemocytometer (Bright-Line Hemacytometer, Sigma Aldrich, Missouri, US).

3.14 Flow cytometry for CD11b and CD62L expression

Neutrophils (2×10^7cells/ml) were incubated in the absence or presence of 50ng/ml TNFα for 20min in 5% CO_2 atmosphere at 37°C. 2.5µl cells were removed and resuspend in 100µl PBS containing 5% FBS. After centrifuging at 900g for 3min, the cell pellet was flicked and resuspended in 10µl PBS with 5% FBS. Two single-label antibodies (1µl each APC-CD11b and PE-CD62L) were mixed into cell suspension to achieve a working concentration. After vortex, cells suspensions with anti-human CDs were incubated at RT in dark for 30min. Cell suspension was replenished with 100µl PBS/5% FBS and centrifuged at 900g for 3min. Cell pellets were resuspended in 50µl PBS/10% FBS and an equal volume of 4% paraformaldehyde was added to fix cells at RT for 15min. Cells suspension with fixing solution was centrifuged 900g for 3min to acquired cells pellet which was resuspended in 200µl PBS/5% FBS to be ready for flow cytometry analysis.

3.15 Luminol-amplified chemiluminescence assay

Neutrophils (2×10^7cells/ml) were incubated in the absence or presence of 50ng/ml TNFα (to prime cells) for 20min in 5% CO_2 atmosphere at 37°C. After prepared master mix of 160µl was added in each wells of 96-well white plates (the master mixture included: 158.8µl HBSS, 1µl luminol with finial conc. of 10µM and 0.2µl stimulus of fMLP with finial conc. 1µM or PMA with finial conc. 100ng/ml), 40µl of the primed-cell suspension was added to the plate quickly. The plate was transferred to the ready luminometer which could read plate every 0.7min as soon as possible. Chemiluminescence was measured and recorded for statistical analysis.

3.16 PI-Annexin V assay

FITC Annexin V Apoptosis Detection Kit with propidium iodide (PI) (Biolegend, San Diego, CA) was used to conduct cells apoptosis assay. The 50ng/ml TNFα treated and untreated neutrophils (conc. 2×107 cells/ml) of 25µl were centrifuged at 900g for

3min and supernatant discarded. After pelleted cells were washed with cold PBS/10%FBS of 300µl, cells were resuspended in 100µl Annexin V binding buffer in 5ml tube. The cell suspension was added with 5µL FITC Annexin V and 10µL PI solution sequentially to incubate 15min at RT in the dark. Stained cells suspension was replenished with 400µl Annexin V binding buffer. Cells were captured and analyzed by flow cytometry: BD LSR II (San Jose, CA, USA). Annexin V signals were recorded on FITC channel and PI signals were captured on PE-Texas Red channel. Untreated neutrophils without staining was set as control cells of Annexin V^- /PI^- and their intensity histogram adjusted to less than 10^3.

Part C: NDMV Isolation, Purification and Properties

3.17 NDMV releasing and isolation

Freshly isolated neutrophils (2×10^7 cells/ml) were stimulated with recombinant human TNFα (50ng/ml, Biolegend) for 20min at 37°C. Neutrophils and media were centrifuged at 4400g for 15min at 4°C to remove neutrophils. Thereafter, supernatant was centrifuged again at 13,000g for 2 min at 4°C to remove platelets. NDMV were pelleted by ultra-centrifugation at 100,000g for 60 min at 4°C. Microvesicle pellets were re-suspended in 100µl sterile particle-free PBS (0.02µm filtered), used fresh or frozen at -80°C until using for microRNA sequencing.

3.18 Electron microscopy assay

Pelleted NDMV were fixed for 3h in PBS with 2% glutaraldehyde and 2% paraformaldehyde (PFA), then examined by transmission electron microscopy of negative staining and scanning electron microscopy to ascertain extracellular vesicles morphology and diameter. TEM copper grid was floated on 10µl NDMV mixture for 10min, 1×PBS droplet and deionized water was used for washing in turn. The NDMV attached grid was floated on 10µl uranyl acetate and lead citrate to stain for 1min. Eventually, this TEM grid was imaged by JOEL JEM-1400 Plus TEM operated at 80-100kV (JEOL, Peabody, US).

For SEM examination, 5µl NDMV mixture was added on to silicon chips, which was dehydrated with series solvents for each 5min: 100% acetone, 100% ethanol and deionized water. Then the samples were conducted with critical point drying and mounted on a SEM stub which was sputter-coated with 40nm gold-palladium alloy. Lastly, samples were observed with a JEOL JSM-7610F SEM operated at 25-50 kV (JEOL, Peabody, US).

3.19 Nanoparticle tracking analysis (NTA)

The size distribution and particle concentration of NDMV were identified by using a NanoSight NS300 (Malvern Panalytical, Malvern, UK) configured with an advanced

sCMOS (scientific complementary metal-oxide-semiconductor) camera and a 405nm laser. The fresh NDMV were diluted 1000 times in particle-free PBS to reach a recommended concentration range from 10^6-10^9 particles/ml. High sensitive camera recorded NDMV Brownian motion in 60s length video for 5 times with camera level 15 under constant flow by syringe pump (flow rate=50) at 25°C. Those successive videos were analyzed automatically on Nanosight NTA 3.1 Software Build 3.1.54 at detective threshold 3. For other settings, viscosity was set to "water", blur size and max jump distance were "automatic". Five samples were analyzed by NTA.

3.20 Flow cytometry of surface protein expression in NDMV

Pelleted untreated neutrophils (UN), 50ng/ml TNFα-treated neutrophils (TN) and Ultra-centrifuged NDMV (MV) resuspended in 49µl antibody binding buffer (10 mm Hepes, pH 7.4, 140 mm NaCl, 2.5 mm CaCl2), before the addition of 1µl Annexin V-FITC, CD11b-FITC, CD14-PE, CD16-PE and CD66-FITC at a 1:100 dilution. Negative control (NC) was set as non-stained neutrophils with fluorescent antibodies. After 10 min incubation in the dark at RT, cells and NDMV were diluted and resuspended in 50µl antibody binding buffer before analysis by flow cytometry using a CytoFlex and CytExpert software (Beckman Coulter, California, US). Before adding samples to process flow cytometry, 1µl microbeads with 1,000nm diameter (ThermoFisher, Massachusetts, US) to identify gating area of microvesicles which predicted size < 1,000nm. Figure 9 shows microbeads and NDMV gating square.

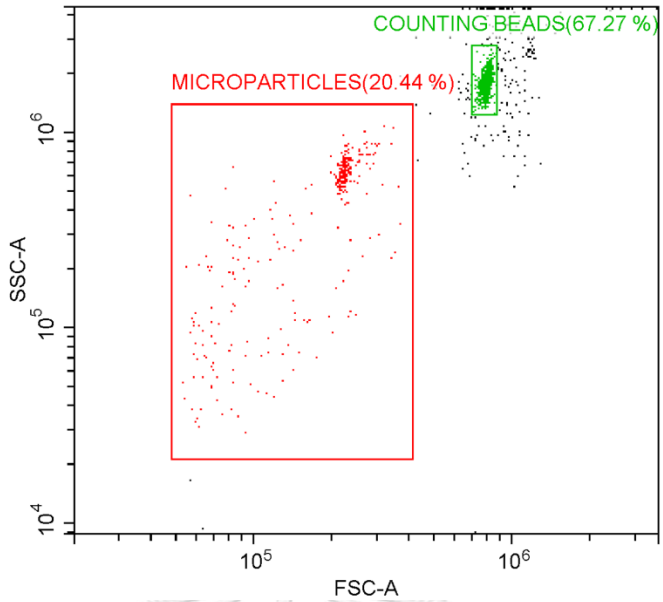

Figure 9. Size reference by microbeads in flow cytometry. Microbeads size was 1,000nm with green plot and gating square. NDMV diameter was less than 1,000nm and displayed with red scatter plots and gating area. NDMV gating area was used for further surface markers expression analysis.

3.21 microRNA sequence

3.21.1 microRNA extract

The miRNeasy Mini Kit (Qiagen, Hilden, Germany) was used to isolate total RNA including microRNA and other small molecular weight small RNAs. TNF-treated/untreated neutrophils and NDMV were pelleted and lysed in 700µl QIAzol reagent in RNase-free microcentrifuge tube. After the lysate was incubated at RT for 5min, chloroform (140µl) was added and mixed completely with lysate. The mixture was incubated at RT for 3min and then centrifuged at 12,000g for 15min at 4°C. The upper aqueous phase was removed into the collection tube and mixed with 100% ethanol of 525µl. The mixture with volume of 700µl was transferred into the mini spin column which was placed in the collection tube. After centrifuge at 10,000g for 15s at RT, the buffer RWT was filled into the mini spin column and centrifuged again. The mini spin column was washed twice by 500µl buffer RPE. The mini spin column bound with total RNA was moved into new collection tube. The membrane of mini spin column was added with 30µl RNase-free water and placed at RT for 1min to

improve RNA dissolution. The eluate was collected by centrifugation at 10,000g for 1min. The obtained 30µl eluate were transferred to the membrane and centrifuged twice.

3.21.2 Agarose gel electrophoresis for RNA integrity

The 1% solid agarose gel was placed in an electrophoresis gel box and covered with 1×TAE. The RNA sample of 1000ng was mixed with 6× loading buffer of 5µl and 100% formamide 15µl. After loading RNA mixture into a relevant well of the agarose gel, the electrophoresis started at 80V for 30min. The whole agarose gel was stained by 0.5µg/mL EtBr solution for 15min, then washed gel 3 times by DEPC-treated water. RNA bands were visualized on the ultraviolet transilluminator-Gel Doc 1000 (Bio-Rad, CA, USA).

3.21.3 Sequencing microRNA

The microRNA sequence library was prepared on NEBNext® Poly(A) mRNA Magnetic Isolation Module (New England Biolabs), RiboZero Magnetic Gold Kit (Human/Mouse/Rat) (Epicentre, an Illumina Company) and NEB Multiplex Small RNA Library Prep Set for Illumina. TruSeq Rapid SR Cluster Kit (#GD-402-4001, Illumina) was used for microRNA sequence by Illumina NextSeq 500. This experiment was completed by Aksomics Technology Company (China). The raw sequencing data was accessed through quality control to decide what raw data should be used for further analysis. Data analysis progress was shown in Figure 10.

Quality control was processed on Solexa CHASTITY software to filter low quality reads and obtain clean reads. The cutadapt software was used to cut head of clean reads and keep tag with length equal and greater than 15nt, the collect trimmed reads for further analysis. The miRDeep2 software to quantify known microRNA and predict novel microRNA. The R software and its package edgeR was used to analyse different expression to find significant differences after clean reads were standardized by Counts Per Million (CPM) with reference genome (GRCh38) (Figure 11).

Significantly different microRNA was conducted by 2-dimentional cluster analysis and visualized with heatmaps. The different expression of microRNAs will be analysed by Ingenuity Pathway Analysis (IPA) (Qiagen, Redwood, US). The target genes of microRNAs were searched in three databases: TargetScan (Version 6.2) and miRDB (Version 4.0) and miRTarBase on the internet website miRWalk 2.0

(http://mirwalk.umm.uni-heidelberg.de/) (Dweep and Gretz, 2015). These target genes were used for gene ontology analysis, KEGG pathway analysis and Ractome Pathway analysis.

Figure 10. Data analysis flowchart for microRNA sequencing.

Mature_ID	Arm	Pre_ID	Length	Seed	Mature_Sequence
hsa-miR-4677-3p	3p	hsa-mir-4677	22	CUGUGA	UCUGUGAGACCAAAGAACUACU
hsa-miR-4677-5p	5p	hsa-mir-4677	22	UGUUCU	UUGUUCUUUGGUCUUUCAGCCA
hsa-miR-6505-5p	5p	hsa-mir-6505	22	UGGAAU	UUGGAAUAGGGGAUAUCUCAGC
hsa-miR-1911-5p	5p	hsa-mir-1911	23	GAGUAC	UGAGUACCGCCAUGUCUGUUGGG
hsa-miR-4766-3p	3p	hsa-mir-4766	21	UAGCAA	AUAGCAAUUGCUCUUUUGGAA
hsa-miR-6516-5p	5p	hsa-mir-6516	22	UUGCAG	UUUGCAGUAACAGGUGUGAGCA

Mature_ID	Arm	log_2fc	Fold_Change	p_value	q_value
hsa-miR-891a-5p	5p	8.69	411.78	2.43e-22	1.13e-19
hsa-miR-592	5p	8.07	269.38	7.08e-03	3.65e-02
hsa-miR-892a	5p	8.06	266.72	5.00e-15	9.28e-13
hsa-miR-3923	5p	6.86	115.86	3.27e-09	1.26e-07
hsa-miR-431-5p	5p	6.65	100.70	4.87e-02	1.50e-01
hsa-miR-92a-1-5p	5p	-2.89	0.13	9.39e-12	5.81e-10
hsa-let-7c-3p	3p	-2.84	0.14	3.32e-11	1.62e-09
hsa-miR-4768-5p	5p	-2.27	0.21	5.34e-03	2.93e-02
hsa-miR-181b-2-3p	3p	-2.22	0.21	1.31e-07	4.09e-06
hsa-miR-16-1-3p	3p	-2.15	0.23	3.39e-07	9.26e-06

$$CPM = \frac{C \times 10^6}{N}$$

C=number of reads mapped to a reference gen
N=total number of mapped reads in experimen

CPM (counts per million)
RPM (reads per million)
human genomic reference: hg38

software: miRdeep2

Figure 11. Transform reads into CPM and compare group different expression of microRNA.

Part D: NDMV Effects on FLS Function

3.22 MTT assay

The metabolic activity of FLS co-cultured with or without NDMV was evaluated by the 3, (4, 5-dimethylthiazol-2-yl) 2, 5-diphenyl-tetrazolium bromide (MTT) assay. 3,000 FLS were seeded in a 96-well plate for 24h, and then PBS-washed wells were refilled with 60µl DMEM/10%FBS and conditioned media which contained DMEM/10% FBS and different vesicle/cell ratio: 10:1, 20:1, 30:1, 50:1, 100:1, 200:1, 300:1, 400:1 or 10 ng/ml TNFα prior to co-culture for 24h. Media was then removed, then PBS washed 3 times. Subsequently, 100µl culture media with 0.5mg/ml MTT was added in each well and incubated for 4h at 37°C. MTT was removed and replaced with 100µl DMSO to dilute formazan crystals by shaking horizontally for 10min and incubated at 37°C for 30min. The absorbance of dissolved purple crystals in a 96-well plate were measured at 570nm by a microplate reader- Multiskan GO (Thermo Fisher, MA, US). DMSO-diluted FLS without MTT incubation was used as the blanks. The viability of FLS in the control group without NDMV co-culture was set as 100%, which was a relative value to other groups. Each conditioned treatment was repeated 5 times.

3.23 Scratch wound healing assay

10^5 of log phase FLS (Passage 4) were incubated in 6-well tissue culture plates and incubated for 24h to form a monolayer. A 200 µL pipette tip was used to scratch a line and remove cells. Each well was washed twice with 1mL DMEM/10%FBS to remove floating cells. Two mL of DMEM/10%FBS (± NDMV) were added to each well and the plate was incubated for 24h and 48h. Cells were washed twice with PBS and fixed with 300µl 4% PFA for 15min. The cells were then stained with 300µl 0.1% crystal violet for 30min and washed with PBS for 10 times. Images of monolayer cells were captured by microscopy: EVOS M5000 Imaging System (ThermoFisher Scientific, Massachusetts, US). The area of cells between the original scratch lines was evaluated by ImageJ software and % regrowth area was calculated to represent cell proliferation

±NDMV treatments. The percentage of scratch wound regrowth area was set as a baseline 0% after scratching at 0h.

3.24 NDMV labeled by fluorescent PKH26

To quantify the amounts of NDMV taken up by FLS, the phospholipid bilayer membrane of microvesicles was stained by PKH26 Red Fluorescent Cell Linker Kits for General Cell Membrane Labelling (Sigma-Aldrich, St. Louis, US). MV pellets obtained after ultra-centrifugation were resuspended gently in 100µl Diluent C. Equivalent 2× Dye Solution (PKH26 solution : Diluent C = 4µl : 1000µl) was added with the NDMV mixture and incubated for 5min at room temperature (RT). 200µl EV-free serum was used to pause staining for 1min at RT to stop staining. Additional 5ml RPMI 1640/5% EVs-free serum was supplied to wash the PKH26 dyed NDMV and dilute or combine leftover unbound PKH26. Next, the ultra-centrifugation was used to re-pellet PKH26-stained NDMV at 100,000g for 30 min at 4°C which was diluted in 100µl RPMI 1640 and co-cultured immediately with P4 or P5 FLS to measure microvesicles internalization by flow cytometry and confocal microscopy.

3.25 NDMV uptake by flow cytometry

2×10^4 FLS of logarithmic growth phase (Log GP) in P4 were seeded in each well of a 24-well plate and cultured for 24h. Adhered cells were co-cultured with 400µl DMEM/10%FBS and conditioned media and incubated with NDMV (labelled with PKH26) for various time points from 0.5 to 24h. Cells were harvested with 0.25% trypsin and fixed in 4% PFA for 15min at RT. After centrifugation at 900g for 3min at RT, cells were resuspended in 500µl PBS and NDMV uptake was measured by flow cytometry using the LSR II (BD Biosciences, Bedford, US) which was fitted with a 50mW of 488nm blue laser. Forward and side scatter were adjusted to capture an FLS within the gating area. The signals of PKH26 red fluorescence were captured on the PE channel (564-606nm) and analysed by FCS Express 4 Reader (De Novo Software, Glendale, US) and R package “flowCore” “flowQ” and “flowViz”.

3.26 NDMV uptake by confocal microscopy

Before seeding 2×10^4 FLS in logarithmic growth phase of P4 for 24h, tissue-culture treated glass coverslips (WHB Scientific, Shanghai, China) were placed in a 24-well plate. 400µl conditioned media containing labelled NDMV were added for the indicated times, then the plate was washed with DMEM/10%FBS once. Co-cultured cells were fixed with 4% PFA for 15min at RT and washed with PBS twice. 0.5% Triton X-100 (Thermo Fisher, MA, US) was used to permeabilize cells for 10min at RT and then washed in PBS twice. Non-specific binding was blocked with 5% FBS for 30min. Flash Phalloidin Green 488 (Millipore, Billerica, US) at a ratio of 1:100 in PBS was used to stain cellular F-actin for 20min. 300nM DAPI solution (Millipore, Billerica, US) in PBS was used to stain cell nuclei for 5 min. Eventually, coverslips were rinsed with deionized water 3 times and transferred to mount slides with an antifade solution (Millipore, Billerica, US). Slides were viewed on a confocal microscope to capture images: FluoView FV10i (Olympus, Tokyo, Japan) and LSM800 (Zeiss, Oberkochen, Germany).

3.27 Inflammatory cytokines levels by multiplex assay

2ml DMEM/10%FBS was used to culture 10^5 FLS in logarithmic growth phase of P4 for 24h and washed in PBS twice. Adhered cells were co-cultured with DMEM/10%FBS or conditioned medium at the appropriate vesicle/cell ratio and indicated times. Co-cultured media was collected and ultra-centrifugated at 200,000 x g for 60 min at 4°C to remove NDMV and EV for further assay. Cytokines levels in co-cultured media were measured by a commercial kit: Bio-Plex Pro Human Cytokine 17-plex Assay (Biorad, Hercules, US). All processes of testing adhered strictly to the protocol and quick guide from Bio-Plex Pro Assay for Human Cytokines Assay. 50µl diluted magnetic beads was added to an assay plate which was washed twice with Wash Buffer. Co-cultured media 50µl was added to each well and incubate with the beads for 30min at RT with shaking. After washing the plate, 25µl detection antibody was added and incubated for 30min at RT with shaking. The plate was washed 3 times again, and 50µl diluted Streptavidin-Phycoerythrin (SA-PE) added and incubated for 10min. Lastly, 125µl assay buffer was added to resuspend magnetic beads and shaken for 30s. The assay plate was moved to Bio-Plex 200 Systems (Biorad, Hercules, US)

to measure cytokines concentrations. Cytokines detection range illustrated in Table 14.

Table 14. The detectable ranges of 17 human cytokines levels in Bio-Plex Pro Human Cytokine 17-plex Assay.

cytokine	**detection range (pg/ml)**	
	lower	**upper**
IL-1β	3.2	3,261
IL-2	2.1	17,772
IL-4	2.2	3,467
IL-5	3.1	7,380
IL-6	2.3	18,880
IL-7	3.1	6,001
IL-8	1.9	26,403
IL-10	2.2	8,840
IL-12 p70	3.3	13,099
IL-13	3.7	3,137
IL-17	4.9	12,235
G-CSF	2.4	11,565
GM-CSF	63.3	6,039
IFN-γ	92.6	52,719
MCP-1	2.1	1,820
MIP-1β	2	1,726
TNFα	5.8	95,484

Chapter 4. RESULTS

Part A: FLS Culture and Properties

4.1 Contamination detection

Bacterial, fungal and yeast contamination of cell cultures can be visualized by light microscopy and Figure 12A shows black rods that were observed in some FLS cultures which resulted from probable bacterial contamination. Figure 12B shows examples of filaments in cell culture media caused from probable mould contamination. Any contaminated cultures were discarded from our experiments and possible contaminated culture media solutions were discarded. Incubators, biosafety cabinet and others associated equipment were routinely cleaned and sterilized.

Mycoplasma contamination is not detectable by microscopic observation during the cell culture and so a PCR-based method was used to detect mycoplasma contamination. Agarose-gel electrophoresis showed that a PCR product for the positive control (P) was located between 250-300bp shown in Figure 12C. The negative control (N) did not show any PCR products within the 250-300bp this size range. All samples were found not to contain any mycoplasma PCR products among every passage of cultured cells.

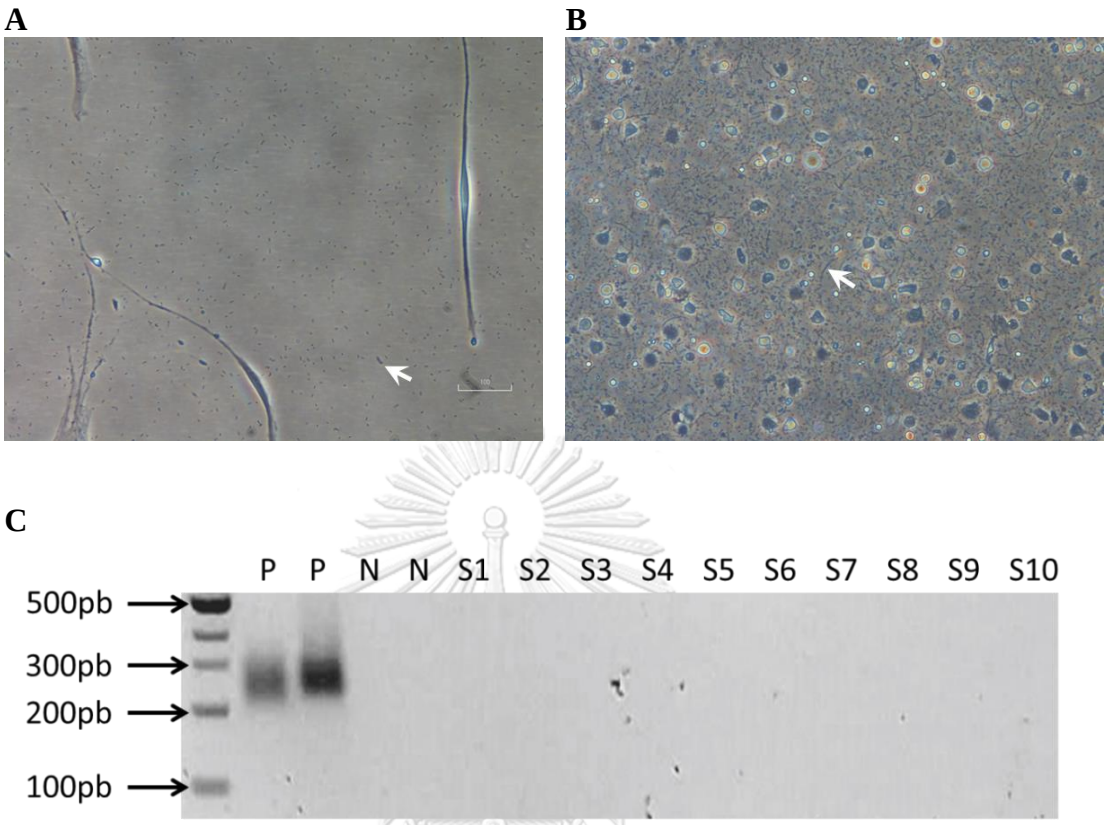

Figure 12. Culture contamination detection. (A) Suspected bacterial contamination was identified under light microscopy. Black rods and dots were sometimes found (white arrows). (B) Fungal contamination could be identified under microscopy. Black filaments were sometimes detected in culture media (white arrow). (C) Mycoplasma contamination was identified by PCR. All tissue and primary cultured cells were not contaminated by mycoplasma.

4.2 Cell growth curve

Primary culture is a fundamental approach to obtain cells from tissues, which included two classical methods: explant/tissue block culture and dispersed/ enzymatic culture. In explant culture, single cells secede radially from tissue, which defined as tissue culture or passage 0. In dispersed culture, tissue was dissociated into single cells by enzymes, which were then seeded into flasks (75cm plastic flask) as passage 0. After single cells proliferated to 85%, cells were sub-cultured into passage 1 until passage 4 for using. During 8-days of culture, 3 phases of growth kinetics were detected: lag phage, exponential phase and the beginning of stationary phase (Figure 13). The growth curve of dispersed cells in culture (passage 1) showed an initial decline below 10,000 cells/ml on days 1, 2 and 3, but this initial decline was not detected in passage 4 cultures, where cell concentrations were above 10,000 cells/ml on days 1, 2 and 3 (Figure 13A). Before day 5, the cell density of passage 1 was lower than that of passage 4 in dispersed cell cultures. Nevertheless, the cell density of passage 1 was higher than that of passage 4 on days 6, 7 and 8. The differences in FLS densities were significant between passage 1 and passage 4 in dispersed cell cultures on day 8 ($p < 0.0079$). No significant differences were found between passage 1 and 4 on other days.

The growth curve of explant cultures in passage 1 showed an initial decline below 10,000 cells/ml on days 1, 2 and 3 also, but the initial decline did not appear in passage 4, whose cell concentrations were above 10,000 cells/ml on day 1, 2 and 3 (Figure 13B). Before day 4, the cell density of passage 1 was lower than that of passage 4 by explant culture. Nevertheless, the cell density of passage 1 was higher than that of passage 4 on days 5, 6, 7 and 8. The differences in cell densities were significant between passage 1 and passage 4 by explant culture on day 8 ($p < 0.0159$). There was no significant difference between those passages on other days.

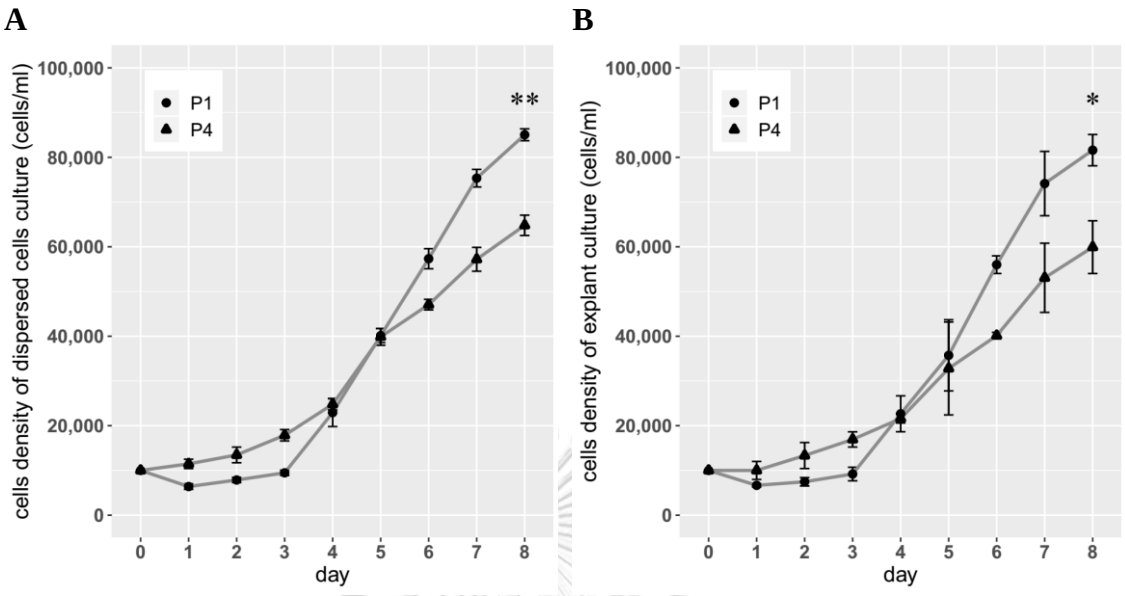

Figure 13. FLS growth curve in passage 1 and 4 by primary culture. (A) The cell growth curve of FLS by dispersed cell culture. On day 8, the cellular density of passage 1 was higher than that of passage 4. (B) The cell growth curve of FLS by explant culture. On day 8, the cellular density of passage 1 was higher than that of passage 4. Values shown are mean (±SE), N=5 separate experiments. Data analyzed with Wilcoxon test. *p<0.05, **p<0.01.

4.3 Cell doubling time

Figure 4.3 shows the doubling time of these dispersed cell cultures which was 62.20 ± 0.45 h (mean ± SE) in passage 1, which was lower than 71.41 ± 1.36 h in passage 4, a difference that was statistically-significant ($p < 0.0079$). The mean cell doubling time in passage 1 was 63.63 ± 1.41h, which was lower than 76.19 ± 4.49h in passage 4 ($p < 0.0159$). However, the population doubling time in passage 1 was not significantly different between dispersed cell cultures and explant cultures ($p = 0.5476$). When compared to passage 4 of explant cultures, the population doubling time of passage 4 of dispersed cell cultures was not significantly different ($p = 0.6905$).

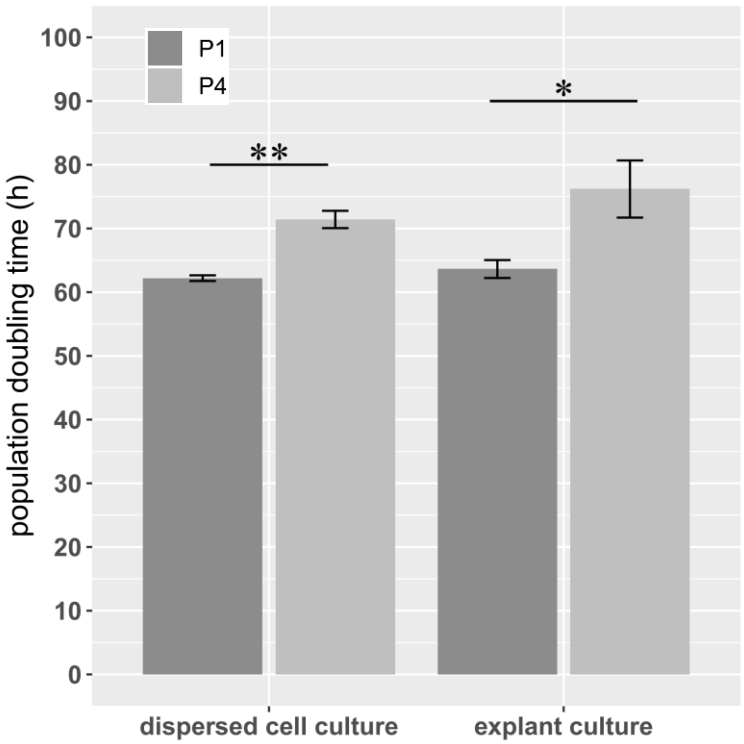

*Figure 14. The cell doubling time of passage 1 cultures and passage 4 cultures: dispersed cell cultures and explant cultures. Values shown are mean (±SE), N=5 separate experiments. Data analyzed with Wilcoxon test. *p<0.05, **p<0.01.*

4.4 Culture duration time

Two different methods were used to isolate FLS. The first was to use explant cultures, allowing the FLS to naturally grow out from the synovium sections. The second was to enzymatically disperse cells by treatment with collagenase and trypsin. 85% confluency of FLS was set as the cell density prior to subculture. The culture duration times were recorded in different passages of dispersed cell cultures and explant cultures (Figure 15). Compared to passage 0, cells in dispersed cell cultures took 4.0 d (±0.9) to reach this level of confluency, while cells in passage 0 of explant cultures took longer to achieve 85% confluency (14.0 ± 1.1 d), a statistically-significant difference (p = 0.0117). For passages 1, 2, 3 and 4, the mean times to achieve 85% cellular confluency by explant cultures were longer than those for dispersed cell cultures, but significant differences were not found. Based on different culture duration time of two methods, dispersed cell cultures were used in all subsequent studies.

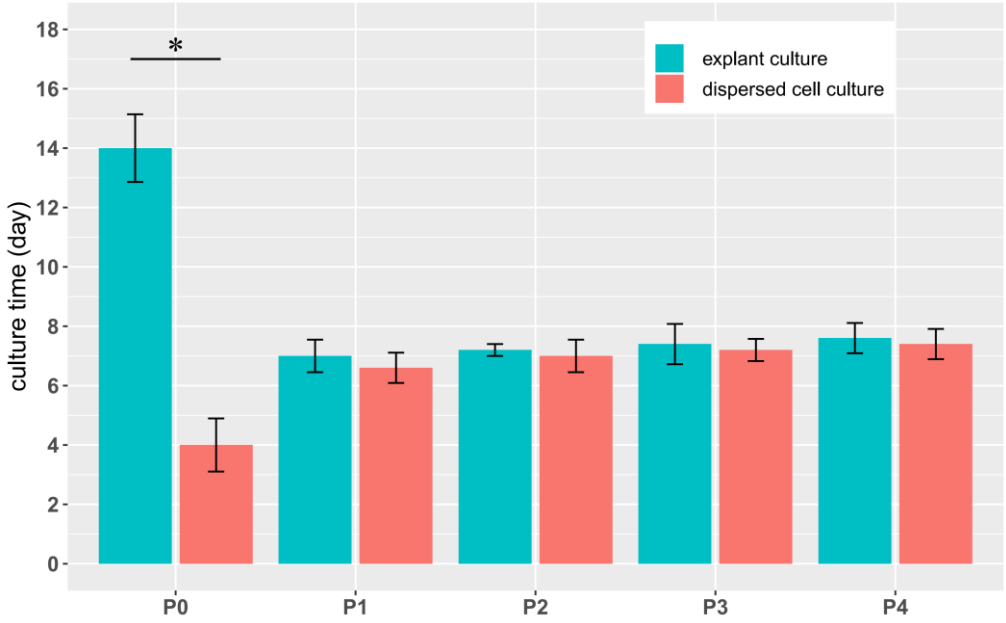

Figure 15. Cell culture time. The culture time in passage 0 of explant cultures to achieve 85% confluency was greater than that of dispersed cells. The time (in days) for explant cultures to achieve 85% confluency was 7.0±1.2, 7.2±0.4, 7.4±1.5 and 7.6±1.1 d, for P1 to P4, respectively, while dispersed cell cultures this time was 6.6±1.1, 7.0±1.3, 7.2±0.8, 7.4±1.1 d. Values shown are mean (±SE), N=5 separate experiments, data analyzed by the Wilcoxon test. *p <0.05.

4.5 Cell cycle kinetics of P1 and P4 of dispersed cells

The cell cycle kinetics can be influenced by different passage stages or FLS purity, and flow cytometry was used to test cell phases of P1 and P4 cultures. In Figure 16A and B, two peaks are apparent, representing G0/G1 (Gap 0 and 1) phases and G2/M (Gap 2 and mitosis) phases, respectively. The trough between peaks represents the cells in S phase (DNA Synthesis). 69.23±0.49% cells of P1 were in G0/G1 phase (Figure 16A), while 73.42±1.05% cells of P4 were in G0/G1 phase (Figure 16B) (p = 0.0362). 14.56±0.36% of P1 cultures were in S phase, which was greater than cells ion P4 (11.43±0.71%) and this difference between P1 and P4 was statistically significant (p = 0.0159). The percentage of P1 cells in G2/M phase was 16.20±0.32% which was not different from that of P4 cultures (15.15±0.74%) (Figure 16C).

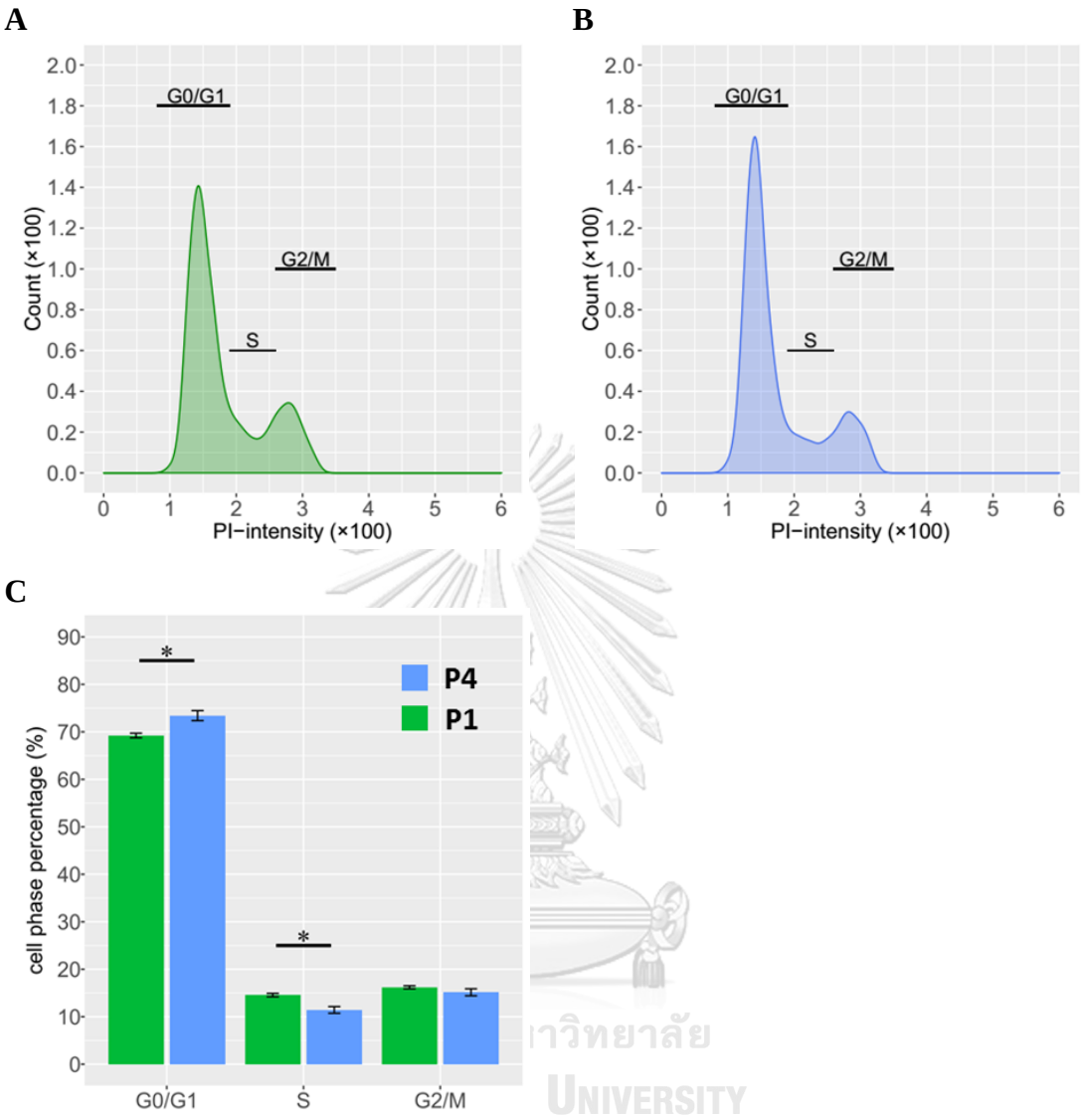

Figure 16. Cell cycle distribution analysis of P1 and P4 cultures. (A) The cell phases were determined by DNA content of P1 cells while in (B), P4 cells were analysed. (C) Percentages of P1 and P4 cells in different phases were analyzed. The percentage of P1 cells in G0/G1 was significantly lower than that of P4 cells, but the percentage of P1 cells in S phase was significantly higher than that of P4 cells. There was no significant difference in the G2/M phase between the different cultures (N=5). Values shown are mean (± SE), with data analyzed by the Wilcoxon test. *$p<0.05$.

4.6. Passage 4 FLS purity increase by dispersed cell culture increase

FLS purity was confirmed by staining cultured cells with fibroblast-positive and -negative antibodies: CD90+, CD55+, CD11b- and CD64- was used to confirm the identity of FLS by flow cytometry. Figure 17 and show an example of the expression of these four CD markers on cultured cells from P1 and P4 from a single patient sample, with the marker set as 0% positive for unstained cells. 74.2% of the cells in P1 were CD90+ and this was increased to 98.9% for P4 cells (Figure 17A). 45.7% of cells were CD55+ in P4 which was increased compared to P1 cells (Figure 17C). The two macrophage markers CD11b and CD64 were decreased from 34.9% to 1.6% and from 19.0% to 5.8%, respectively as culture passage number increased from P1 to P4 (Figure 18A and C).

Five separate knee OA patient samples were cultured and expression of these CD markers determined: results are shown in in Figure 17 and 18. Figure 17B shows that 99.2±0.06% of the cells in P4 were CD90+, which was significantly higher than that of P1 cells (73.5±0.8%, $p = 0.0079$). Figure 17D shows that 35.6±0.50% of the cells in P1 were CD55+, but this was significantly increased to 90.0±2.3% in P4 cells. CD11b+ and CD64+ positive cells decreased from 36.3±0.8% and 23.0±2.8%, respectively in P1, to 1.8±0.4% and 4.6±0.6%, respectively, in P4 ($p < 0.01$) (Figure 18B and D).

In Figure 4.8, the values of CD90 MFI (on a logarithmic scale) in P1 and P4 were 3.0013±0.0101 and 3.8205±0.0100 which were significantly higher than 1.9387±0.0170 in the negative controls (p=0.0002, p<0.0001, respectively). Furthermore, the MFI of CD90 in P4 was significantly greater than that in P1 (p=0.0002). The MFI values of CD55 (logarithmic scale) were 2.3601±0.0172, 3.0312±0.0158 and 3.8290±0.0124 in negative control, P1 and P4 (p<0.001), respectively). The MFI of CD11b was significantly higher in P1 (2.881±0.0173) than in the negative control (2.121±0.0149) and P4 (2.174±0.0369) (p=0.0002 and p=0.0010, respectively). There was no significant difference in MFI for CD11b between the negative controls and P4 cells ($p = 0.1522$). Similarly, there was no significant difference in CD64 expression between negative controls (2.5010±0.0071) and P1 cells (2.6009±0.0318, p=0.0900). However, the MFI of CD64 of P1 cells was higher (3.0937±0.0177) than that of P4 (p<0.001).

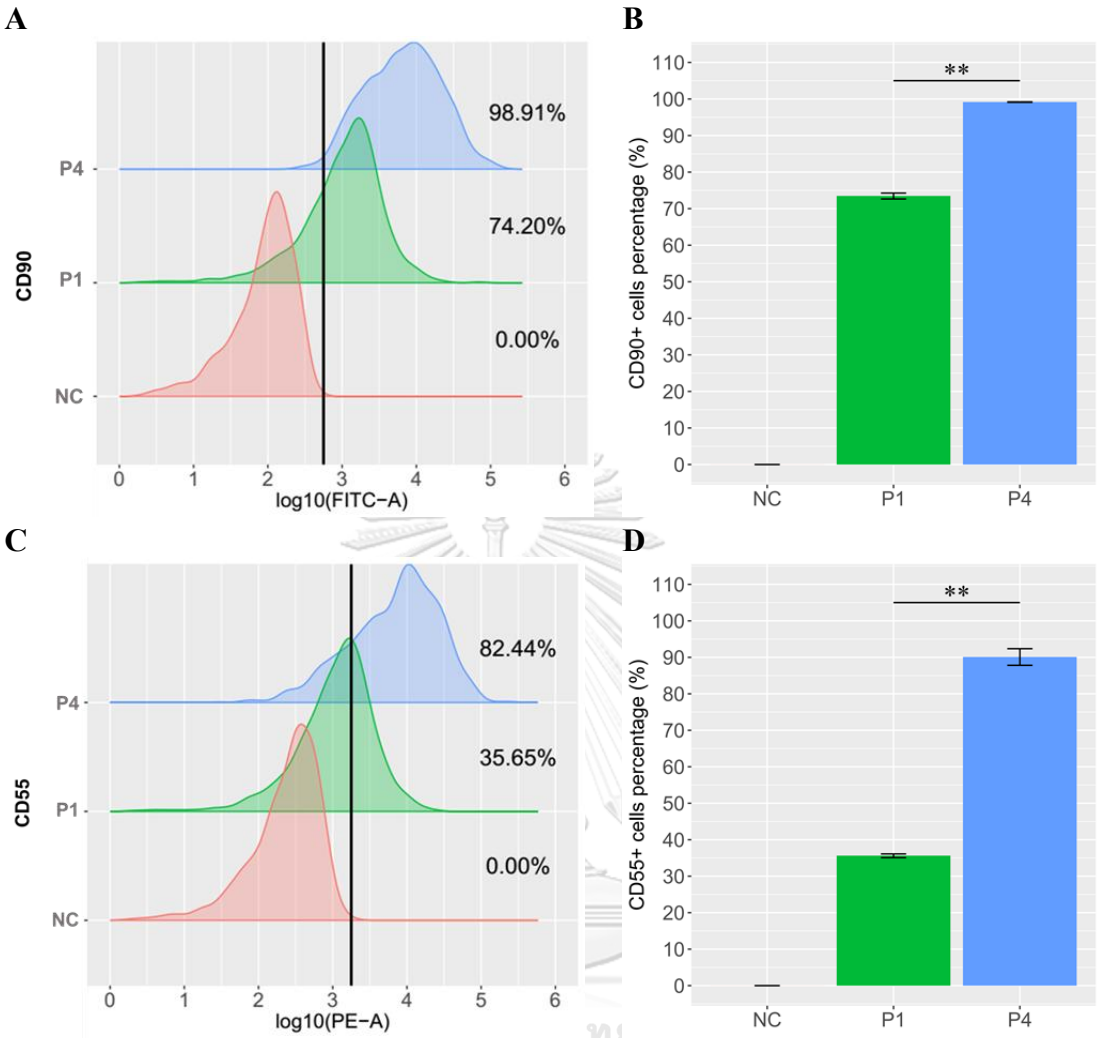

Figure 17. FLS purity of P1 and P4 determined by expression of fibroblast markers. (A) and (C) shows the percentage of CD90+ and CD55+ cells in negative control (Red traces and bars), P1 (green traces and bars) and P4 (blue traces and bars) from a single patient sample. (B) The mean percentage of CD90+ and CD55+ cells in negative control, P1 and P4 from N=5 separate experiments. The percent of CD90+ and CD55+ cells in P1 was significantly lower than in P4. Values shown are mean (± SE). Data analyzed with Wilcoxon test. ** $p<0.01$.

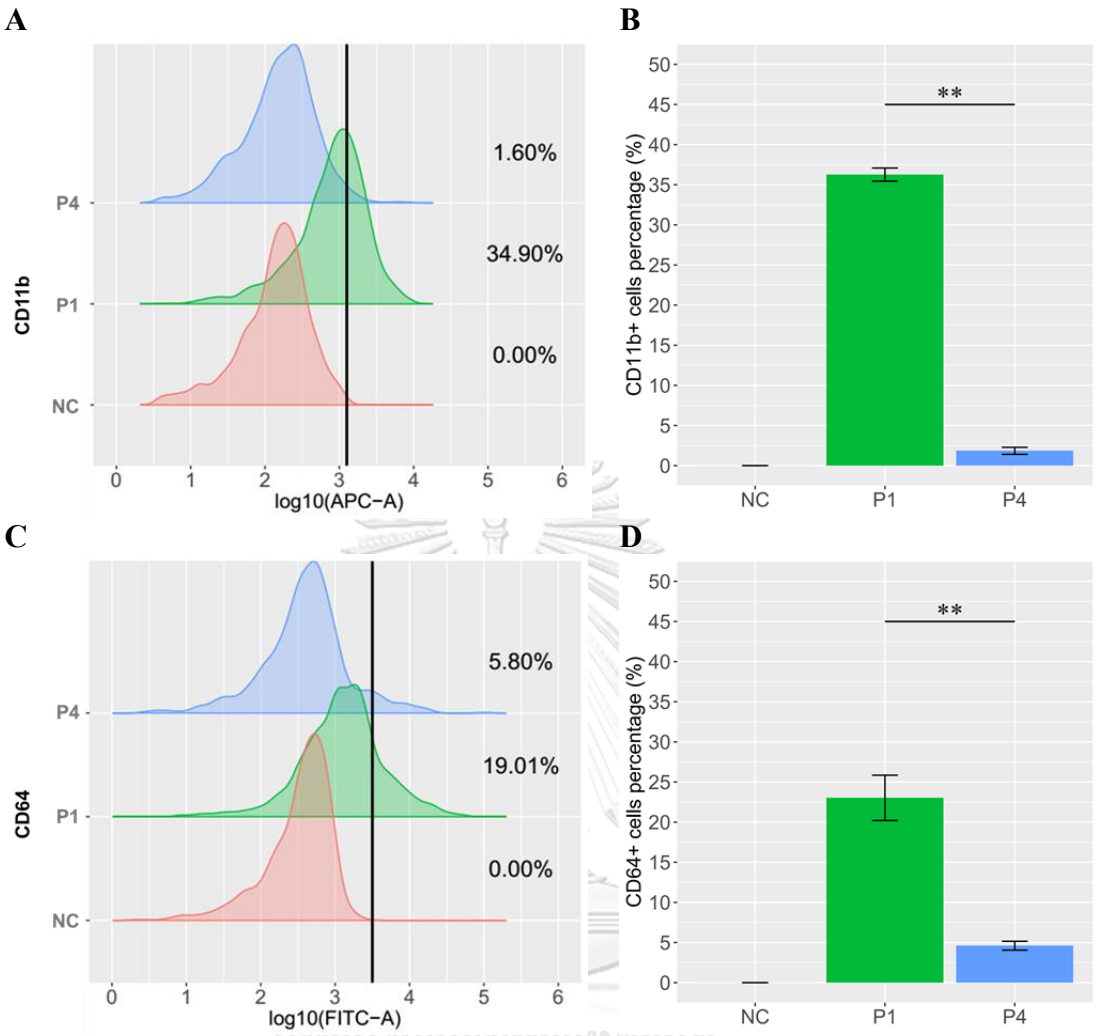

Figure 18. FLS purity of P1 and P4 determined by expression of macrophage markers (A) and (C) shows the percentage of CD11b+ and CD64+ cells in negative controls (Red traces and bars), P1 (green traces and bars) and P4 (blue traces and bars) from a single patient sample. (B) The mean percentage of CD11b+ and CD64+ cells in negative controls, P1 and P4 from N=5 separate experiments. The percent of CD11b+ and CD64+ cells in P1 was significantly higher than in P4. Values shown are mean (± SE). Data analyzed with Wilcoxon test. **p<0.01.

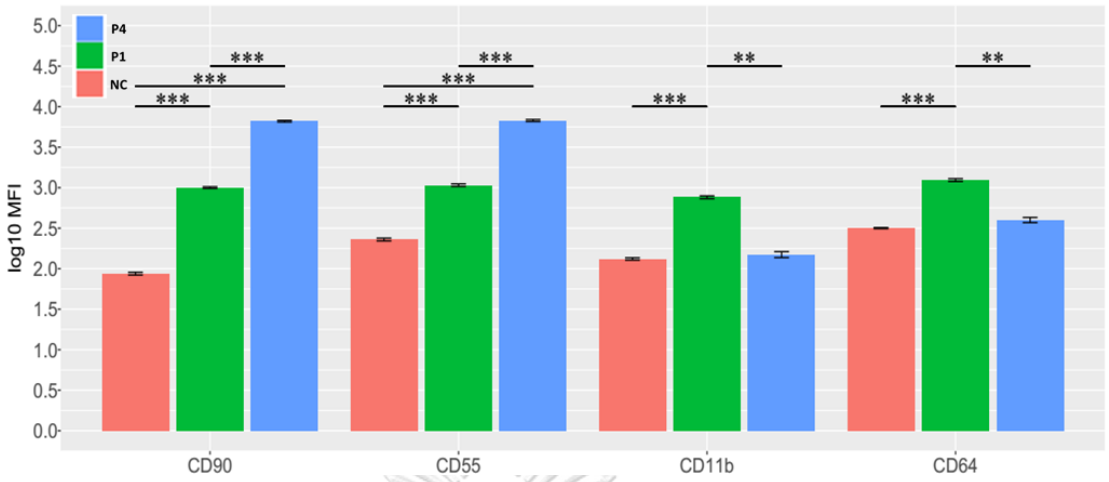

Figure 19. MFI values (logarithmic scale) of positive and negative fibroblast CDs markers. The logarithm values of CD90+ and CD55+ cells in P4 were higher than in the negative controls and P1. The values of CD11b+ and CD64+ cells in P4 were higher than in negative controls (NC) or P1. Values shown are mean (± SE). Data analyzed with Conover test. $^{**}p<0.01$, $^{***}p<0.001$.

Part B: Neutrophil Isolation and Functional Assays

4.7 Neutrophil purity by microscopy

Isolated cells on cytospins were stained with Wright's stain to identify the level of purity and types of contaminating cells. In Figure 20, all cell nuclei were stained blue and typically, the neutrophil nucleus contained 2-5 lobes while the cytoplasm stained pink. Eosinophils were identified as their cytoplasm stained bright red while basophil cytoplasm (very rarely detected) was dark blue by Wright's staining. The nucleus of lymphocytes was distinct from that of granulocytes and was round and stained dark blue (Figure 20A). The purity of neutrophils isolated by Polymorphprep by this visual determination was 98.15±0.05% while contaminating cells comprised: eosinophils 0.84±0.07%; basophils, 0.19±0.05%; mononuclear phagocytes 0.36±0.06% and lymphocytes 0.46±0.05 (Figure 20B).

4.8 Neutrophils purity by flow cytometry

The purity of isolated neutrophils was also measured by flow cytometry. Firstly, single cells (singlets) were gated to separate doublets of cells (Figure 21A). Neutrophils in the gated singlets were identified by their characteristic FSC-H and SSC-H properties. By this method, neutrophil purity was calculated as 98.25% and monocytes percentages were 1.75% (result from a single experiment, Figure 21B). In 5 separate experiments, neutrophil percentage was calculated as 98.50±0.19% and monocyte percentage contamination was 1.50±0.19% (Figure 21C).

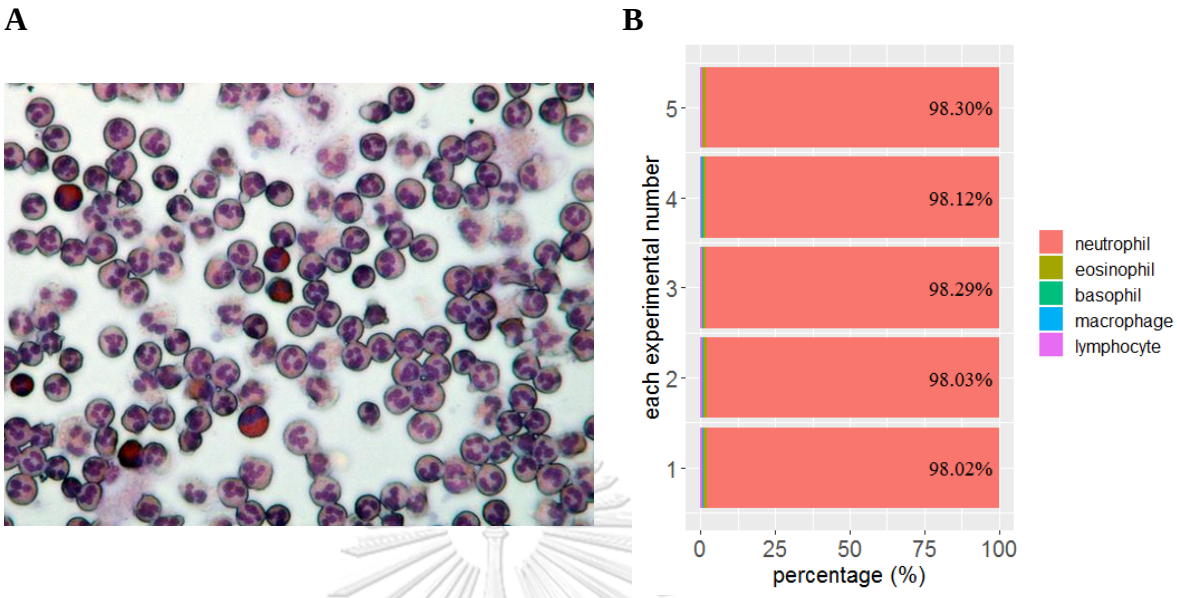

Figure 20. Image of isolated neutrophils stained by Wright's solution and visualized by light microscopy. (A) Neutrophils' nuclei stained by methylene blue was identified as 2-5 lobes and their cytoplasm contained granules stained pink by eosin red. The eosinophil cytoplasm is bright red and again, the nuclei are identified as 2-5 lobes. 100× (B) The purity of 5 separate preparations of neutrophils isolated by Polymorphprep was approximately 95-99%. Other types of leukocytes comprised 1-5% of all cells.

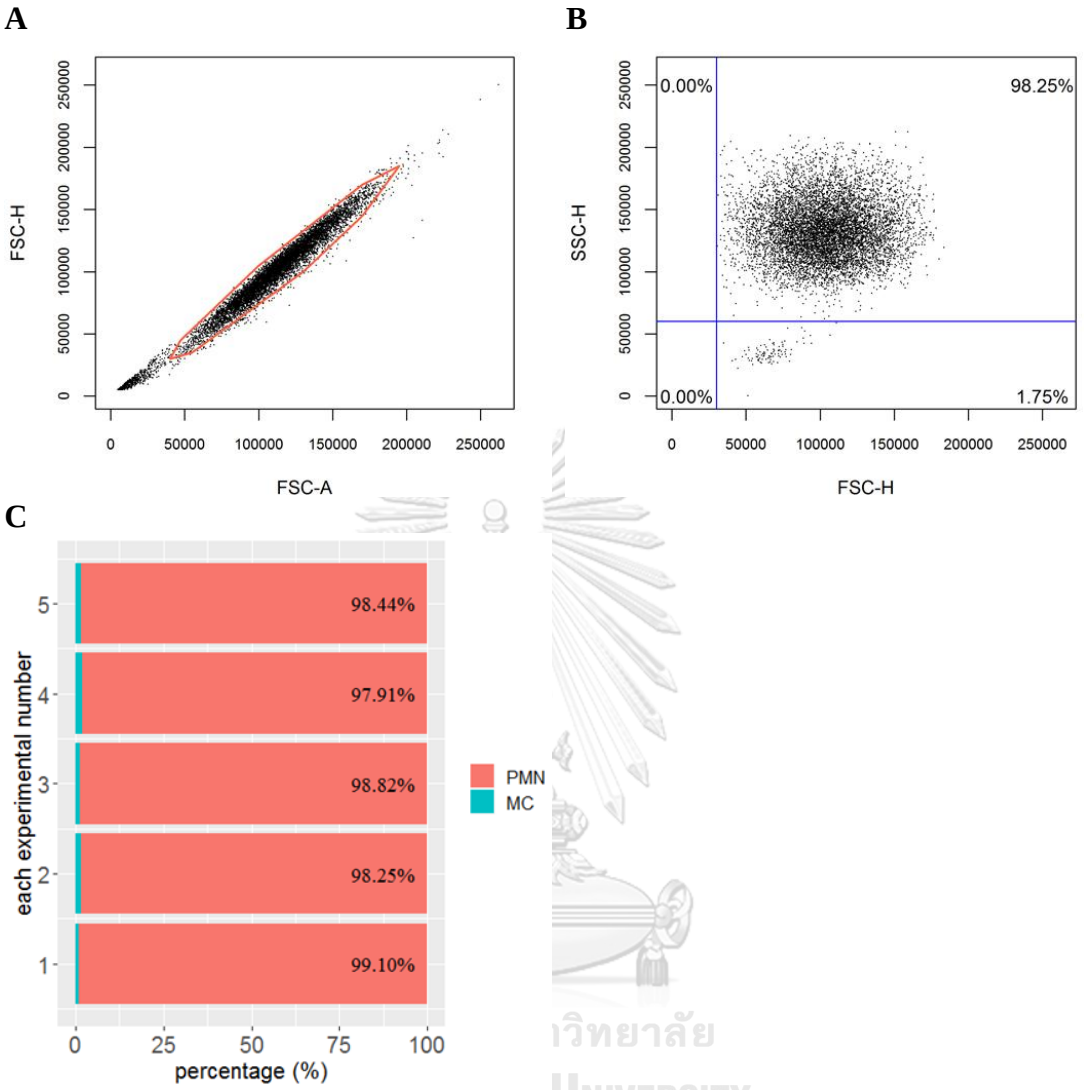

Figure 21. Flow cytometry analysis of neutrophil purity. (A) separation of singlets and doublets in a FSC-A and FSC-H plot. (B) scatter plot of neutrophils by FSC-H and SSC-H channel in a single experiment. (C) Summary of neutrophil and monocyte purity from five individual experiments.

4.9 Inhibition of chemotactic migration of neutrophils treated with TNFα

The effects of various treatments on human neutrophil migration was examined utilizing a modified transwell assay containing upper and lower chambers. In these experiments, neutrophils migrated into the lower chamber under the influence of neutrophil chemotactic factor, fMLP (10^{-8}mol/L) placed in the lower chamber. The neutrophils from sepsis patients were used as a positive control as these have decreased migration (Zonneveld et al., 2016). 5×10^6 neutrophils were added into the upper chamber and after incubation for 90min at 37°C, neutrophils that had migrated into the lower chamber were counted by a hemocytometer. Cell migration (%) was calculated as the number of neutrophils in lower chamber divided by total neutrophils number added in the upper chamber. Compared to the percentage migration of untreated neutrophils (88.2±1.3%), the TNFα (50ng/ml) treated neutrophil migration was decreased to 76.2±2.2% (p = 0.0001). As a positive control, the migration of neutrophils from sepsis patients was 49.60±2.09%, which was significantly lower than TNFα-treated or -untreated neutrophil migration (p = 0.0001) (Figure 22).

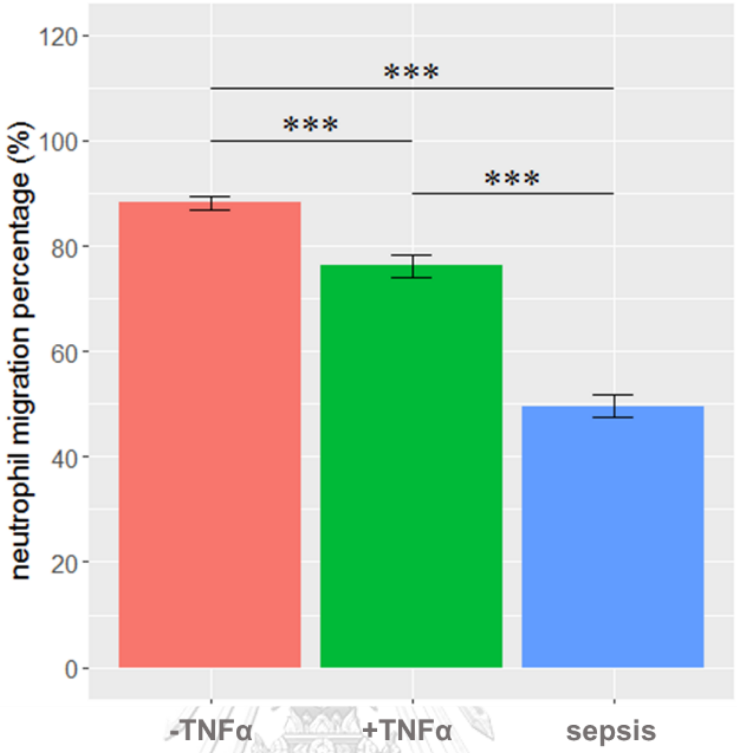

Figure 22. Effects of TNFα on fMLP-induced neutrophil chemotaxis measured in a transwell assay. Cells were incubated in the absence (-) or presence (+) of 50ng/ml-TNFα-treated: sepsis neutrophils were not treated with TNFα. 5×10^{6} cells were added into the upper chamber and incubated for 90min at 37°C. FMLP 10^{-8}mol/L was the chemotactic factor in lower chamber. The migration percentages were 88.2%, 76.2% and 49.6 in untreated neutrophils, TNFα-treated neutrophils and sepsis neutrophils, respectively. Cell migration (%) was calculated as the number of neutrophils in lower chamber divided by total neutrophils number added in upper chamber. The data were mean ± S.E. of five independent experiments. ***p<0.001.

4.10 CD11b and CD62L expression on the surface of TNFα-treated and untreated neutrophils

We then measured the effects of TNFα, at the concentration used to produce microvesicles (50ng/mL) on CD11b and CD62L expression of neutrophils. Neutrophils were therefore incubated for 20 min in the absence (control) and presence of 50ng/mL TNFα at 37°C. Previous work has shown that TNFα can up-regulate and down-regulate, respectively, levels of these receptors (Headland et al., 2015). The expression of CD11b and CD62L on freshly-isolated neutrophils and TNFα treated neutrophils are shown in Figure 23. In untreated, control neutrophils, 74.8% of the neutrophil population was CD11b+, while in TNFα treated neutrophils 86.1% of the cells were CD11b+ (Figure 23A). The MFI of CD11b in TNFα treated neutrophils was raised to 13580.54±1.02 MFI, compared to 7146.74±1.01 MFI untreated neutrophils (p = 0.0079) (Figure 23B). In comparison, 99.5% of control neutrophils were CD62L+ neutrophils while in TNFα-treated neutrophils <1% of the cells were CD11b+ (Figure 23C). The MFI of CD62L in untreated neutrophils was 114698.80±1.01 MFI, while this decreased to an MFI of 55.90±1.01 in TNFα-treated neutrophils (p = 0.0079) (Figure 23D).

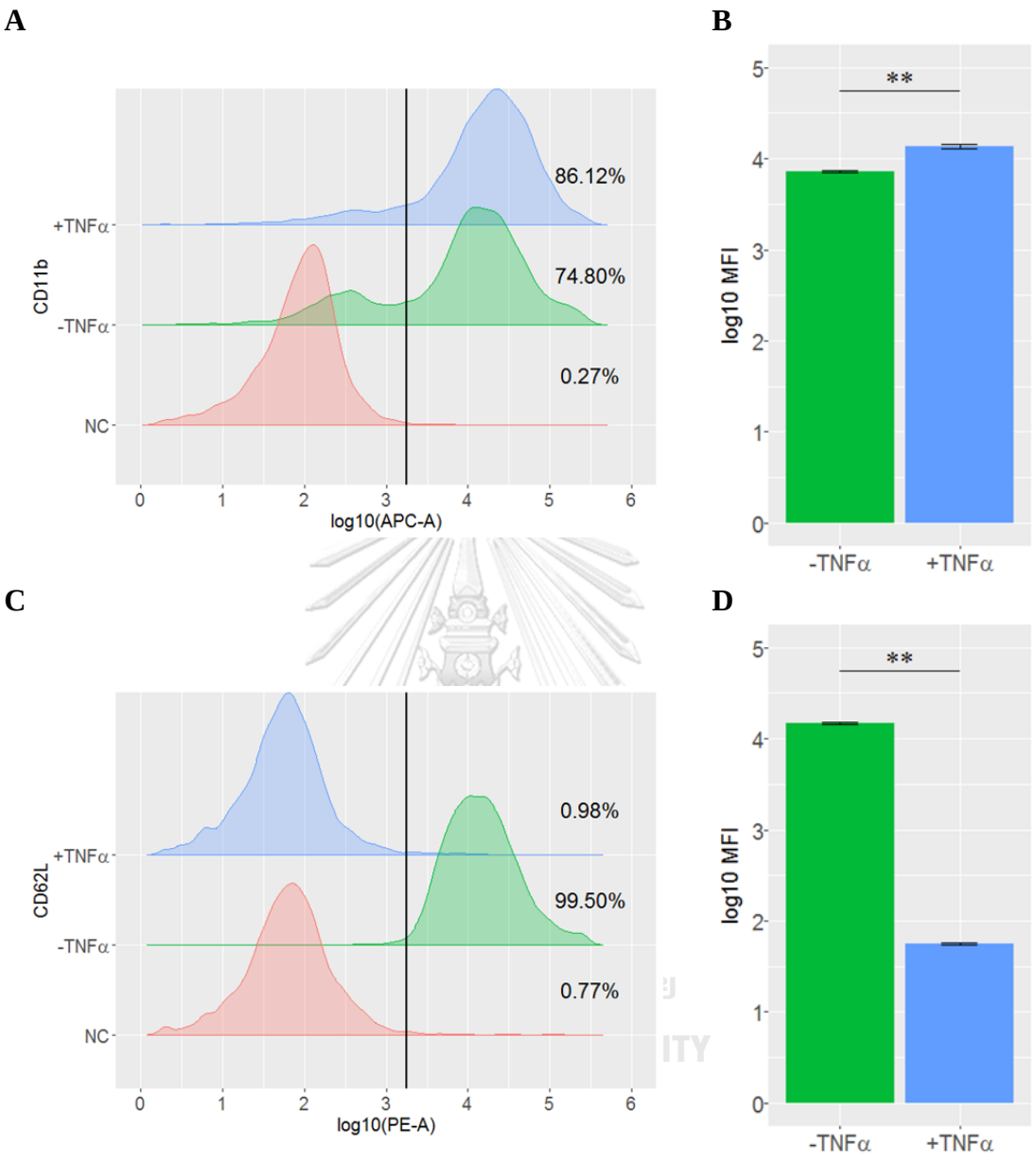

Figure 23. CD11b and CD62L surface expression on neutrophils by direct flow cytometry. (A) and (B) CD11b expression on neutrophils ± 50ng/mL TNFα for 20min. (C) and (D) CD62L expression on neutrophils with/out treatment of TNFα, as above. The data are expressed as mean ± S.E. of five independent experiments. $^{**}p<0.01$.

4.11 Respiratory burst activity of TNFα treated neutrophils

TNFα directly stimulated luminol-amplified chemiluminescence (CL) of human neutrophils, but the response was low compared to levels of CL stimulated by fMLP and PMA. For TNFα treatment, chemiluminescence values were between 5000 to 15000 AU (arbitrary units) and this increased slowly over a 30min period (Figure 24A). However, neutrophils pre-incubated with high-dose TNFα (50 ng/mL) displayed marked enhancement of chemiluminescence after stimulation with fMLP and PMA. However, the maximal responses and time to peak response were different between fMLP and PMA stimulation. The peak of CL was highest (32329 AU) at 40s after fMLP stimulation, while after 4min, the CL curve of TNFα primed/ fMLP stimulated cells overlapped with that of TNFα priming. CL responses after 30min were not significantly different (p=0.1925, Figure 24B). The peak of CL was highest (65695 AU) 200s after PMA stimulation, the peak value of which was increased 2-fold compared to fMLP stimulation. The total CL over 30min was significantly different between neutrophils activated with TNFα alone and neutrophils pre-incubated with TNFα and stimulated with PMA (p<0.0001). In comparison to the CL response of TNFα activation alone and TNF followed by fMLP, the CL average of TNFα plus PMA was significantly higher (p<0.0001).

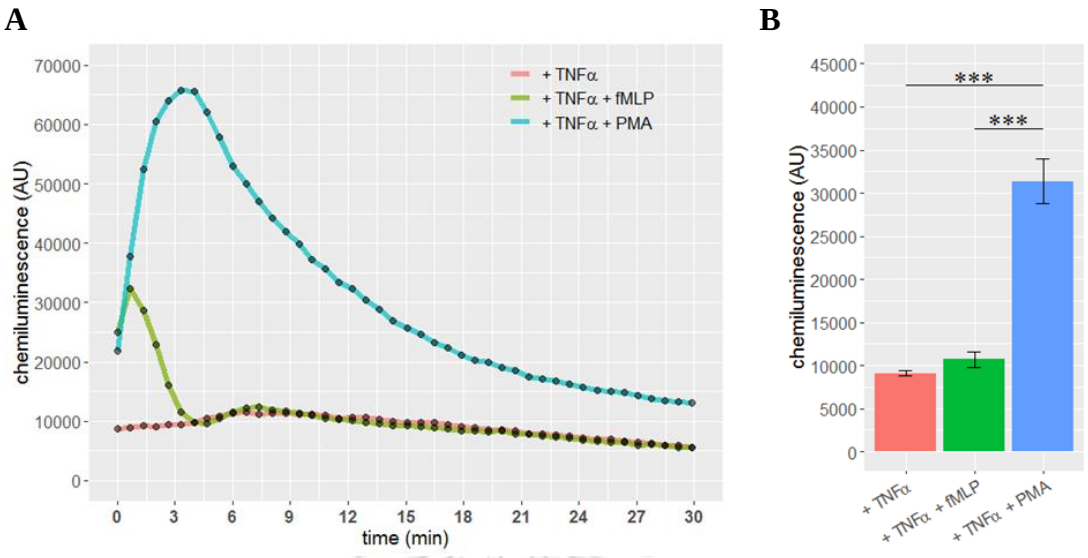

Figure 24. Effect of TNFα on neutrophil luminol-amplified chemiluminescence stimulated by fMLP and PMA. (A) Representative time-dependent curves with TNFα only and TNFα pre-treatment followed by fMLP and PMA stimulation. (B) summary data of total CL showing mean ± S.E. of 5 independent experiments. ***p<0.001

4.12 Apoptosis of untreated and TNFα treated neutrophils

To measure the effects of TNFα (at the concentration and incubation time used to make microvesicles) on neutrophil death, an Annexin V and Propidium Iodide (PI) apoptosis assay was conducted. Freshly-isolated neutrophils were incubated without (control) and with 50ng/ml TNFα for 20min at 37°C after which time neutrophils were stained with Annexin-V FITC and PI prior to flow cytometry. Apoptosis levels of freshly-isolated neutrophils were comparable to those of untreated controls (Figure 25A and B). The numbers of viable (non-apoptotic) neutrophils were not significantly different between untreated neutrophils and TNF-treated cells (98.01±0.28% v.s. 97.80±0.22%, respectively, p=0.0952) (Figure 25C). The numbers of early apoptotic and late apoptotic/necrotic neutrophils were also not significantly different between samples (p=0.1508 and p=0.3095 respectively). The percentage of early apoptotic cells was 0.79 ±0.03% in untreated neutrophils and 0.86 ±0.03% in TNF-treated neutrophils (Figure 25D), while the percentage of late apoptotic/necrotic cells was 1.20 ±0.26% in untreated neutrophils and 1.74±0.22% in TNF-treated neutrophils (Figure 25E).

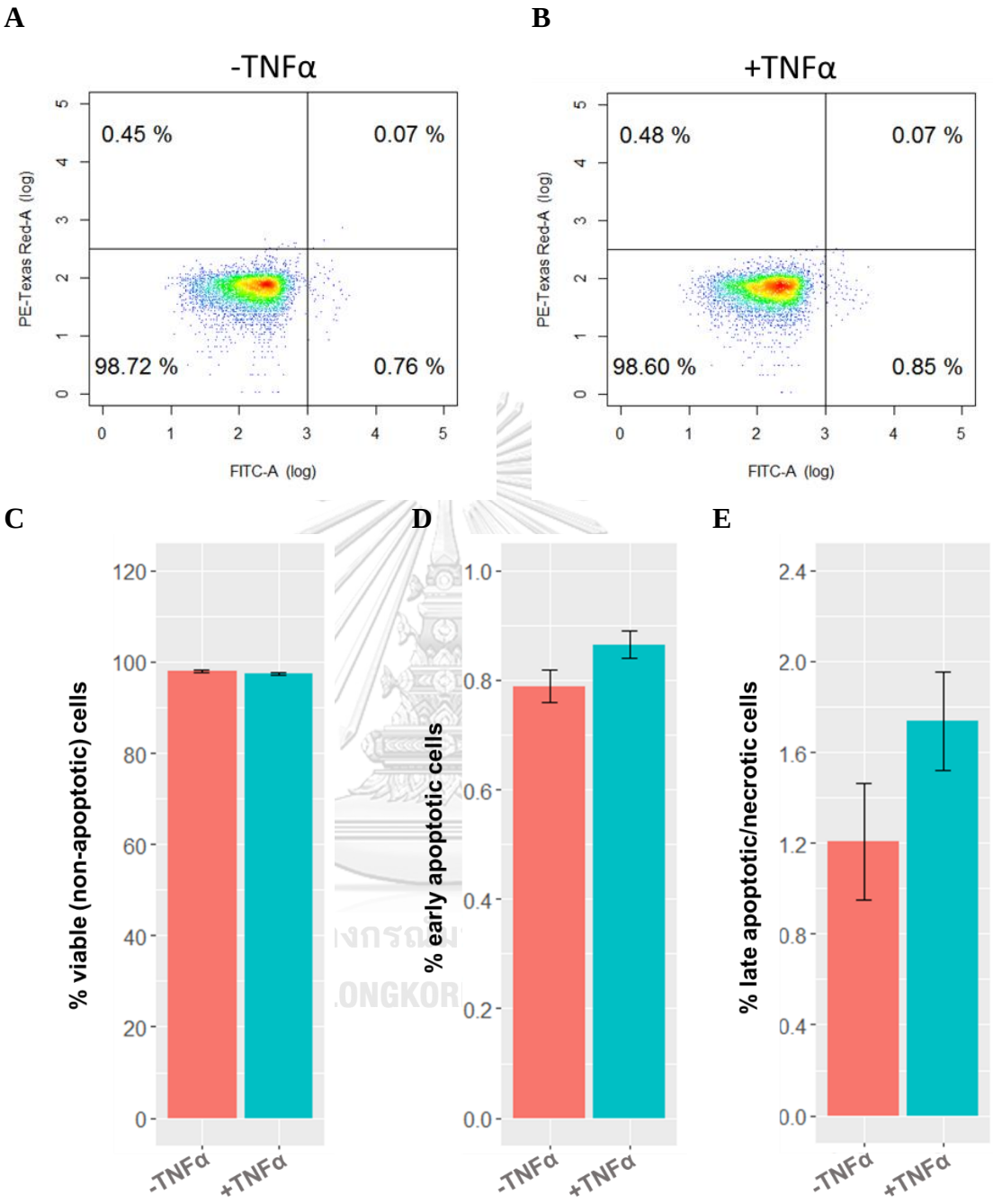

Figure 25. Annexin–V FITC/PI assay to measure neutrophil apoptosis. (A) Neutrophils were incubated in the absence (-TNFα, A) or presence (-TNFα, B) of 50 ng/mL of TNFα for 20 min. Early apoptotic cells (annexin V positive, PI negative) are seen in the lower right quadrant while late apoptotic/necrotic cells (annexin-positive and PI-positive) are seen in the upper right quadrant. Cells in the lower left quadrant are viable (non-apoptotic) cells, with dead cells in the upper left. In (C)-(E)

neutrophils were incubated in the absence or presence of TNFα showing viable (non-apoptotic cells) in (C), early apoptotic cells (annexin-positive and PI-negative) and in (D) and late/necrotic cells (annexin-positive and PI-positive) in (E). The data were mean ± S.E. of five independent experiments.

Part C: NDMV Isolation, Purification and Properties

4.13 Morphological and size characteristics of NDMV measured by TEM and SEM

Electron microscopy is often used to confirm the identity of EVs, and their size is characteristic of the type of EVs. TEM showed that the NDMV prepared and isolated in this study resembled a cup (minus a handle) and their size ranged from 200 to 500nm in diameter (Figure 26A). When visualised by SEM, NDMV had an irregular spherical appearance, with an uneven surface, and their size again mainly ranged from 200 to 500nm in diameter (Figure 26B), but some vesicles were smaller than 100nm. NDMV diameter was measured by Image J software. The average of minimum diameter from SEM and TEM is shown in Figure 26C-E. The minimum diameter measured by SEM (111.03 ±6.04nm) was lower than that measured by TEM (203.23±14.63nm), and this difference was statistically significant (p<0.0001) (Figure 26C). The maximum diameter measured by SEM (138.26±7.61nm) was lower than that measured by TEM (260.95±19.52nm), and again, this difference was significant (p<0.0001) (Figure 26D). The average diameter measured by TEM's (204.20±9.16nm) was significantly greater than that measured by SEM (124.64±6.54nm) (p<0.0001) (Figure 26E). These significant differences in NDMV diameter measured by these two techniques could be due to the various processing steps of TEM and SEM: e.g. isolated NDMV were dehydrated by acetone and ethanol for SEM.

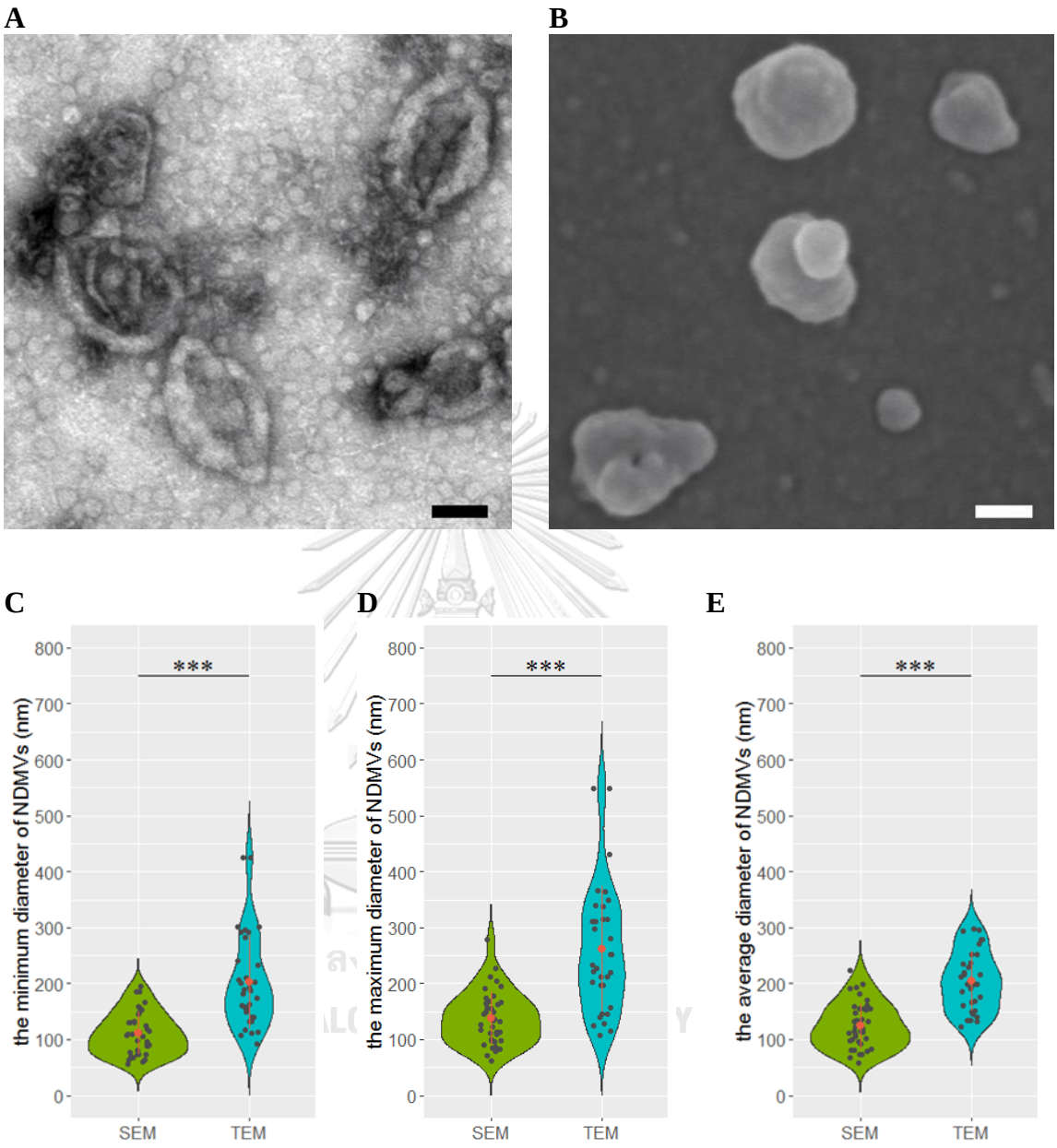

Figure 26. Images of NDMV by SEM and TEM. (A) TEM image of NDMV. (B) SEM image of NDMV. (C-E) show minimum, maximum and average diameter of NDMV, respectively, determined by Image J. The data shown are mean ± S.E. of five separate samples. Welch Two sample t-test was used to analyse these quantitative data. ***p<0.001.

4.14 Nanoparticle tracking assay (NTA) to characterize NDMV

NDMV were also characterised by Nanoparticle Tracking Analysis (NTA). As the NDMV pass through a laser beam, light was scattered and the Brownian motion of the particles can be recorded using this technique (Figure 27A). Figure 27B-E shows NTA report of NDMV concentration and size. By this methodology, the diameter of the NDMV ranged from 38.41 to 1000.00nm, with a mean value 232.3 ± 8.9nm. NDMV with a diameter of <100nm comprised approximately to 2-3% of the total population. The NDMV concentration was calculated as 3.8×10^{8} ± 1.9×10^{7} particles/mL by this method. This analysis revealed that MV were present as 4 discrete sub-populations, based on their size (Figure 27F) with the greatest proportion with a diameter of between 100-150nm.

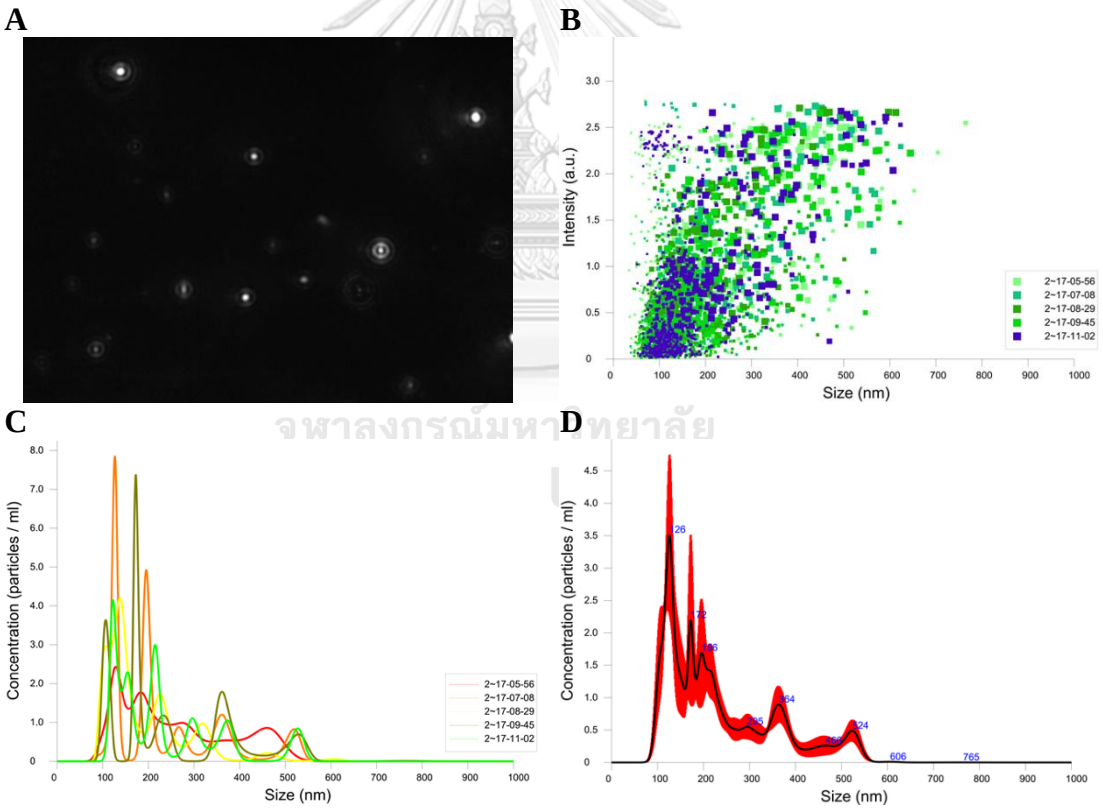

E

NANOSIGHT

Results

Stats: Merged Data

Mean:	235.4 nm
Mode:	125.7 nm
SD:	122.0 nm
D10:	114.7 nm
D50:	195.4 nm
D90:	427.5 nm

Stats: Mean +/- Standard Error

Mean:	235.7 +/- 11.9 nm
Mode:	137.4 +/- 9.1 nm
SD:	119.1 +/- 6.7 nm
D10:	114.6 +/- 3.9 nm
D50:	193.6 +/- 11.9 nm
D90:	414.2 +/- 28.5 nm
Concentration:	3.85e+008 +/- 1.03e+007 particles/ml
	19.5 +/- 0.5 particles/frame
	22.3 +/- 2.1 centres/frame

F

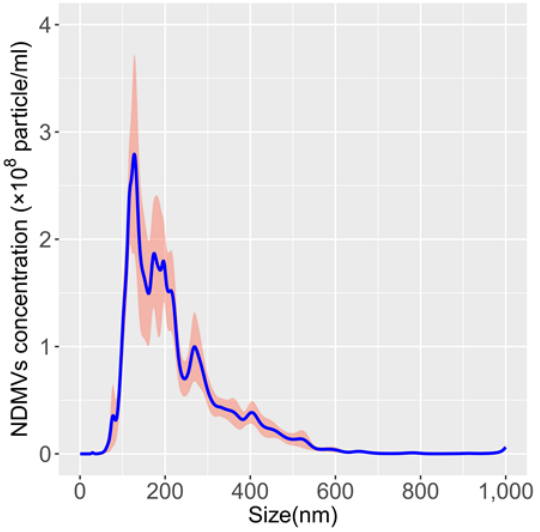

Figure 27. NTA of isolated NDMV from TNFα treated neutrophils. (A) Superimposed images captured by NTA demonstrating Brownian motion of highlighted white particles. (B) Dissimilar colours and areas of squares represent NDMV scattered light intensity and size from the 5 individual videos/measurement of each sample. (C) The graph shows the distribution of NDMV size versus their concentration (10^7 particles/ml). Each curve with distinct colour represents measurements from different samples. (D) Nanosight NTA software calculated average of NDMV size and concentration automatically by finite track length adjustment (FTLA) and plotted their relationship by 5 individual videos of one sample. The black line represents NDMV distribution of size and concentration average from 5 videos of one NDMV sample. The red trace shows the standard error of the means. (E) Text report displayed statistical description from 5 videos of one NDMV sample. D10 was used to represent intercepts for 10% of cumulative metrics, D50 for 50% and D90 for 90%. (F) Size distribution against concentration of NDMV was plotted from 5 independent samples were measured by NTA for 5 videos of each sample. The blue curve represents the mean concentrations of differently-sized NDMV while the pink trace shows standard errors of means.

4.15 Annexin V expression on the surface of NDMV

To confirm annexin V expression on the surface of neutrophils surface, flow cytometry was utilized to measure mean fluorescent intensity (MFI) on untreated neutrophils (UN), TNFα treated neutrophils (TN) and NDMV. Negative control (NC) was set as non-stained neutrophils. Figure 28A shows histograms of FITC-anti annexin V labeled cells and microvesicles. No significant differences were detected in the surface expression of annexin V on NC and UN (p=0.1979) or NC and TN (p=0.1182) (Figure 28B). The MFI of annexin V on UN and TN were not significantly different, which is consistent with previous results in Figure 25. However, annexin V expression on the surface of NDMV was significantly higher than that of UN or TN (p<0.0001).

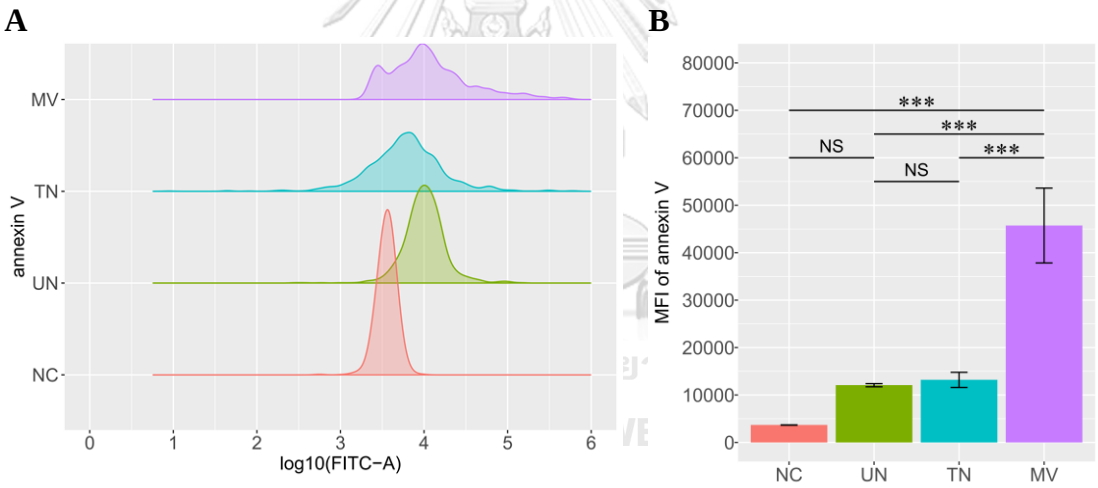

Figure 28. FITC-Annexin V expression on the surface of neutrophils and NDMV. (A) Histogram of log10 (FITC-A) annexin V of untreated neutrophils (UN), TNFα treated neutrophils (TN) and NDMV. NC was negative control of neutrophils in the absence of annexin V. (B) Annexin V MFI on the surface of UN, TN and NDMV showing mean±S.E. of five separate experiments. Tukey multiple comparisons of means was used for statistical analysis. ***p<0.001. NS = not significant.

4.16 CD11b expression on the surface of NDMV

After 50ng/ml TNFα treatment for 20min, CD11b expression increased on the surface membrane of neutrophils. Flow cytometry was then used to measure CD11b expression on the surface of intact neutrophils and NDMV. Mean fluorescent intensity (MFI) was measured on untreated, control neutrophils (UN), TNFα treated neutrophils (TN) and NDMV. Negative control (NC) was set as non-stained neutrophils. Figure 29A shows histogram of FITC-anti CD11b labeled cells and microvesicles, indicating that expression of this receptor increased following TNF treatment, but this receptor was only present at low levels on the surface of NDMV. Figure 29B shows that CD11b expression on TN was significantly increased compared to UN (p<0.0001), which was consistent with previous results (Figure 23). CD11b expression on the surface of UN, TN and NDMV were significantly higher than NC (p<0.0001, respectively). The CD11b MFI on NDMV was significantly lower than on both UN and TN (p<0.0001).

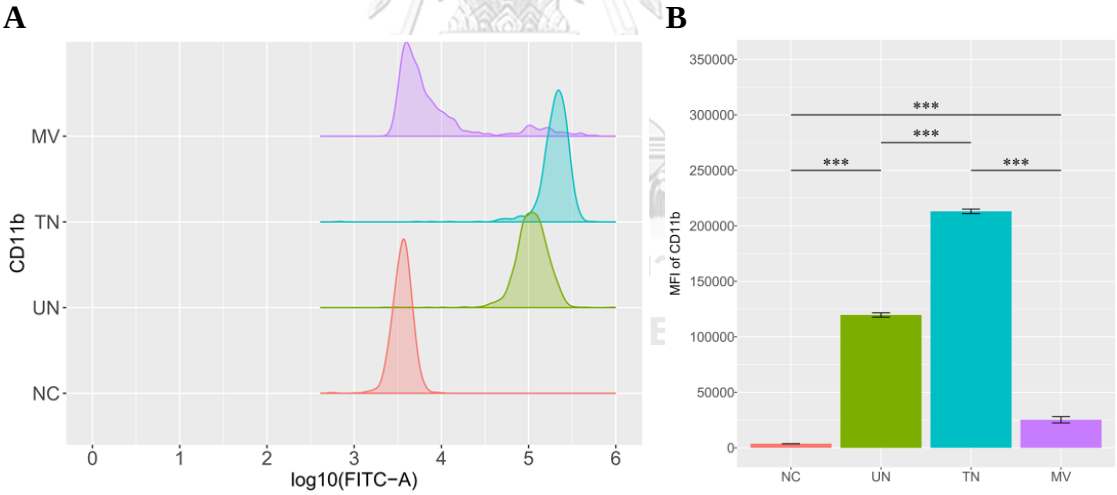

Figure 29. FITC-CD11b expression on the surface of neutrophils and NDMV. (A) Histogram of log10(FITC-A) CD11b of untreated, control neutrophils (UN), TNFα treated neutrophils (TN) and NDMV. NC was negative control of neutrophils without fluorescent antibody staining. (B) CD11b MFI on the surface of NC, UN, TN and NDMV showing mean ± S.E. of five separate experiments. Tukey multiple comparisons of means was used for statistical analysis. ***p<0.001. NS = not significant.

4.17 CD14 expression on NDMV surface

After 50ng/ml TNFα treatment for 20min, CD14 expression decreased on the surface membrane of neutrophils. Flow cytometry was then used to measure CD14 expression on the surface of intact neutrophils and NDMV. Mean fluorescent intensity (MFI) was measured on untreated, control neutrophils (UN), TNFα treated neutrophils (TN) and NDMV. Negative control (NC) was set as non-stained neutrophils with CD14. Figure 30A shows histograms of PE-anti CD14 labeled cells and NDMV. Figure 30B shows that the MFI of CD14 expression on UN and TN were significantly higher than NC (p<0.0001), while CD14 expression on UN was significantly higher than on TN (p<0.0001). Both UN and TN surface expression of CD14 were significantly greater than on NDMV's. Although CD14 MFI on NDMV was higher than NC, there was no significant difference between expression levels (p=0.2043).

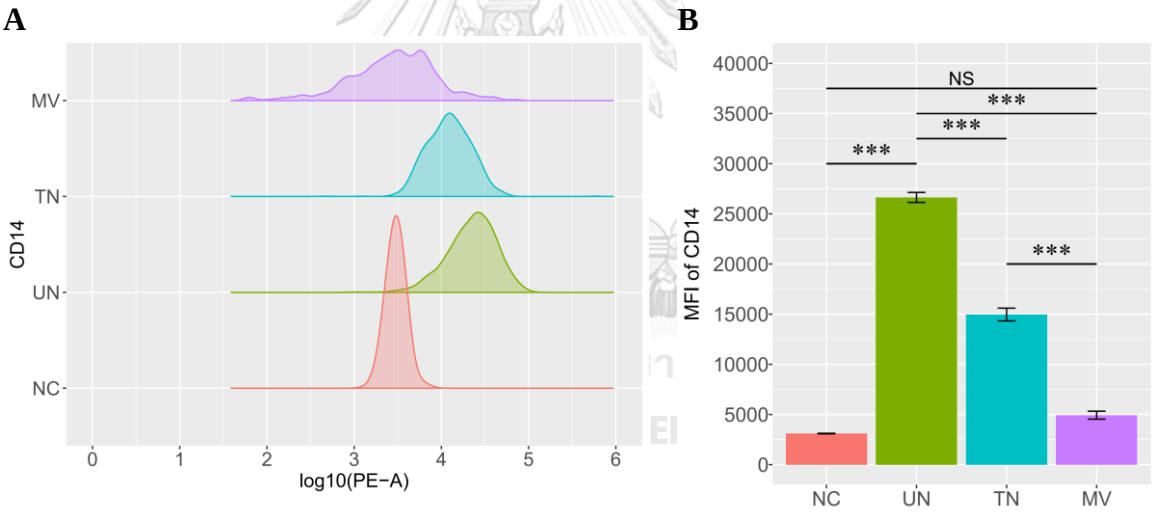

Figure 30. PE-CD14 expression on the surface of neutrophils and NDMV. (A) Histograms of log10 (PE-A) CD14 of control, untreated neutrophils (UN), TNFα treated neutrophils (TN) and NDMV. NC was negative control of neutrophils without fluorescent antibody staining. (B) CD14 MFI on the surface of UN, TN and NDMV shown as mean ± S.E. of five separate experiments. Tukey multiple comparisons of means was used for statistical analysis. ***p<0.001. NS = not significant.

4.18 CD63 expression on NDMV surface

CD63 expression was then measured on the surface of neutrophils ± treatment with 50ng/ml TNFα for 20min, and on the surface of NDMV by flow cytometry. Negative control (NC) was set as non-stained neutrophils with CD63. Mean fluorescent intensity (MFI) was measured on untreated, control neutrophils (UN), TNFα treated neutrophils (TN) and NDMV. Figure 31A shows histograms of PE-anti CD63 labeled cells and NDMV. There were no significant differences in CD63 MFI between NC and UN (p=0.9898) or between NC and TN (Figure 31B, p=0.9789). CD63 expression on UN and TN was also not significantly different (p=0.9998). However, CD63 expression on the surface of NDMV was higher than on NC and UN (p=0.0190, p=0.0455, respectively). No significant differences were found between CD63 expression on TN and NDMV (p=0.0575).

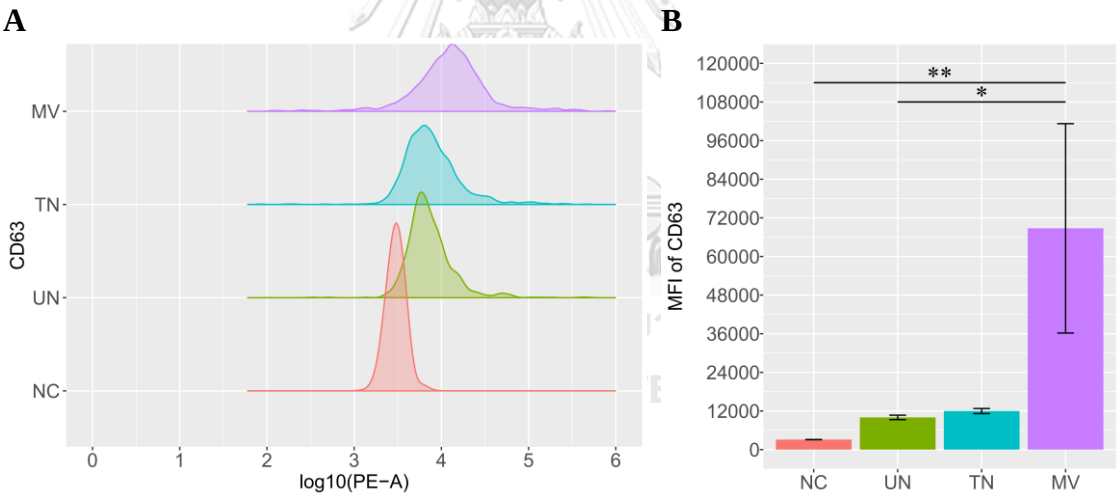

Figure 31. PE-CD63 expression on the surface of neutrophils and NDMV. (A) Histograms of log10 (PE-A) CD63 of control, untreated neutrophils (UN), TNFα treated neutrophils (TN) and NDMV. NC was negative control of neutrophils without fluorescent antibody staining. (B) CD63 MFI on the surface of UN, TN and NDMV expressed as mean ± S.E. of five separate experiments. Tukey multiple comparisons of means was used for statistical analysis. *p<0.05, **p<0.001.

4.19 CD66 expression on NDMV surface

CD66 expression was then measured on the surface of neutrophils ± treatment with 50ng/ml TNFα for 20min, and on the surface of NDMV by flow cytometry. Negative control (NC) was set as non-stained neutrophils with CD66. Mean fluorescent intensity (MFI) was measured on untreated, control neutrophils (UN), TNFα treated neutrophils (TN) and NDMV. Figure 32A shows histograms of FITC-anti CD66 labeled cells and MV and Figure 32B demonstrates that the MFI of CD66 expression on UN and TN were significantly higher than on NC (p<0.0001), while CD66 expression on UNs was significantly lower than TN's (p<0.0001). Both UN and TN surface expression of CD66 were significantly higher than on NDMV (p<0.0001, respectively). There was no significant difference between CD66 MFI on NDMV and NC (p=0.9208).

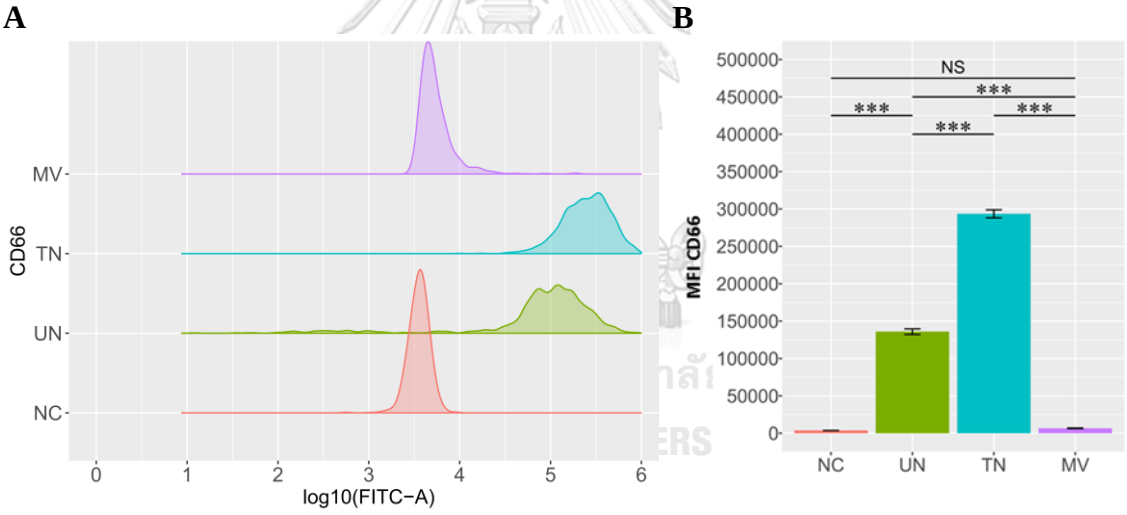

Figure 32. FITC-CD66 expression on the surface of neutrophils and NDMV. (A) Histograms of log10 (FITC-A) CD66 of TNFα untreated neutrophils (UN), TNFα treated neutrophils (TN) and NDMV. NC was negative control of neutrophils without fluorescent antibody staining. (B) CD66 MFI on the surface of UN, TN and NDMV with data shown mean ± S.E. of five separate experiments. Tukey multiple comparisons of means was used for statistical analysis. ***p<0.001. NS = not significant.

4.20 RNA isolation and characterisation from NDMV and neutrophils

Before conducting microRNA sequencing, extracted total RNA (including microRNA) quality and concentration was assayed by Nanodrop 2000/2000c Spectrophotometers (ThermoFisher, Massachusetts, US). Total RNA samples extracted from untreated neutrophils (N), TNFα treated neutrophils (T) and neutrophil-derived microvesicles (M) from three separate volunteers (given notations of 9, 10 and 11). Whole blood (50ml) was divided into two applications: 10ml for untreated neutrophils (N), 40ml for TNFα-treated neutrophils (T) and NDMV (M) generation. For spectrophotometry, the optical density (OD) 260/280 ratio should be close to 2.0 for pure RNA. The OD 260/280 ratio of cellular RNA were acceptable between 1.83 to 1.99, as well as an RNA concentration over 50ng/µl (Table 15).

Table 15. Total RNA concentration from neutrophils and NDMV and their 260/280 ratio.

Sample No.	Concentration (ng/µl)	OD 260/280
N9	67.6	1.83
N10	64.7	1.86
N11	65.4	1.91
T9	211.8	1.89
T10	289.3	1.99
T11	265.1	1.94
M9	36.6	1.42
M10	31.6	1.37
M11	25.1	1.31

RNA integrity was also measured by agarose gel electrophoresis (Figure 33). The 28S and 18S ribosomal RNA bands (upper two bands in each lane) of untreated

and treated neutrophils had bright intensity. However, while 5S ribosomal RNA bands (lowest bands) were observed, they were diffuse as they were of lower molecular weight.

The 28S and 18S ribosomal RNA bands were fairly sharp, intense bands. The intensity of the upper band should be about twice that of the lower band. Smaller, more diffuse bands representing low molecular weight RNAs (tRNA and 5S ribosomal RNA) may be present. It is normal to see a diffuse smear of ethidium bromide staining material migrating between the 18S and 28S ribosomal bands, probably comprised of mRNA and other heterogeneous RNA species. DNA contamination of the RNA preparation would have been evident as a high molecular weight smear or band migrating above the 28S ribosomal RNA band, but this was not evident. Degradation of the RNA will be reflected by smearing of ribosomal RNA bands. However, ribosomal RNA bands were not present in NDMV lanes: M9, M10 and M11. NDMV could cargo more small RNA with low molecular weight, such as microRNA.

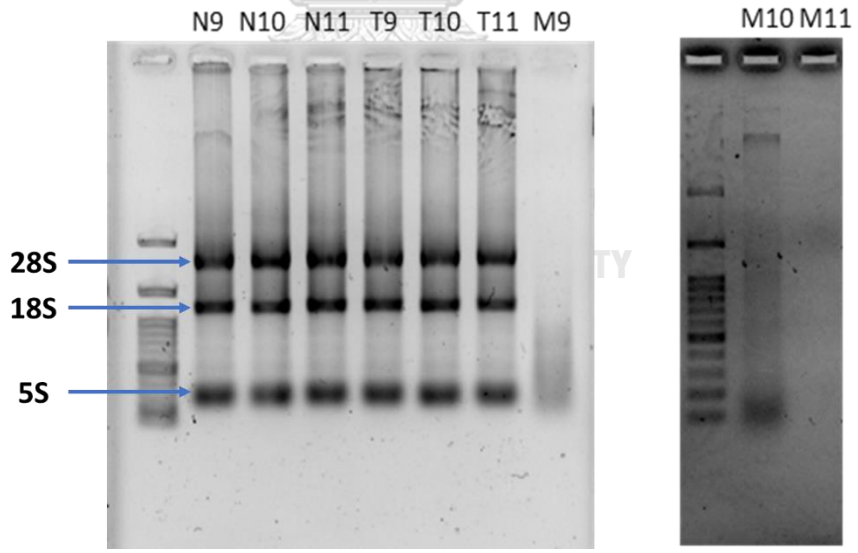

Figure 33. Total RNA integrity examination by agrose gel electrophoresis. Extracted RNA of untreated (N) and treated neutrophils (T) include 28S, 18S and 5S ribosomal RNA. Those specific ribosomal RNA were absent in neutrophils-derived microvesicles (M). Lane 1 of each gel is a DNA marker (100-3,000bp) (Cleaver Scientific, Warwickshire, UK).

4.21 Characterisation of microRNA isolated from neutrophils and NDMV

Micro-RNAs were isolated from untreated, control neutrophils (UN), neutrophils treated for 20 min with 50 ng/mL TNFα and from NDMV (prepared after treatment of neutrophils for 20 min with 50ng/mL TNFα, as described in Methods). After extraction of these microRNAs, they were sequenced, mapped and expression levels were compared between the three samples. The top 15 different expressions of microRNAs in comparisons are shown in (Table 16 and 17). Apart from identifying the range of microRNAs expressed in these three samples, comparisons were also made of those microRNAs that were up- or down-regulated between samples. Venn diagrams were used to visualize microRNAs that were differentially expressed between samples (Figure 34). These were compared as follows: A, upregulated microRNA in NDMV compared with untreated, control neutrophils (UN)- 220 microRNA; B, upregulated microRNA in NDMV compared with TNFα treated neutrophils (TN)- was 186 microRNA; C, upregulated microRNA in UN compared with TN- 125 microRNA; D, upregulated microRNA in TN compared to UN- 122 microRNA. Figure 34 shows overlapping section or microRNA among each microRNA groups. The covering area between ellipse A and B contained 159 microRNAs in Table 18. There were 128 microRNA from intersection of A and D excluded from the overlap of C and D sets. The microRNAs, with low level in UN and TN, can still be loaded into NDMV. Overlapping 23 microRNAs of A and B ellipses were likewise enriched in UN than TN. However, the number of microRNA in intersection of A and B sets, enriched in TN and UN as well, was only 8. The 159 microRNAs, enclosed by NDMV, do not only up-regulate in comparison to untreated neutrophils, but also to TNFα treated neutrophils. These 159 microRNAs maintain high levels in NDMV regardless of that neutrophils were or not treated with TNFα. These 159 enriched microRNA were further analysed for target genes prediction, GO and KEGG pathways analysis.

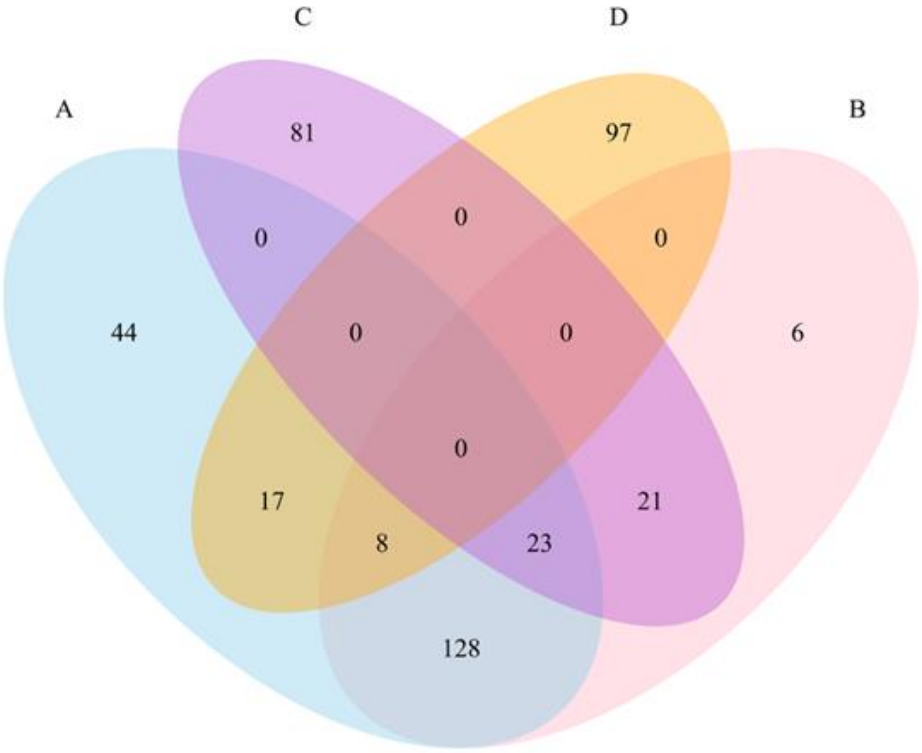

Note: A, up-regulated miRNA of NDMV vs untreated Neutrophils (N=3); B, up-regulated miRNA of NDMV vs treated Neutrophils (N=3); C, up-regulated miRNA of untreated vs treated Neutrophils (N=3); D, up-regulated miRNA of treated vs untreated Neutrophils (N=3).

Figure 34. Venn Images of upregulated microRNA among control, untreated neutrophils (UN), TNFα treated neutrophils (TN) and NDMV. The number in overlapping section stands for specific microRNAs were listed in Table 12.

Table 16. The example of top 15 different expression microRNAs in comparison of NDMV (M) and untreated neutrophils (N).

Mature_ID	different expression statistic				CPM	
	log2(FC)	FC	*p* value	q value	M	N
hsa-miR-1-3p	5.305238797	39.53994057	1.64501E-35	1.44925E-32	8.958658865	3.653420068
hsa-miR-133a-3p	5.93035462	60.98382011	6.71317E-34	1.97144E-31	6.614250799	0.683896179
hsa-miR-133b	5.60904336	48.80791981	1.43634E-21	3.16354E-19	4.455247025	-1.153796336
hsa-miR-26a-2-3p	-4.827003427	0.035231179	2.15234E-20	3.79242E-18	3.439822664	8.266826091
hsa-miR-12136	-4.988676471	0.031496242	3.67422E-19	5.39498E-17	2.762875579	7.75155205
hsa-miR-205-5p	4.459438089	22.00009866	2.13627E-17	2.68865E-15	4.10759461	-0.351843479
hsa-miR-1255a	3.652579957	12.57581467	4.88781E-17	5.3827E-15	5.267752978	1.615173021
hsa-miR-21-3p	-3.613130649	0.081722058	9.55639E-16	9.35464E-14	5.449126286	9.062256936
hsa-miR-3168	5.178229197	36.2078146	2.68724E-15	2.36746E-13	3.994863471	-1.183365727
hsa-miR-340-3p	3.10470749	8.60221083	6.37029E-15	5.10203E-13	8.349627987	5.244920497
hsa-miR-122-5p	5.586749298	48.05948548	9.93806E-15	7.29619E-13	11.28650188	5.69975258
hsa-miR-203a-3p	3.939236639	15.34010698	2.34812E-13	1.5913E-11	5.464917361	1.525680723
hsa-let-7a-5p	3.13003893	8.754585841	5.74703E-13	3.16446E-11	14.64958317	11.51954424
hsa-miR-206	4.532706174	23.14624363	1.25261E-12	6.13083E-11	5.573657377	1.040951202
hsa-miR-214-3p	4.89227578	29.69762759	2.45007E-12	1.13606E-10	3.461939461	-1.430336319

Note: *p* value is from the exact test by negative binomial distribution. Q value is the false discovery rate (FDR) adjusted *p* value. FC: fold change; CMP: counts per million.

Table 17. The example of top 15 different expression microRNAs in comparison of NDMV (M) and treated neutrophils (T).

Mature ID	different expression statistic				CPM	
	log2(FC)	FC	*p* value	q value	M	T
hsa-miR-1307-5p	-4.539160878	0.043010691	2.14267E-22	1.92626E-19	4.788000782	9.327161661
hsa-miR-15a-5p	-4.473574165	0.045011138	6.4213E-22	2.88637E-19	6.194935087	10.66850925
hsa-miR-1-3p	3.987610119	15.86318017	6.57932E-20	1.11767E-17	8.697462359	4.70985224
hsa-miR-12136	-5.308993738	0.025225143	5.64421E-20	1.11767E-17	2.505441923	7.814435661
hsa-miR-18a-5p	-4.15835556	0.056002865	8.61625E-20	1.11767E-17	3.465801936	7.624157496
hsa-miR-3168	10.08923735	1089.339061	5.62813E-20	1.11767E-17	3.768864766	-6.320372588
hsa-miR-3613-5p	-4.127465516	0.057214891	8.70266E-20	1.11767E-17	6.683502376	10.81096789
hsa-miR-340-3p	3.403986509	10.58527253	1.09343E-18	1.22875E-16	8.100237391	4.696250882
hsa-miR-101-5p	-5.742561098	0.018677419	2.73557E-18	2.73253E-16	-0.329583545	5.412977553
hsa-miR-26a-2-3p	-4.640548163	0.040091823	5.44071E-18	4.89119E-16	3.20629657	7.846844733
hsa-miR-133b	4.865630909	29.15418138	7.90624E-18	5.92309E-16	4.199230262	-0.666400647
hsa-miR-29c-3p	-4.144653302	0.056537296	7.5491E-18	5.92309E-16	6.598332539	10.74298584
hsa-miR-4785	-5.361484063	0.024323859	1.37902E-17	9.53647E-16	-0.101387878	5.260096185
hsa-miR-21-3p	-3.946546323	0.064859139	1.51463E-16	9.72612E-15	5.221739202	9.168285525
hsa-miR-590-5p	-10.35666581	0.000762663	4.49978E-16	2.69687E-14	-6.320372588	4.036293218

Note: *p* value is from the exact test by negative binomial distribution. Q value is the false discovery rate (FDR) adjusted *p* value. FC: fold change; CMP: counts per million.

Table 18. MicroRNA quantity and name of overlapping section in figure 4.8.

Set intersection	quantity	microRNA
A∩B	159	Total microRNA of A∩B∩C and A∩B∩D and (A∩B) ∉ (C∪D)
A∩B∩C	23	hsa-miR-1290, hsa-miR-340-3p, hsa-let-7c-5p, hsa-miR-3143, hsa-miR-744-5p, hsa-miR-223-5p, hsa-miR-128-3p, hsa-miR-148a-3p, hsa-miR-3605-5p, hsa-miR-99a-5p, hsa-miR-4508, hsa-miR-424-3p, hsa-miR-3158-3p, hsa-miR-2115-3p, hsa-miR-4746-5p, hsa-miR-200a-5p, hsa-miR-22-5p, hsa-miR-3186-5p, hsa-miR-34b-3p, hsa-miR-9-3p, hsa-miR-941, hsa-miR-218-5p, hsa-miR-16-2-3p
A∩B∩D	8	hsa-miR-1-3p, hsa-miR-10b-5p, hsa-miR-214-3p, hsa-miR-1255a, hsa-let-7e-5p, hsa-miR-30a-3p, hsa-miR-409-3p, hsa-miR-320d
(A∩B) ∉ (C∪D)	128	hsa-miR-3168, hsa-miR-4488, hsa-miR-4497, hsa-miR-122-5p, hsa-miR-124-3p, hsa-miR-133b, hsa-miR-1269b, hsa-miR-219a-2-3p, hsa-miR-6869-5p, hsa-miR-133a-3p, hsa-miR-615-3p, hsa-miR-206, hsa-miR-4492, hsa-miR-4510, hsa-miR-184, hsa-miR-125b-1-3p, hsa-miR-4654, hsa-miR-203a-3p, hsa-miR-129-5p, hsa-miR-10400-5p, hsa-miR-122-3p, hsa-miR-10398-3p, hsa-miR-4516, hsa-miR-205-5p, hsa-miR-125b-2-3p, hsa-miR-4638-5p, hsa-miR-369-5p, hsa-miR-30c-2-3p, hsa-miR-3179, hsa-miR-511-5p, hsa-miR-137-3p, hsa-miR-7704, hsa-miR-455-3p, hsa-miR-149-5p, hsa-miR-433-3p, hsa-miR-214-5p, hsa-miR-455-5p, hsa-miR-125b-5p, hsa-miR-490-3p, hsa-miR-377-5p, hsa-miR-365b-5p, hsa-miR-4773, hsa-miR-7973, hsa-miR-323a-3p, hsa-miR-371b-5p, hsa-miR-129-1-3p, hsa-miR-204-5p, hsa-miR-6818-3p, hsa-miR-505-5p, hsa-miR-4443, hsa-miR-6741-3p, hsa-miR-3202, hsa-miR-195-3p, hsa-miR-4449, hsa-miR-1827, hsa-let-7d-5p, hsa-miR-193b-3p, hsa-miR-138-5p, hsa-miR-127-3p, hsa-miR-139-5p, hsa-miR-877-3p, hsa-miR-330-3p, hsa-miR-3909, hsa-miR-3177-3p, hsa-miR-6779-5p, hsa-miR-485-3p, hsa-miR-708-3p, hsa-miR-1273h-5p, hsa-let-7a-5p, hsa-miR-659-5p, hsa-miR-4781-3p, hsa-miR-4467, hsa-miR-370-3p, hsa-miR-766-5p, hsa-miR-4676-5p, hsa-miR-497-5p, hsa-miR-100-5p, hsa-miR-423-3p, hsa-miR-9-5p, hsa-miR-493-3p, hsa-miR-6842-5p, hsa-miR-486-3p, hsa-miR-342-5p, hsa-miR-3138, hsa-miR-92a-1-5p, hsa-miR-4742-3p, hsa-miR-4755-5p, hsa-miR-320b, hsa-miR-329-3p, hsa-miR-3690, hsa-miR-224-5p, hsa-miR-485-5p, hsa-miR-6130, hsa-miR-6813-5p, hsa-miR-382-3p, hsa-miR-5009-5p, hsa-miR-581, hsa-miR-1246, hsa-miR-493-5p, hsa-miR-7844-5p, hsa-miR-3150b-5p, hsa-miR-320c, hsa-miR-6842-3p, hsa-miR-382-5p, hsa-miR-6502-5p, hsa-miR-139-3p, hsa-miR-942-5p, hsa-miR-450a-2-3p, hsa-miR-625-5p, hsa-miR-4685-3p, hsa-miR-30a-5p, hsa-miR-4473, hsa-miR-6852-5p, hsa-miR-193a-5p, hsa-miR-26a-5p, hsa-miR-671-3p, hsa-miR-10399-3p, hsa-miR-6866-5p, hsa-miR-320a-3p, hsa-miR-423-5p, hsa-miR-1301-3p, hsa-miR-641, hsa-miR-331-3p, hsa-miR-365a-3p, hsa-miR-365b-3p, hsa-miR-628-3p, hsa-miR-196a-5p, hsa-miR-30c-5p
A∩B∩C∩D	0	---

A: up-regulated miRNA of NDMV vs untreated Neutrophils, B: up-regulated miRNA of NDMV vs treated Neutrophils; C: up-regulated miRNA of untreated vs treated Neutrophils, D: up-regulated miRNA of treated vs untreated neutrophils.

4.22 Target genes prediction of NDMV-enriched microRNA

To confirm the identity of the messenger RNA (mRNA) or gene expression pattern that was influenced by each microRNA, the binding sites of the 159 microRNAs enriched in NDMV, compared to neutrophils treated with TNFα, was predicted by analysis via two databases: TargetScan (Version 6.2) and miRDB (Version 4.0). The TarPmiR algorithm was used to improve the predicted precision and reliability based platform- miRWalk 2.0 (http://mirwalk.umm.uni-heidelberg.de/) (Dweep and Gretz, 2015). Predicted microRNA targets were classified into validated and non-validated sub-groups by data resource-miRTarBase.

Target genes, that were predicted by only one database alone (either TargetScan or miRDB), were excluded from further analyses. Predicted target genes, which were listed in both TargetScan and miRDB were used for next step analysis. In total, 657,394 genes were predicted by either resource alone, but 7,978 target genes were predicted in both TargetScan and miRDB. Of these, 1,258 target genes were further validated by miRTarBase. Figure 35 illustrates a network of 49 microRNA interacting with their target gene and some of these target genes are shared within the network. The 10 predicted target genes and their properties are listed in Table 19.

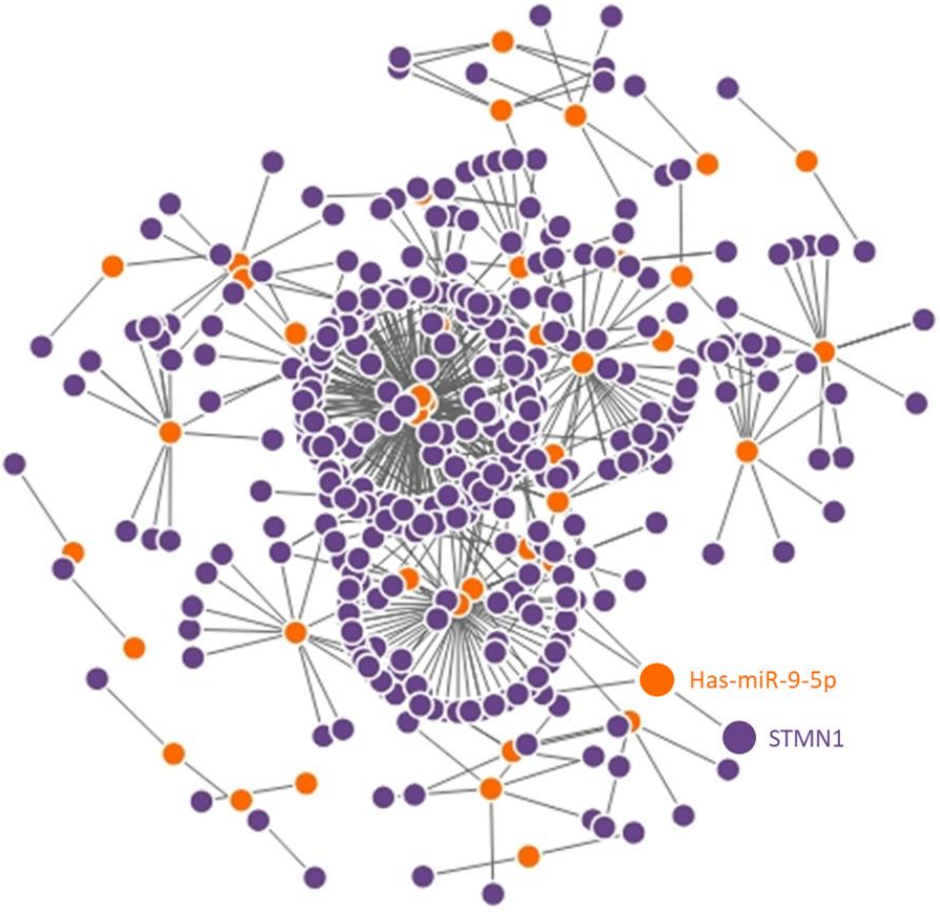

Figure 35. Typical microRNA and their target genes predicted by TargetScan and miRDB. There are 159 target genes were predicted by TargetScan, miRDB, but only predicted target genes of 49 microRNAs were available by miRTarBase. Orange dots represent microRNAs; violet dots represent predicted target genes. The selected pot shows microRNA name or its interactive gene name. The more violet pots interact with one orange pot displays the more predicted gene could regulated by this microRNA.

Table 19. Examples of 10 microRNA and their predicted target genes.

microRNA	Target gene symbol	P value	AREs	M/E motif	Pairing number	TargetScan	miRDB	miRTarBase
hsa-miR-139-5p	ROCK2	1	0.879	19.837	14	1	1	YES
hsa-miR-1-3p	NXT2	1	0.809	11.351	18	1	1	YES
hsa-miR-330-3p	CMPK1	1	0.803	8.763	18	1	1	--
hsa-miR-148a-3p	CS	1	0.794	9.309	13	1	1	--
hsa-let-7c-5p	BACH1	0.961	0.779	4.957	15	1	1	YES
hsa-miR-30c-5p	RAPGEF2	1	0.779	7.570	15	1	1	--
hsa-miR-218-5p	RLIM	1	0.765	8.303	15	1	1	--
hsa-miR-30a-5p	PTPN4	1	0.765	7.371	18	1	1	--
hsa-miR-10b-5p	XRN1	1	0.765	10.398	11	1	1	--
hsa-miR-138-5p	ATP11C	1	0.765	9.964	17	1	1	--

Notes: *p* value means binding probability: higher values are more significant and were automatically computed by TarPmiR by random forest method. AREs (AU-rich elements) represent transcript AU content 30nt in up- or down-stream interactions. M/E motif reflects probabilities of microRNA paired with target gene at various areas (Ding et al., 2016). Validated genes were listed in the miRTarBase column.

4.23 Gene ontology: molecular function (MF) of target genes

The Gene Ontology (GO) project provides structured, controlled terms describing the functions of gene products, as well as the association of these terms with the gene products performing these functions. It is specifically designed for supporting the computational representation of biological systems (Ashburner et al., 2000, Acencio et al., 2019). It is categorized into three domains and associated annotations: molecular function (MF); biological process (BP) and cellular component (CC). 159 microRNAs were differently expressed in NDMV compared with both untreated neutrophils (ellipse A) and TNFα treated neutrophils (ellipse B), as shown in Figure 34 and Table 10. Furthermore, 7,978 target genes of these 159 microRNAs were grouped with these three items, analysed by R packages: "systemPipeR", "biomaRt" and "systemPipeRdata".

For MF classification, 66 annotations of MF were found with significant differences (p<0.05). The top 25 significantly-different MF are shown in Figure 36. The most significant MF of target genes was protein binding (GO:0005515) with an adjusted p value of 1.7703×10^{-23} and highest enrichment score of 19.8745. There were 1562 target genes associated with this term, all of which interacted selectively and non-covalently with any protein or protein complex. The second most significant term of GO was DNA-binding/transcription factor activity, RNA polymerase II-specific (GO:0000981) and was associated with 231 predicted genes. This term of MF involved a protein or a protein complex that interacts selectively and non-covalently with a specific DNA sequence (sometimes referred to as a motif) within the regulatory region of a RNA polymerase II-transcribed gene to modulate transcription. Regulatory regions include promoters (proximal and distal) and enhancers. The third most significant term with p values of 5.3332×10^{-20} was regulatory region nucleic acid binding (GO:0001067), and there were 197 target genes involved in this term interacting selectively and non-covalently with a nucleic acid region that regulates a nucleic acid-based process. Such processes include transcription, DNA replication, and DNA repair. In summary, enriched microRNA in NDMV regulate a wide range of molecular functions: DNA transcription, mRNA translation, protein expression and various enzymes' activities.

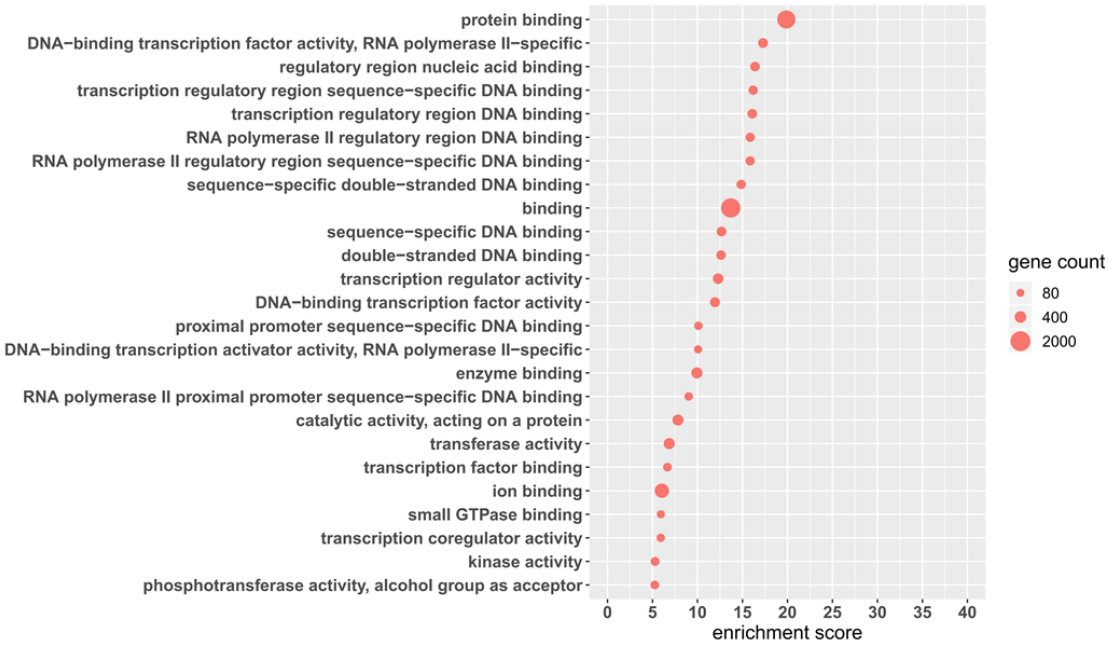

Figure 36. Representative top 25 term with significant differences of MF for target genes.

4.24 Gene ontology: biological process (BP) of target genes

475 terms of BP were found to be significantly enriched in NDMV (p<0.05). The top 25 significantly different BP are shown in Figure 37 The terms with highest enrichment score (13.6949) in BP of target genes was nervous system development (GO:0007399), but the number of target genes interacted with NDMV microRNAs related to GO:0007399 was not highest for this term. The term of cellular process (GO:0009987) contained the most target genes (17,946). This term related to any process that is carried out at the cellular level, but not necessarily restricted to a single cell. For example, cell communication occurs in more than one cell such as cells to cells communication, but also occurs at the cellular level. The second and third most enriched BP processes were protein modification (GO:0036211) and cellular protein modification (GO:0006464) process. These two terms are related to the covalent alteration of one or more amino acids occurring in proteins, peptides and nascent polypeptides. In addition, metabolic processes were also highly enriched.

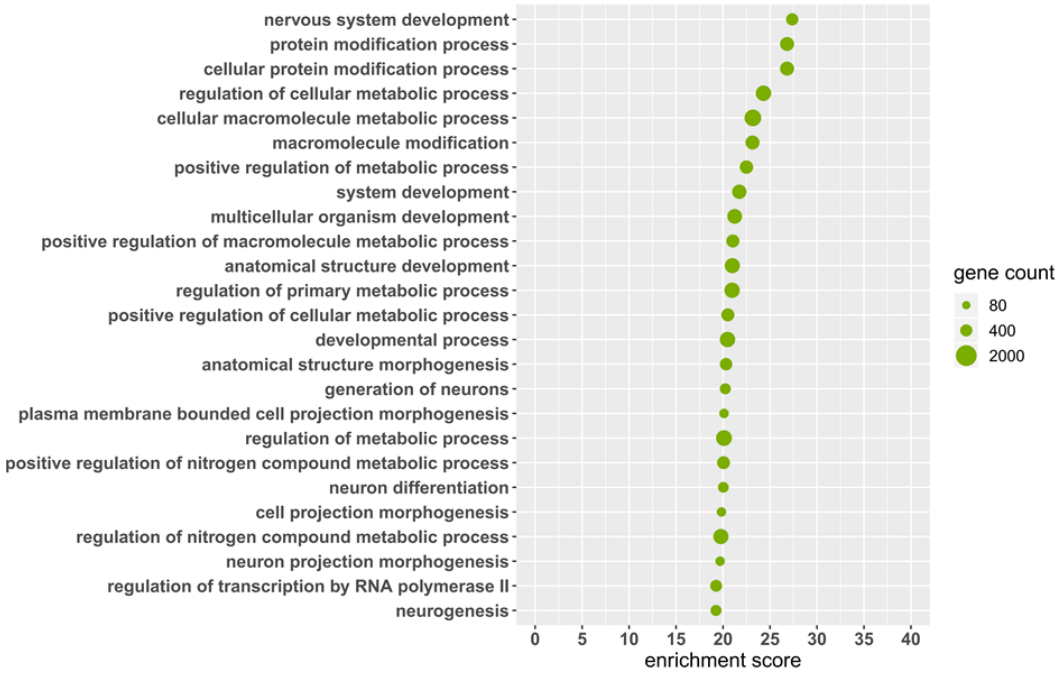

Figure 37. Representative top 25 term with enrichment scores of BP for target genes.

4.25 Gene ontology: cellular components (CC) of target genes

Significant differences were found in 81 terms of CC (p<0.05) with the top 25 significantly different CC are shown in Figure 38. The top 2 terms with highest enrichment scores were intracellular part (GO:0044424) and intracellular (GO:0005622) with enrichment scores of 37.1 and 36.8, respectively. GO:0044424 is an obsolete term of CC, that has now been replaced by GO:0005622. The term intracellular or cellular component related to the living contents of a cell, contained within (but not including) the plasma membrane, usually taken to exclude large vacuoles and masses of secretory or ingested material. In eukaryotes, it includes the nucleus and cytoplasm.

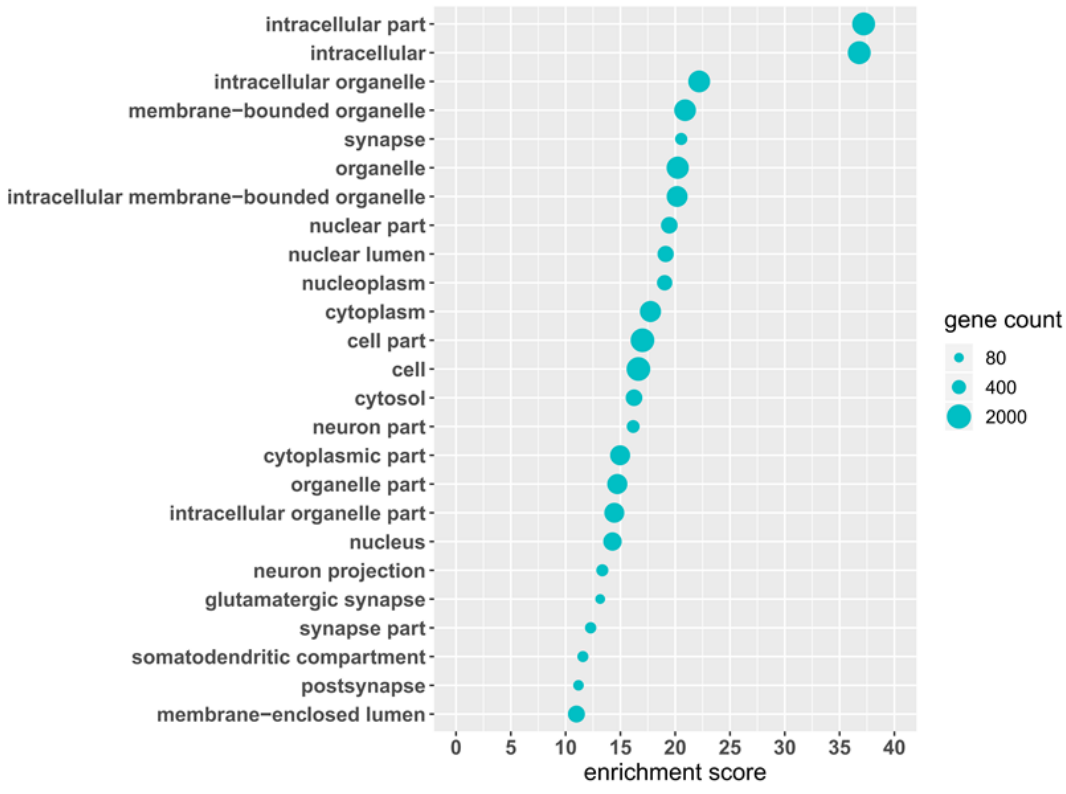

Figure 38. Representative top 25 term with enrichment scores of CC for target genes.

4.26 Kyoto Encyclopedia of Genes and Genomes (KEGG) pathways of target genes

To confirm potential interactions among microRNAs and molecules in cells, KEGG pathways were analysed. 7,978 target genes regulated by the 159 microRNAs were analysed by the R packages: "clusterProfiler", "org.Hs.eg.db" and "enrichplot".

In total, 101 KEGG pathways were significantly different (adjusted $p < 0.05$) and the top 25 significantly different pathways are shown in Figure 39A. Two major signaling pathways were identified as having the highest gene ratio (related target genes counts/total predicted target genes): PI3K-AKT and MAPK signaling pathways with gene ratios of 0.0907 and 0.0833 (adjusted p=1.02×10^{-7} and 8.93×10^{-9}). Gene ration was the number of target genes related to a specific signaling pathway divided by the number of total predicted target genes. This analysis identified 74 target genes interacting in the PI3K-AKT signaling pathway, and 68 target genes were involved in the MAPK signaling pathway. The third highest gene ratio identified (axon guidance) did not share any target genes with other top 25 pathways (Figure 39B). The PI3K-AKT signaling pathway shared 26 target genes with the MAPK signaling pathway: AKT3, MAPK1, KITLG, FGF7, IGF1, BDNF, VEGFC, HGF, NGF, FGF1, FASLG, NRAS, SOS1, ERBB4, NGFR, KIT, FGF2, IGF1R, EFNA1, PRKCA, FGFR2, MET, INSR, FGF17, IGF2 and TP53 (Figure 40 and Figure 41). In the Ras signaling pathway, with a gene ratio of 0.0612, the active Ras is capable to regulate cellular function through components of the PI3K-AKT and MAPK signaling pathways. Hyaluronic acid (HA) is an essential proteoglycan secreted by FLS, which was main proteoglycan regulated in "proteoglycans in cancer" with gene ratio of 0.0600.

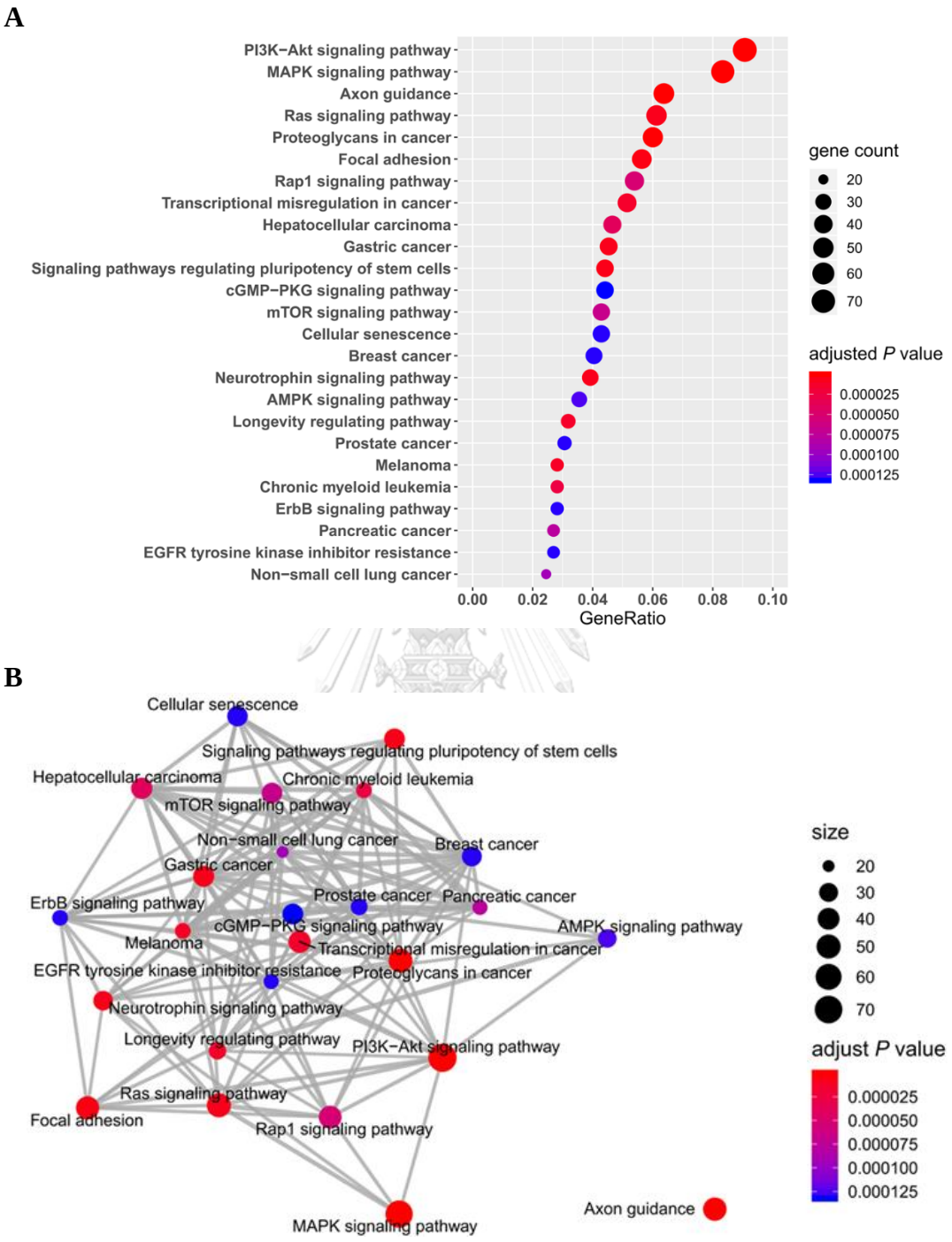

Figure 39. KEGG pathways analysis of target genes. (A) Dotplot of top 25 pathways with lowest adjusted *p* value and highest genes ratios. (B) Network of top 25 pathways with significant differences of target genes.

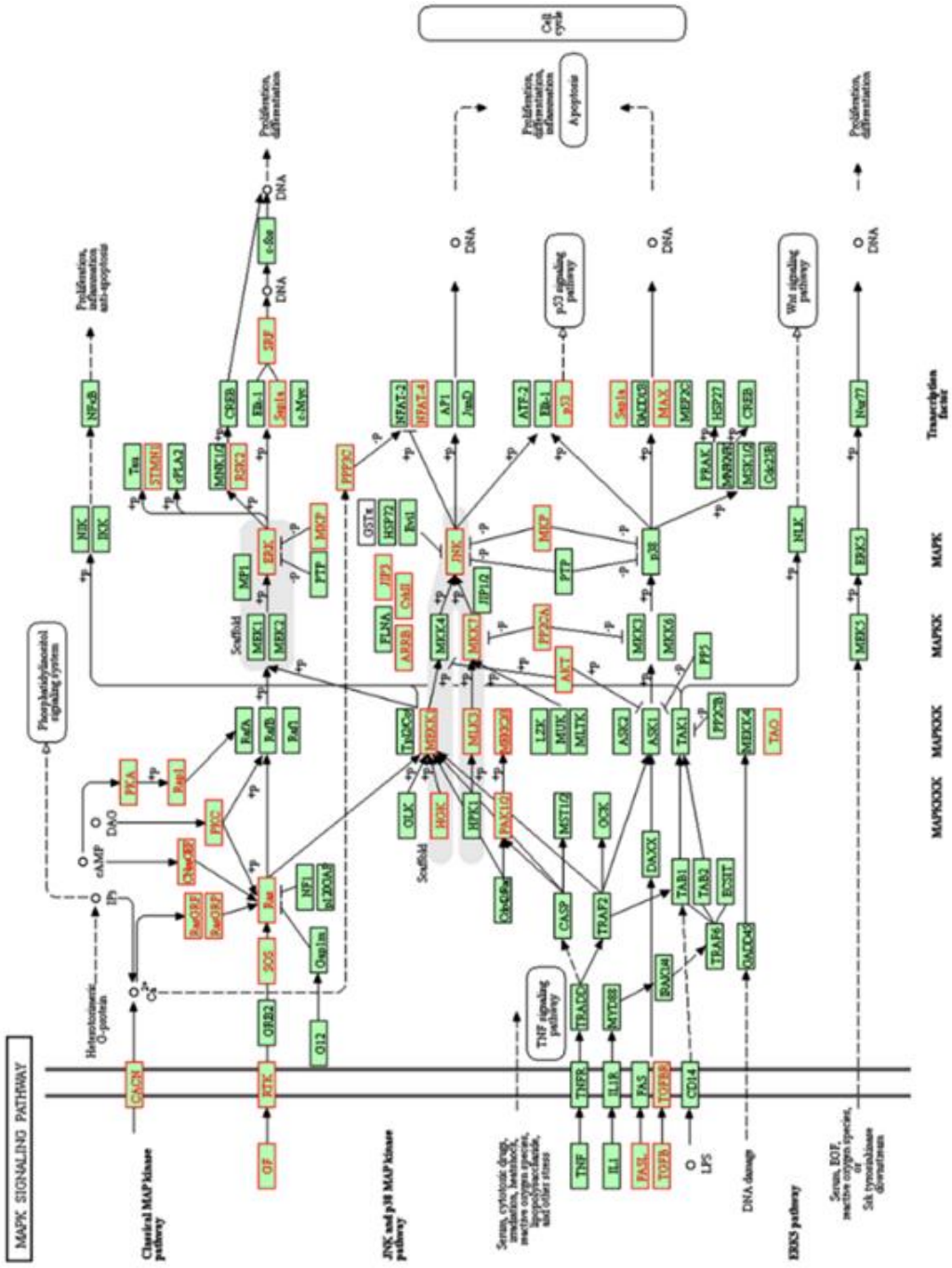

Figure 40. The components involved in MAPK signaling pathway. Red boxes and text represent factors that interacted with NDMV microRNA. Green boxes and text represent factors that are involved in identical signaling pathway and their locations.

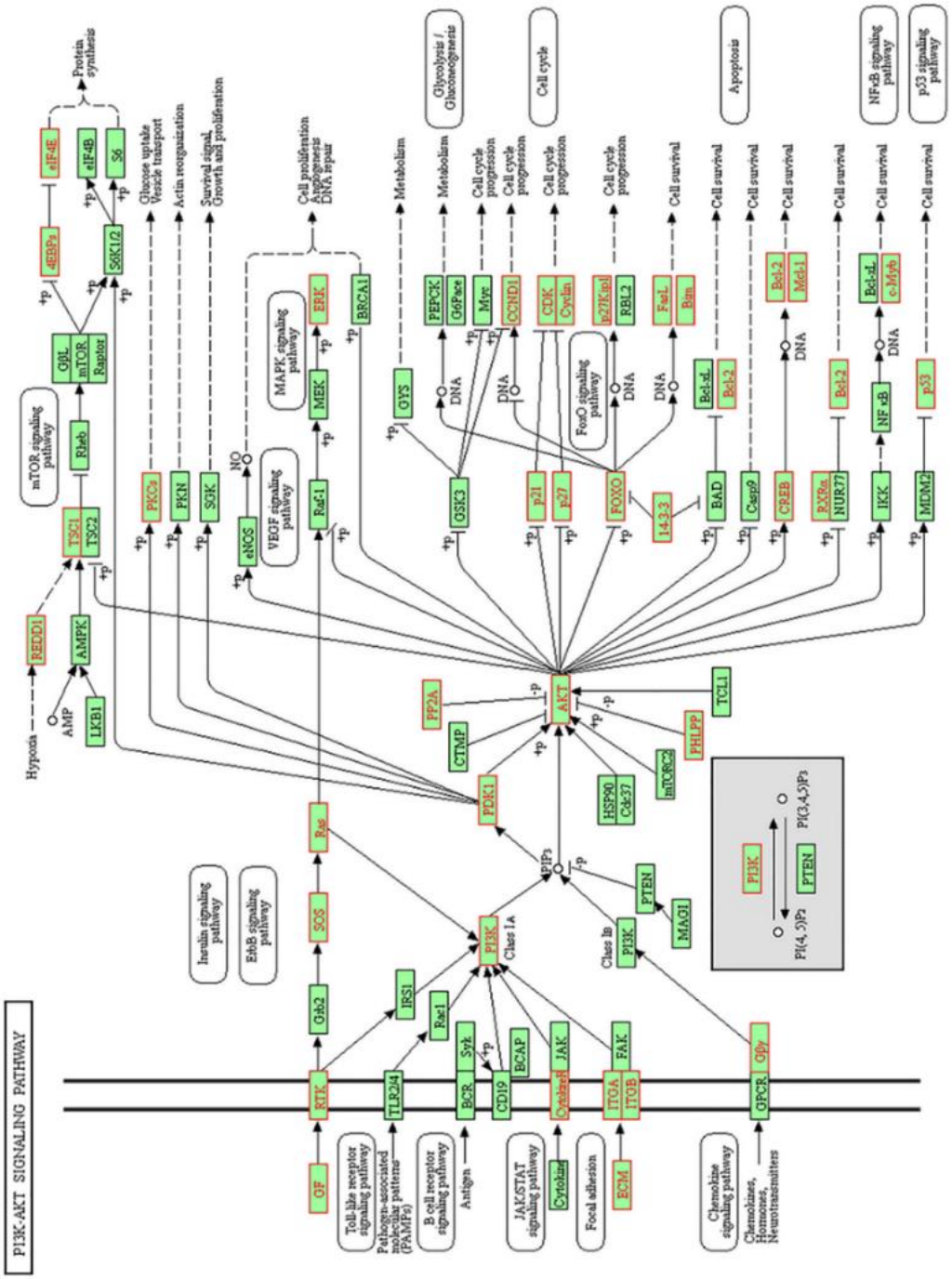

Figure 41. The components involved in PI3K-AKT signaling pathway. Red boxes and text represent factors that interact with NDMV microRNA. Green boxes and text represent factors that are involved in identical signaling pathway and their locations.

Part D: NDMV Effects on FLS function

4.27 Effects of NDMV on FLS Viability

To determine the viability of FLS after exposure to TNFα and NDMV, cellular metabolic activity was determined by the MTT assay. The viability of FLS treated with 10 ng/ml TNFα for 24h was not significantly different to that of untreated controls, incubated in the absence of TNFα. However, when FLS were exposed to NDMV at ratios of 200, 300 and 400 per cell for 24h, the cell viabilities were decreased to 63%, 58% and 69%, respectively ($p < 0.01$). However, after incubation of FLS with NDMV at ratios of 10, 30, 50 and 100 per FLS for 24h, there were no significant differences in viability compared to control (untreated) cells (Figure 42A).

The effect of incubation time on the viability of FLS following incubation with NDMV was then investigated. FLS were incubated with NDMV at a ratio of 100 NDMV per cell and at time periods, viability was measured by the MTT assay and compared to that of untreated controls. In the absence of NDMV, MTT activity increased in line with the increase in cell number (Figure 42B). FLS viability was unaffected by incubation with this concentration of NDMV for up to 24h incubation, but by 48h incubation, FLS viability was significantly decreased (p=0.0079, Figure 42B). Therefore, in subsequent experiments, FLS were incubated with NDMV at a ratio of 1:100 for 24h as these experimental conditions had no detrimental effect in the viability of the FLS.

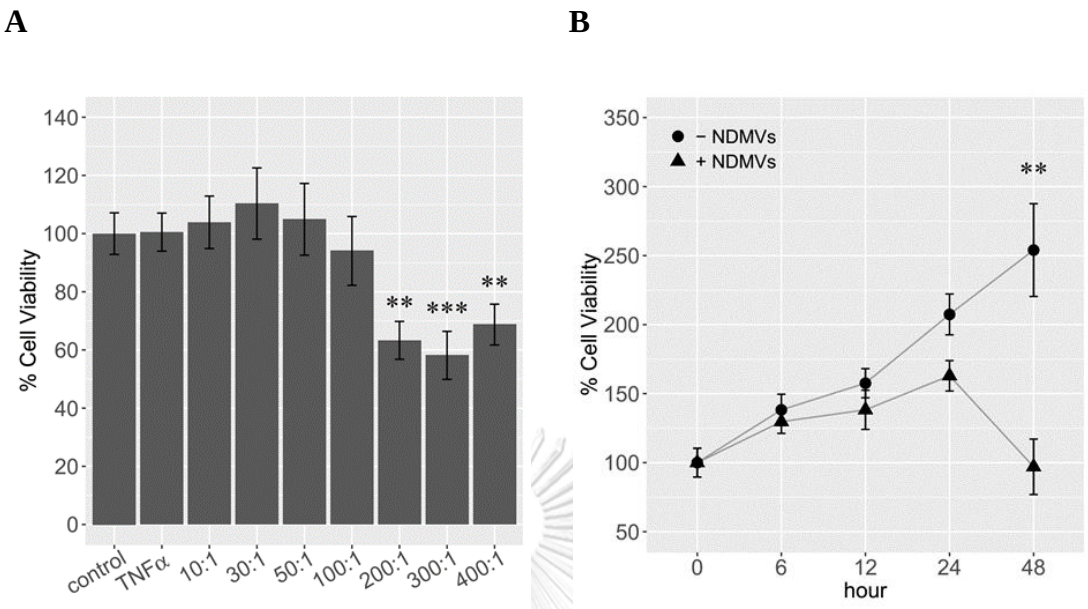

Figure 42. Cell viabilities of FLS incubated with different ratios of NDMV over time. (A) FLS were co-cultured TNFα alone (10 ng/mL) or NDMV at particle:cell ratios of 10, 30, 50, 100, 200, 300, and 400 for 24 h. Control cell viability is designated as 100% for cells incubated in the absence of TNFα after 24 h incubation. (B) Cell viabilities of FLS incubated in the absence (●) or presence (▲) of NDMV at a ratio of 1:100 over a 48h incubation period. Initial cell viability at time 0h is defined as 100%. Values shown are mean ± SE, N=5 separate experiments. Data analyzed with Wilcoxon test compared to controls or test group. $^{**}p<0.01$, $^{***}p<0.001$.

4.28 NDMV effect on FLS immigration

The scratch wound healing assay was used to measure NDMV effects on FLS migration and proliferation. Figure 43A shows captured images of FLS with/without NDMV treatment at time 0h, 24h and 48h culture. At 24h, a few FLS proliferated across the green line to the blank (scratched out) area in both the untreated and NDMV-treated samples. The wound healing area (WHA) of untreated cells was 26.83±2.98% which was higher than that of NDMV-treated which was 15.65±4.06%: these differences were not significant in Figure 43B (p=0.1598). After FLS monolayers were cultured ± NDMV for 48h, the WHA increased to 56.00±4.73% in untreated cells, whereas the WHA decreased into 13.21±7.06% in FLS treated NDMV for 48h in Figure 43B (p=0.0079). Therefore, the NDMV inhibited FLS proliferation and migration.

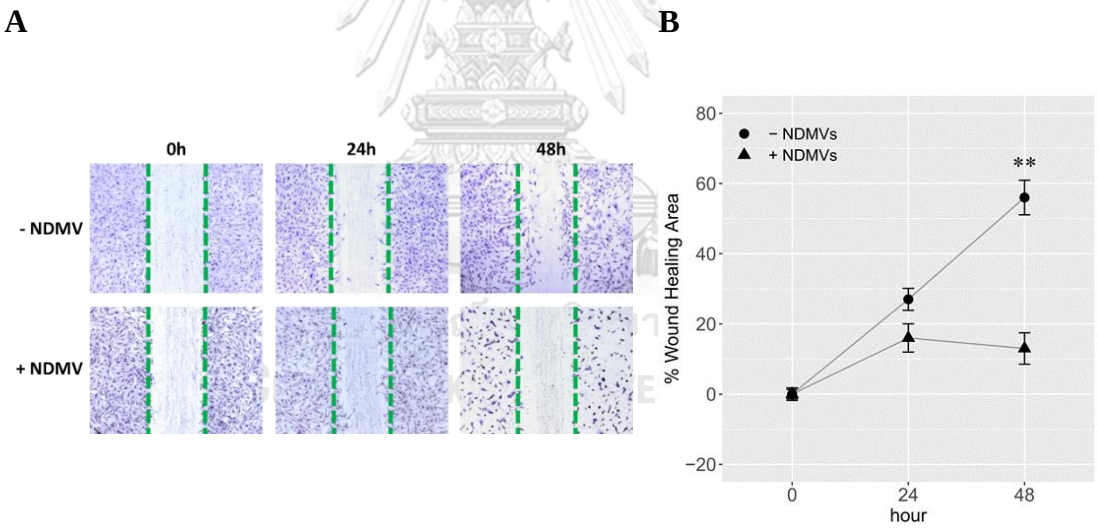

Figure 43. Percentages of wound healing area (WHA) after synovial fibroblast monolayer scratching ± treatment with NDMV at 0h, 24h and 48h. Cell monolayers shown are representative from N=5 experiments (A). WHA percentages were quantified by the ImageJ software (B). Values shown were mean (±SE, N=5), Wilcox test was used for statistical analysis. **p<0.01.

4.29 FLS internalisation of NDMV by FLS: measurement by flow cytometry

To measure and quantify uptake of NDMV by FLS, cells were co-cultured with PKH26-labelled NDMV at a ratio of 1:100 for different time periods and then analyzed by flow cytometry. Uptake of labeled NDMV by FLS was detected as early as 0.5h after addition, increased by 6h incubation, but uptake was not increased further by 24 h incubation (Figure 44A). After 1h incubation, 3.6% of FLS took up NDMV and by 6h incubation over 35% of the cells stained positive for NDMV uptake: by 24h incubation, 37% of the FLS stained positive. Calculation of uptake as a fold change in MFI revealed a 1.25 increase by 0.5h (compared to vehicle control), rising to the 2.4 fold increase by 6h, which was largely unaltered by 24h (2.1-fold) and 48h (2.6-fold) (Figure 44B).

A

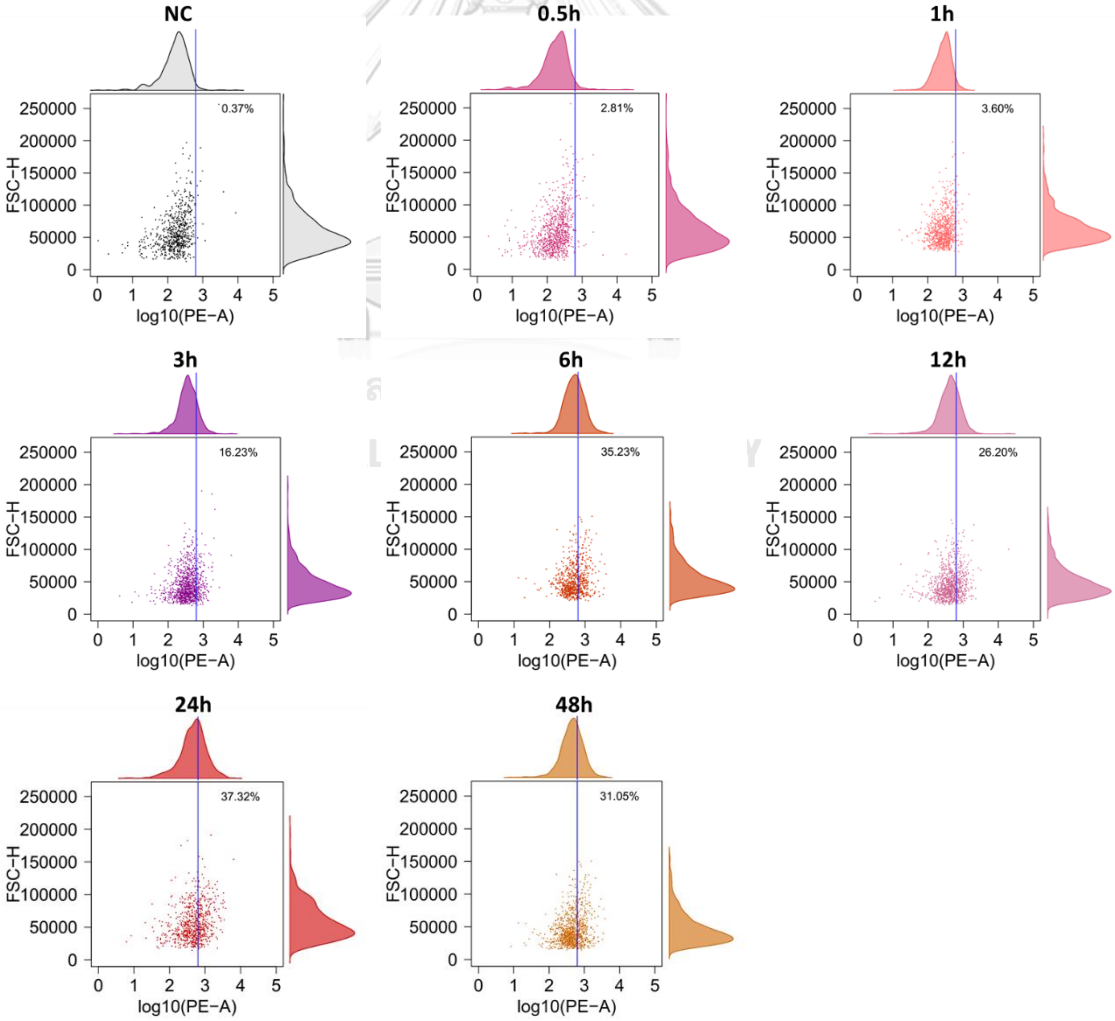

B

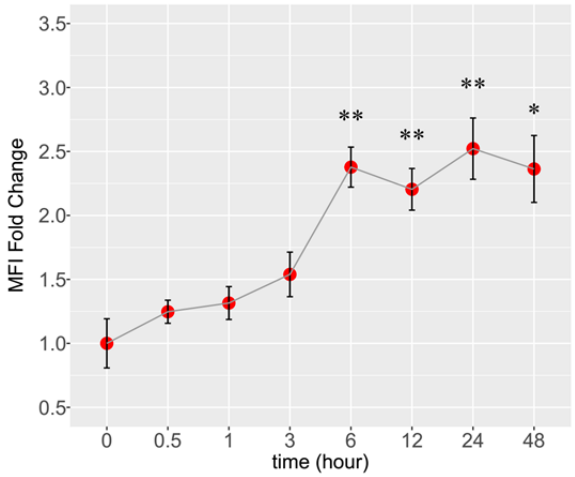

Figure 44. Measurement of NDMV uptake by flow cytometry. (A) Shows scatter plot of untreated, control FLS, and 1h, 6h and 24h after addition of NDMV at a ratio of 1:100. The vertical line is the gating threshold to identify NDMV-negative and -positive FLS. The upper and right panels are density curves of target fluorescence in FLS and cell size. (B) The mean MFI fold change over time of incubation of FLS with labelled NDMV. Data were normalized to FLS in the absence of NDMV. Each point represents the mean (± SE) from 5 separate experiments. *p<0.05, **p<0.01.

4.30 FLS internalisation of NDMV by FLS: analysis by confocal microscopy

Confocal microscopy was used to confirm uptake and internalisation of PKH26-labeled NDMV by FLS. Cells were incubated with NDMV for 24h and then stained for visualisation of the actin cytoskeleton using phalloidin and the nucleus using DAPI. Z-stack images were then collected to reconstruct 3D images of the samples. This analysis revealed that single and multiple NDMV were localized in the cytoplasm of the FLS, in equivalent focal planes as the actin cytoskeleton (Figure 45A and B). This experimental approach confirmed that NDMV were internalised by FLS in a time-dependent manner: labeled NDMV was found inside of one FLS on 1h co-culture; but all FLS took NDMV up on 6h and 24h. (Figure 45C). The number of FLS internalized NDMV in a confocal image was quantified by the percentage of NDMV-labelled positive FLS. The percentage of positive FLS was in a time-dependent way: 25.94%, 94.16% and 94.64 for 1h, 6h and 24h, respectively (Figure 45D).

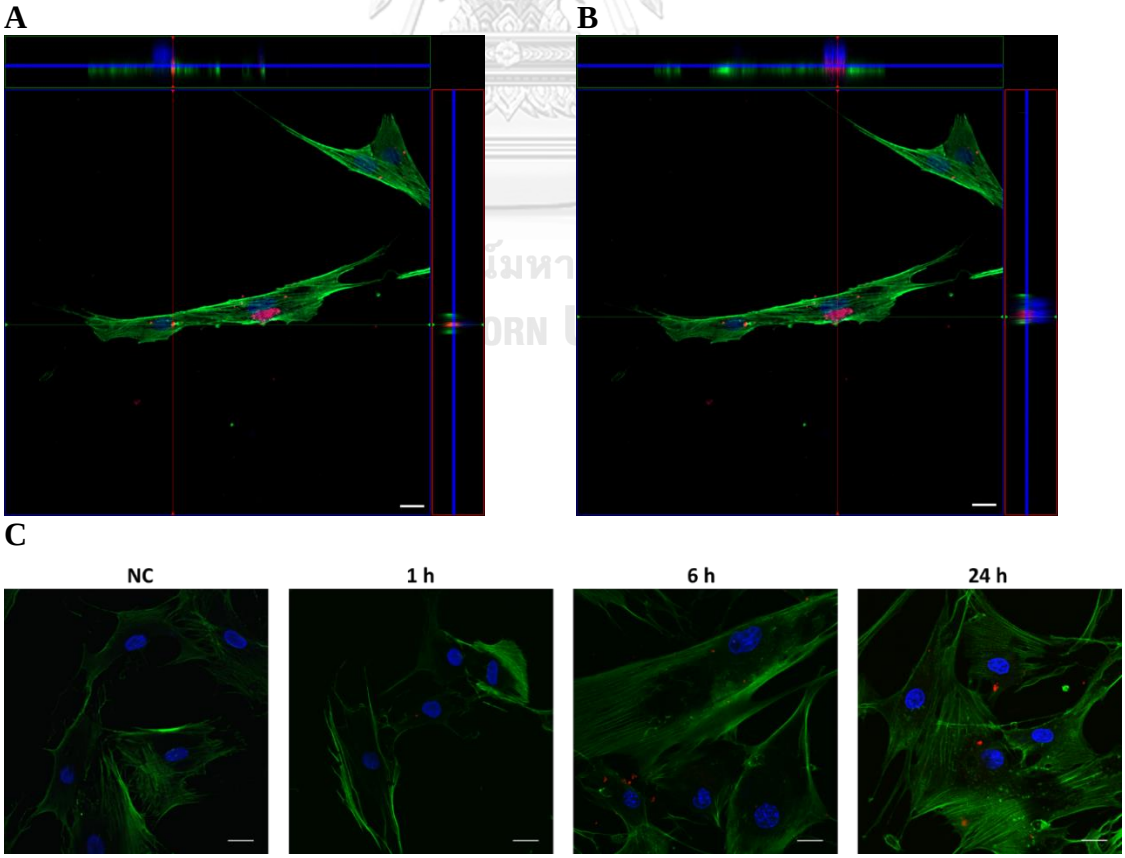

D

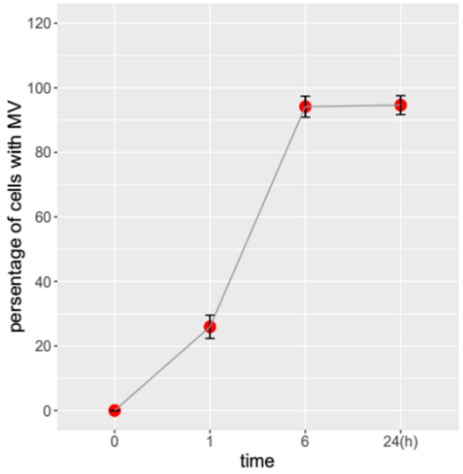

Figure 45. Visualisation of NDMV internalised within FLS by confocal microscopy. NDMV were incubated with FLS at a ratio of 100:1. (A) and (B) Show representative images of three-dimensional analysis after 24h incubation. Nuclei were stained by DAPI (blue) and actin by phalloidin (green), whereas NDMV were labelled by PKH26 (red). Middle images are optical sections; upper and right panels are vertical cross sections (red and green lines) of NDMV from confocal Z stack series. (C) Representative images at 1h, 6h and 24h. Scale bar: 20µm. (D) The number of FLS internalizing labelled NDMV was quantified into percentage of cells with MV normalized by total amount of FLS. Each point represented mean (± SE), N=5.

4.31 NDMV effects on cytokines expression by TNFα-stimulated FLS

We then measured the effects of NDMV on the ability of FLS to secrete a range of cytokines after incubation for 6h and 24 h in the presence and absence of TNFα. In these experiments, we determined the effects of NDMV alone on FLS cytokine expression and the ability of NDMV to affect TNFα regulated expression, after co-incubation of FLS with NDMV plus TNFα. Of the cytokines analysed, all except IL-1β, IL-7, IL-10, IL-12, IL-13 and GM-CSF were detected in FLS culture medium, as the level of IL-7, IL-12 and IL-13 were could not recorded by Multiplex system and low values obtained for IL-1β, IL-10 and GM-CSF were out detectable range and hence could not be reliably quantified.

The addition of TNFα alone significantly stimulated the secretion of IL-2, IL-4, IL-5, IL-6, IL-8, IFNγ, MCP-1 and MIP-1 from FLS ($p<0.05$, Figure 46). TNFα also significantly elevated IL-17 and G-CSF expression by FLS, and while this increased expression was statistically significant, the magnitude of this increase was not as great as that for other cytokines and chemokines, largely because of more variable expression rates by unstimulated FLS. The addition of NDMV alone to FLS for 6h and 24h had little effect on cytokine expression, except for a significant decrease in endogenous IL-6, IFNγ and MCP-1 expression. However, when co-incubated with TNFα, NDMV significantly decreased TNFα induced expression of IL-5, IL-6, IL-8, IL-17, G-CSF, IFNγ, MCP-1 and MIP-1 ($p<0.05$, Figure 46). In contrast, NDMV had no significant effect on TNFα induced IL-2 and IL-4 expression, showing that their inhibitory effect on cytokine expression was selective.

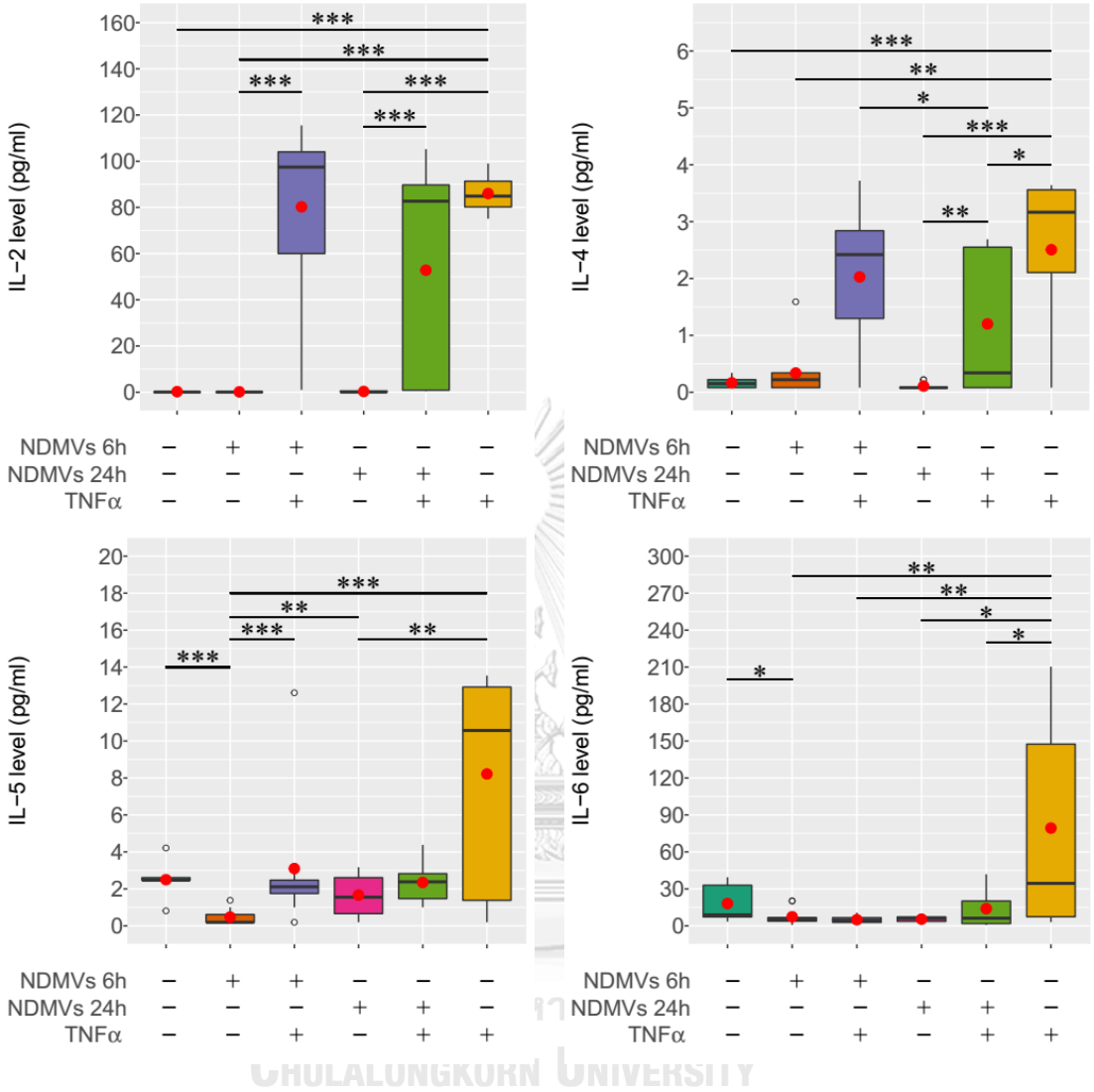

Figure 46. Inflammatory cytokine and chemokine levels in FLS and NDMV co-culture supernatants. Cytokine levels after incubation as follows: control; + NDMV 6h - TNFα; + NDMV 24h -TNFα; + NDMV 6h + TNFα; + NDMV 24h +TNFα and + TNFα. TNFα induces FLS to produce 10 cytokines, which are prohibited by NDMV pre-treatment. The cytokines inhibition of NDMV is significantly improved at 24h than 6h. Cytokine levels were analyzed with Conover test: dots (●) in box plots represent mean values (± S.E. N=5). *p < 0.05; ** p < 0.01; *** p < 0.001.

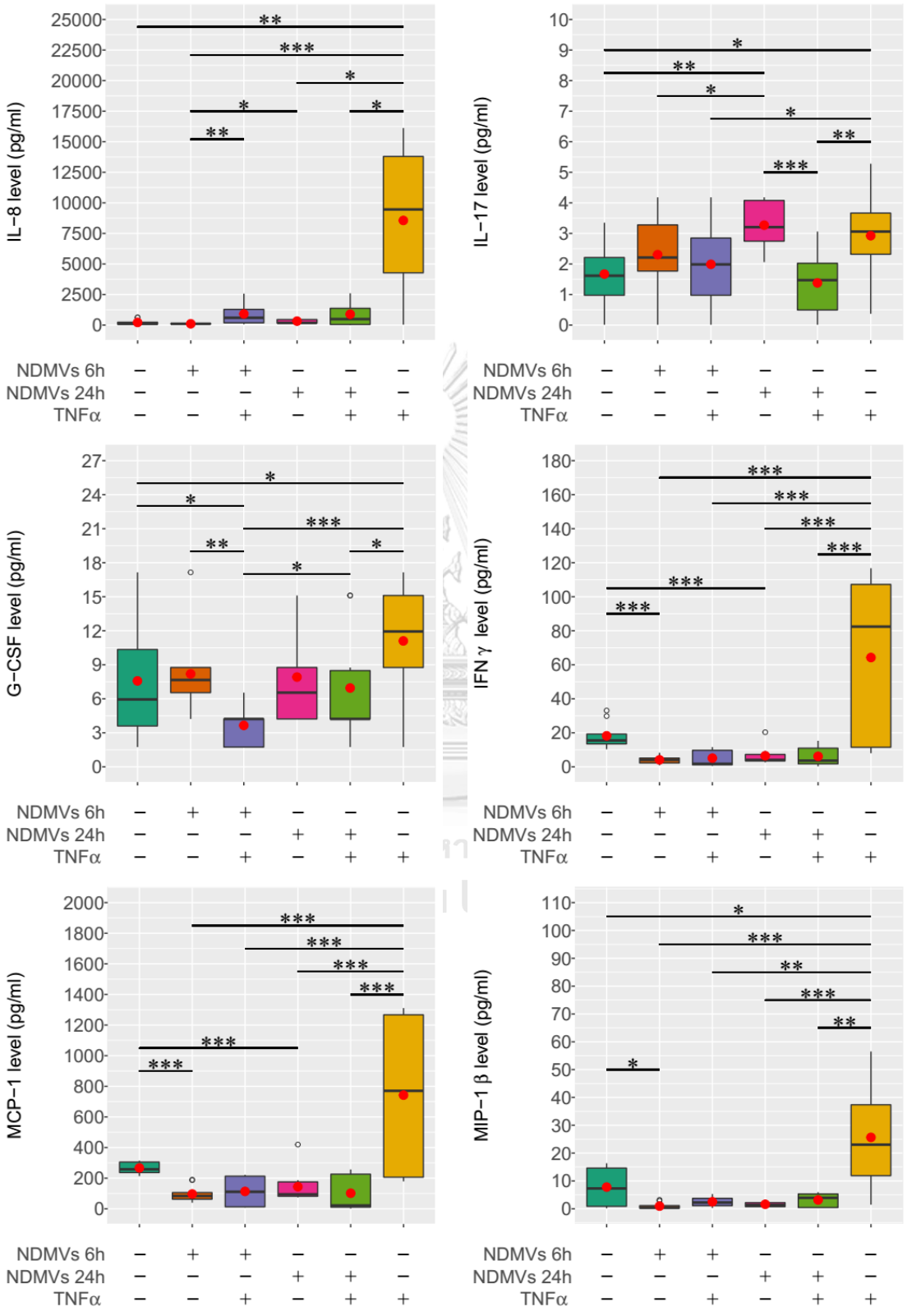

Continued Figure 46

4.32 Heatmap and cluster analysis of NDMV effects on cytokines expression

Hierarchical cluster analysis via heatmaps demonstrated relationships between patterns of cytokine expression in the presence and absence of TNFα and NDMV (Figure 47). This demonstrates that cytokine expression in the absence of TNFα was largely unaffected by treatment with NDMV: control and NDMV exposure for 6h or 24h were lower and these clustered together. However, in the presence of TNFα and NDMV, the patterns of cytokine expression clustered, but two patterns were apparent: down-regulated expression of IL-17, G-CSF, IL-8, MIP-1β, MCP-1, IL-5, IL-6 and IFNγ after NDMV exposure for 6h and 24h, while in contrast, IL-2 and IL-4 were down-regulated by NDMV after 24h treatment.

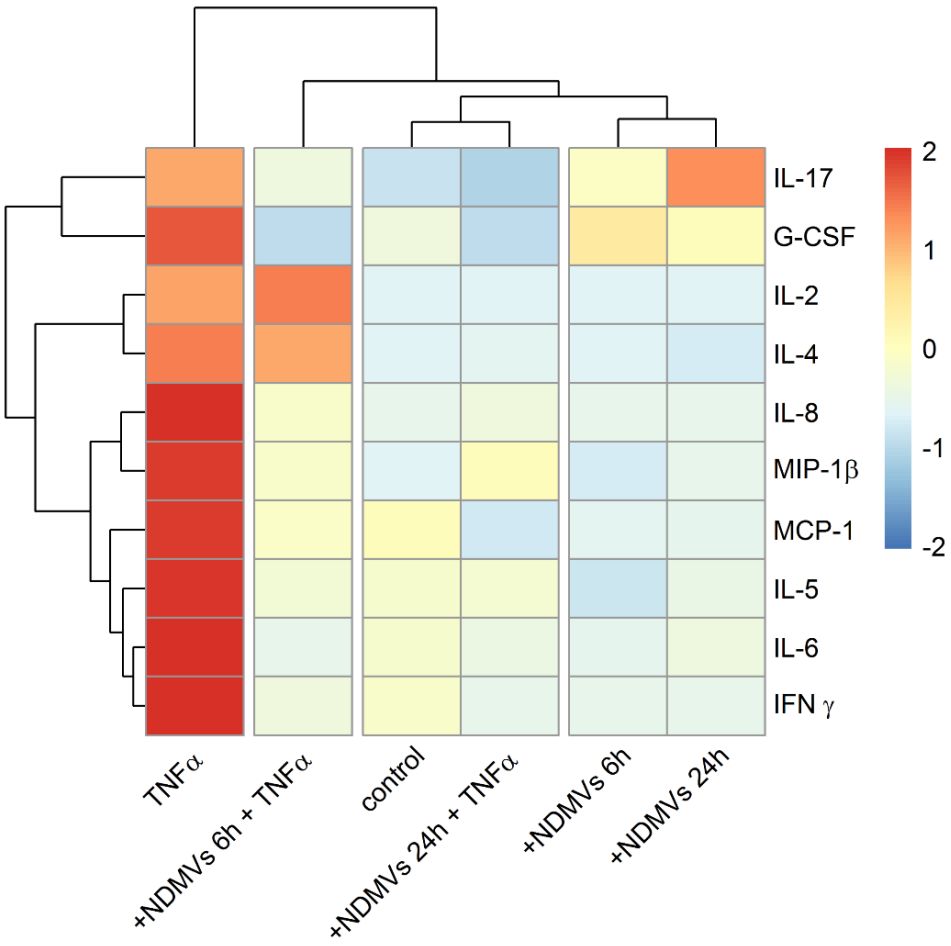

Figure 47. Heatmap of concentrations of inflammatory cytokines in cultured media of FLS with/without NDMV and TNFα. Median values were first standardized into z-score based on each cytokine level in different groups. The Hierarchical Method was then used for cluster analysis on this standardised data. Colour codes represent high (red), intermediate (white) and low (blue) expression.

Chapter 5. DISCUSSION

5.1 Characteristics of FLS

In addition to FLS and MLS, synovial tissues contain various numbers and types of cells, such as lymphocytes, macrophages, endothelial cells, DC, etc. that had to be removed during the isolation of FLS prior to their culture and characterisation. Free cells in suspension (lymphocytes and granulocytes) could be removed by medium changes and sub-culture, but adherent cells (macrophages, MLS, endothelial cells and DC) were progressively eliminated from the cultures during successive passages and culture *in vitro*. Therefore, total numbers of cells usually decreased over the first few days (by day 4) in culture in P1 as these cells were progressively lost. However, we observed typical growth curve of P4 FLS showing an "S" shape curve of cell proliferation. Additionally, the doubling times of cells was higher in P4 than P1, which demonstrated higher proliferation rates in P1. However, the proliferation rates of FLS by two different isolation methods (explant and dispersed) were identical. Xiao *et al*. reported that high purity of FLS (<99%) could be obtained from dispersed cells culture compared to explant cultures(Xiao et al., 2010). Both methods are acceptable to obtain FLS.

After dispersed cells were cultured in P1 to P4, the time of cellular confluency to achieve 85% were very comparable from 6.5 to 7.5 days in comparison of explant culture in P1 and P4. However, the time of 85% confluency was different between dispersed cells culture and explant culture, as enzymatic methods could effectively shorten process of "tissues to cells" from 14 days to 4 days. In this respect, the dispersed cell culture method resulted in cultures of high purity of FLS and well-preserved FLS characteristics, as well as a short culture period. As a result, the method of dispersing cells by two-enzymes (collagenase and trypsin) was used in our experiments.

To distinguish between FLS and MLS is often problematic by visualization on the light microscope, but the high density of rough Endoplasmic Reticulum (rER) present in FLS can be detected by electron microscopy, which indicates high biosynthetic activity of these cells that secrete large quantities of molecules into the synovial joint. In addition to morphological properties of FLS detectable by EM, their membrane surface makers are different to those of MLS. The FLS positive markers are CD90 (Thymocyte differentiation antigen-1, Thy-1), CD55 (decay accelerating factor, DAF), CD106 (vascular cell adhesion molecule-1, VCAM-1), uridine diphosphoglucose dehydrogenase (UD-PGD) and vimentin (Zimmermann et al., 2000). CD90 and vimentin may also be expressed on mesenchymal stem/stromal cells (MSC) and fibroblasts that originate from other tissues (Peduto et al., 2018). Fibroblasts of the sub-intimal layer also express CD55, CD106 and UD-PGD (Xiao et al., 2010). The negative markers of FLS are positive markers for MLS, such as CD11b and CD64. In my experiments, CD55+ and CD90+ synoviocytes were the most prominent cells by passage 4 (83-85% CD55+, 98-99% CD90+,), while CD11b+ and CD64+ synoviocytes decreased to 1-2% and 5-6%, respectively, of the population by this time.

As FLS purity increased from P1 to P4, there were more synoviocytes in G0/G1 phase and fewer in S phase because long cell culture periods influence the cell cycle, proliferation, transcription factor activity and differentiation (Zimmermann et al., 2000). Gu *et al*. found that the percentage of human umbilical cord MSC in G1 phase increased as cell passage number increased, meanwhile, while those in S phase decreased, and the percentage in G2 phase did not alter significantly (Gu et al., 2016). These researchers demonstrated that long-term primary culture could increase intracellular oxidative stress of cells to promote variations in the cell cycle. In addition, long-term primary culture could increase the probability of trisomy 7 in synoviocytes to affect cellular proliferation by Ki-67 protein (Ermis et al., 1995). Finally, long-term primary culture could induce accumulation of reactive oxygen species (ROS) and shorten telomere length during *in vitro* passage of FLS. Sun and his colleagues found that exogenous telomerase addition preserved FLS growth rate to maintain the population doubling time (Sun et al., 2004). In our experiments, we

observed that it was difficult to trypsinize P10 FLS and most of the recovered FLS did not adhered to new flasks or culture plates.

5.2 Neutrophil function

Isolation of functionally-competent neutrophils was a fundamental step for experiments aimed at preparing neutrophil-derived microvesicles (NDMV). Polymorphprep was used to isolate neutrophils from whole blood of healthy volunteers, a process that could be completed within 2 h. Thomas *et al.* indicated that Polymorphprep was a reliable method to obtain highly-pure neutrophils (purity > 95%) and that contaminating cells (< 5%) did not have a statistically-significant impact on general gene expression of TNFα treated neutrophils (Thomas et al., 2015). Neutrophil purity was over 98% in our experiments as indicated by microscopy and flow cytometry examinations.

As neutrophils were exposed to TNFα at a high dose (50ng/ml) and for a short time (20min) for the preparation of NDMV, it was important to determine the cell characteristics and functions after this TNFα exposure. Several neutrophil surface antigens can be up-regulated (e.g. CD11b) or down-regulated (e.g. CD62L), after exposure to TNFα (Wittmann et al., 2004, Headland et al., 2015). These receptors are crucial for neutrophil adhesion, recruitment and migration. In addition, increased CD11b on neutrophils can interact with CD54/Intercellular Adhesion Molecule 1 of endothelial cells to increase neutrophil accumulation in inflammatory foci (Krieger et al., 2004). However, CD62L on the neutrophil surface is decreased after TNFα treatment, by activating Tumor Necrosis Factor-α-Converting Enzyme (TACE) via the p38 MAPK pathway (Ivetic, 2018, Killock and Ivetic, 2010). CD62L on neutrophils normally controls rolling on and off the endothelial bed, but its shedding triggers tighter adhesion with the endothelium.

Wittmann *et al*. demonstrated that CD11b up-regulation and CD62L down-regulation were associated with TNFα priming and fMLP stimulation of the neutrophil respiratory burst (Wittmann et al., 2004). In our experiments, high-dose TNFα primed neutrophils were further stimulated by fMLP and PMA to produce ROS (Reactive Oxygen Species), that were higher than after TNFα treatment alone. Moreover, ROS induced by PMA was higher than fMLP, as fMLP required Formyl

Peptide Receptor 1/2 (FPR1/2) while PMA is a phorbol ester that is transported passively across the cell membrane (Tan et al., 1998, Thomas et al., 2000, He and Ye, 2017). Barnes *et al.* (2012) also reported that low-dose TNFα primed neutrophils generated more ROS after both fMLP and PMA stimulation than in control (non-TNFα) group (Barnes et al., 2012).

It was then necessary to determine whether this TNFα treatment induced changes in other neutrophil functions. The first of these tested was the effect on apoptosis. It was found that high-dose and short-time incubation with TNFα only induced about 1% of the neutrophils to undergo apoptosis. When incubated *in vitro*, around 60% of neutrophils undergo apoptosis by 24h (Savill et al., 1990), and previous research found that high-dose TNFα (10ng/ml and 100ng/ml) and low-dose (1ng/ml) induced neutrophil apoptosis after overnight and 3h incubation (van den Berg et al., 2001, Takeda et al., 1993). However, another study showed that different concentrations of TNFα (1, 10 and 100ng/ml) could not significantly affect neutrophil apoptosis after 1-2min incubation (Salamone et al., 2001). They likewise showed that 10ng/ml TNFα induced neutrophil apoptosis by 0.5, 1 and 3h. Furthermore, Cross *et al.* showed that TNFα possessed dual features on neutrophil apoptosis in a dose-dependent manner (Cross et al., 2008); low-dose TNFα (1ng/ml) had an anti-apoptotic role on neutrophils by inducing Bfl-1 while high-dose TNFα (10ng/ml and 100ng/ml) promoting neutrophil apoptosis by Mcl-1 degradation after 2, 3 and 6h exposures. However, 10ng/ml TNFα could induce anti-apoptotic gene expression by neutrophils after 1h exposures (and 3h and 6h) (Chiewchengchol et al., 2016). In my experiments, 50ng/ml of TNFα was used to treat neutrophils for 20min to generate MV and this was not shown to induce morphological changes associated with apoptosis, supporting previous publications (Headland et al., 2015, Rhys et al., 2018, Dalli et al., 2008).

Neutrophil migration was suppressed by TNFα pretreatment in our experiments. In fact, fMLP and TNFα were effective chemoattractants for neutrophils and induced polarization, adherence and transmigration. It has been shown that TNFα-induced adherence and migration was blocked by PI3K and MAPK inhibitors (Kamata et al., 2004, Suzuki et al., 2001). However, TNFα blocked the capability for cytoskeleton reorganisation of neutrophils which may result in decreased neutrophil chemotaxis

induced by fMLP (Kutsuna et al., 2004, Kato and Kitagawa, 2006). Therefore, it can be concluded that for the preparation of NDMV, this treatment with TNFα did not induce apoptosis.

5.3 Properties of NDMV

The various types of EV that are produced and shed from donor cells are categorized by size, composition and assembly mechanism. EV classification is based on their size, but there is considerable overlap in sizes of different types of EV and their actual sizes may be dependent on the method of isolation and purification (Van der Pol et al., 2014, Van der Pol et al., 2016, Arraud et al., 2014). The conventional method to isolate EV is centrifugation and it has been reported that NDMV-enriched fractions can be prepared by centrifugation at 20,000 or 15,700 ×g (Pliyev et al., 2014, Rhys et al., 2018). However, NDMV are usually prepared by ultra-centrifugation at 100,000 ×g, conditions that we used in our study (Table 2.5.3). Electron microscopy is a standard method to measure EV size to identify the EV type. EV are irregular spheres under electron microscopy, and EV can be used to measure maximum and minimum diameters. The minimum, maximum and average diameters of EV measured by TEM were larger by those measured by SEM. This could be a varying result from the different sample preparations, as EV samples were dehydrated with series of solvent for each of 5min (acetone and ethanol). The EV diameter measured by TEM was 80 nm, which was larger than the average measured by SEM. However, all EV average diameters were >100nm as measured by TEM. NTA confirmed these findings: analysis of these vesicles by NTA showed that 97-98% of isolated NDMV were in the size range of 100-1000nm. Therefore, the morphology and size characteristics of NDMV in our experiments were consistent with our expectations and previous reports (Ajikumar et al., 2019, Finkielsztein et al., 2018).

TNFα can stimulate neutrophils to change the surface expression of CD markers and receptors through degranulation and shedding (Galligan and Yoshimura, 2003). Neutrophil granules comprise 4 types: primary/azurophil granules (CD63+, CD68+), secondary/specific granules (CD11b+, CD15+, CD66+, CD67+), tertiary/gelatinase granules (CD11b+) and secretory vesicles (CD11b+, CD14+, CD10+, CD13+, CD45+). Expression of CD66 and CD14 were not significantly different between MV

and untreated control neutrophils (Vols et al., 2017, Lawrence et al., 2018). Expression of CD66 and CD14 were not significantly different between MV and untreated control neutrophils (Elbim et al., 2001, Galligan and Yoshimura, 2003, Rørvig et al., 2013). Secretory vesicles contain CD14 which binds lipopolysaccharide (LPS) to increase TNFα production and release by neutrophils (Takeshita et al., 1998, Ishii et al., 1993). Niel *et al*. demonstrated that melanocyte-derived exosomes could express CD63, which could modulate endosomal arrangement that is dependent upon the Endosomal Sorting Complex Required for Transport (ESCRT) process (Van Niel et al., 2011, van Niel et al., 2018). Primary granules contain abundant MPO, which was one protein present in EV (Dalli et al., 2013, Vols et al., 2017). We demonstrated that NDMV expressed surface markers from primary and tertiary granules of neutrophils. Dali *et al*. reported in their proteomic supplementary data that Annexin V also was abundant on NDMV in their proteomic supplementary data (Dalli et al., 2013). which was consistent with our flow cytometry results which showed that more Annexin V was expressed on NDMV than on treated and untreated neutrophils. The function of Annexin V on NDMV and the role that this may play on recipient cells is unknown. Vascular smooth muscle, chondrocytes, osteoblasts and macrophages have all been shown to generate MV or matrix vesicles expressing Annexin V (Kapustin et al., 2011, New et al., 2013, Xiao et al., 2007, Genge et al., 2007). These MV with abundant Annexin V may bind with phosphatidylserine and/or S100A9 to develop a nucleation complex for physiological calcification and matrix mineralization (Krohn et al., 2016).

5.4 NDMV carried microRNAs

There were 159 predominant microRNAs detected in NDMV prepared which were released from TNFα treated neutrophils which contained 220 microRNAs compared to untreated cells. 5% of microRNAs were identical in TNFα treated neutrophils and untreated cells. 18% microRNAs overlapped with up-regulated microRNAs from untreated neutrophils compared treated cells. Squadrito *et al*. found that microRNAs were not randomly loaded in EV, but selectively loaded into macrophage-derived EV in response to various forms of macrophage activation (Squadrito et al., 2014). In total, 657,394 genes were predicted to interact with the 159 microRNAs identified in our

NDMV preparations, and the target genes included protein- or DNA-binding, proteins or metabolic process and intracellular components. NDMV could profoundly influence FLS by their microRNA.

EV incorporated microRNAs are a way to transport such molecules to target cells and avoiding RNase degradation in extracellular fluids. Thus, microRNAs within EVs retain their integrity and activation potential that would persist until internalization by the target cells (Turturici et al., 2014, Asghar et al., 2019). Alexander *et al*. (2015) found that MV contained microRNA-155 and microRNA-146a that could be internalized by marrow-derived DCs whose microRNA-155 and 146a levels were then elevated to detectable levels in mouse model (Alexander et al., 2015). In this study, TNFα and IL-6 concentrations were regulated by these microRNA-loaded EV. However, NDMV in our experiments did not contain these two microRNA, rather microRNA-3168, 4488, 124-3p, 10398-3p, 1290 and 6968-5p in NDMV were increased in TNFα-exposed neutrophils by 2-fold.

5.5 PI3K/Akt and MAPK signaling pathways may be regulated by NDMV microRNA

PI3K-AKT and MAPK were the two most significant signaling pathways that were predicted to be regulated by predicted target genes of NDMV microRNAs according to the KEGG database. PI3K-AKT is a crucial pathway that contributes to the inflammatory response, cell growth or proliferation and cellular apoptosis (Lu and Qian, 2019, Huang et al., 2019, Li et al., 2018). The activation of PI3K-AKT could induce the downstream pathway, Nuclear Factor kappa-light-chain-enhancer of activated B cells (NF-κB) to regulate inflammatory cytokine expression and the p53 signaling pathway to regulate gene expression (Schabbauer et al., 2004). PI3K-AKT activation could also initiate mTOR which would stimulate NF-κB to up-regulate inflammatory gene expression, especially, including iNOS, COX-2, IL etc. (Shabab et al., 2017). The MAPK signaling pathway is also important in the regulation of inflammatory cytokine expression via NF-κB and Jun in FLS (Du et al., 2019, Rosillo et al., 2019, Namba et al., 2017). Previous work has demonstrated that exogenous microRNAs (microRNA-145, 143-3p or 451) modulated pro-inflammatory cytokines

(TNFα, IL-1β or IL-6) through PI3K/AKT and MAPK/mTOR pathways (Zhong et al., 2018, Yang et al., 2018, Wang et al., 2015).

5.6 NDMV effect on FLS

In this thesis, we have isolated NDMV from TNFα treated human neutrophils and measured their effects on the function of FLS prepared from OA synovium, especially the ability of FLS to express cytokines and chemokines that can promote synovitis. We show that NDMV can inhibit the expression of a variety of pro-inflammatory molecules that are released by FLS following stimulation with TNFα. Our data thus add to the growing body of evidence to show that, under certain experimental and perhaps disease conditions, NDMV exert anti-inflammatory effects.

NDMV expressed annexin A1, CD66b, CD62L on their cell surface (as do intact neutrophils) and myeloperoxidase (MPO) in line with previous publications (Headland et al., 2015, Pitanga et al., 2014). MPO is an efficient peroxidase that may elicit oxidative damage and produce cytotoxic hypochlorous acid (HOCl) and other oxidants in inflammatory conditions (Pattison and Davies, 2006). MPO has been detected in synovial fluid of OA patients and is elevated in RA patients, and intra-articular injection of MPO increased the severity of arthritis in a mouse model (Nzeusseu Toukap et al., 2014, Lefkowitz et al., 1999). Internalised NDMV could induce MPO accumulation and intracellular activity that might interfere with FLS viability, proliferation and migration. The scratch-wound assay showed that NDMV slowed down FLS migration, as indicated by a decrease in the wound healing area. However, high-dose (V/C>100) and long-term (>24h) NDMV treatments were harmful to FLS viability and biological activity. The mechanisms of NDMV that result in internalisation generally include endocytosis, micropinocytosis, phagocytosis or membrane fusion etc. (Mulcahy et al., 2014). Endocytosis is a major mechanism of EVs uptake by recipient cells into the endosomal compartment which may then be transported to lysosomes (Lázaro-Ibáñez et al., 2017, Tian et al., 2013, Montecalvo et al., 2012). EVs internalisation is dependent on EVs dose, treatment time and the nature of the recipient cells. In our experiments, NDMV internalised by FLS with approximately 35% of cells taking up labelled NDMV over a 6 h to 48h period.

As a member of the pro-inflammatory family of cytokines, TNFα is generated by cells such as neutrophils, macrophages or adipocytes to induce systemic inflammation (Bulló et al., 2003). TNFα has been detected in synovial fluid, plasma and synovial membrane of OA patients, and may activate both tissue cells and infiltrating immune cells (Mabey et al., 2016, Kapoor et al., 2011, Han et al., 2001, Stannus et al., 2010). NDMV have been shown to possess anti-inflammatory activity and promote inflammatory resolution, and in our experiments, NDMV could depress most inflammatory cytokines expressed by TNFα activated FLS (L Johnson et al., 2014). While IL-7, IL-12 p70 and IL-13 expression was undetectable, IL-5, IL-6, IFN-γ and MCP-1 expression levels were not significantly different between control and TNFα treated FLS. However, expression of these latter 4 pro-inflammatory cytokines were decreased by NDMV in non-activated FLS (Muhl and Pfeilschifter, 2003, Finnerty et al., 2006). This finding was contradictory to that of Mesri *et al*. (1999) who reported that IL-6 and MCP1 were elevated by NDMV via JNK1 signaling pathway in endothelial cells (Mesri and Altieri, 1999). Our experiments suggest that the effects of NDMV are dependent on the nature and function of the target cells, or that the effects are dose and time-dependent. Expression of the pro-inflammatory chemokine, IL-8 was suppressed by NDMV pre-treatment of TNFα-activated FLS activator for 24h. Previous research has also shown that NDMV could decrease IL-8 secretion by macrophages activated with zymosan or LPS (Gasser et al., 2003). The three family members of receptor tyrosine kinases (RTKs) - Tyro3, AXL and MER (TAM) - could be activated through binding with phosphatidylserine (PtdSer) which was carried on NDMV. Moreover, the FLS and synovial micromass (composition of macrophages and FLS at a ratio of 1 to 5) expressed these three TAM which decreased pro-inflammatory cytokines expression by up-regulation of the suppressor of cytokine signaling (SOCS) protein 1 and 3 (Rhys et al., 2018, Ruiz-Heiland et al., 2014, Waterborg et al., 2018a, Waterborg et al., 2018b). IL-1β is a classical pro-inflammatory cytokine whose levels are also increased in synovium and synovial fluid of OA patients. Rhys *et al*. (2018) found that NDMV-carried phosphatidylserine that could bind with its receptors MER (MER tyrosine kinase) of macrophages to block IL-1β expression via phosphoinositide 3-kinase (PI3K) and signal transducer and activator of transcription 1 (STAT1) signaling pathway (Rhys et

al., 2018). NDMV prevented IL-1β produced by TNFα stimulated FLS at both 6h and 24h in our study, which might result from regulation of the TAM-SOCS signaling axis.

Additionally, we found that NDMV did not decrease IL-10 secretion but TNFα prevented FLS from releasing more IL-10 into culture supernatants, which was blocked by NDMV pre-treatment. Pro-inflammatory levels of IL-17 levels are elevated in serum, synovial fluid and inflamed synovium in OA and are associated with disease severity (Deligne et al., 2015, Chen et al., 2014). IL-17 can enhance MMPs expression and up-regulate expression of the pro-inflammatory cytokines: IL-1β, IL-6, IL-8 and TNFα in FLS from OA patients (Honorati et al., 2006, Agarwal et al., 2008). Interestingly, NDMV could up-regulate IL-17 levels released from FLS, but this effect was depressed in the presence of TNFα which increased IL-17 expression after 24h incubation. The anti-inflammatory cytokine, IL-4 was not altered in FLS stimulated with NDMV in the absence of TNFα, similarly to the pro-inflammatory IL-2. However, IL-4 expression decreased in FLS incubated with NDMV in the presence of TNFα by 24h incubation (but not by 6h), suggesting that NDMV do not only regulate expression of inflammatory cytokines, but also cytokines such as IL-4 that play regulatory roles in immune and inflammatory function. TNFα up-regulated expression of M-CSF and GM-CSF in our experiment, in line with previous reports (Watanabe et al., 2017), but GM-CSF secretion was significantly higher in NDMV 24h pre-treatment plus TNFα stimulation than TNFα treatment alone in this study. Furthermore, NDMV might probably modulate FLS via their carried an amount of microRNA cargo, because there microRNAs could up and down-regulate gene expression and translation, such as TNFα-related kinases (Valinezhad Orang et al., 2014).

5.7 Limitation of this study

Although FLS of high purity were successfully obtained by enzymatic primary culture, highly-pure neutrophils were efficiently separated from whole blood of volunteers and NDMV were effectively isolated from neutrophils, several limitations of this study should be clearly stated. This study is a descriptive research to investigate NDMV effects on FLS rather than mechanistic research, that could, for example use inhibitors

or microRNA mimics to define the underlying molecular processes. It is impossible to investigate one specific protein or RNA function in the target cells, as NDMV are "information packages" with multiple components. Synovitis in the patients from whom we obtained the samples, could be in different phases of arthritis and influenced by systemic and local factors. MV are rarely released from untreated/healthy neutrophils, and so this study did not contain a control group of microvesicles derived from healthy neutrophils. In the microRNA sequencing experiments, cells and NDMV were collected from 3 samples and for the NDMV microRNA experiments, those with low mapping rate were excluded from analysis. Clearly, such low abundance microRNAs may still have biological significance. Furthermore, *in vivo*, synovitis is likely to be associated with, and induced by several different mediators, but this *in vitro* study we modelled cellular inflammation in FLS by use of a single cytokine: TNFα. This research work did not include animal models of synovitis to verify the cell-based conclusions. Finally, only 17 inflammatory cytokines were measured in culture media of FLS and others may be involved in regulation of OA synovitis.

Chapter 6. CONCLUSIONS AND OUTLOOK

In conclusion, in addition to their potential role in cartilage function to benefit chondrocytes and cartilage repair, NDMV were capable of controlling inflammatory responses of FLS through direct contact with macrophages to upload Annexin A1 and phosphatidylserine (PS) (Headland et al., 2015, Headland and Norling, 2015, Rhys et al., 2018). Large quantities of NDMV were produced by non-apoptotic neutrophils stimulated by high dose, short term TNFα and their surface proteins, Annexin A1 or A5, PS, CD11b and CD63, may bind with ligands of FLS to initiate endocytosis to internalize NDMV. Various types of microRNAs were contained within NDMV that may be liberated in the cytoplasm of FLS by lysosomes to regulate gene expression, such as binding to target mRNAs to initiate post-transcriptional control. PI3K-Akt and MAPK signaling pathways, two classical and inflammation-related signaling pathways, were predicted to be most significant regulated by NDMV-carried microRNA. Inhibition of these pathways would prevent downstream signaling pathway, such as NF-κB and p53 signaling pathways, to decrease cytokine and chemokine expression, such as IL-6, IFNγ, MCP-1 etc. Our experimental work supported previous studies that demonstrated NDMV possess anti-inflammatory properties to suppress inflammatory responses of FLS. Figure 48 suggests possible mechanisms and pathways regulated by NDMV. Our work encourages further studies to reveal mechanisms of how NDMV limit inflammation of the synovium and subsequent damage of cartilage in OA and RA.

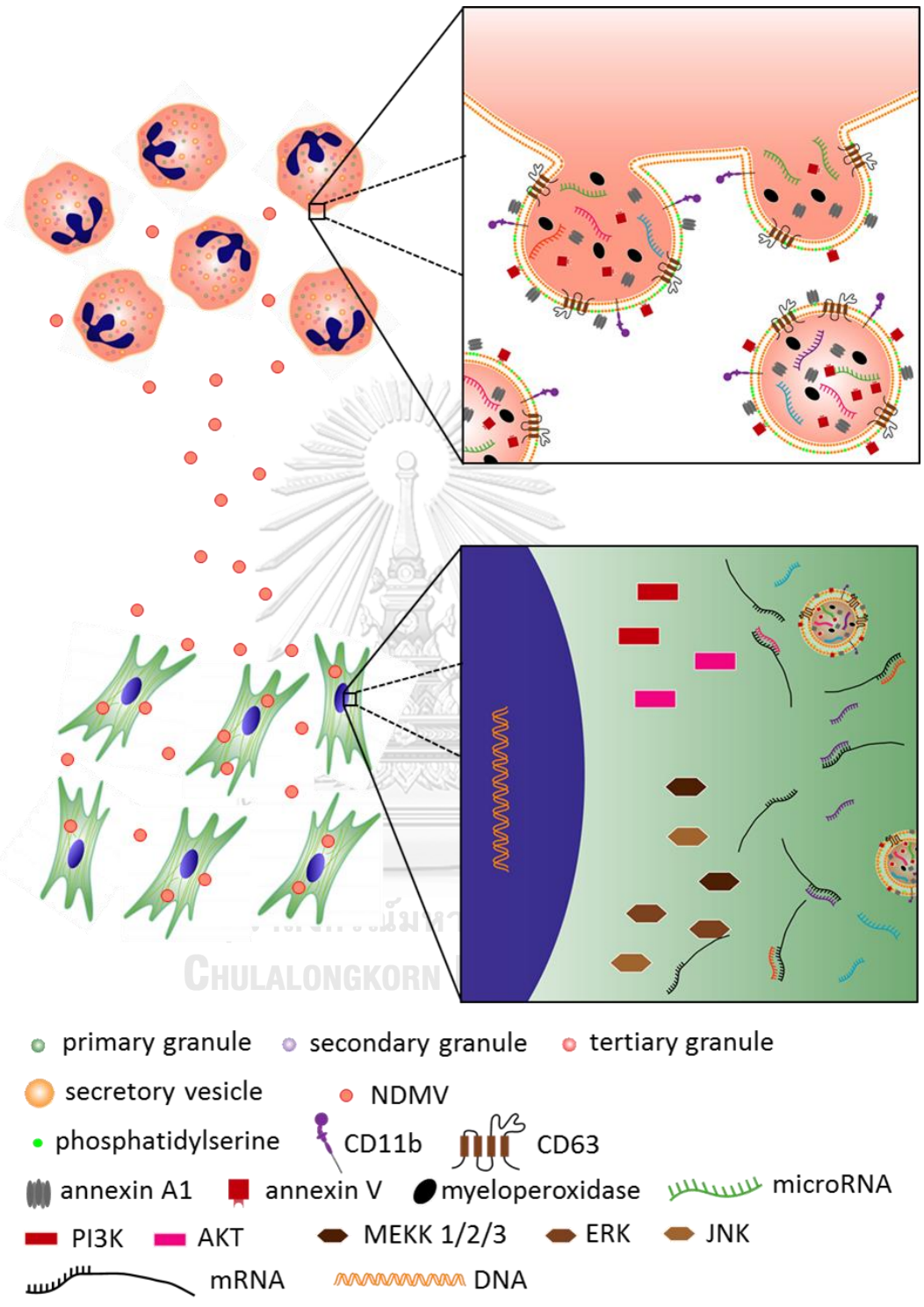

Figure 48. Possible mechanisms of NDMV inhibition of inflammatory responses of FLS via NDMV uploaded microRNA targeting PI3K-Akt and MAPK signaling pathway.

In spite of the interest in EV and NDMV, there are still many unsolved questions to explore and investigate. EV are the “inflammation packages” composed of “good guys” and “bad guys”, so EV influences on target cells depend on resultant overall balance of all of their contents and components and the nature of the target cell. A major factor will be the efficiency with which they are internalized by the target cell. NDMV could be a suitable biomarker to improve precision of diagnosis and a suitable experimental tool for correction of inflammatory disease, especially in arthritis. Further work is needed to confirm if NDMV will be a potential approach to protect cartilage degradation and suppress synovitis in OA and RA. By identifying how stimulants facilitate neutrophils to generate MV and by characterising how NDMV modulate recipient cells via their uploaded components, could enable researchers and doctors to use NDMV in clinical practice for alleviating patient’s pain and improve their quality of life.

APPENDIX

Appendix A / KOOS: Knee Injury and Osteoarthritis Outcome Score

This survey asks for your view about your knee.

Symptoms

These questions should be answered thinking of your knee symptoms during the last week.

S1. Do you have swelling in your knee?

Never	Rarely	Sometimes	Often	Always

S2. Do you feel grinding, hear clicking or any other type of noise when your knee moves?

Never	Rarely	Sometimes	Often	Always

S3. Does your knee catch or hang up when moving?

Never	Rarely	Sometimes	Often	Always

S4. Can you straighten your knee fully?

Always	Often	Sometimes	Rarely	Never

S5. Can you bend your knee fully?

Stiffness

The following questions concern the amount of joint stiffness you have experienced during the last week in your knee. Stiffness is a sensation of restriction or slowness in the ease with which you move your knee joint.

S6. How severe is your knee joint stiffness after first wakening in the morning?

None	Mild	Moderate	Severe	Extreme

S7. How severe is your knee stiffness after sitting, lying or resting **later in the day**?

None	Mild	Moderate	Severe	Extreme

Pain

P1. How often do you experience knee pain?

Never	Monthly	Weekly	Daily	Always

What amount of knee pain have you experienced the last week during the following activities?

P2. Twisting/pivoting on your knee

None	Mild	Moderate	Severe	Extreme

P3. Straightening knee fully

None	Mild	Moderate	Severe	Extreme

P4. Bending knee fully

None	Mild	Moderate	Severe	Extreme

P5. Walking on flat surface

None	Mild	Moderate	Severe	Extreme

P6. Going up or down stairs

None	Mild	Moderate	Severe	Extreme

P7. At night while in bed

None	Mild	Moderate	Severe	Extreme

P8. Sitting or lying

None	Mild	Moderate	Severe	Extreme

P9. Standing upright

None	Mild	Moderate	Severe	Extreme

Function, daily living

The following questions concern your physical function. By this we mean your ability to move around and to look after yourself. For each of the following activities please indicate the degree of difficulty you have experienced in the last week due to your knee.

A1. Descending stairs

None	Mild	Moderate	Severe	Extreme

A2. Ascending stairs

None	Mild	Moderate	Severe	Extreme

For each of the following activities please indicate the degree of difficulty you have experienced in the **last week** due to your knee.

A3. Rising from sitting

None	Mild	Moderate	Severe	Extreme

A4. Standing

None	Mild	Moderate	Severe	Extreme

A5. Bending to floor/pick up an object

None	Mild	Moderate	Severe	Extreme

A6. Walking on flat surface

None	Mild	Moderate	Severe	Extreme

A7. Getting in/out of car

None	Mild	Moderate	Severe	Extreme

A8. Going shopping

None	Mild	Moderate	Severe	Extreme

A9. Putting on socks/stockings

None	Mild	Moderate	Severe	Extreme

A10. Rising from bed

None	Mild	Moderate	Severe	Extreme

A11. Taking off socks/stockings

None	Mild	Moderate	Severe	Extreme

A12. Lying in bed (turning over, maintaining knee position)

None	Mild	Moderate	Severe	Extreme

A13. Getting in/out of bath

None	Mild	Moderate	Severe	Extreme

A14. Sitting

None	Mild	Moderate	Severe	Extreme

A15. Getting on/off toilet

None	Mild	Moderate	Severe	Extreme

For each of the following activities please indicate the degree of difficulty you have experienced in the last week due to your knee.

A16. Heavy domestic duties (moving heavy boxes, scrubbing floors, etc)

None	Mild	Moderate	Severe	Extreme

A17. Light domestic duties (cooking, dusting, etc)

None	Mild	Moderate	Severe	Extreme

Function, sports and recreational activities

The following questions concern your physical function when being active on a higher level. The questions should be answered thinking of what degree of difficulty you have experienced during the last week due to your knee.

SP1. Squatting

None	Mild	Moderate	Severe	Extreme

SP2. Running

None	Mild	Moderate	Severe	Extreme

SP3. Jumping

None	Mild	Moderate	Severe	Extreme

SP4. Twisting/pivoting on your injured knee

None	Mild	Moderate	Severe	Extreme

SP5. Kneeling

None	Mild	Moderate	Severe	Extreme

Quality of Life

Q1. How often are you aware of your knee problem?

Never	Monthly	Weekly	Daily	Constantly

Q2. Have you modified your lifestyle to avoid potentially damaging activities to your knee?

Not at all	Mildly	Moderately	Severely	Totally

Q3. How much are you troubled with lack of confidence in your knee?

Not at all	Mildly	Moderately	Severely	Extremely

Q4. In general, how much difficulty do you have with your knee?

None	Mild	Moderate	Severe	Extreme

Appendix B / ISOA: Indices of Severity and Disease Activity for Osteoarthritis

Sections for index:(1) Pain or discomfort; (2) Maximum distance walked; (3) Activities of daily living.

Pain or Discomfort

Parameter	Finding	Points
Pain or discomfort during nocturnal bed rest	None	0
	Only on movement or in certain positions	1
	Without movement	2
Duration of morning stiffness or pain after getting up	None	0
	< 15 minutes	1
	>= 15 minutes	2
Remaining standing for 30 minutes increases pain	No	0
	Yes	1
Pain on walking	None	0
	Only after walking some distance	1
	Early after starting	2
Pain or discomfort after getting up from sitting without use of arms	No	0
	Yes	1

Maximum Distance Walked

Parameter	Finding	Points
Maximum distance walked	Unlimited	0
	> 1 kilometer but limited	1
	About 1 kilometer (about 15 minutes)	2
	About 500 - 900 meters (about 8-15 minutes)	3
	From 300 - 500 meters	4

	From 100 - 300 meters	5
	< 100 meters	6
Walking aids required	None	0
	1 walking stick or crutch	1
	2 walking sticks or crutches	2

Activities of Daily Living

Parameter	Finding	Points
Able to climb up a standard flight of stairs	Easily	0
	With mild difficulty	0.5
	With moderate difficulty	1.0
	With marked difficulty	1.5
	Impossible	2.0
Able to climb down a standard flight of stairs	Easily	0
	With mild difficulty	0.5
	With moderate difficulty	1.0
	With marked difficulty	1.5
	Impossible	2.0
Able to squat or bend at the knee	Easily	0
	With mild difficulty	0.5
	With moderate difficulty	1.0
	With marked difficulty	1.5
	Impossible	2.0
Able to walk on uneven ground	Easily	0
	With mild difficulty	0.5
	With moderate difficulty	1.0
	With marked difficulty	1.5
	Impossible	2.0

Appendix C / WOMAC: Western Ontario and McMaster Universities Arthritis Index

The WOMAC consists of 24 items divided into 3 subscales: pain (5 items); stiffness (2 items); physical function (17 items). The WOMAC is available in 5-point Likert-type and 100mm Visual Analog formats.

Section A: pain

Think about the pain you felt during the last 48 hours caused by the arthritis in your knee or hip. Select the number that best describes your pain. Question: How much pain have you had:

item	None	Mild	Moderate	Severe	Extreme
1. When walking in a flat surface?	0	1	2	3	4
2. When going up or down stairs?	0	1	2	3	4
3. At night while in bed? (that is pain that disturbs your sleep)	0	1	2	3	4
4. While sitting or lying down?	0	1	2	3	4
5. While standing?	0	1	2	3	4

Section B: stiffness

Think about the stiffness (not pain) you felt during the last 48 hours caused by the arthritis in your knee or hip. Stiffness is a sensation of decreased ease in moving your joint. Select the number that best describes your stiffness:

item	None	Mild	Moderate	Severe	Extreme
6. How severe has your stiffness been after you first woke up in the morning?	0	1	2	3	4
7. How severe has your stiffness been after sitting or lying down or while resting later in the day?	0	1	2	3	4

Section C: difficulty performing daily activities

Think about the difficulty you had in doing the following daily physical activities during the last 48 hours caused by the arthritis in your knee or hip. By this we mean your ability to move around and take care of yourself. Select the number that best describes your difficulty. Question: How much difficulty have you had:

item	None	Mild	Moderate	Severe	Extreme
8. when going down the stairs?	0	1	2	3	4
9. when going up the stairs?	0	1	2	3	4
10. when getting up from a sitting position?	0	1	2	3	4
11. while standing?	0	1	2	3	4
12. when bending to the floor?	0	1	2	3	4
13. when walking on a flat surface?	0	1	2	3	4
14. getting in or out of a car, or getting on or off a bus?	0	1	2	3	4
15. while going shopping?	0	1	2	3	4
16. when putting on your socks or panty hose or stockings?	0	1	2	3	4
17. when getting out of bed?	0	1	2	3	4
18. when taking off your socks or panty hose or stockings?	0	1	2	3	4
19. when lying in bed?	0	1	2	3	4
20. when getting in or out of the bathtub?	0	1	2	3	4
21. while sitting?	0	1	2	3	4
22. when getting on or off the toilet?	0	1	2	3	4
23. while doing heavy household chores?	0	1	2	3	4
24. while doing light household chores?	0	1	2	3	4

Appendix D / Heatmaps of microRNA Different Expression in Neutrophils and NDMV

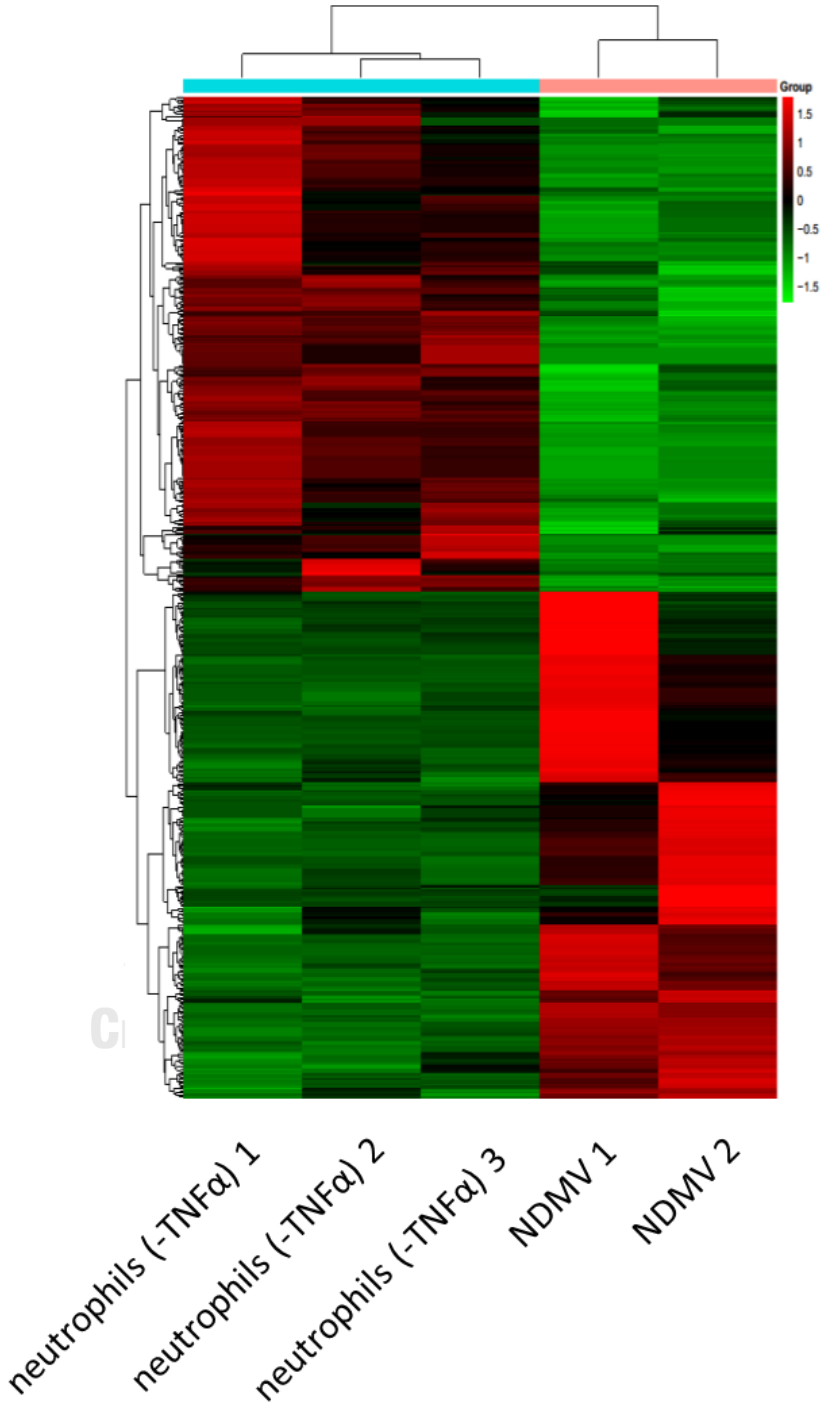

Figure D1. Different expression of microRNA in TNFα-untreated neutrophils and NDMV.

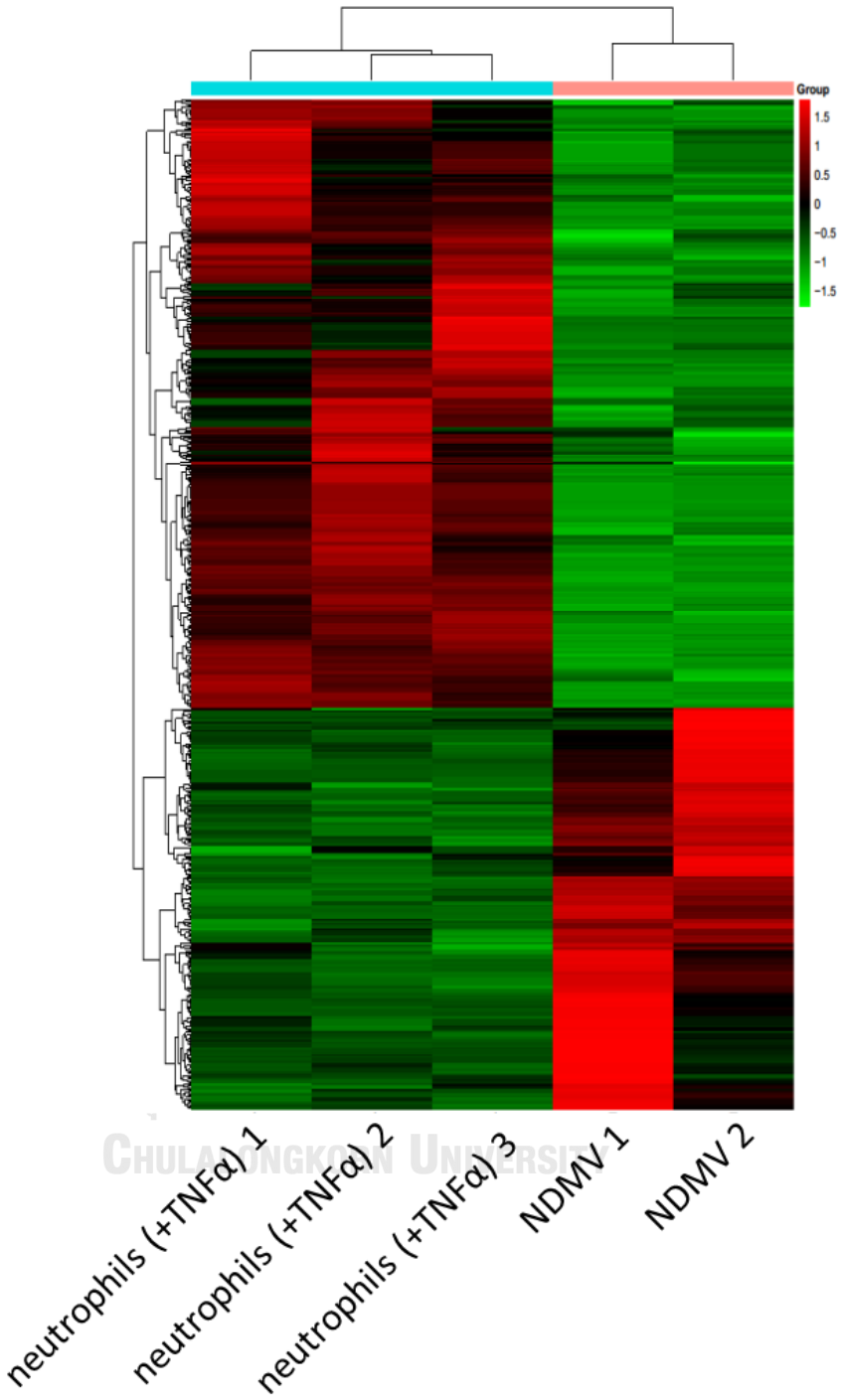

Figure D2. Different expression of microRNA in TNFα-treated neutrophils and NDMV.

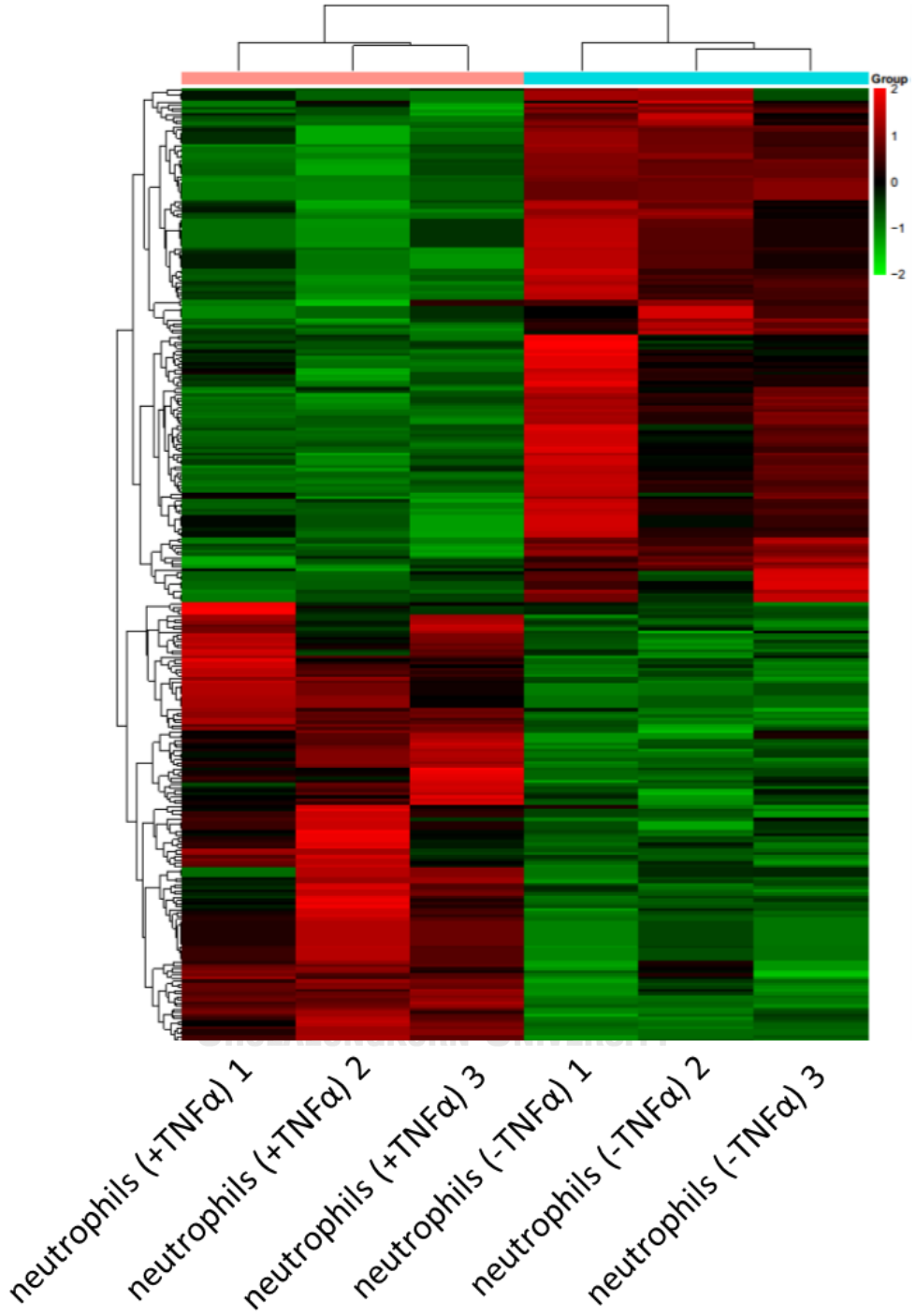

Figure D3. Different expression of microRNA in TNFα-treated and untreated neutrophils.

Appendix E / Reactome Pathway Analysis of NDMV microRNA

Reactome is an open pathway database for bioinformatic analysis (https://reactome.org). It provides another available approach to process big data of target gene. We used the analysed results of Reactome pathway to compare with that of KEGG. The following table shows probable pathway ($p < 0.05$) related with NDMV microRNA of 159. Red words in description were related to PI3K-Akt and MAPK signaling pathway.

Table E. Reactome pathway of NDMV microRNA

ID	Description	GeneRatio	qvalue
R-HSA-9006934	Signaling by Receptor Tyrosine Kinases	93/1156	5.74735E-06
R-HSA-112316	Neuronal System	74/1156	0.001242358
R-HSA-5663202	Diseases of signal transduction	69/1156	0.001242358
R-HSA-9006925	Intracellular signaling by second messengers	54/1156	0.006055974
R-HSA-5683057	MAPK family signaling cascades	54/1156	0.003584897
R-HSA-9006931	Signaling by Nuclear Receptors	49/1156	0.029773722
R-HSA-9607240	FLT3 Signaling	49/1156	0.005510192
R-HSA-112315	Transmission across Chemical Synapses	45/1156	0.032398328
R-HSA-1257604	PIP3 activates AKT signaling	45/1156	0.022315083
R-HSA-5684996	MAPK1/MAPK3 signaling	42/1156	0.040735265
R-HSA-5673001	RAF/MAP kinase cascade	42/1156	0.031485128
R-HSA-8939211	ESR-mediated signaling	40/1156	0.016671707
R-HSA-1483257	Phospholipid metabolism	37/1156	0.030933667
R-HSA-397014	Muscle contraction	37/1156	0.027731091
R-HSA-112314	Neurotransmitter receptors and postsynaptic signal transmission	37/1156	0.022315083
R-HSA-6811442	Intra-Golgi and retrograde Golgi-to-ER traffic	36/1156	0.027785156
R-HSA-5576891	Cardiac conduction	28/1156	0.019287451
R-HSA-73887	Death Receptor Signaling	27/1156	0.030933667
R-HSA-194840	Rho GTPase cycle	26/1156	0.040476774
R-HSA-166520	Signaling by NTRKs	26/1156	0.001954227
R-HSA-2219528	PI3K/AKT Signaling in Cancer	26/1156	0.001954227
R-HSA-199418	Negative regulation of the PI3K/AKT network	25/1156	0.007607503
R-HSA-9006936	Signaling by TGF-beta family members	25/1156	0.003584897
R-HSA-6811558	PI5P, PP2A and IER3 Regulate PI3K/AKT Signaling	23/1156	0.012211791

R-HSA-5173105	O-linked glycosylation	22/1156	0.042165819
R-HSA-187037	Signaling by NTRK1 (TRKA)	22/1156	0.001954227
R-HSA-442755	Activation of NMDA receptors and postsynaptic events	21/1156	0.015713737
R-HSA-193704	p75 NTR receptor-mediated signaling	20/1156	0.040476774
R-HSA-74752	Signaling by Insulin receptor	20/1156	0.006055974
R-HSA-9009391	Extra-nuclear estrogen signaling	20/1156	0.005510192
R-HSA-170834	Signaling by TGF-beta Receptor Complex	20/1156	0.003584897
R-HSA-190236	Signaling by FGFR	19/1156	0.029938298
R-HSA-6794362	Protein-protein interactions at synapses	19/1156	0.029938298
R-HSA-1483255	PI Metabolism	19/1156	0.022315083
R-HSA-422356	Regulation of insulin secretion	19/1156	0.011951844
R-HSA-2219530	Constitutive Signaling by Aberrant PI3K in Cancer	19/1156	0.008660319
R-HSA-375165	NCAM signaling for neurite out-growth	19/1156	0.001954227
R-HSA-8986944	Transcriptional Regulation by MECP2	18/1156	0.003584897
R-HSA-2428928	IRS-related events triggered by IGF1R	18/1156	0.001242358
R-HSA-2428924	IGF1R signaling cascade	18/1156	0.001242358
R-HSA-2404192	Signaling by Type 1 Insulin-like Growth Factor 1 Receptor (IGF1R)	18/1156	0.001242358
R-HSA-74751	Insulin receptor signaling cascade	18/1156	0.001242358
R-HSA-204998	Cell death signaling via NRAGE, NRIF and NADE	17/1156	0.034373093
R-HSA-5654738	Signaling by FGFR2	17/1156	0.027147437
R-HSA-373755	Semaphorin interactions	17/1156	0.010219801
R-HSA-9614085	FOXO-mediated transcription	17/1156	0.010219801
R-HSA-1226099	Signaling by FGFR in disease	17/1156	0.008125866
R-HSA-109606	Intrinsic Pathway for Apoptosis	17/1156	0.001954227
R-HSA-199992	trans-Golgi Network Vesicle Budding	16/1156	0.041188869
R-HSA-193648	NRAGE signals death through JNK	16/1156	0.010219801
R-HSA-3000171	Non-integrin membrane-ECM interactions	15/1156	0.021341993
R-HSA-6794361	Neurexins and neuroligins	15/1156	0.014426919
R-HSA-112399	IRS-mediated signaling	15/1156	0.004461806
R-HSA-1433557	Signaling by SCF-KIT	15/1156	0.001954227
R-HSA-8853659	RET signaling	15/1156	0.001715811
R-HSA-2173793	Transcriptional activity of SMAD2/SMAD3:SMAD4 heterotrimer	14/1156	0.005510192
R-HSA-1660499	Synthesis of PIPs at the plasma membrane	13/1156	0.040735265
R-HSA-5654736	Signaling by FGFR1	13/1156	0.029837407
R-HSA-109704	PI3K Cascade	13/1156	0.012211791

R-HSA-5655253	Signaling by FGFR2 in disease	13/1156	0.010385519
R-HSA-419037	NCAM1 interactions	13/1156	0.009268756
R-HSA-5655302	Signaling by FGFR1 in disease	13/1156	0.004461806
R-HSA-2559585	Oncogene Induced Senescence	12/1156	0.004461806
R-HSA-9022692	Regulation of MECP2 expression and activity	12/1156	0.004461806
R-HSA-114452	Activation of BH3-only proteins	12/1156	0.002253121
R-HSA-5654743	Signaling by FGFR4	11/1156	0.040476774
R-HSA-5654741	Signaling by FGFR3	11/1156	0.034487419
R-HSA-5654696	Downstream signaling of activated FGFR2	11/1156	0.006055974
R-HSA-187687	Signaling to ERKs	10/1156	0.032398328
R-HSA-5654687	Downstream signaling of activated FGFR1	10/1156	0.019938575
R-HSA-4090294	SUMOylation of intracellular receptors	10/1156	0.015713737
R-HSA-442742	CREB1 phosphorylation through NMDA receptor-mediated activation of RAS signaling	10/1156	0.015713737
R-HSA-452723	Transcriptional regulation of pluripotent stem cells	10/1156	0.004461806
R-HSA-5654716	Downstream signaling of activated FGFR4	9/1156	0.024622519
R-HSA-5654708	Downstream signaling of activated FGFR3	9/1156	0.015713737
R-HSA-9634638	Estrogen-dependent nuclear events downstream of ESR-membrane signaling	9/1156	0.012426358
R-HSA-2173795	Downregulation of SMAD2/3: SMAD4 transcriptional activity	9/1156	0.010219801
R-HSA-5654695	PI-3K cascade: FGFR2	9/1156	0.010219801
R-HSA-5655332	Signaling by FGFR3 in disease	9/1156	0.008025745
R-HSA-8853338	Signaling by FGFR3 point mutants in cancer	9/1156	0.008025745
R-HSA-8934593	Regulation of RUNX1 Expression and Activity	9/1156	0.001954227
R-HSA-400685	Sema4D in semaphorin signaling	8/1156	0.040735265
R-HSA-5654700	FRS-mediated FGFR2 signaling	8/1156	0.040735265
R-HSA-9006115	Signaling by NTRK2 (TRKB)	8/1156	0.040735265
R-HSA-3232118	SUMOylation of transcription factors	8/1156	0.01467157
R-HSA-1433559	Regulation of KIT signaling	8/1156	0.004461806
R-HSA-1181150	Signaling by NODAL	7/1156	0.040735265
R-HSA-2028269	Signaling by Hippo	7/1156	0.040735265
R-HSA-5654720	PI-3K cascade: FGFR4	7/1156	0.040735265
R-HSA-416700	Other semaphorin interactions	7/1156	0.034373093
R-HSA-5654710	PI-3K cascade: FGFR3	7/1156	0.027922803
R-HSA-881907	Gastrin-CREB signaling pathway via PKC and MAPK	7/1156	0.027922803
R-HSA-9022699	MECP2 regulates neuronal receptors and channels	7/1156	0.021496752
R-HSA-392517	Rap1 signaling	7/1156	0.015713737

R-HSA-5637810	Constitutive Signaling by EGFRvIII	6/1156	0.040476774
R-HSA-5637812	Signaling by EGFRvIII in Cancer	6/1156	0.040476774
R-HSA-169893	Prolonged ERK activation events	6/1156	0.030718533
R-HSA-418359	Reduction of cytosolic Ca++ levels	6/1156	0.030718533
R-HSA-170968	Frs2-mediated activation	6/1156	0.015713737
R-HSA-5655291	Signaling by FGFR4 in disease	6/1156	0.010682553
R-HSA-8853334	Signaling by FGFR3 fusions in cancer	6/1156	0.007452663
R-HSA-8875555	MET activates RAP1 and RAC1	5/1156	0.041204888
R-HSA-9614399	Regulation of localization of FOXO transcription factors	5/1156	0.041204888

Appendix F / IPA(Qiagen)

Qiagen integrity pathway analysis (IPA) was a user-friendly software to interpret bioinformatic data. 159 microRNA of different expression in neutrophils and NDMV was used to predict their probable network shown in Figure F.

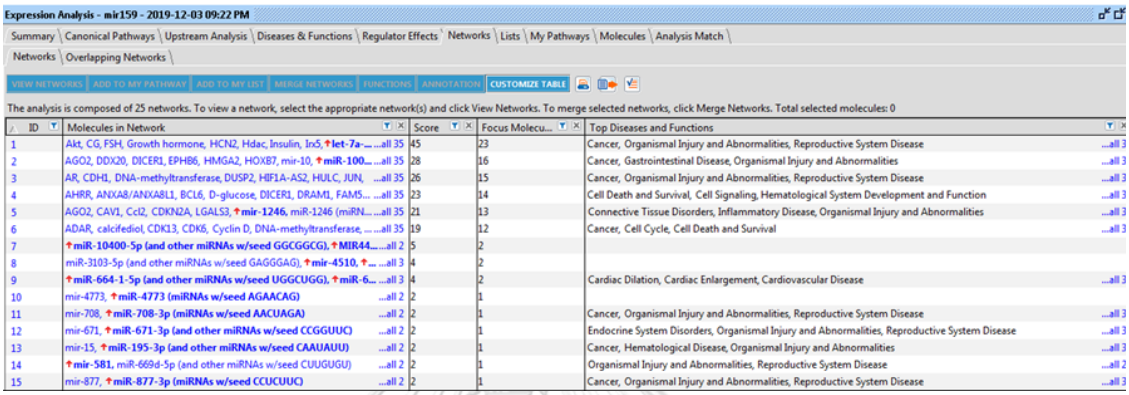

Expression Analysis - mir159 - 2019-12-03 09:22 PM

Summary | Canonical Pathways | Upstream Analysis | Diseases & Functions | Regulator Effects | Networks | Lists | My Pathways | Molecules | Analysis Match

Networks | Overlapping Networks

VIEW NETWORKS | ADD TO MY PATHWAY | ADD TO MY LIST | MERGE NETWORKS | FUNCTIONS | ANNOTATION | CUSTOMIZE TABLE

The analysis is composed of 25 networks. To view a network, select the appropriate network(s) and click View Networks. To merge selected networks, click Merge Networks. Total selected molecules: 0

ID	Molecules in Network	Score	Focus Molecu...	Top Diseases and Functions
1	Akt, CG, FSH, Growth hormone, HCN2, Hdac, Insulin, In5, ↑let-7a-... ...all 35	45	23	Cancer, Organismal Injury and Abnormalities, Reproductive System Disease ...all 3
2	AGO2, DDX20, DICER1, EPHB6, HMGA2, HOXB7, mir-10, ↑miR-100... ...all 35	28	16	Cancer, Gastrointestinal Disease, Organismal Injury and Abnormalities ...all 3
3	AR, CDH1, DNA-methyltransferase, DUSP2, HIF1A-AS2, HULC, JUN, ...all 35	26	15	Cancer, Organismal Injury and Abnormalities, Reproductive System Disease ...all 3
4	AHRR, ANXA8/ANXA8L1, BCL6, D-glucose, DICER1, DRAM1, FAM5... ...all 35	23	14	Cell Death and Survival, Cell Signaling, Hematological System Development and Function ...all 3
5	AGO2, CAV1, Ccl2, CDKN2A, LGALS3, ↑mir-1246, miR-1246 (miRN... ...all 35	21	13	Connective Tissue Disorders, Inflammatory Disease, Organismal Injury and Abnormalities ...all 3
6	ADAR, calcifediol, CDK13, CDK6, Cyclin D, DNA-methyltransferase, ...all 35	19	12	Cancer, Cell Cycle, Cell Death and Survival ...all 3
7	↑miR-10400-5p (and other miRNAs w/seed GGCGGCG), ↑MIR44... ...all 2	5	2	
8	miR-3103-5p (and other miRNAs w/seed GAGGGAG), ↑mir-4510, ↑... ...all 3	4	2	
9	↑miR-664-1-5p (and other miRNAs w/seed UGGCUGG), ↑miR-6... ...all 3	4	2	Cardiac Dilation, Cardiac Enlargement, Cardiovascular Disease ...all 3
10	mir-4773, ↑miR-4773 (miRNAs w/seed AGAACAG) ...all 2	2	1	
11	mir-708, ↑miR-708-3p (miRNAs w/seed AACUAGA) ...all 2	2	1	Cancer, Organismal Injury and Abnormalities, Reproductive System Disease ...all 3
12	mir-671, ↑miR-671-3p (and other miRNAs w/seed CCGGUUC) ...all 2	2	1	Endocrine System Disorders, Organismal Injury and Abnormalities, Reproductive System Disease ...all 3
13	mir-15, ↑miR-195-3p (and other miRNAs w/seed CAAUAUU) ...all 2	2	1	Cancer, Hematological Disease, Organismal Injury and Abnormalities ...all 3
14	↑mir-581, miR-669d-5p (and other miRNAs w/seed CUUGUGU) ...all 2	2	1	Organismal Injury and Abnormalities, Reproductive System Disease ...all 2
15	mir-877, ↑miR-877-3p (miRNAs w/seed CCUCUUC) ...all 2	2	1	Cancer, Organismal Injury and Abnormalities, Reproductive System Disease ...all 3

Figure F1. List of molecules in network and their score evaluated by IPA.

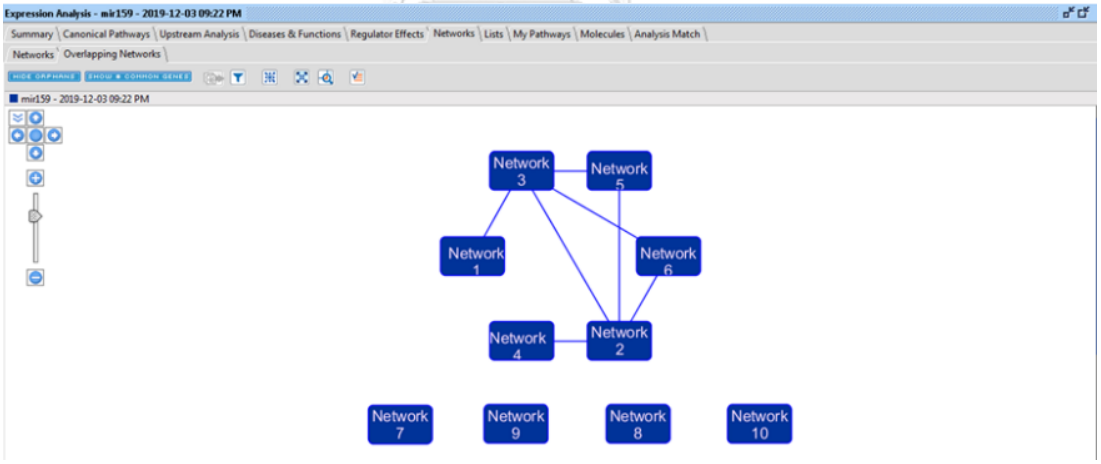

Figure F2. Connection of top 10 networks

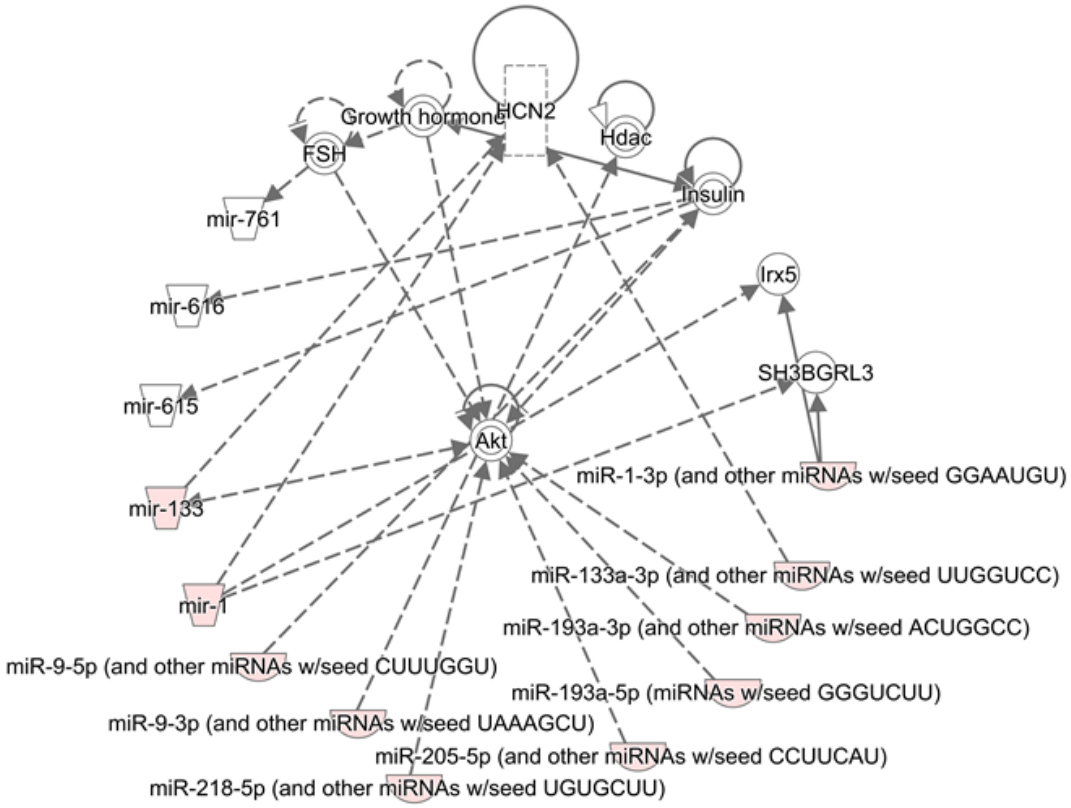

Figure F3. Interaction of target genes and NDMV microRNA in Network 1. As NDMV microRNA were exogenous small RNA, up-stream molecules of microRNA were excluded from photograph.

Appendix G / Pre-treatment of NDMV and Treatment of TNFα to FLS

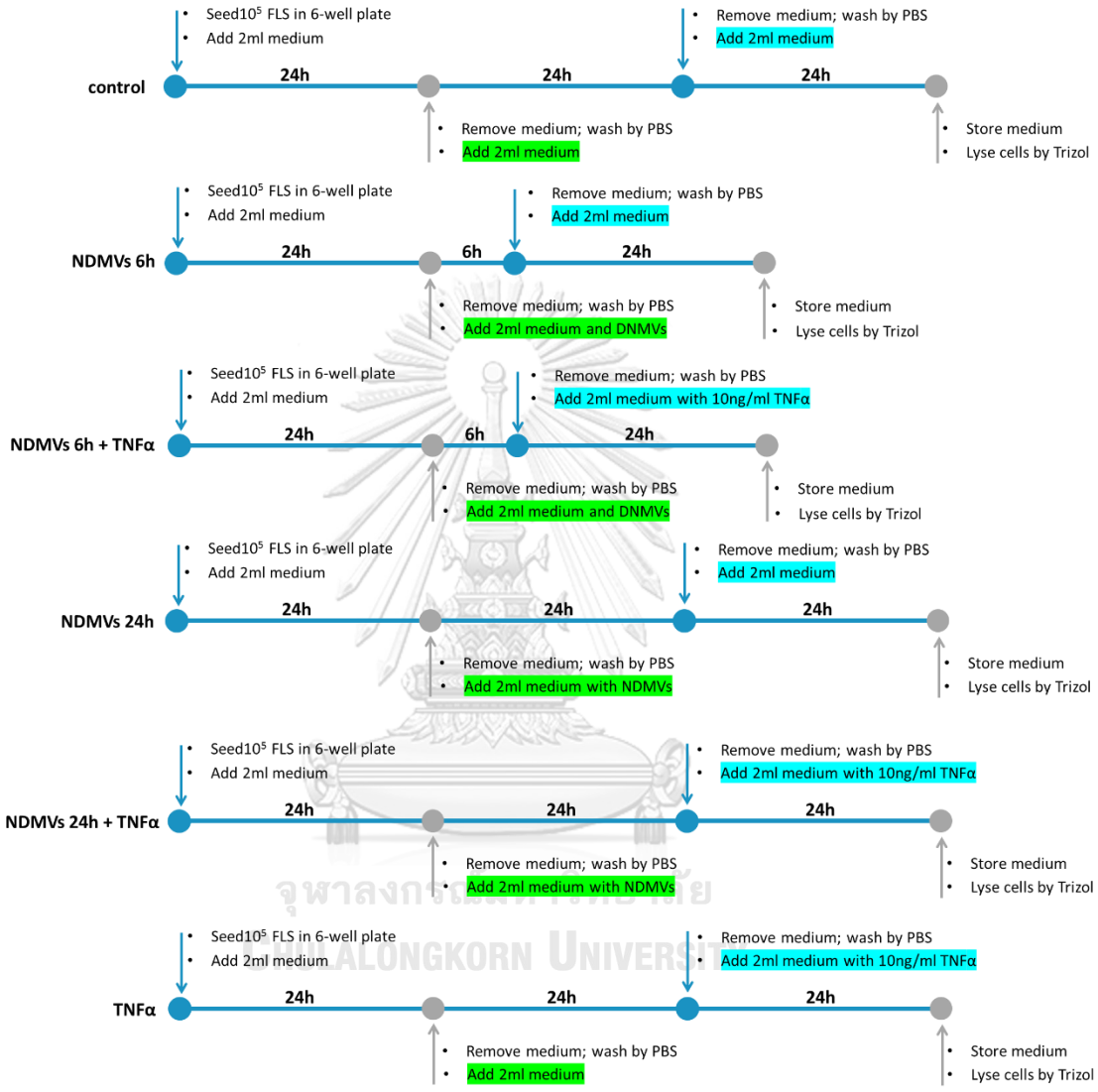

Figure G. The schedule of NDMV to pre-treat FLS on 6, 24h after FLS adhere to 6-well plates.

ABBREVIATIONS

Abbreviation	Full Name
AB	Apoptotic Bodies
ACPA	Anti-Citrullinated Protein Antibodies
ANCA	Anti-Neutrophil Cytoplasmic Antibody
APC	Allophycocyanin
BMI	Body Mass Index
BP	Biological Process
C5a	Cleavage of Complement Component C5
CC	Cellular Component
CCL	Chemokine (C-C Motif) Ligand
CD	Cluster of Difference
COX	Cyclooxygenase
CPM	Counts per Million
CRP	C-Reactive Protein
CXCL	Chemokine (C-X-C Motif) Ligand
DAF	Decay Accelerating Factor
DAS	Disease Activity Score
DC	Dendritic Cells
DEPC	Diethyl Pyrocarbonate
DIP	Distal Interphalangeal
DMARD	Disease-Modifying Antirheumatic Drugs
DMEM	Dulbecco's Modified and Eagle's Medium
D-NAME	N Omega-Nitro-D-Arginine Methyl Ester Hydrochloride
ECM	Extracellular Matrix

EDTA	Ethylenediaminetetraacetic Acid
EM	Electron Microscopy
ER	Endoplasmic Reticulum
ESCRT	Endosomal Sorting Complex Required for Transport
EULAR	European League Against Rheumatism
EV	Extracellular Vesicles
Exo	Exosomes
FBS	Fetal Bovine Serum
FITC	Fluorescein Isothiocyanate
FLS	Fibroblast-Like Synoviocytes
fMLP	N-Formylmethionyl-Leucyl-Phenylalanine
FOX	Forkhead Box
FPR	Formyl Peptide Receptor
GO	Gene Ontology
HBSS	Hanks' Balanced Salt Solution
HE	Hematoxylin and Eosin
HLA	Human Leukocyte Antigen
IFN	Interferon
IL	Interleukin
IPA	Ingenuity Pathway Analysis
ISOA	Indices of Severity and Disease Activity for Osteoarthritis
JNK	C-Jun N-Terminal Kinases
KEGG	Kyoto Encyclopedia of Genes and Genomes
KL grade	Kellgren and Lawrence Grade
KOOS	Knee Injury and Osteoarthritis Outcome Score

L-NAME	N Omega-Nitro-L-Arginine Methyl Ester Hydrochloride
Log GP	Logarithmic Growth Phase
LPS	Lipopolysaccharides
MAPK	Mitogen-Activated Protein Kinase
MCP	Monocyte Chemoattractant Protein
MDMC	Monocyte-Derived Microvesicles
MerTK	Mer-Receptor Tyrosine Kinase
MF	Molecular Function
MFI	Mean Fluorescent Index
MGC	Multinucleated Giant Cells
MHC	Major Histocompatibility Complex
MLS	Macrophage-Like Synoviocytes
MMP	Matrix Metalloproteinases
MPO	Myeloperoxidase
MRI	Magnetic Resonance Imaging
MSC	Mesenchymal Stem Cells
MSCs	Mesenchymal Stem Cells
mTOR	Mammalian Target of Rapamycin
MTP	Metatarsophalangeal
MTT	3, (4, 5-Dimethylthiazol-2-yl) 2, 5-Diphenyl-Tetrazolium Bromide
MTX	Methotrexate
MV	Microvesicles
MVB	Multivesicular Bodies
NDMV	Neutrophil-Derived Microvesicles
NF-κB	Nuclear Factor Kappa B

NK cells	Natural Killer Cells
NSAID	Non-Steroidal Anti-Inflammatory Drugs
NTA	Nanoparticle Tracking Analysis
OA	Osteoarthritis
OD	Optical Density
Onc	Oncosomes
PBMC	Peripheral Blood Mononuclear Cell
PBS	Phosphate-Buffered Saline
PCR	Polymerase Chain Reaction
PE	Phycoerythrin
PFA	Paraformaldehyde
PGE	Prostaglandin E
PI	Propidium Iodide
PI3K	Phosphoinositide 3-Kinase
PIP	Proximal Interphalangeal
PKB/AKT	Protein Kinase B
PMA	Para-Methoxyamphetamine
PMN	Polymorphonuclear Neutrophils
poly-HEMA	Poly-2-Hydoroxyethyl Methacrylate
PtdSer	Phosphatidylserine
RA	Rheumatoid Arthritis
RANKL	Rank-Ligand
RF	Rheumatoid Factors
RNAK	Receptor Activator of Nuclear Factor Kappa B
ROS	Reactive Oxygen Species

RT	Room Temperature
RTK	Receptor Tyrosine Kinases
RT-PCR	Reverse Transcription-Polymerase Chain Reaction
SA-PE	Streptavidin-Phycoerythrin
SEM	Scanning Electron Microscopy
SER	Erythrocyte Sedimentation Rate
SF	Synovial Fluid
SLE	Systemic Lupus Erythematosus
SOCS	Suppressor of Cytokine Signaling
STAT	Signal Transducer and Activator of Transcription
TACE	Tumor Necrosis Factor-A-Converting Enzyme
TAM	Tyro3, AXL and MER
TDMV	T Cell-Derived Microvesicles
TEM	Transmission Electron Microscopy
TGFβ	Transforming Growth Factor Beta
Th	T Helper Cells
Thy-1	Thymocyte Differentiation Antigen-1
TLR	Toll-Like Receptor
TNFα	Tumor Necrosis Factor Alpha
TRAF	TNF Receptor-Associated Factor
UD-PGD	Uridine Diphosphoglucose Dehydrogenase
ULN	Upper Limit of Normal
UV	Ultra-Violate
VAS	Visual Analogue Scale
VCAM	Vascular Cell Adhesion Molecule

TRAF	TNF Receptor-Associated Factor
UD-PGD	Uridine Diphosphoglucose Dehydrogenase

REFERENCES

ABD-EL-HAFEZ, A. A., EL-DEEB, A., ESMAIL, M. & AL SERNAGAWY, R. 2014. Ultrastructural characteristics of synovial fluid cells in rheumatoid arthritis and osteoarthritis. *Tanta Medical Journal,* 42**,** 21.

ACENCIO, M. L., LÆGREID, A. & KUIPER, M. 2019. The Gene Ontology Resource: 20 years and still GOing strong.

AGARWAL, S., MISRA, R. & AGGARWAL, A. 2008. Interleukin 17 levels are increased in juvenile idiopathic arthritis synovial fluid and induce synovial fibroblasts to produce proinflammatory cytokines and matrix metalloproteinases. *The Journal of rheumatology,* 35**,** 515-519.

AJIKUMAR, A., LONG, M. B., HEATH, P. R., WHARTON, S. B., INCE, P. G., RIDGER, V. C. & SIMPSON, J. E. 2019. Neutrophil-Derived Microvesicle Induced Dysfunction of Brain Microvascular Endothelial Cells In Vitro. *International journal of molecular sciences,* 20**,** 5227.

ALETAHA, D., NEOGI, T., SILMAN, A. J., FUNOVITS, J., FELSON, D. T., BINGHAM, C. O., 3RD, BIRNBAUM, N. S., BURMESTER, G. R., BYKERK, V. P., COHEN, M. D., COMBE, B., COSTENBADER, K. H., DOUGADOS, M., EMERY, P., FERRACCIOLI, G., HAZES, J. M., HOBBS, K., HUIZINGA, T. W., KAVANAUGH, A., KAY, J., KVIEN, T. K., LAING, T., MEASE, P., MENARD, H. A., MORELAND, L. W., NADEN, R. L., PINCUS, T., SMOLEN, J. S., STANISLAWSKA-BIERNAT, E., SYMMONS, D., TAK, P. P., UPCHURCH, K. S., VENCOVSKY, J., WOLFE, F. & HAWKER, G. 2010a. 2010 Rheumatoid arthritis classification criteria: an American College of Rheumatology/European League Against Rheumatism collaborative initiative. *Arthritis Rheum,* 62**,** 2569-81.

ALETAHA, D., NEOGI, T., SILMAN, A. J., FUNOVITS, J., FELSON, D. T., BINGHAM III, C. O., BIRNBAUM, N. S., BURMESTER, G. R., BYKERK, V. P. & COHEN, M. D. 2010b. 2010 rheumatoid arthritis classification criteria: an American College of Rheumatology/European League Against Rheumatism collaborative initiative. *Arthritis & Rheumatism,* 62**,** 2569-2581.

ALEXANDER, M., HU, R., RUNTSCH, M. C., KAGELE, D. A., MOSBRUGER, T. L., TOLMACHOVA, T., SEABRA, M. C., ROUND, J. L., WARD, D. M. &

O'CONNELL, R. M. 2015. Exosome-delivered microRNAs modulate the inflammatory response to endotoxin. *Nature communications,* 6**,** 7321.

ALTMAN, R., ASCH, E., BLOCH, D., BOLE, G., BORENSTEIN, D., BRANDT, K., CHRISTY, W., COOKE, T. D., GREENWALD, R., HOCHBERG, M. & ET AL. 1986. Development of criteria for the classification and reporting of osteoarthritis. Classification of osteoarthritis of the knee. Diagnostic and Therapeutic Criteria Committee of the American Rheumatism Association. *Arthritis Rheum,* 29**,** 1039-49.

AREND, W. P. & FIRESTEIN, G. S. 2012. Pre-rheumatoid arthritis: predisposition and transition to clinical synovitis. *Nature Reviews Rheumatology,* 8**,** 573.

ARNETT, F. C., EDWORTHY, S. M., BLOCH, D. A., MCSHANE, D. J., FRIES, J. F., COOPER, N. S., HEALEY, L. A., KAPLAN, S. R., LIANG, M. H. & LUTHRA, H. S. 1988. The American Rheumatism Association 1987 revised criteria for the classification of rheumatoid arthritis. *Arthritis & Rheumatism: Official Journal of the American College of Rheumatology,* 31**,** 315-324.

ARRAUD, N., LINARES, R., TAN, S., GOUNOU, C., PASQUET, J. M., MORNET, S. & BRISSON, A. R. 2014. Extracellular vesicles from blood plasma: determination of their morphology, size, phenotype and concentration. *Journal of Thrombosis and Haemostasis,* 12**,** 614-627.

ASGHAR, S., LITHERLAND, G. J., LOCKHART, J. C., GOODYEAR, C. S. & CRILLY, A. 2019. Exosomes in intercellular communication and implications for osteoarthritis. *Rheumatology,* 59**,** 57-68.

ASHBURNER, M., BALL, C. A., BLAKE, J. A., BOTSTEIN, D., BUTLER, H., CHERRY, J. M., DAVIS, A. P., DOLINSKI, K., DWIGHT, S. S., EPPIG, J. T., HARRIS, M. A., HILL, D. P., ISSEL-TARVER, L., KASARSKIS, A., LEWIS, S., MATESE, J. C., RICHARDSON, J. E., RINGWALD, M., RUBIN, G. M. & SHERLOCK, G. 2000. Gene ontology: tool for the unification of biology. The Gene Ontology Consortium. *Nature genetics,* 25**,** 25-29.

BARNES, T. C., ANDERSON, M. E., EDWARDS, S. W. & MOOTS, R. J. 2012. Neutrophil-derived reactive oxygen species in SSc. *Rheumatology,* 51**,** 1166-1169.

BARTOK, B. & FIRESTEIN, G. S. 2010. Fibroblast-like synoviocytes: key effector cells in rheumatoid arthritis. *Immunological reviews,* 233**,** 233-255.

BULLÓ, M., GARCÍA-LORDA, P., MEGIAS, I. & SALAS-SALVADÓ, J. 2003. Systemic inflammation, adipose tissue tumor necrosis factor, and leptin expression. *Obesity research,* 11**,** 525-531.

CHAIAMNUAY, P., DARMAWAN, J., MUIRDEN, K. & ASSAWATANABODEE, P. 1998. Epidemiology of rheumatic disease in rural Thailand: a WHO-ILAR COPCORD study. Community Oriented Programme for the Control of Rheumatic Disease. *The Journal of rheumatology,* 25**,** 1382-1387.

CHEN, B., DENG, Y., TAN, Y., QIN, J. & CHEN, L.-B. 2014. Association between severity of knee osteoarthritis and serum and synovial fluid interleukin 17 concentrations. *Journal of International Medical Research,* 42**,** 138-144.

CHEN, T. S., LAI, R. C., LEE, M. M., CHOO, A. B. H., LEE, C. N. & LIM, S. K. 2009. Mesenchymal stem cell secretes microparticles enriched in pre-microRNAs. *Nucleic acids research,* 38**,** 215-224.

CHEN, Y. C., HO, C. W., TSAI, H. H. & WANG, J. S. 2015. Interval and continuous exercise regimens suppress neutrophil-derived microparticle formation and neutrophil-promoted thrombin generation under hypoxic stress. *Clin Sci (Lond),* 128**,** 425-36.

CHIEWCHENGCHOL, D., WRIGHT, H. L., THOMAS, H. B., LAM, C. W., ROBERTS, K. J., HIRANKARN, N., BERESFORD, M. W., MOOTS, R. J. & EDWARDS, S. W. 2016. Differential changes in gene expression in human neutrophils following TNF-α stimulation: Up-regulation of anti-apoptotic proteins and down-regulation of proteins involved in death receptor signaling. *Immunity, inflammation and disease,* 4**,** 35-44.

COCUCCI, E. & MELDOLESI, J. 2015. Ectosomes and exosomes: shedding the confusion between extracellular vesicles. *Trends Cell Biol,* 25**,** 364-72.

COLLADO, P., NAREDO, E., CALVO, C., GAMIR, M. L., CALVO, I., GARCIA, M. L., MERINO, R., GRANA, J., BUSTABAB, S. & GARRIDO, J. 2013. Reduced joint assessment vs comprehensive assessment for ultrasound detection of synovitis in juvenile idiopathic arthritis. *Rheumatology (Oxford),* 52**,** 1477-84.

COOPER, C., DENNI SON, E., EDWARDS, M. & LITWIC, A. 2013. Epidemiology of osteoarthritis. *Medicographia,* 35**,** 145-51.

CRESCITELLI, R., LÄSSER, C., SZABÓ, T. G., KITTEL, A., ELDH, M.,

DIANZANI, I., BUZÁS, E. I. & LÖTVALL, J. 2013. Distinct RNA profiles in subpopulations of extracellular vesicles: apoptotic bodies, microvesicles and exosomes. *Journal of extracellular vesicles,* 2**,** 20677.

CROSS, A., MOOTS, R. J. & EDWARDS, S. W. 2008. The dual effects of TNFα on neutrophil apoptosis are mediated via differential effects on expression of Mcl-1 and Bfl-1. *Blood,* 111**,** 878-884.

CROSS, M., SMITH, E., HOY, D., CARMONA, L., WOLFE, F., VOS, T., WILLIAMS, B., GABRIEL, S., LASSERE, M. & JOHNS, N. 2014. The global burden of rheumatoid arthritis: estimates from the global burden of disease 2010 study. *Annals of the rheumatic diseases,* 73**,** 1316-1322.

CUMPELIK, A., ANKLI, B., ZECHER, D. & SCHIFFERLI, J. A. 2016. Neutrophil microvesicles resolve gout by inhibiting C5a-mediated priming of the inflammasome. *Ann Rheum Dis,* 75**,** 1236-45.

DALLI, J., MONTERO-MELENDEZ, T., NORLING, L. V., YIN, X., HINDS, C., HASKARD, D., MAYR, M. & PERRETTI, M. 2013. Heterogeneity in neutrophil microparticles reveals distinct proteome and functional properties. *Molecular & Cellular Proteomics,* 12**,** 2205-2219.

DALLI, J., NORLING, L. V., MONTERO-MELENDEZ, T., FEDERICI CANOVA, D., LASHIN, H., PAVLOV, A. M., SUKHORUKOV, G. B., HINDS, C. J. & PERRETTI, M. 2014. Microparticle alpha-2-macroglobulin enhances pro-resolving responses and promotes survival in sepsis. *EMBO Mol Med,* 6**,** 27-42.

DALLI, J., NORLING, L. V., RENSHAW, D., COOPER, D., LEUNG, K.-Y. & PERRETTI, M. 2008. Annexin 1 mediates the rapid anti-inflammatory effects of neutrophil-derived microparticles. *Blood,* 112**,** 2512-2519.

DANIEL, L., FAKHOURI, F., JOLY, D., MOUTHON, L., NUSBAUM, P., GRUNFELD, J.-P., SCHIFFERLI, J., GUILLEVIN, L., LESAVRE, P. & HALBWACHS-MECARELLI, L. 2006. Increase of circulating neutrophil and platelet microparticles during acute vasculitis and hemodialysis. *Kidney international,* 69**,** 1416-1423.

DE LANGE-BROKAAR, B. J., IOAN-FACSINAY, A., VAN OSCH, G. J., ZUURMOND, A.-M., SCHOONES, J., TOES, R. E., HUIZINGA, T. W. &

KLOPPENBURG, M. 2012. Synovial inflammation, immune cells and their cytokines in osteoarthritis: a review. *Osteoarthritis and cartilage,* 20**,** 1484-1499.

DELIGNE, C., CASULLI, S., PIGENET, A., BOUGAULT, C., CAMPILLO-GIMENEZ, L., NOURISSAT, G., BERENBAUM, F., ELBIM, C. & HOUARD, X. 2015. Differential expression of interleukin-17 and interleukin-22 in inflamed and non-inflamed synovium from osteoarthritis patients. *Osteoarthritis Cartilage,* 23**,** 1843-52.

DEQUEKER, J. & LUYTEN, F. 2008. The history of osteoarthritis-osteoarthrosis. *Annals of the rheumatic diseases,* 67**,** 5-10.

DIAZ-TORNE, C., SCHUMACHER, H., YU, X., GOMEZ-VAQUERO, C., DAI, L., CHEN, L., CLAYBURNE, G., EINHORN, E., SACHDEVA, R. & SINGH, J. 2007. Absence of histologic evidence of synovitis in patients with Gulf War veterans' illness with joint pain. *Arthritis Care & Research,* 57**,** 1316-1323.

DING, J., LI, X. & HU, H. 2016. TarPmiR: a new approach for microRNA target site prediction. *Bioinformatics,* 32**,** 2768-2775.

DISTLER, J. H., JUNGEL, A., HUBER, L. C., SEEMAYER, C. A., REICH, C. F., 3RD, GAY, R. E., MICHEL, B. A., FONTANA, A., GAY, S., PISETSKY, D. S. & DISTLER, O. 2005a. The induction of matrix metalloproteinase and cytokine expression in synovial fibroblasts stimulated with immune cell microparticles. *Proc Natl Acad Sci U S A,* 102**,** 2892-7.

DISTLER, J. H., JÜNGEL, A., HUBER, L. C., SEEMAYER, C. A., REICH, C. F., GAY, R. E., MICHEL, B. A., FONTANA, A., GAY, S. & PISETSKY, D. S. 2005b. The induction of matrix metalloproteinase and cytokine expression in synovial fibroblasts stimulated with immune cell microparticles. *Proceedings of the National Academy of Sciences,* 102**,** 2892-2897.

DOHERTY, M., WATT, I. & DIEPPE, P. 1983. Influence of primary generalised osteoarthritis on development of secondary osteoarthritis. *The Lancet,* 322**,** 8-11.

DU, H., ZHANG, X., HUANG, X., ZENG, Y., CHEN, H., WANG, S., WU, J., LI, Q., ZHU, W. & LI, H. 2019. A Novel Phytochemical, DIM, Inhibits Proliferation, Migration, Invasion and TNFα Induced Inflammatory Cytokine Production of Synovial Fibroblasts From Rheumatoid Arthritis Patients by Targeting MAPK and AKT/mTOR Signal Pathway. *Frontiers in immunology,* 10**,** 1620.

DUARTE, T. A., NORONHA-DUTRA, A. A., NERY, J. S., RIBEIRO, S. B., PITANGA, T. N., LAPA, E. S. J. R., ARRUDA, S. & BOECHAT, N. 2012. Mycobacterium tuberculosis-induced neutrophil ectosomes decrease macrophage activation. *Tuberculosis (Edinb),* 92**,** 218-25.

DWEEP, H. & GRETZ, N. 2015. miRWalk2. 0: a comprehensive atlas of microRNA-target interactions. *Nature methods,* 12**,** 697-697.

EKEN, C., GASSER, O., ZENHAEUSERN, G., OEHRI, I., HESS, C. & SCHIFFERLI, J. A. 2008. Polymorphonuclear neutrophil-derived ectosomes interfere with the maturation of monocyte-derived dendritic cells. *The Journal of Immunology,* 180**,** 817-824.

EKEN, C., MARTIN, P. J., SADALLAH, S., TREVES, S., SCHALLER, M. & SCHIFFERLI, J. A. 2010. Ectosomes released by polymorphonuclear neutrophils induce a MerTK-dependent anti-inflammatory pathway in macrophages. *J Biol Chem,* 285**,** 39914-21.

EKEN, C., SADALLAH, S., MARTIN, P. J., TREVES, S. & SCHIFFERLI, J. A. 2013. Ectosomes of polymorphonuclear neutrophils activate multiple signaling pathways in macrophages. *Immunobiology,* 218**,** 382-92.

ELBIM, C., KATSIKIS, P. D. & ESTAQUIER, J. 2009. Neutrophil apoptosis during viral infections. *The open virology journal,* 3**,** 52-59.

ELBIM, C., REGLIER, H., FAY, M., DELARCHE, C., ANDRIEU, V., EL BENNA, J. & GOUGEROT-POCIDALO, M.-A. 2001. Intracellular pool of IL-10 receptors in specific granules of human neutrophils: differential mobilization by proinflammatory mediators. *The Journal of Immunology,* 166**,** 5201-5207.

ERMIS, A., HENN, W., REMBERGER, K., HOPF, C., HOPF, T. & ZANG, K. D. 1995. Proliferation enhancement by spontaneous multiplication of chromosome 7 in rheumatic synovial cells in vitro. *Human genetics,* 96**,** 651-654.

FAM, A. G., MORAVA-PROTZNER, I., PURCELL, C., YOUNG, B. D., BUNTING, P. S. & LEWIS, A. J. 1995. Acceleration of experimental lapine osteoarthritis by calcium pyrophosphate microcrystalline synovitis. *Arthritis & Rheumatism: Official Journal of the American College of Rheumatology,* 38**,** 201-210.

FELSON, D. T. 1990. Epidemiology of the rheumatic diseases. *Current opinion in*

rheumatology, 2**,** 301-308.

FINKIELSZTEIN, A., MASCARENHAS, L., BUTIN-ISRAELI, V. & SUMAGIN, R. 2018. Isolation and Characterization of Neutrophil-derived Microparticles for Functional Studies. *J Vis Exp*.

FINNERTY, C. C., HERNDON, D. N., PRZKORA, R., PEREIRA, C. T., OLIVEIRA, H. M., QUEIROZ, D. M., ROCHA, A. M. & JESCHKE, M. G. 2006. Cytokine expression profile over time in severely burned pediatric patients. *Shock,* 26**,** 13-19.

FRANSEN, M., BRIDGETT, L., MARCH, L., HOY, D., PENSERGA, E. & BROOKS, P. 2011. The epidemiology of osteoarthritis in Asia. *International journal of rheumatic diseases,* 14**,** 113-121.

FRISELL, T., HOLMQVIST, M., KÄLLBERG, H., KLARESKOG, L., ALFREDSSON, L. & ASKLING, J. 2013. Familial risks and heritability of rheumatoid arthritis: role of rheumatoid factor/anti–citrullinated protein antibody status, number and type of affected relatives, sex, and age. *Arthritis & Rheumatism,* 65**,** 2773-2782.

FURUZAWA-CARBALLEDA, J. & ALCOCER-VARELA, J. 1999. Interleukin-8, interleukin-10, intercellular adhesion molecule-1 and vascular cell adhesion molecule-1 expression levels are higher in synovial tissue from patients with rheumatoid arthritis than in osteoarthritis. *Scandinavian journal of immunology,* 50**,** 215-222.

GABRIEL, S. E. & MICHAUD, K. 2009. Epidemiological studies in incidence, prevalence, mortality, and comorbidity of the rheumatic diseases. *Arthritis research & therapy,* 11**,** 229.

GALLIGAN, C. & YOSHIMURA, T. 2003. Phenotypic and functional changes of cytokine-activated neutrophils. *The Neutrophil: An Emerging Regulator of Inflammatory and Immune Response.* Karger Publishers.

GARSTANG, S. V. & STITIK, T. P. 2006. Osteoarthritis: epidemiology, risk factors, and pathophysiology. *American journal of physical medicine & rehabilitation,* 85**,** S2-S11.

GASSER, O., HESS, C., MIOT, S., DEON, C. & SANCHEZ, J.-C. 2003. Characterisation and properties of ectosomes released by human polymorphonuclear neutrophils. *Experimental cell research,* 285**,** 243-257.

GASSER, O. & SCHIFFERLI, J. A. 2004. Activated polymorphonuclear neutrophils

disseminate anti-inflammatory microparticles by ectocytosis. *Blood,* 104**,** 2543-2548.

GASSER, O. & SCHIFFERLI, J. A. 2005. Microparticles released by human neutrophils adhere to erythrocytes in the presence of complement. *Experimental cell research,* 307**,** 381-387.

GENGE, B. R., WU, L. N. & WUTHIER, R. E. 2007. In vitro modeling of matrix vesicle nucleation synergistic stimulation of mineral formation by annexin A5 and phosphatidylserine. *Journal of Biological Chemistry,* 282**,** 26035-26045.

GOMEZ, I., WARD, B., SOUILHOL, C., RECARTI, C., ARIAANS, M., JOHNSTON, J., BURNETT, A., MAHMOUD, M., LUONG, L. A., WEST, L., LONG, M., PARRY, S., WOODS, R., HULSTON, C., BENEDIKTER, B., NIESPOLO, C., BAZAZ, R., FRANCIS, S., KISS-TOTH, E., VAN ZANDVOORT, M., SCHOBER, A., HELLEWELL, P., EVANS, P. C. & RIDGER, V. 2020. Neutrophil microvesicles drive atherosclerosis by delivering miR-155 to atheroprone endothelium. *Nature communications,* 11**,** 214-214.

GONZALEZ-CANO, P., MONDRAGON-FLORES, R., SANCHEZ-TORRES, L. E., GONZALEZ-POZOS, S., SILVA-MIRANDA, M., MONROY-OSTRIA, A., ESTRADA-PARRA, S. & ESTRADA-GARCIA, I. 2010. Mycobacterium tuberculosis H37Rv induces ectosome release in human polymorphonuclear neutrophils. *Tuberculosis (Edinb),* 90**,** 125-34.

GOTIS-GRAHAM, I. & MCNEIL, H. P. 1997. Mast cell responses in rheumatoid synovium. Association of the MCTC subset with matrix turnover and clinical progression. *Arthritis & Rheumatism: Official Journal of the American College of Rheumatology,* 40**,** 479-489.

GREGERSEN, P. K., SILVER, J. & WINCHESTER, R. J. 1987. The shared epitope hypothesis. An approach to understanding the molecular genetics of susceptibility to rheumatoid arthritis. *Arthritis & Rheumatism: Official Journal of the American College of Rheumatology,* 30**,** 1205-1213.

GU, Y., LI, T., DING, Y., SUN, L., TU, T., ZHU, W., HU, J. & SUN, X. 2016. Changes in mesenchymal stem cells following long-term culture in vitro. *Molecular medicine reports,* 13**,** 5207-5215.

GUDURIC-FUCHS, J., O'CONNOR, A., CAMP, B., O'NEILL, C. L., MEDINA, R. J.

& SIMPSON, D. A. 2012. Selective extracellular vesicle-mediated export of an overlapping set of microRNAs from multiple cell types. *BMC genomics,* 13**,** 357.

GUERMAZI, A. 2019. Imaging the synovium in OA. *Osteoarthritis and Cartilage,* 27**,** S17.

GUERMAZI, A., HAYASHI, D., ROEMER, F. W., ZHU, Y., NIU, J., CREMA, M. D., JAVAID, M. K., MARRA, M. D., LYNCH, J. A. & EL-KHOURY, G. Y. 2014. Synovitis in knee osteoarthritis assessed by contrast-enhanced magnetic resonance imaging (MRI) is associated with radiographic tibiofemoral osteoarthritis and MRI-detected widespread cartilage damage: the MOST study. *The Journal of rheumatology,* 41**,** 501-508.

GUIDELINES, A. C. O. R. S. O. R. A. 2002. Guidelines for the management of rheumatoid arthritis: 2002 update. *Arthritis & Rheumatism,* 46**,** 328-346.

GYORGY, B., SZABO, T. G., TURIAK, L., WRIGHT, M., HERCZEG, P., LEDECZI, Z., KITTEL, A., POLGAR, A., TOTH, K., DERFALVI, B., ZELENAK, G., BOROCZ, I., CARR, B., NAGY, G., VEKEY, K., GAY, S., FALUS, A. & BUZAS, E. I. 2012. Improved flow cytometric assessment reveals distinct microvesicle (cell-derived microparticle) signatures in joint diseases. *PLoS One,* 7**,** e49726.

HAN, C. W., CHOI, J. H., KIM, J. M., KIM, W. Y., LEE, K. Y. & OH, G. T. 2001. Glucocorticoid-mediated repression of inflammatory cytokine production in fibroblast-like rheumatoid synoviocytes is independent of nuclear factor-kappaB activation induced by tumour necrosis factor alpha. *Rheumatology (Oxford),* 40**,** 267-73.

HAYWOOD, L., MCWILLIAMS, D. F., PEARSON, C. I., GILL, S. E., GANESAN, A., WILSON, D. & WALSH, D. A. 2003. Inflammation and angiogenesis in osteoarthritis. *Arthritis Rheum,* 48**,** 2173-7.

HE, H.-Q. & YE, R. 2017. The formyl peptide receptors: diversity of ligands and mechanism for recognition. *Molecules,* 22**,** 455.

HEADLAND, S. E., JONES, H. R., NORLING, L. V., KIM, A., SOUZA, P. R., CORSIERO, E., GIL, C. D., NERVIANI, A., DELL'ACCIO, F., PITZALIS, C., OLIANI, S. M., JAN, L. Y. & PERRETTI, M. 2015. Neutrophil-derived microvesicles enter cartilage and protect the joint in inflammatory arthritis. *Sci Transl Med,* 7**,** 315ra190.

HEADLAND, S. E. & NORLING, L. V. 2015. The resolution of inflammation: Principles and challenges. *Semin Immunol,* 27**,** 149-60.

HESS, C., SADALLAH, S., HEFTI, A., LANDMANN, R. & SCHIFFERLI, J.-A. 1999. Ectosomes released by human neutrophils are specialized functional units. *The Journal of Immunology,* 163**,** 4564-4573.

HONG, C. W. 2018. Extracellular Vesicles of Neutrophils. *Immune Netw,* 18**,** e43.

HONG, Y., ELEFTHERIOU, D., HUSSAIN, A. A., PRICE-KUEHNE, F. E., SAVAGE, C. O., JAYNE, D., LITTLE, M. A., SALAMA, A. D., KLEIN, N. J. & BROGAN, P. A. 2012a. Anti-neutrophil cytoplasmic antibodies stimulate release of neutrophil microparticles. *Journal of the American Society of Nephrology,* 23**,** 49-62.

HONG, Y., ELEFTHERIOU, D., HUSSAIN, A. A., PRICE-KUEHNE, F. E., SAVAGE, C. O., JAYNE, D., LITTLE, M. A., SALAMA, A. D., KLEIN, N. J. & BROGAN, P. A. 2012b. Anti-neutrophil cytoplasmic antibodies stimulate release of neutrophil microparticles. *J Am Soc Nephrol,* 23**,** 49-62.

HONORATI, M., NERI, S., CATTINI, L. & FACCHINI, A. 2006. Interleukin-17, a regulator of angiogenic factor release by synovial fibroblasts. *Osteoarthritis and Cartilage,* 14**,** 345-352.

HUANG, C. C., CHIOU, C. H., LIU, S. C., HU, S. L., SU, C. M., TSAI, C. H. & TANG, C. H. 2019. Melatonin attenuates TNF-α and IL-1β expression in synovial fibroblasts and diminishes cartilage degradation: Implications for the treatment of rheumatoid arthritis. *Journal of pineal research,* 66**,** e12560.

HUNTER, M. P., ISMAIL, N., ZHANG, X., AGUDA, B. D., LEE, E. J., YU, L., XIAO, T., SCHAFER, J., LEE, M.-L. T. & SCHMITTGEN, T. D. 2008. Detection of microRNA expression in human peripheral blood microvesicles. *PloS one,* 3**,** e3694.

ISHII, Y., WANG, Y., HAZIOT, A., DEL VECCHIO, P., GOYERT, S. & MALIK, A. 1993. Lipopolysaccharide binding protein and CD14 interaction induces tumor necrosis factor-alpha generation and neutrophil sequestration in lungs after intratracheal endotoxin. *Circulation research,* 73**,** 15-23.

IVETIC, A. 2018. A head-to-tail view of L-selectin and its impact on neutrophil behaviour. *Cell Tissue Res,* 371**,** 437-453.

IWANAGA, T., SHIKICHI, M., KITAMURA, H., YANASE, H. & NOZAWA-

INOUE, K. 2000. Morphology and functional roles of synoviocytes in the joint. *Archives of histology and cytology,* 63**,** 17-31.

JORDAN, J. M., HELMICK, C. G., RENNER, J. B., LUTA, G., DRAGOMIR, A. D., WOODARD, J., FANG, F., SCHWARTZ, T. A., ABBATE, L. M. & CALLAHAN, L. F. 2007. Prevalence of knee symptoms and radiographic and symptomatic knee osteoarthritis in African Americans and Caucasians: the Johnston County Osteoarthritis Project. *The Journal of rheumatology,* 34**,** 172-180.

JUNGEL, A., DISTLER, O., SCHULZE-HORSEL, U., HUBER, L. C., HA, H. R., SIMMEN, B., KALDEN, J. R., PISETSKY, D. S., GAY, S. & DISTLER, J. H. 2007. Microparticles stimulate the synthesis of prostaglandin E(2) via induction of cyclooxygenase 2 and microsomal prostaglandin E synthase 1. *Arthritis Rheum,* 56**,** 3564-74.

JUTRAS, B. L., LOCHHEAD, R. B., KLOOS, Z. A., BIBOY, J., STRLE, K., BOOTH, C. J., GOVERS, S. K., GRAY, J., SCHUMANN, P., VOLLMER, W., BOCKENSTEDT, L. K., STEERE, A. C. & JACOBS-WAGNER, C. 2019. Borrelia burgdorferi peptidoglycan is a persistent antigen in patients with Lyme arthritis. *Proc Natl Acad Sci U S A,* 116**,** 13498-13507.

KAMATA, N., KUTSUNA, H., HATO, F., KATO, T., OSHITANI, N., ARAKAWA, T. & KITAGAWA, S. 2004. Activation of human neutrophils by granulocyte colony-stimulating factor, granulocyte-macrophage colony-stimulating factor, and tumor necrosis factor α: role of phosphatidylinositol 3-kinase. *International journal of hematology,* 80**,** 421-427.

KAPOOR, M., MARTEL-PELLETIER, J., LAJEUNESSE, D., PELLETIER, J.-P. & FAHMI, H. 2011. Role of proinflammatory cytokines in the pathophysiology of osteoarthritis. *Nature Reviews Rheumatology,* 7**,** 33-42.

KAPUSTIN, A. N., DAVIES, J. D., REYNOLDS, J. L., MCNAIR, R., JONES, G. T., SIDIBE, A., SCHURGERS, L. J., SKEPPER, J. N., PROUDFOOT, D. & MAYR, M. 2011. Calcium regulates key components of vascular smooth muscle cell–derived matrix vesicles to enhance mineralization. *Circulation research,* 109**,** e1-e12.

KATO, T. & KITAGAWA, S. 2006. Regulation of neutrophil functions by proinflammatory cytokines. *International journal of hematology,* 84**,** 205-209.

KILLOCK, D. J. & IVETIC, A. 2010. The cytoplasmic domains of TNFalpha-converting enzyme (TACE/ADAM17) and L-selectin are regulated differently by p38 MAPK and PKC to promote ectodomain shedding. *Biochem J,* 428**,** 293-304.

KNIJFF-DUTMER, E. A., KOERTS, J., NIEUWLAND, R., KALSBEEK-BATENBURG, E. M. & VAN DE LAAR, M. A. 2002. Elevated levels of platelet microparticles are associated with disease activity in rheumatoid arthritis. *Arthritis Rheum,* 46**,** 1498-503.

KRENN, V., MORAWIETZ, L., BURMESTER, G. R., KINNE, R., MUELLER - LADNER, U., MULLER, B. & HAUPL, T. 2006. Synovitis score: discrimination between chronic low - grade and high - grade synovitis. *Histopathology,* 49**,** 358-364.

KRIEGER, M., SCOTT, M. P., MATSUDAIRA, P. T., LODISH, H. F., DARNELL, J. E., ZIPURSKY, L., KAISER, C. & BERK, A. 2004. Molecular cell biology. *San Francisco*.

KROHN, J. B., HUTCHESON, J. D., MARTÍNEZ - MARTÍNEZ, E. & AIKAWA, E. 2016. Extracellular vesicles in cardiovascular calcification: expanding current paradigms. *The Journal of physiology,* 594**,** 2895-2903.

KURREEMAN, F. A., PADYUKOV, L., MARQUES, R. B., SCHRODI, S. J., SEDDIGHZADEH, M., STOEKEN-RIJSBERGEN, G., VAN DER HELM, A. H., ALLAART, C. F., VERDUYN, W. & HOUWING-DUISTERMAAT, J. 2007. A candidate gene approach identifies the TRAF1/C5 region as a risk factor for rheumatoid arthritis. *PLoS medicine,* 4**,** e278.

KUTSUNA, H., SUZUKI, K., KAMATA, N., KATO, T., HATO, F., MIZUNO, K., KOBAYASHI, H., ISHII, M. & KITAGAWA, S. 2004. Actin reorganization and morphological changes in human neutrophils stimulated by TNF, GM-CSF, and G-CSF: the role of MAP kinases. *American Journal of Physiology-Cell Physiology,* 286**,** C55-C64.

L JOHNSON, B., W KUETHE, J. & C CALDWELL, C. 2014. Neutrophil derived microvesicles: emerging role of a key mediator to the immune response. *Endocrine, Metabolic & Immune Disorders-Drug Targets (Formerly Current Drug Targets-Immune, Endocrine & Metabolic Disorders)* [Online], 14.

LANA, J. F. D. S. D. & RODRIGUES, B. L. 2019. Osteoarthritis as a Chronic

Inflammatory Disease: A Review of the Inflammatory Markers. *Osteoarthritis.* IntechOpen.

LAWRENCE, R. C., FELSON, D. T., HELMICK, C. G., ARNOLD, L. M., CHOI, H., DEYO, R. A., GABRIEL, S., HIRSCH, R., HOCHBERG, M. C., HUNDER, G. G., JORDAN, J. M., KATZ, J. N., KREMERS, H. M., WOLFE, F. & NATIONAL ARTHRITIS DATA, W. 2008. Estimates of the prevalence of arthritis and other rheumatic conditions in the United States. Part II. *Arthritis Rheum,* 58**,** 26-35.

LAWRENCE, S. M., CORRIDEN, R. & NIZET, V. 2018. The ontogeny of a neutrophil: mechanisms of granulopoiesis and homeostasis. *Microbiol. Mol. Biol. Rev.,* 82**,** e00057-17.

LÁZARO-IBÁÑEZ, E., NEUVONEN, M., TAKATALO, M., THANIGAI ARASU, U., CAPASSO, C., CERULLO, V., RHIM, J. S., RILLA, K., YLIPERTTULA, M. & SILJANDER, P. R.-M. 2017. Metastatic state of parent cells influences the uptake and functionality of prostate cancer cell-derived extracellular vesicles. *Journal of extracellular vesicles,* 6**,** 1354645.

LEE, J. C., ESPÉLI, M., ANDERSON, C. A., LINTERMAN, M. A., POCOCK, J. M., WILLIAMS, N. J., ROBERTS, R., VIATTE, S., FU, B. & PESHU, N. 2013. Human SNP links differential outcomes in inflammatory and infectious disease to a FOXO3-regulated pathway. *Cell,* 155**,** 57-69.

LEFKOWITZ, D. L., GELDERMAN, M. P., FUHRMANN, S. R., GRAHAM, S., STARNES III, J. D., LEFKOWITZ, S. S., BOLLEN, A. & MOGUILEVSKY, N. 1999. Neutrophilic myeloperoxidase–macrophage interactions perpetuate chronic inflammation associated with experimental arthritis. *Clinical immunology,* 91**,** 145-155.

LI, H., XIE, S., QI, Y., LI, H., ZHANG, R. & LIAN, Y. 2018. TNF−α increases the expression of inflammatory factors in synovial fibroblasts by inhibiting the PI3K/AKT pathway in a rat model of monosodium iodoacetate−induced osteoarthritis. *Experimental and therapeutic medicine,* 16**,** 4737-4744.

LU, X. & QIAN, J. 2019. Downregulated MEG3 participates in rheumatoid arthritis via promoting proliferation of fibroblast−like synoviocytes. *Experimental and therapeutic medicine,* 17**,** 1637-1642.

MABEY, T., HONSAWEK, S., TANAVALEE, A., YUKTANANDANA, P.,

WILAIRATANA, V. & POOVORAWAN, Y. 2016. Plasma and synovial fluid inflammatory cytokine profiles in primary knee osteoarthritis. *Biomarkers,* 21**,** 639-644.

MANCUSO, P., RAMAN, S., GLYNN, A., BARRY, F. & MURPHY, J. M. 2019. Mesenchymal Stem Cell Therapy for Osteoarthritis: The Critical Role of the Cell Secretome. *Frontiers in bioengineering and biotechnology,* 7**,** 9-9.

MEEHAN, B., RAK, J. & DI VIZIO, D. 2016. Oncosomes - large and small: what are they, where they came from? *Journal of extracellular vesicles,* 5**,** 33109-33109.

MESRI, M. & ALTIERI, D. C. 1998. Endothelial cell activation by leukocyte microparticles. *The Journal of Immunology,* 161**,** 4382-4387.

MESRI, M. & ALTIERI, D. C. 1999. Leukocyte microparticles stimulate endothelial cell cytokine release and tissue factor induction in a JNK1 signaling pathway. *Journal of Biological Chemistry,* 274**,** 23111-23118.

MO, Y.-Q., DAI, L., ZHENG, D.-H., ZHU, L.-J., WEI, X.-N., PESSLER, F., SHEN, J. & ZHANG, B.-Y. 2011. Synovial infiltration with CD79a-positive B cells, but not other B cell lineage markers, correlates with joint destruction in rheumatoid arthritis. *The Journal of rheumatology,* 38**,** 2301-2308.

MOHAMED, R. H., PASHA, H. F. & EL-SHAHAWY, E. E. 2012. Influence of TRAF1/C5 and STAT4 genes polymorphisms on susceptibility and severity of rheumatoid arthritis in Egyptian population. *Cellular immunology,* 273**,** 67-72.

MOLL, C., BOGAS, M., GOMEZ-PUERTA, J. A., CELIS, R., VAZQUEZ, I., RODRIGUEZ, F., KANTEREWICZ, E., SANMARTI, R. & CANETE, J. D. 2009. Macroscopic features of knee synovitis in early untreated Behcet disease and psoriatic arthritis. *Clin Rheumatol,* 28**,** 1053-7.

MONTECALVO, A., LARREGINA, A. T., SHUFESKY, W. J., STOLZ, D. B., SULLIVAN, M. L., KARLSSON, J. M., BATY, C. J., GIBSON, G. A., ERDOS, G. & WANG, Z. 2012. Mechanism of transfer of functional microRNAs between mouse dendritic cells via exosomes. *Blood,* 119**,** 756-766.

MUHL, H. & PFEILSCHIFTER, J. 2003. Anti-inflammatory properties of pro-inflammatory interferon-gamma. *Int Immunopharmacol,* 3**,** 1247-55.

MULCAHY, L. A., PINK, R. C. & CARTER, D. R. F. 2014. Routes and mechanisms of extracellular vesicle uptake. *Journal of extracellular vesicles,* 3**,** 10.3402/jev.v3.24641.

MULLAN, R. H., MATTHEWS, C., BRESNIHAN, B., FITZGERALD, O., KING, L., POOLE, A. R., FEARON, U. & VEALE, D. J. 2007. Early changes in serum type II collagen biomarkers predict radiographic progression at one year in inflammatory arthritis patients after biologic therapy. *Arthritis & Rheumatism: Official Journal of the American College of Rheumatology,* 56**,** 2919-2928.

MYASOEDOVA, E., CROWSON, C. S., KREMERS, H. M., THERNEAU, T. M. & GABRIEL, S. E. 2010. Is the incidence of rheumatoid arthritis rising?: results from Olmsted County, Minnesota, 1955–2007. *Arthritis & Rheumatism,* 62**,** 1576-1582.

NAMBA, S., NAKANO, R., KITANAKA, T., KITANAKA, N., NAKAYAMA, T. & SUGIYA, H. 2017. ERK2 and JNK1 contribute to TNF-α-induced IL-8 expression in synovial fibroblasts. *PloS one,* 12**,** e0182923.

NEW, S. E., GOETTSCH, C., AIKAWA, M., MARCHINI, J. F., SHIBASAKI, M., YABUSAKI, K., LIBBY, P., SHANAHAN, C. M., CROCE, K. & AIKAWA, E. 2013. Macrophage-derived matrix vesicles: an alternative novel mechanism for microcalcification in atherosclerotic plaques. *Circulation research,* 113**,** 72-77.

NOLAN, S., DIXON, R., NORMAN, K., HELLEWELL, P. & RIDGER, V. 2008. Nitric oxide regulates neutrophil migration through microparticle formation. *The American journal of pathology,* 172**,** 265-273.

NZEUSSEU TOUKAP, A., DELPORTE, C., NOYON, C., FRANCK, T., ROUSSEAU, A., SERTEYN, D., RAES, M., VANHAEVERBEEK, M., MOGUILEVSKY, N. & NEVE, J. 2014. Myeloperoxidase and its products in synovial fluid of patients with treated or untreated rheumatoid arthritis. *Free radical research,* 48**,** 461-465.

OEHLER, S., NEUREITER, D., MEYER-SCHOLTEN, C. & AIGNER, T. 2002. Subtyping of osteoarthritic synoviopathy. *Clinical and experimental rheumatology,* 20**,** 633-640.

OKADA, Y., WU, D., TRYNKA, G., RAJ, T., TERAO, C., IKARI, K., KOCHI, Y., OHMURA, K., SUZUKI, A. & YOSHIDA, S. 2014. Genetics of rheumatoid arthritis contributes to biology and drug discovery. *Nature,* 506**,** 376.

ORR, C., SOUSA, E., BOYLE, D. L., BUCH, M. H., BUCKLEY, C. D., CAÑETE, J. D., CATRINA, A. I., CHOY, E. H., EMERY, P. & FEARON, U. 2017. Synovial tissue research: a state-of-the-art review. *Nature reviews. Rheumatology,* 13**,** 463-475.

OSANI, M. C., VAYSBROT, E. E., ZHOU, M., MCALINDON, T. E. & BANNURU, R. R. 2019. Duration of Symptom Relief and Early Trajectory of Adverse Events for Oral NSAID s in Knee Osteoarthritis: A Systematic Review and Meta - analysis. *Arthritis care & research*.

PATTISON, D. & DAVIES, M. 2006. Reactions of myeloperoxidase-derived oxidants with biological substrates: gaining chemical insight into human inflammatory diseases. *Current medicinal chemistry,* 13**,** 3271-3290.

PEARLE, A., SCANZELLO, C., GEORGE, S., MANDL, L., DICARLO, E., PETERSON, M., SCULCO, T. & CROW, M. 2007. Elevated high-sensitivity C-reactive protein levels are associated with local inflammatory findings in patients with osteoarthritis. *Osteoarthritis and Cartilage,* 15**,** 516-523.

PEAT, G., THOMAS, E., DUNCAN, R., WOOD, L., HAY, E. & CROFT, P. 2006. Clinical classification criteria for knee osteoarthritis: performance in the general population and primary care. *Annals of the rheumatic diseases,* 65**,** 1363-1367.

PEDUTO, L., SANSONETTI, P. J. & NIGRO, G. 2018. Intestinal Stem Cells and Their Niche at Homeostasis and Under Stress. *Advances in Stem Cells and their Niches.* Elsevier.

PESSLER, F., CHEN, L., DAI, L., GOMEZ-VAQUERO, C., DIAZ-TORNE, C., PAESSLER, M., SCANZELLO, C., CAKIR, N., EINHORN, E. & SCHUMACHER, H. 2008a. A histomorphometric analysis of synovial biopsies from individuals with Gulf War Veterans' Illness and joint pain compared to normal and osteoarthritis synovium. *Clinical rheumatology,* 27**,** 1127-1134.

PESSLER, F., DAI, L., DIAZ-TORNE, C., GOMEZ-VAQUERO, C., PAESSLER, M., ZHENG, D., EINHORN, E., RANGE, U., SCANZELLO, C. & SCHUMACHER, H. 2008b. The synovitis of "non-inflammatory" orthopaedic arthropathies: a quantitative histological and immunohistochemical analysis. *Annals of the rheumatic diseases,* 67**,** 1184-1187.

PETTIT, A. R., AHERN, M. J., ZEHNTNER, S., SMITH, M. D. & THOMAS, R. 2001. Comparison of differentiated dendritic cell infiltration of autoimmune and osteoarthritis synovial tissue. *Arthritis & Rheumatism: Official Journal of the American College of Rheumatology,* 44**,** 105-110.

PITANGA, T. N., DE ARAGAO FRANCA, L., ROCHA, V. C., MEIRELLES, T., BORGES, V. M., GONCALVES, M. S., PONTES-DE-CARVALHO, L. C., NORONHA-DUTRA, A. A. & DOS-SANTOS, W. L. 2014. Neutrophil-derived microparticles induce myeloperoxidase-mediated damage of vascular endothelial cells. *BMC Cell Biol,* 15**,** 21.

PLIYEV, B. K., KALINTSEVA, M. V., ABDULAEVA, S. V., YARYGIN, K. N. & SAVCHENKO, V. G. 2014. Neutrophil microparticles modulate cytokine production by natural killer cells. *Cytokine,* 65**,** 126-129.

PRIETO-POTIN, I., LARGO, R., ROMAN-BLAS, J. A., HERRERO-BEAUMONT, G. & WALSH, D. A. 2015. Characterization of multinucleated giant cells in synovium and subchondral bone in knee osteoarthritis and rheumatoid arthritis. *BMC Musculoskelet Disord,* 16**,** 226.

REICH, N., BEYER, C., GELSE, K., AKHMETSHINA, A., DEES, C., ZWERINA, J., SCHETT, G., DISTLER, O. & DISTLER, J. H. 2011. Microparticles stimulate angiogenesis by inducing ELR(+) CXC-chemokines in synovial fibroblasts. *J Cell Mol Med,* 15**,** 756-62.

REIN, S., OKOGBAA, J., HAGERT, E., MANTHEY, S. & LADD, A. 2019. Histopathological analysis of the synovium in trapeziometacarpal osteoarthritis. *Journal of Hand Surgery (European Volume)***,** 1753193419848600.

RHYS, H. I., DELL'ACCIO, F., PITZALIS, C., MOORE, A., NORLING, L. V. & PERRETTI, M. 2018. Neutrophil Microvesicles from Healthy Control and Rheumatoid Arthritis Patients Prevent the Inflammatory Activation of Macrophages. *EBioMedicine,* 29**,** 60-69.

ROLLE, N. A., JAN, I., SIBBITT, W. L., BAND, P. A., HASELER, L. J., HAYWARD, W. A., MURUGANANDAM, M., EMIL, N. S., FANGTHAM, M. & BANKHURST, A. D. 2019. Extractable synovial fluid in inflammatory and non-inflammatory arthritis of the knee. *Clinical Rheumatology***,** 1-9.

RØRVIG, S., ØSTERGAARD, O., HEEGAARD, N. H. & BORREGAARD, N. 2013. Proteome profiling of human neutrophil granule subsets, secretory vesicles, and cell membrane: correlation with transcriptome profiling of neutrophil precursors. *Journal of leukocyte biology,* 94**,** 711-721.

ROSILLO, M. Á., ALARCÓN-DE-LA-LASTRA, C., CASTEJÓN, M. L., MONTOYA, T., CEJUDO-GUILLÉN, M. & SÁNCHEZ-HIDALGO, M. 2019. Polyphenolic extract from extra virgin olive oil inhibits the inflammatory response in IL-1β-activated synovial fibroblasts. *British Journal of Nutrition,* 121**,** 55-62.

RUDERMAN, E. M. 2012. Overview of safety of non-biologic and biologic DMARDs. *Rheumatology,* 51**,** vi37-vi43.

RUIZ-HEILAND, G., ZHAO, Y., DERER, A., BRAUN, T., ENGELKE, K., NEUMANN, E., MUELLER-LADNER, U., LIU, Y., ZWERINA, J. & SCHETT, G. 2014. Deletion of the receptor tyrosine kinase Tyro3 inhibits synovial hyperplasia and bone damage in arthritis. *Annals of the rheumatic diseases,* 73**,** 771-779.

SACITHARAN, P. K. 2019. Ageing and Osteoarthritis. *In:* HARRIS, J. R. & KOROLCHUK, V. I. (eds.) *Biochemistry and Cell Biology of Ageing: Part II Clinical Science.* Singapore: Springer Singapore.

SAITO, I., KOSHINO, T., NAKASHIMA, K., UESUGI, M. & SAITO, T. 2002. Increased cellular infiltrate in inflammatory synovia of osteoarthritic knees. *Osteoarthritis and cartilage,* 10**,** 156-162.

SALAMONE, G., GIORDANO, M., TREVANI, A. S., GAMBERALE, R., VERMEULEN, M., SCHETTINNI, J. & GEFFNER, J. R. 2001. Promotion of neutrophil apoptosis by TNF-α. *The Journal of Immunology,* 166**,** 3476-3483.

SALT, E. & CROFFORD, L. 2012. Rheumatoid arthritis: new treatments, better outcomes. *The Nurse Practitioner,* 37**,** 16-22.

SARMANOVA, A., HALL, M., MOSES, J., DOHERTY, M. & ZHANG, W. 2016. Synovial changes detected by ultrasound in people with knee osteoarthritis–a meta-analysis of observational studies. *Osteoarthritis and cartilage,* 24**,** 1376-1383.

SAVILL, J., DRANSFIELD, I., HOGG, N. & HASLETT, C. 1990. Vitronectin receptor-mediated phagocytosis of cells undergoing apoptosis. *Nature,* 343**,** 170.

SCHABBAUER, G., TENCATI, M., PEDERSEN, B., PAWLINSKI, R. & MACKMAN, N. 2004. PI3K-Akt pathway suppresses coagulation and inflammation in endotoxemic mice. *Arteriosclerosis, thrombosis, and vascular biology,* 24**,** 1963-1969.

SHABAB, T., KHANABDALI, R., MOGHADAMTOUSI, S. Z., KADIR, H. A. & MOHAN, G. 2017. Neuroinflammation pathways: a general review. *International*

Journal of Neuroscience, 127**,** 624-633.

SHANAJ, S. & DONLIN, L. T. 2019. Synovial Tissue: Cellular and Molecular Phenotyping. *Current rheumatology reports,* 21**,** 52.

SHEN, G., KRIENKE, S., SCHILLER, P., NIESSEN, A., NEU, S., ECKSTEIN, V., SCHILLER, M., LORENZ, H. M. & TYKOCINSKI, L. O. 2017. Microvesicles released by apoptotic human neutrophils suppress proliferation and IL-2/IL-2 receptor expression of resting T helper cells. *Eur J Immunol,* 47**,** 900-910.

SLANSKY, E., LI, J., HAUPL, T., MORAWIETZ, L., KRENN, V. & PESSLER, F. 2010. Quantitative determination of the diagnostic accuracy of the synovitis score and its components. *Histopathology,* 57**,** 436-43.

SLATER, T. W., FINKIELSZTEIN, A., MASCARENHAS, L. A., MEHL, L. C., BUTIN-ISRAELI, V. & SUMAGIN, R. 2017. Neutrophil Microparticles Deliver Active Myeloperoxidase to Injured Mucosa To Inhibit Epithelial Wound Healing. *J Immunol,* 198**,** 2886-2897.

SMITH, M. D. 2011. Suppl 1: The Normal Synovium. *The open rheumatology journal,* 5**,** 100.

SMITH, M. D., O'DONNELL, J., HIGHTON, J., PALMER, D. G., ROZENBILDS, M. & ROBERTS-THOMSON, P. J. 1992. Immunohistochemical analysis of synovial membranes from inflammatory and non-inflammatory arthritides: scarcity of CD5 positive B cells and IL2 receptor bearing T cells. *Pathology,* 24**,** 19-26.

SQUADRITO, M. L., BAER, C., BURDET, F., MADERNA, C., GILFILLAN, G. D., LYLE, R., IBBERSON, M. & DE PALMA, M. 2014. Endogenous RNAs modulate microRNA sorting to exosomes and transfer to acceptor cells. *Cell reports,* 8**,** 1432-1446.

STANNUS, O., JONES, G., CICUTTINI, F., PARAMESWARAN, V., QUINN, S., BURGESS, J. & DING, C. 2010. Circulating levels of IL-6 and TNF-α are associated with knee radiographic osteoarthritis and knee cartilage loss in older adults. *Osteoarthritis and cartilage,* 18**,** 1441-1447.

STEINER, G., TOHIDAST-AKRAD, M., WITZMANN, G., VESELY, M., STUDNICKA-BENKE, A., GAL, A., KUNAVER, M., ZENZ, P. & SMOLEN, J. 1999. Cytokine production by synovial T cells in rheumatoid arthritis. *Rheumatology (Oxford,*

England), 38**,** 202-213.

SUMMERS, C., RANKIN, S. M., CONDLIFFE, A. M., SINGH, N., PETERS, A. M. & CHILVERS, E. R. 2010. Neutrophil kinetics in health and disease. *Trends in immunology,* 31**,** 318-324.

SUN, Y., FIRESTEIN, G. S., WENGER, L., HUANG, C. Y. & CHEUNG, H. S. 2004. Telomerase-transduced osteoarthritic fibroblast-like synoviocyte cell line. *Biochem Biophys Res Commun,* 323**,** 1287-92.

SUZUKI, K., HASEGAWA, T., SAKAMOTO, C., ZHOU, Y.-M., HATO, F., HINO, M., TATSUMI, N. & KITAGAWA, S. 2001. Cleavage of mitogen-activated protein kinases in human neutrophils undergoing apoptosis: role in decreased responsiveness to inflammatory cytokines. *The Journal of Immunology,* 166**,** 1185-1192.

TAK, P. P., SMEETS, T. J., DAHA, M. R., KLUIN, P. M., MEIJERS, K. A., BRAND, R., MEINDERS, A. E. & BREEDVELD, F. C. 1997. Analysis of the synovial cell infiltrate in early rheumatoid synovial tissue in relation to local disease activity. *Arthritis & Rheumatism: Official Journal of the American College of Rheumatology,* 40**,** 217-225.

TAKAHASHI, T., BABOOLAL, T. G., LAMB, J., HAMILTON, T. W. & PANDIT, H. G. 2019. Is Knee Joint Distraction a Viable Treatment Option for Knee OA?—A Literature Review and Meta-Analysis. *J Knee Surg,* 32**,** 788-795.

TAKEDA, Y., WATANABE, H., YONEHARA, S., YAMASHITA, T., SALTO, S. & SENDO, F. 1993. Rapid acceleration of neutrophil apoptosis by tumor necrosis factor-α. *International Immunology,* 5**,** 691-694.

TAKESHITA, S., NAKATANI, K., TAKATA, Y., KAWASE, H., SEKINE, I. & YOSHIOKA, S. 1998. Interferon-gamma (IFN-γ) and tumor necrosis factor-alpha (TNF-α) enhance lipopolysaccharide binding to neutrophils via CD14. *Inflammation research,* 47**,** 101-103.

TAN, A. S., AHMED, N. & BERRIDGE, M. V. 1998. Acute regulation of glucose transport after activation of human peripheral blood neutrophils by phorbol myristate acetate, fMLP, and granulocyte-macrophage colony-stimulating factor. *Blood,* 91**,** 649-55.

THOMAS, H. B., MOOTS, R. J., EDWARDS, S. W. & WRIGHT, H. L. 2015. Whose

gene is it anyway? The effect of preparation purity on neutrophil transcriptome studies. *PLoS One,* 10**,** e0138982.

THOMAS, Y., SCHIFF, M., BELKADI, L., JURGENS, P., KAHHAK, L. & BENVENISTE, J. 2000. Activation of human neutrophils by electronically transmitted phorbol-myristate acetate. *Med Hypotheses,* 54**,** 33-9.

TIAN, T., ZHU, Y. L., HU, F. H., WANG, Y. Y., HUANG, N. P. & XIAO, Z. D. 2013. Dynamics of exosome internalization and trafficking. *Journal of cellular physiology,* 228**,** 1487-1495.

TIMAR, C. I., LORINCZ, A. M., CSEPANYI-KOMI, R., VALYI-NAGY, A., NAGY, G., BUZAS, E. I., IVANYI, Z., KITTEL, A., POWELL, D. W., MCLEISH, K. R. & LIGETI, E. 2013. Antibacterial effect of microvesicles released from human neutrophilic granulocytes. *Blood,* 121**,** 510-8.

TOBÓN, G. J., YOUINOU, P. & SARAUX, A. 2010. The environment, geo-epidemiology, and autoimmune disease: Rheumatoid arthritis. *Autoimmunity reviews,* 9**,** A288-A292.

TURBICA, I., GALLAIS, Y., GUEGUEN, C., THARINGER, H., AL SABBAGH, C., GORGES, R., GARY-GOUY, H., KERDINE-ROMER, S., PALLARDY, M., MASCARELL, L., GLEIZES, A. & CHOLLET-MARTIN, S. 2015. Ectosomes from neutrophil-like cells down-regulate nickel-induced dendritic cell maturation and promote Th2 polarization. *J Leukoc Biol,* 97**,** 737-49.

TURTURICI, G., TINNIRELLO, R., SCONZO, G. & GERACI, F. 2014. Extracellular membrane vesicles as a mechanism of cell-to-cell communication: advantages and disadvantages. *American Journal of Physiology-Cell Physiology,* 306**,** C621-C633.

VALDES, A. M. & STOCKS, J. 2018. Osteoarthritis and ageing. *European Medical Journal Rheumatology,* 3**,** 116-123.

VALINEZHAD ORANG, A., SAFARALIZADEH, R. & KAZEMZADEH-BAVILI, M. 2014. Mechanisms of miRNA-Mediated Gene Regulation from Common Downregulation to mRNA-Specific Upregulation. *International journal of genomics,* 2014**,** 970607-970607.

VAN DEN BERG, J. M., WEYER, S., WEENING, J. J., ROOS, D. & KUIJPERS, T. W. 2001. Divergent effects of tumor necrosis factor α on apoptosis of human

neutrophils. *Journal of leukocyte biology,* 69**,** 467-473.

VAN DER HEIJDE, D. M. 1996. Plain X-rays in rheumatoid arthritis: overview of scoring methods, their reliability and applicability. *Bailliere's clinical rheumatology,* 10**,** 435-453.

VAN DER POL, E., BÖING, A., GOOL, E. & NIEUWLAND, R. 2016. Recent developments in the nomenclature, presence, isolation, detection and clinical impact of extracellular vesicles. *Journal of Thrombosis and Haemostasis,* 14**,** 48-56.

VAN DER POL, E., COUMANS, F., GROOTEMAAT, A., GARDINER, C., SARGENT, I., HARRISON, P., STURK, A., VAN LEEUWEN, T. & NIEUWLAND, R. 2014. Particle size distribution of exosomes and microvesicles determined by transmission electron microscopy, flow cytometry, nanoparticle tracking analysis, and resistive pulse sensing. *Journal of Thrombosis and Haemostasis,* 12**,** 1182-1192.

VAN NIEL, G., CHARRIN, S., SIMOES, S., ROMAO, M., ROCHIN, L., SAFTIG, P., MARKS, M. S., RUBINSTEIN, E. & RAPOSO, G. 2011. The tetraspanin CD63 regulates ESCRT-independent and-dependent endosomal sorting during melanogenesis. *Developmental cell,* 21**,** 708-721.

VAN NIEL, G., D'ANGELO, G. & RAPOSO, G. 2018. Shedding light on the cell biology of extracellular vesicles. *Nature reviews Molecular cell biology,* 19**,** 213.

VERSUS ARTHRITIS 2013. Prevalence of osteoarthritis in England and local authorities: Reading.

VOLS, S., SIONOV, R. V. & GRANOT, Z. 2017. Always look on the bright side: anti-tumor functions of neutrophils. *Current pharmaceutical design,* 23**,** 4862-4892.

WANG, Z.-C., LU, H., ZHOU, Q., YU, S.-M., MAO, Y.-L., ZHANG, H.-J., ZHANG, P.-C. & YAN, W.-J. 2015. MiR-451 inhibits synovial fibroblasts proliferation and inflammatory cytokines secretion in rheumatoid arthritis through mediating p38MAPK signaling pathway. *International journal of clinical and experimental pathology,* 8**,** 14562.

WATANABE, S., OGURA, N., AKUTSU, M., KAWASHIMA, M., HATTORI, T., YANO, T., ITO, K. & KONDOH, T. 2017. Interleukin-1β and Tumor Necrosis Factor-α Synergistically Induce Expression of Colony Stimulating Factors in Synovial Fibroblasts from the Human Temporomandibular Joint. *International Journal of Oral-*

Medical Sciences, 15**,** 74-84.

WATERBORG, C. E., BEERMANN, S., BROEREN, M. G., BENNINK, M. B., KOENDERS, M. I., VAN LENT, P. L., VAN DEN BERG, W. B., VAN DER KRAAN, P. M. & VAN DE LOO, F. A. 2018a. Protective role of the MER tyrosine kinase via efferocytosis in rheumatoid arthritis models. *Frontiers in immunology,* 9.

WATERBORG, C. E., BROEREN, M. G., BLANEY DAVIDSON, E. N., KOENDERS, M. I., VAN LENT, P. L., VAN DEN BERG, W. B., VAN DER KRAAN, P. M. & VAN DE LOO, F. A. 2018b. The level of synovial AXL expression determines the outcome of inflammatory arthritis, possibly depending on the upstream role of TGF-β1. *Rheumatology,* 58**,** 536-546.

WEGNER, N., LUNDBERG, K., KINLOCH, A., FISHER, B., MALMSTRÖM, V., FELDMANN, M. & VENABLES, P. J. 2010. Autoimmunity to specific citrullinated proteins gives the first clues to the etiology of rheumatoid arthritis. *Immunological reviews,* 233**,** 34-54.

WITTMANN, S., ROTHE, G., SCHMITZ, G. & FRÖHLICH, D. 2004. Cytokine upregulation of surface antigens correlates to the priming of the neutrophil oxidative burst response. *Cytometry Part A: The Journal of the International Society for Analytical Cytology,* 57**,** 53-62.

WOOD, M. J., LECKENBY, A., REYNOLDS, G., SPIERING, R., PRATT, A. G., RANKIN, K. S., ISAACS, J. D., HANIFFA, M. A., MILLING, S. & HILKENS, C. M. 2019. Macrophage proliferation distinguishes 2 subgroups of knee osteoarthritis patients. *JCI insight,* 4.

WOOLF, A. D. & PFLEGER, B. 2003. Burden of major musculoskeletal conditions. *Bulletin of the World Health Organization,* 81**,** 646-656.

XIAO, C.-Y., PAN, Y.-F. & GUO, X.-H. 2010. Primary cultured of fibroblast-like synoviocytes and their biological feature [J]. *China Medical Engineering,* 2.

XIAO, Z., CAMALIER, C. E., NAGASHIMA, K., CHAN, K. C., LUCAS, D. A., CRUZ, M. J. D. L., GIGNAC, M., LOCKETT, S., ISSAQ, H. J. & VEENSTRA, T. D. 2007. Analysis of the extracellular matrix vesicle proteome in mineralizing osteoblasts. *Journal of cellular physiology,* 210**,** 325-335.

YAMIN, R., BERHANI, O., PELEG, H., AAMAR, S., STEIN, N., GAMLIEL, M.,

HINDI, I., SCHEIMAN-ELAZARY, A. & GUR, C. 2019. High percentages and activity of synovial fluid NK cells present in patients with advanced stage active Rheumatoid Arthritis. *Scientific reports,* 9**,** 1351.

YANG, Z., WANG, J., PAN, Z. & ZHANG, Y. 2018. miR-143-3p regulates cell proliferation and apoptosis by targeting IGF1R and IGFBP5 and regulating the Ras/p38 MAPK signaling pathway in rheumatoid arthritis. *Experimental and therapeutic medicine,* 15**,** 3781-3790.

YUDOH, K., MATSUNO, H., NAKAZAWA, F., YONEZAWA, T. & KIMURA, T. 2000. Reduced expression of the regulatory CD4+ T cell subset is related to Th1/Th2 balance and disease severity in rheumatoid arthritis. *Arthritis & Rheumatism: Official Journal of the American College of Rheumatology,* 43**,** 617-627.

ZENG, Q. Y., CHEN, R., DARMAWAN, J., XIAO, Z. Y., CHEN, S. B., WIGLEY, R., LE CHEN, S. & ZHANG, N. Z. 2008. Rheumatic diseases in China. *Arthritis Res Ther,* 10**,** R17.

ZHANG, W., DOHERTY, M., LEEB, B., ALEKSEEVA, L., ARDEN, N., BIJLSMA, J., DINÇER, F., DZIEDZIC, K., HÄUSELMANN, H. & HERRERO-BEAUMONT, G. 2007. EULAR evidence based recommendations for the management of hand osteoarthritis: report of a Task Force of the EULAR Standing Committee for International Clinical Studies Including Therapeutics (ESCISIT). *Annals of the rheumatic diseases,* 66**,** 377-388.

ZHONG, F., XU, J., YANG, X., ZHANG, Q., GAO, Z., DENG, Y., ZHANG, L. & YU, C. 2018. miR‐145 eliminates lipopolysaccharides‐induced inflammatory injury in human fibroblast‐like synoviocyte MH7A cells. *Journal of cellular biochemistry,* 119**,** 10059-10066.

ZIMMERMANN, T., KUNISCH, E., PFEIFFER, R., HIRTH, A., STAHL, H.-D., SACK, U., LAUBE, A., LIESAUS, E., ROTH, A. & PALOMBO-KINNE, E. 2000. Isolation and characterization of rheumatoid arthritis synovial fibroblasts from primary culture—primary culture cells markedly differ from fourth-passage cells. *Arthritis Research & Therapy,* 3**,** 72.

ZONNEVELD, R., MOLEMA, G. & PLÖTZ, F. B. 2016. Analyzing neutrophil morphology, mechanics, and motility in sepsis: options and challenges for novel bedside

technologies. *Critical care medicine,* 44**,** 218-228.

VITA

NAME	Dong Zhan
DATE OF BIRTH	03, December, 1984
PLACE OF BIRTH	Qujing, Yunnan Province, P.R.China
INSTITUTIONS ATTENDED	University of Liverpool
HOME ADDRESS	Room 201, Bld. D, Run Ya Yuan, Tian Run Kang Yuan, Junxian Street, Chenggong District, Kunming, Yunnan Province, P.R.China.
PUBLICATION	1. Relationships between blood leukocyte mitochondrial DNA copy number and inflammatory cytokines in knee osteoarthritis. Zhan D, Tanavalee A, Tantavisut S, Ngarmukos S, Edwards SW, Honsawek S. Journal of Zhejiang University-SCIENCE B. 2019:1-11. 2. Reduction of leukocyte mitochondrial DNA copy number in knee osteoarthritis. Zhan D, Honsawek S. Chulalongkorn Medical Journal. 2019;63(3):207-209. 3. Association of adiponectin gene polymorphisms with knee osteoarthritis. Zhan D, Thumtecho S, Tanavalee A, Yuktanandana P, Anomasiri W, Honsawek S. World journal of orthopedics. 2017;8(9):719. 4. Association of adiponectin +276G/T polymorphism with knee osteoarthritis. Zhan D, Yuktanandana P, Anomasiri W, Tanavalee A, Honsawek S. Biomedical reports. 2014;2(2):229-232. 5. Study on clinical characteristics of thyroid nodules. Luo J, Feng J, Zhan D, Meng Q, Shen Y. Chinese General Practice. 2018;21(36):4445-4452,4458. (Chinese) 6. Telomere length in peripheral blood leukocytes is associated with severity of biliary atresia. Udomsinprasert W, Poovorawan Y, Chongsrisawat V, Vejchapipat P, Zhan D, Honsawek S. PloS one. 2015;10(7). 7. Plasma and synovial fluid sclerostin are inversely associated with radiographic severity of knee osteoarthritis. Mabey T, Honsawek S, Tanavalee A, Wilairatana V, Yuktanandana P, Saetan N, Zhan D. Clinical biochemistry. 2014;47(7-8):547-51. 8. Neutrophil-derived microvesicles modulate expression

of inflammatory cytokines by fibroblast-like synoviocytes. Scientific Reports 2020. Revised and reviewed.
9. Isolation of microvesicles from human circulating neutrophils. Bio-protocol 2020. Accepted/ In press.

AWARD RECEIVED None